Liquid Sloshing in Containers with Flexibility

A thesis submitted in fulfillment of the requirements for the degree of Doctor of Philosophy

School of Engineering and Science

Faculty of Health, Engineering and Science

Victoria University

Melbourne, Australia

by

Marija Gradinscak

MAY 2009

Summary

Sloshing is the low frequency oscillations of the free surface of a liquid in a partially filled container. The dynamic response of structures holding the liquid can be significantly influenced by these oscillations, and their interaction with the sloshing liquid could lead to instabilities. It is critical to predict and to control sloshing in order to maintain safe operations in many engineering applications, such as in-ground storage and marine transport of liquid cargo, aerospace vehicles and earthquake-safe structures.

Contributions to the state of knowledge in predicting and controlling sloshing are the main objectives of the proposed research. To this end, a numerical model has been developed to enable reliable predictions of liquid sloshing. The numerical results are compared with experimental results to determine the accuracy of the numerical model. Further, the research addresses the employment of intentionally induced sloshing to control structural oscillations. The novelty of this research is in its use of a flexible container. Results indicate that intentionally introduced flexibility of the container is capable of producing effective control. The practical application of the proposed research is in the early design stages of engineering systems for which liquid sloshing plays a significant part in structural loading.

Declaration

I, Marija Gradinscak, declare that the PhD thesis entitled Liquid Sloshing in Containers with Flexibility is no more than 100,000 words in length including quotes and exclusive of tables, figures, appendices, bibliography, references and footnotes. This thesis contains no material that has been submitted previously, in whole or in part, for the award of any other academic degree or diploma. Except where otherwise indicated, this thesis is my own work.

Signature: [redacted]

Date: 7/08/2009

Acknowledgments

The research and execution of this thesis would not have been possible without the support, advice and comments from those who have taken the time to either contribute or inquire into what has been keeping me busy for the last few years. I am grateful for every person with whom I have discussed the subject for in some way they have each contributed to the end result of this thesis.

Special acknowledgment must go to my supervisors; Associate Professor Özden F. Turan and Dr Eren S. Semercigil for their encouragement and guidance during the course of this investigation. For the generous contribution of their time during the preparation of the draft, I am extremely grateful.

Thanks also go to my parents, Nikola and Tinka for creating the opportunity for me to pursue this path. Great thanks to my son Marin and daughter Mariana for supporting me in a difficult time.

And finally I would like to dedicate this thesis to my late husband Zlatko who encouraged and supported my passion and gave me the strength and belief to finish.

Table of Contents

List of Illustrations

List of Tables

Chapter 1

Introduction

The liquid surface in a partially full container can move back and forth (in standing or traveling waves) at discrete natural frequencies. This low frequency oscillation of the liquid is defined as sloshing. In Figure 1.1, L indicates the width of the container (also the wavelength), and H the height of the static liquid level. The shaded area indicates the expected shape of the free surface at its fundamental mode. Sloshing at the fundamental frequency mobilizes the largest amount of liquid, and may produce excessive structural loads that can lead to structural failure. Welt et al. (1992) showed that sloshing resulting from external forces is critical when the excitation frequency is close to the fundamental sloshing frequency.

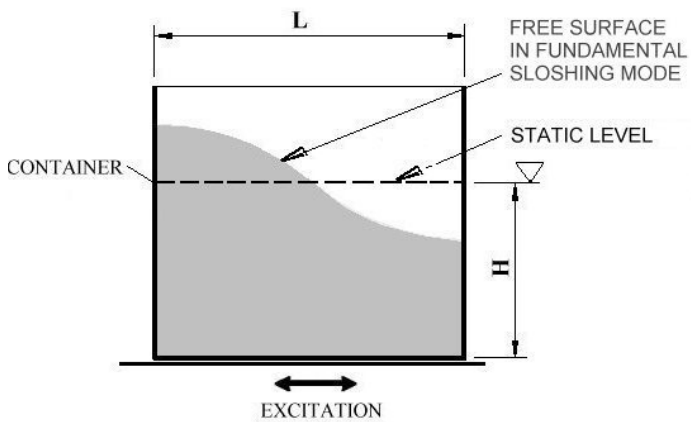

Figure 1.1: Liquid sloshing in a rigid container

It is critical to predict and to control sloshing in order to maintain safe operation in many engineering applications, such as in ground and marine transport of liquid cargo, aerospace vehicles and earthquake–safe structures. Most commonly, the harmful effect of sloshing is experienced in transportation and storage of liquid cargo, Popov et al. (1992). In marine engineering, sloshing plays a significant role in defining maneuverability and safety of vessels, Fotia et al. (2000).

The inherent flexibility of a liquid container is usually treated as a problem since achieving a perfectly rigid container is a practical impossibility. Container flexibility, on the other hand, may be treated as a design parameter to gain benefit, rather than a nuisance to overcome. The novelty of the presented thesis is to investigate the required flexibility parameters of a container to achieve either the suppression of its content or to utilize intentionally induced sloshing as a vibration control agent for light and flexible structures. To the best of the author's knowledge, this is the first attempt to make use of flexibility as a design parameter in the control of liquid sloshing. Most of the reported efforts in this thesis are of numerical nature. Limited simple experiments are presented to validate some of the numerical predictions.

The research in this thesis is divided into three areas. Firstly, the observations from extensive numerical predictions of liquid sloshing in a container with flexible walls are presented. Efforts are summarized to determine the tuning condition of the container flexibility to the dynamics of sloshing liquid for effective sloshing control. Second area of the focus deals with improving the design of the flexible container to facilitate effective sloshing control. Thirdly, liquid sloshing has been utilized for the purposes of controlling structural vibrations. Hence, as mentioned earlier, the general objective in this research is to explore the possibilities of using the flexibility of the container as a design parameter. To clarify the specific objectives, a brief description of the content of each chapter is given next. Each of these chapters is presented as a self-contained entity, with its own relevant literature and conclusions.

Chapter 2 explores the possibility of using a container with flexible walls to control the sloshing of its liquid content. The flexibility of a container may be employed to suppress excessive sloshing only when there is a strong interaction between the container and the liquid. This strong interaction is ideally achieved when the fundamental structural frequency of the container, in the direction of sloshing, is tuned to the fundamental sloshing frequency. However, this ideal condition may not be possible and multiple vibration modes may be involved in the process, due to the structural complexity of the container and strong fluid-structure interactions.

The flexible container used in this study has its critical frequencies higher than the sloshing frequencies involved. Hence, tuning requires lowering the container frequencies. The method chosen to lower these frequencies is to add mass to the container. Control in the order of 80% has been demonstrated to be possible as compared to the sloshing levels observed with a rigid container. The following list includes the published work relevant to this chapter:

***Gradinscak, M. Semercigil, S. E. and Turan**, **Ö. F.,** 2001, Sloshing Control with Container Flexibility, 14th Australasian Fluid Mechanics Conference, Adelaide University, Adelaide, Australia.*

***Gradinscak, M., Semercigil, S. E. and Turan**, **Ö. F.,** 2002, Design of Flexible Containers for Sloshing Control, Proceedings of ASME FEDSM'02, ASME 2002 Fluids Engineering Division Summer Meeting, Montreal, Quebec, Canada.*

***Güzel, U. B, Gradinscak, M., Semercigil, S. E. and Turan**, **Ö. F.,** 2004, Control of Liquid Sloshing in Flexible Containers: Part 1. Added Mass, 15th Australasian Fluid Mechanics Conference, University of Sydney, Sydney, Australia.*

***Güzel, U. B., Gradinscak, M., Semercigil, S. E. and Turan**, **Ö. F.,** 2005, Tuning Flexible Containers for Sloshing Control, Proceedings of the IMAC-XXIII: A Conference and Exposition on Structural Dynamics, January 31-February 3, Orlando, Florida.*

***Gradinscak, M., Semercigil, S. E. and Turan**, **Ö. F.,** 2006, Liquid Sloshing in Flexible Containers, Part 1: Tuning Container Flexibility for Sloshing Control, Fifth International conference on CFD in the Process Industries, CSIRO, Melbourne, Australia, 13-15 December.*

Chapter 3 deals with improvement of the container design by adding auxiliary structural elements to it. The motivation for this chapter comes from the observations made in Chapter 2 when rather large structural deflections are required to achieve the reported levels of sloshing control. These large deflections may be difficult to accommodate in some practical applications. Hence, it is desirable to limit them while maintaining the effectiveness of control.

Large deflections are observed at the open top of the container, away from the centre of the container. Hence, rigid links (or straps) which are attached at the opposite sides of the open top, may limit these outward deflections. Observations are reported in Chapter 3, to limit the container deflections to practical levels, with almost identical levels of sloshing control to that reported in Chapter 3. Findings of this chapter are reported in:

***Gradinscak, M., Güzel, U. B, Semercigil, S. E. and Turan**, **Ö. F.,** 2004, Control of Liquid Sloshing in Flexible Containers: Part 2. Added Straps, 15th Australasian Fluid Mechanics Conference, University of Sydney, Sydney, Australia.*

Tuned liquid dampers may be employed for structural vibration control, similar to that of a classical tuned vibration absorber. For such cases, the fundamental sloshing frequency is tuned at a critical frequency of the structure to be controlled. The pressure forces, as a result of the intentionally induced liquid sloshing, are used as control forces. Such an absorber has the benefits of being effective and practically free of maintenance. The work presented in Chapter 4 demonstrates the effects of container flexibility on structural vibration control. The supression of structural response can improve by up to 80% as compared to that can be obtained with a tuned sloshing absorber with a rigid container. Work related to this chapter has been presented in:

***Gradinscak, M. Semercigil, S. E. and Turan**, **Ö. F.,** 2006, Liquid Sloshing in Flexible Containers, Part2: Using a Sloshing Absorber With a Flexible Container for Structural Control, Fifth International conference on CFD in the Process Industries, CSIRO, Melbourne, Australia, 13-15 December.*

Chapter 5 of this thesis summarises the efforts presented in the earlier content chapters, and presents recommendations to further the findings. Since the working principles of the classical tuned vibration absorber is the starting point of most the presented material of this thesis, Appendix A is allocated for a summary of tuned vibration absorbers, for completeness. Appendix B presents results obtained in forty second time frames of the simulation for suppression of sloshing in a flexible container. Appendix C presents results obtained for 5% and 10% structural damping of the container and its effect on displacement of the controlled structure. Appendix D presents the effect of different mass ratios on the structure's displacement when liquid dampers are applied.

Chapter 2

CONTROL OF LIQUID SLOSHING USING A FLEXIBLE CONTAINER

2.1 Introduction

This chapter presents the outcomes of investigations conducted into the possibility of using a container with flexible walls to achieve an effective control of liquid sloshing. It is the primary contribution of this thesis to the state of knowledge. The chapter is organized as follows:

- Section 2.2 presents the literature review of the relevant previous work concerning liquid sloshing.
- Section 2.3 gives detailed explanations of the finite element model developed to simulate liquid–flexible structure interaction.
- Section 2.4 deals with the further details of the numerical process.
- Section 2.5 discusses numerical observations.
- Section 2.6 outlines relevant experimental observations.
- Section 2.7 reiterates the primary findings on employing container flexibility in suppressing liquid sloshing and their significance.

2.2 Background

Sloshing generally refers to the low-frequency oscillations of the free surface of a liquid in a partially filled container. When liquid mass represents a large percentage of the total mass of a structure, sloshing could induce disturbance to its stability. This is mainly contributed to by the induced dynamic loads and shift of the centre of gravity.

The study of sloshing is critical both industrially and environmentally, thus attracting research and academic literature which explores sloshing and attempts to control its impact. Study of sloshing generally proves challenging due to the presence of strong flow interactions with its container. These interactions become even more challenging if the container is flexible. The primary cause of these greater complexities is the moving boundaries of the fluid as the flexible container deforms under the effect of dynamic sloshing loads. As a result, the dynamic responses of a flexible container may be significantly different than that with rigid walls.

2.2.1 Literature Review

Early research on sloshing in flexible containers can be found in Kana and Abramson (1966) which reports experiments to determine the response of a cylindrical elastic tank. Experiments revealed nonlinearity in the deformation of the shell wall when the elastic shell contained liquid with a free surface. High frequency, small amplitude vibration excitation of the elastic structure, in a circumferential mode, led to a low frequency, large amplitude free surface motion of the liquid, in a rotationally symmetric mode. The complexity of this phenomenon was acknowledged in their research and simplifications were used in this reference, to obtain analytical solutions for restricted ranges of input conditions.

Haroun and Housner (1981) and Veletos (1984) developed a mechanical model for flexible tanks. The liquid-tank system was converted into an equivalent spring-mass system which brought hydrodynamic simplification. Jain and Medhekar (1993a, 1993b) draw attention to this mechanical model and suggest separate models for rigid and flexible tanks. They recommend that the Haroun and Housner (1981) model be used for a flexible tank, and Veletsos (1984) model to be used for a rigid tank. Malhotra et al. (2000) continued to investigate the possibilities of simplification of the previously developed flexible tank model, but their results are not significantly different from the rigid container model. These mechanical models convert the container-liquid system into an equivalent spring-mass system and considerably simplify the analyses.

Chen and Haroun (1994) and Jeong and Kim (1998) report investigations on container flexibility with a primary interest to determine natural frequencies and mode shapes of containers with liquid. Chen and Haroun (1994) report a numerical model for a two-dimensional system consisting of a liquid and a flexible tank. The liquid was considered to be inviscid, incompressible and irrotational. The model required the addition of artificial energy dissipation to stabilize the numerical simulation. Jeong and Kim (1998) present an analytical method for determining the natural frequency of shells filled with liquid. In this research, liquid movement was restricted by rigid plates placed at the top and bottom of the shell. Analytical solutions were validated with finite element analyses using a commercial code. No constraints were applied to the free surface nodes of the fluid elements for the sloshing fluid model.

Tang (1994) reports results of an investigation on the dynamic response of a tank containing two different liquids under seismic excitation. Both analytical and numerical approaches are considered. Research is based on assumptions that, in its fixed-base condition, the tank-liquid system responds in its fundamental mode of vibration as a single-degree-of-freedom system and that the convective component of the response is not affected by the soil-structure-interaction.

Yao et al. (1994) develop a numerical model to simulate three-dimensional waves in narrow tanks. Energy dissipation was added to match predicted wave amplitudes to experimental data. Takahara et al. (1995) simulated sloshing of fluid in cylindrical tanks subjected to pitching excitation at a frequency in the neighborhood of the lowest resonant frequency. The nonlinearity of the liquid surface oscillation and the nonlinear coupling between the dominant modes and other modes are considered in the response analysis of the sloshing motion. The equations governing the amplitude of liquid surface motions are derived and the stability analysis of each motion is conducted. Equivalent damping terms were added to their formulation to account for the energy dissipation.

Movement of vessels containing liquid is a common operation in the packaging industry. Yano et al. (2002) reported research on a container gradually accelerating on an inclined path, paying special attention to the suppression of the sloshing. Garrido (2003) investigates modeling efforts of sloshing in a rectangular container which is first accelerated, and then decelerated due to frictional forces. Results obtained from a pendulum model and experiments are reported as satisfactory whilst acknowledging the limitations of the simplicity of the model. Grundelius and Bernhardsson (2000) investigate industrially relevant problems of movement of a carton container, from one position to another in the packaging machine. An open container with liquid has to be moved without excessive sloshing. It is acknowledged that the severity of sloshing depends on how the package is accelerated and on the properties of the liquid. It proposes an iterative learning control approach and attempts to find an open loop acceleration reference using the obtained results in the next iteration with repeating the same procedure until the desired outcome have been accomplished.

For flexible structures, only recently researchers begin to use the fully nonlinear theory to explain more accurately the phenomenon of flow physics associated with liquid sloshing. Pal et al. (2003) study non-linear free surface oscillation of a liquid inside elastic containers using the finite element technique. The finite element method based on two-dimensional fluid and structural elements is used for the numerical simulation. A numerical scheme is developed on the basis of a mixed Eulerian–Lagrangian approach, with velocity potential as the unknown nodal variable in the fluid domain and displacements as unknowns in the structural domain. Numerical results obtained by this investigation for rigid containers are first compared with existing solutions to validate the code for non-linear sloshing without fluid–structure coupling. Bauer et al. (2004) employ an elastic membrane in a rigid container, resulting in considerable reduction of liquid sloshing. Although theoretical and numerical observations compare favorably, cases are restricted to a membrane in axisymetric motion. Wang et al. (2004) use a finite element method to study sloshing in a two dimensional rectangular container subjected to random excitation. The method is based on fully nonlinear wave potentional theory based on the finite element method. Mitra and Sinhamahapatra (2005) present a new pressure-based Galerkin finite element that could handle flexible walls, but the cases are restricted to linear problems with small amplitude waves.

Anderson (2000) mentions for the first time, the possibility of using container flexibility for the control of liquid sloshing. Numerical predictions show that the sloshing wave amplitude can be significantly reduced by tuning the interaction of the flexible container with liquid sloshing. Experiments were carried out to verify the numerical model. Gradinscak et al. (2001, 2002 and 2006) and Guzel et al. (2004, 2005) report the design potential of flexible containers for significant reduction of sloshing. The flexibility of a container may be employed to suppress excessive sloshing only when there is a strong interaction between the container and the liquid. This strong interaction is achieved when the fundamental structural frequency, in the direction of the sloshing, is tuned to the fundamental sloshing frequency of liquid. Throughout this thesis the research is discussed in further detail.

2.2.2 Summary of literature review

In summary, the published work of the previous research has certainly provided direction for further research throughout this thesis. The author gratefully acknowledges these contributions. However, a good portion of the current research has been restricted to the approximation, and unavoidable simplification, of the liquid sloshing problem. On the other hand, the complexity of sloshing, such as non-linearity and 'liquid-structure interaction' problem has to be fully addressed in order to produce realistic and practical solutions for control. Reporting of container flexibility as a design tool to control sloshing has not been found in the literature. It is the intention of this thesis to explore such possibility and demonstrate its promise.

In this thesis, the dynamic interaction of a flexible container and liquid sloshing is utilized for the purpose of controlling liquid sloshing. The primary concern is the reduction of liquid sloshing using container flexibility. This concept is a novel one. This work is important in applications involving the storage and transportation of liquid goods where sloshing can either damage the liquid product or compromise the structural integrity of the container. In practice, the advantages of using a flexible container are two fold. First, if sloshing of liquid is suppressed effectively, then the safety of the intended operation is enhanced. Secondly, a flexible container is lighter than its rigid counterpart which should result in cost reductions and material savings.

2.3 Numerical Model and Procedure

2.3.1 Description of the model and test conditions

ANSYS (2002) finite element analyses package was used to model the flexible container and the sloshing liquid. The flexible container used for the numerical model was of aluminium, an open top rectangular prism of 1.6 m in length, 0.4 m in width and 0.4 m in height. The wall thickness was 1 mm. The container was filled with water to a depth of 0.3 m. The total weight of the container was 6 kg. The Young's modulus, Poisson ratio and mass density of aluminum are taken to be of 70e9 N/m^2, 0.3 and 2700 kg/m^3, respectively. Structural damping applied for the full finite element model was taken to be

1% of the critical damping in the fundamental mode of the container without liquid. The container was modeled with two-dimensional rectangular shell elements. Three dimensional brick elements were used to model the liquid. Fluid-structure interaction was achieved by coupling the liquid displacement with that of the container walls with relative velocity vector in the direction of the normal equal to zero. Hence, the liquid was constrained by the walls.

The objective of the simulation was to obtain the displacement histories at several locations of both the container and liquid. Sloshing was induced by imposing a transient 5 mm – sinusoidal displacement of one cycle to the base of the container in y-direction, as shown in Figure 2.3.1. The frequency of this disturbance was chosen to be 1.34 Hz, which is the fundamental sloshing frequency of a rigid container of the same dimensions, Milne-Thomson (1968). In Equation (1) below, a closed form expression is given of the fundamental sloshing frequency, where h and d are the liquid height and container width, respectively.

$$f = \frac{1}{2\pi}\sqrt{\frac{g\pi}{d}\tanh\left(\frac{\pi h}{d}\right)} \qquad (1)$$

The concept of using a flexible container to control sloshing of a liquid is similar to that of using a tuned absorber to control excessive vibrations of a mechanical oscillator. For completeness, a brief description of the tuned vibration absorber is given in Appendix A. For a tuned absorber, the natural frequency of the absorber is tuned to that of the structure to be controlled, to maintain minimum oscillation amplitudes, whilst this same absorber is also put in resonance intentionally. Here, the sloshing liquid is taken to be analogous to the structure to be controlled, whereas the flexible container is expected to act like the tuned absorber.

Tuning the container dynamics to that of the sloshing liquid is attempted by adding point masses on the flexible container. Two masses are added directly above the "observed container node" indicated in Figure 2.3.1, on the free edge of the flexible walls.

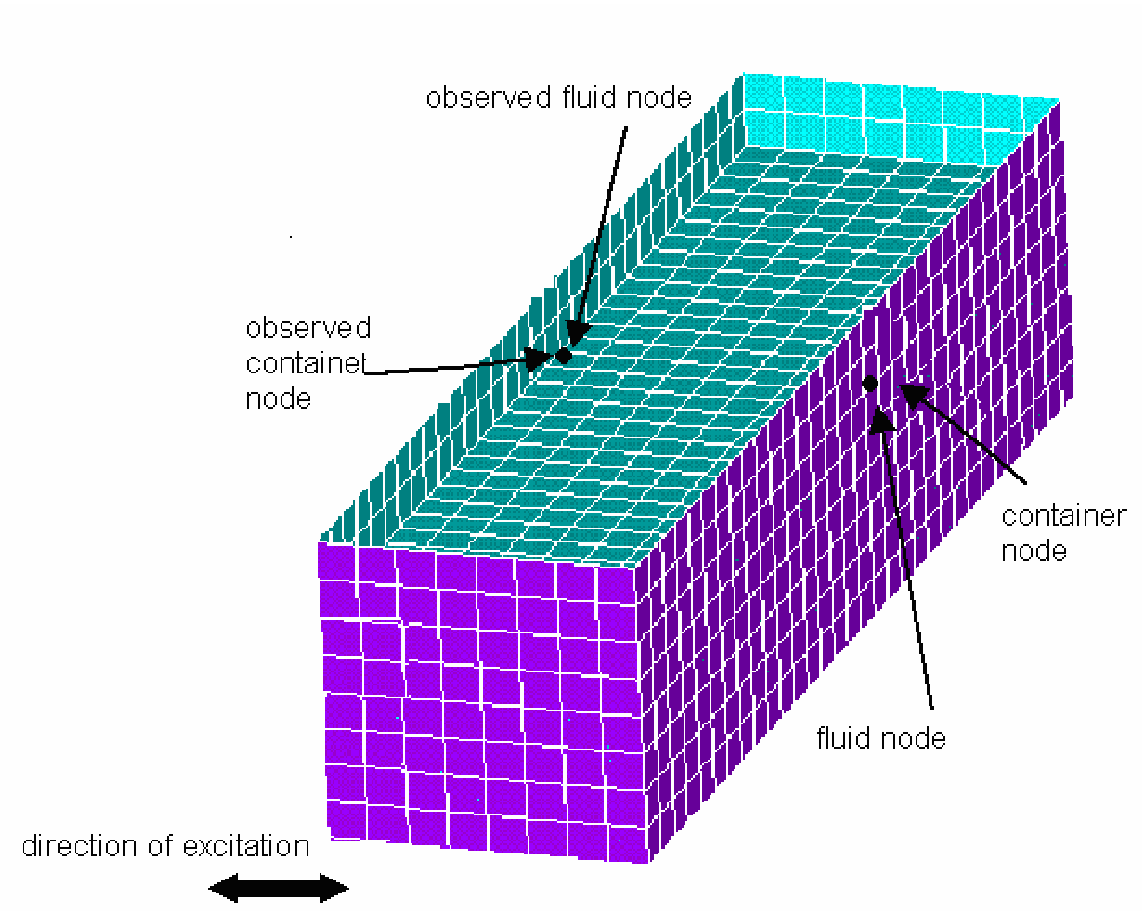

Figure 2.3.1: The numerical model and the location of the observed nodes.

The finite element model of the container was created using two-dimensional rectangular shell elements, SHELL63 (ANSYS 2002) with the characteristics as shown in Figure 2.3.2 below. This element is defined by four nodes with constant thickness and with six degrees of freedom at each node. The element thickness was varied in numerical simulations for elastic and rigid definitions of the container. As outlined earlier, 0.001 m (1 mm) wall thickness is assigned to the flexible container. This thickness was increased to 0.005 m (5 mm) in order to predict the response of a rigid container having the same dimensions as those of the flexible container.

Numerous trials were undertaken with the intention to verify grid cell size and its explanation proceeds in this chapter. As an outcome from those trials, the grid cell size of 50mmx50mm was selected as sufficient for numerical accuracy for both container and liquid models. The full finite element model of the container was discretised into 896 elements.

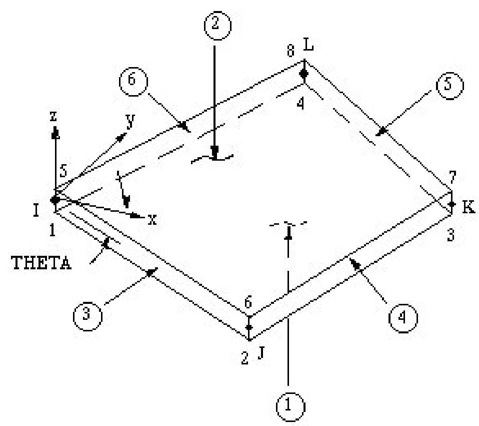

Figure 2.3.2: Two-dimensional rectangular shell finite element.

FLUID80 (ANSYS 2002), three-dimensional brick finite elements were used to model the liquid. The total weight of the liquid content is 192kg. The brick finite element is shown in Figure 2.3.3, which is defined by eight nodes having three degrees of freedom at each node. The parameters for the finite element model were defined for a homogeneous, inviscid, irrotational and incompressible liquid.

The complex physical behavior of the free surface liquid utilizes formulations of nonlinear wave theory and is defined by the gravity springs attached to each node of the liquid. The full liquid finite element model was discretised into 1536 elements.

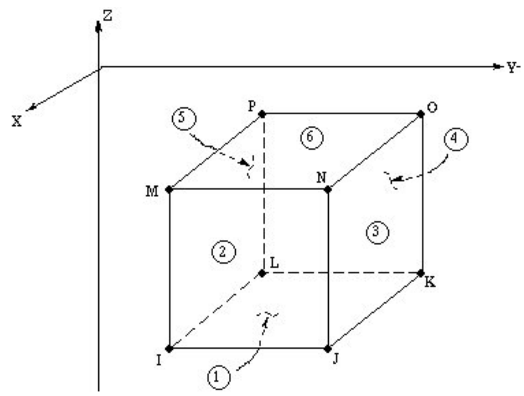

Figure 2.3.3: Three-dimensional brick finite element.

To control sloshing, the objective is to tune the container's fundamental natural frequency to the fundamental sloshing frequency. The tuning has been attempted by adding mass elements at the top edge and in the middle of the 1.6 m long sides of the container. The structural mass element, MASS21 (ANSYS 2002), is defined as a single node as shown in Figure 2.3.4.

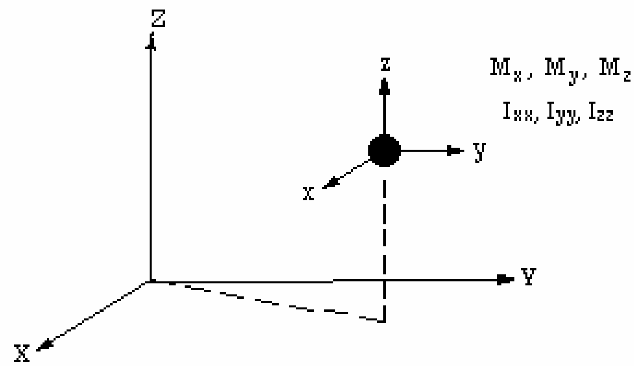

Figure 2.3.4: Structural mass element

Liquid boundary conditions are shown in Figure 2.3.5. These boundary conditions have been defined using separate coincident nodes for each liquid element. These nodes were then coupled with the structural elements in the direction normal to the interface.

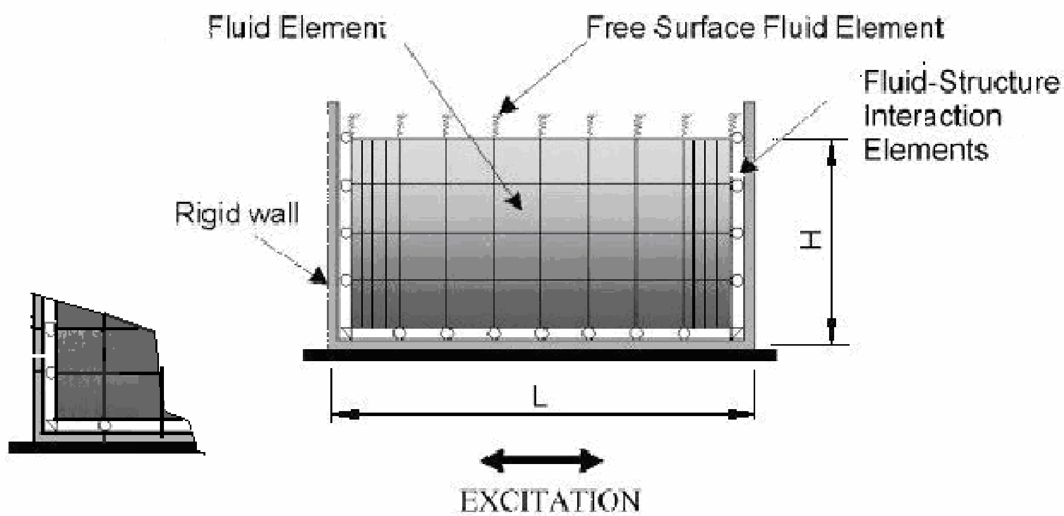

Figure 2.3.5: Liquid-Structure interaction model.

2.4 Computational Simulations

The dynamic response and natural frequencies of both the liquid and the container are influenced by strong interactions between them. The strong interaction between liquid and container is achieved when the fundamental frequency of the liquid (in the direction of sloshing) is tuned to the fundamental frequency of the container.

The response of the container's structure depends primarily on its natural frequencies, damping characteristics, and the frequency content of the time-varying loads. Eigenvalue modal analysis has been used first to determine the container's natural frequencies and mode shapes. Three mode shapes of oscillation of the container are obtained and given in Figure 2.4.1. Natural frequencies for different added masses are determined and are given in Table 2.4.1.

The first mode shape of oscillation, in Figure 2.4.1 (a), shows that oscillations along the longest walls of the container are out of phase. The second mode shape of oscillation in Figure 2.4.1 (b), shows that the oscillations along the longest walls are in phase, whilst the third and higher modes showed much clearer separation of frequencies, Figure 2.4.1 (c). The first and second modes are plate modes with the first one an out-of-phase mode, and the second one is an in-phase mode Third mode is at the added mass location.

a)

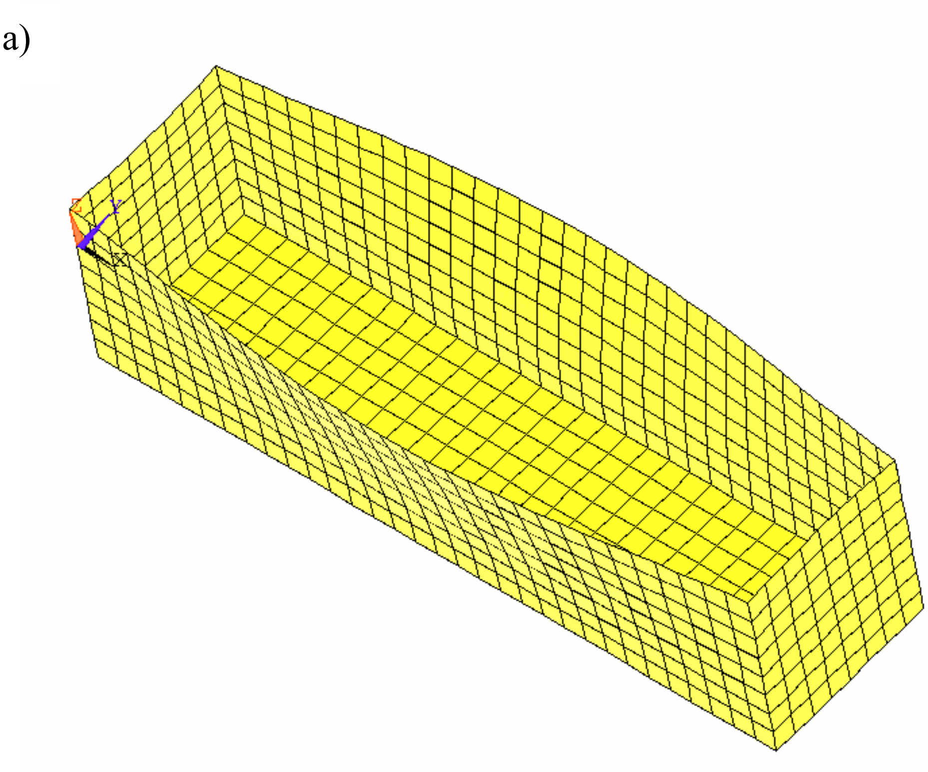

b)

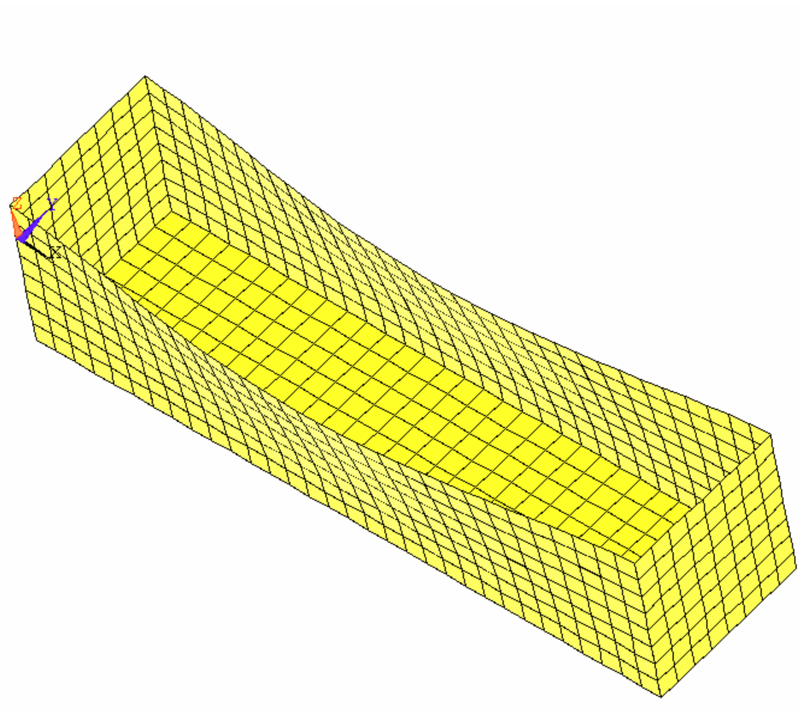

c)

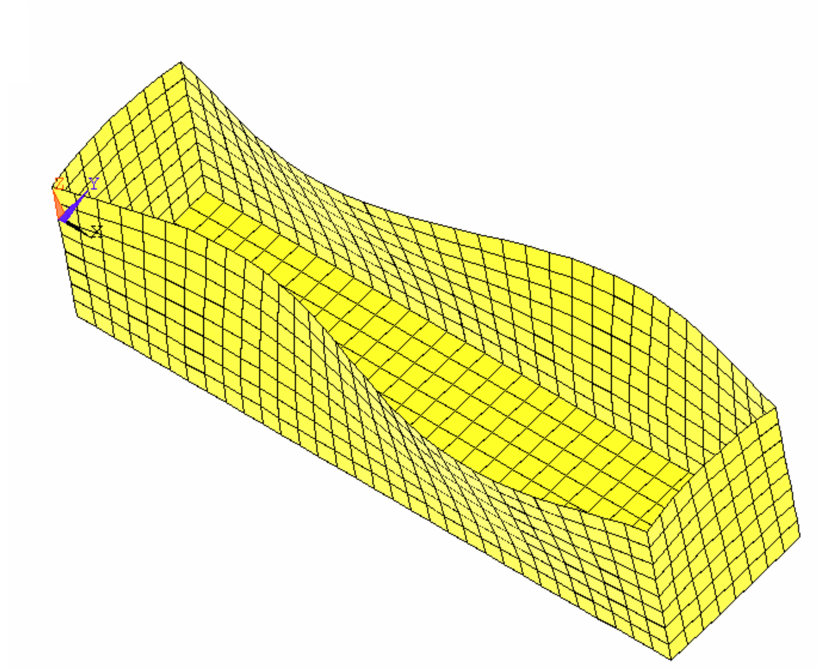

Figure 2.4.1.: Mode shapes of oscillation for the container with 0 kg point mass and no liquid.

From Table 2.4.1, the frequency for the simulation without mass is significantly higher than the theoretical fundamental sloshing frequency of liquid, which is calculated at 1.34 Hz. By adding masses those natural frequencies of the container become closer to sloshing frequency. However, it should be remembered that the frequencies changed when container contained liquid. Hence, the information in Figure 2.4.1 and Table 2.4.1 are for identification purposes only.

Table 2.4.1 First, second and third natural frequencies of the container without liquid for different masses. Selective cases were experimentally verified at the fundamental mode.

Mass [kg]	1^{st} natural frequency [Hz]	2^{nd} natural frequency [Hz]	3^{rd} natural frequency [Hz]
0	6.38	6.47	9.25
3	1.41	1.42	9.25
5	1.1	1.1	9.25
7	0.94	0.94	9.25
9	0.83	0.83	9.25
11	0.75	0.75	9.25
13	0.69	0.69	9.25

2.4.1 Selection of Mesh Size

As mentioned earlier in this chapter, the container walls have been represented with standard shell elements in the FEA model. 3-D fluid elements have been used for the liquid in the container. The container is meshed with square elements of 0.05 m x 0.05 m size and the liquid is meshed with cubic elements of 0.05 m x 0.05 m x 0.05 m size. The solution is independent of the mesh size at this resolution. Grid independence has been verified by testing 0.025 m square and cubic elements for the same selected cases of forty second runs. These results are presented in Figures 2.4.1.1 to 2.4.1.3.

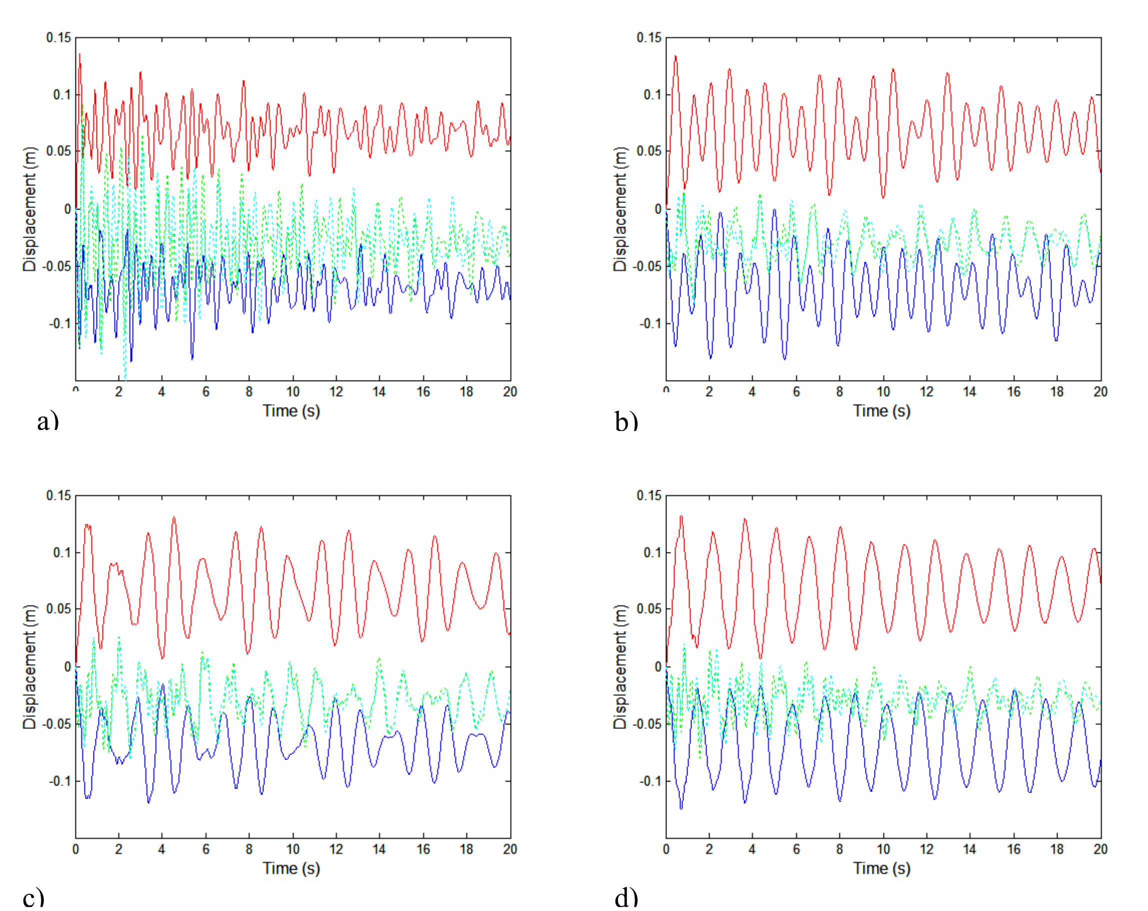

Figure 2.4.1.1: Predicted displacement histories of chosen fluid and structure nodes in a flexible container with various added masses, for the 25 mm mesh size and 10 ms time steps runs. Point mass amounts: (a) 0 kg, (b) 5 kg, (c) 9 kg, (d) 13 kg.

Figure 2.4.1.1 gives the displacement histories of the container and fluid nodes for 0.025 m mesh size tests. Figure 2.4.1.4 gives the displacement histories of the container and fluid nodes for 0.05 m mesh size tests. Top and bottom solid lines in red and blue indicate the container nodes. Dashed lines in the middle in green indicate the fluid node displacement histories. Very similar displacement patterns are seen in Figure 2.4.1.1 with 0.025 m mesh, in comparison to Figure 2.4.1.4 with 0.05 m mesh, for 0 kg, 5 kg, 9 kg, 13 kg added point masses cases, respectively, indicating negligible difference between 0.025 m and 0.05 m mesh sizes.

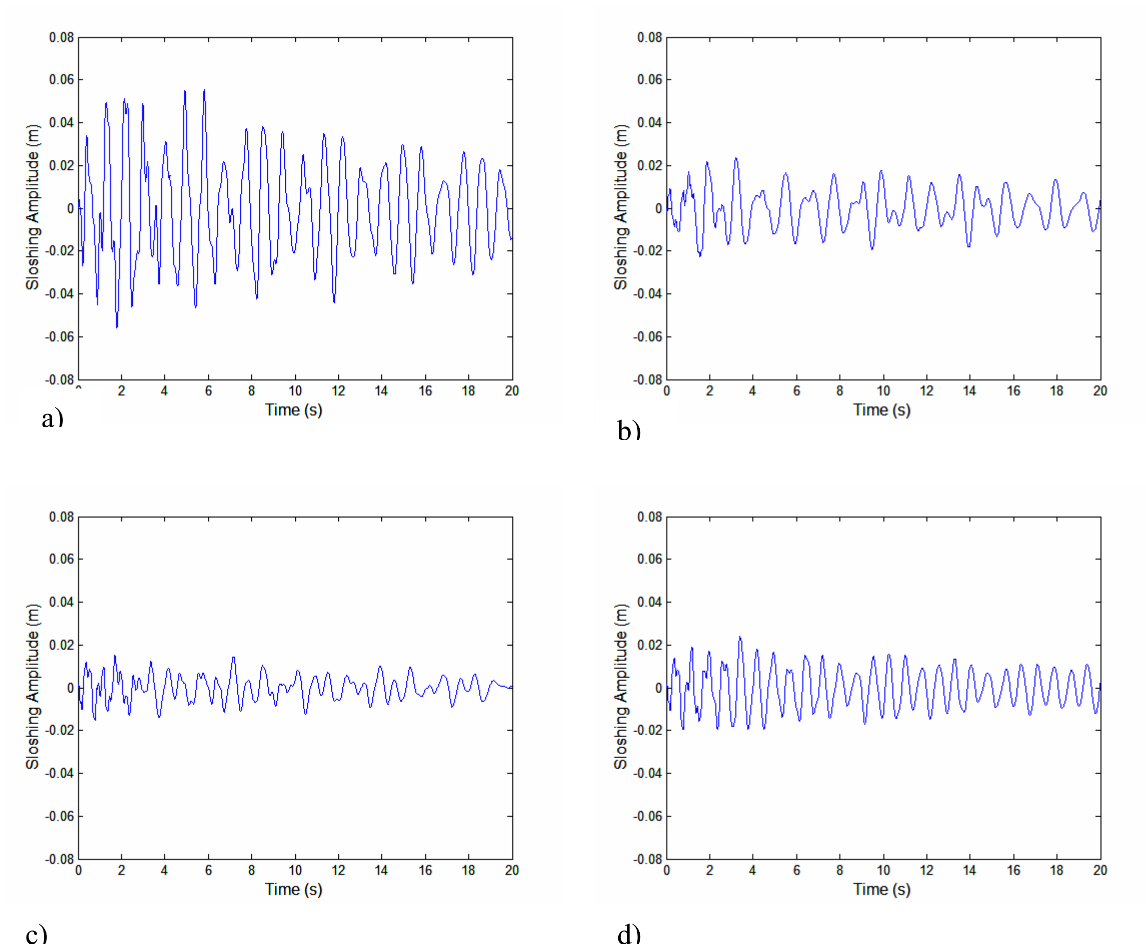

Figure 2.4.1.2: Predicted sloshing amplitude of chosen fluid nodes in a flexible container with various added masses, for the 25 mm mesh size and 10 ms time steps runs. Point mass amounts: (a) 0 kg, (b) 5 kg, (c) 9 kg, (d) 13 kg.

Sloshing amplitudes for the selected cases with 0.025 m mesh size are shown in Figure 2.4.1.2. Figure 2.4.1.5 gives the sloshing amplitude for 0.05 m mesh size tests. The high sloshing amplitude around 0.05 m for the case with 0 kg point mass is gradually decreasing until the 9 kg point mass case in Figure 2.4.1.2 (c) to a level just below 0.02 m. The tuning effect is assumed to be lost beyond this point as seen in Figure 2.4.1.2 (d), where sloshing amplitude is increasing back to above 0.02 m. Figure 2.4.1.5 give the same sloshing histories obtained with the 0.05 m mesh size. Differences between respective plots for the selected cases are again insignificant.

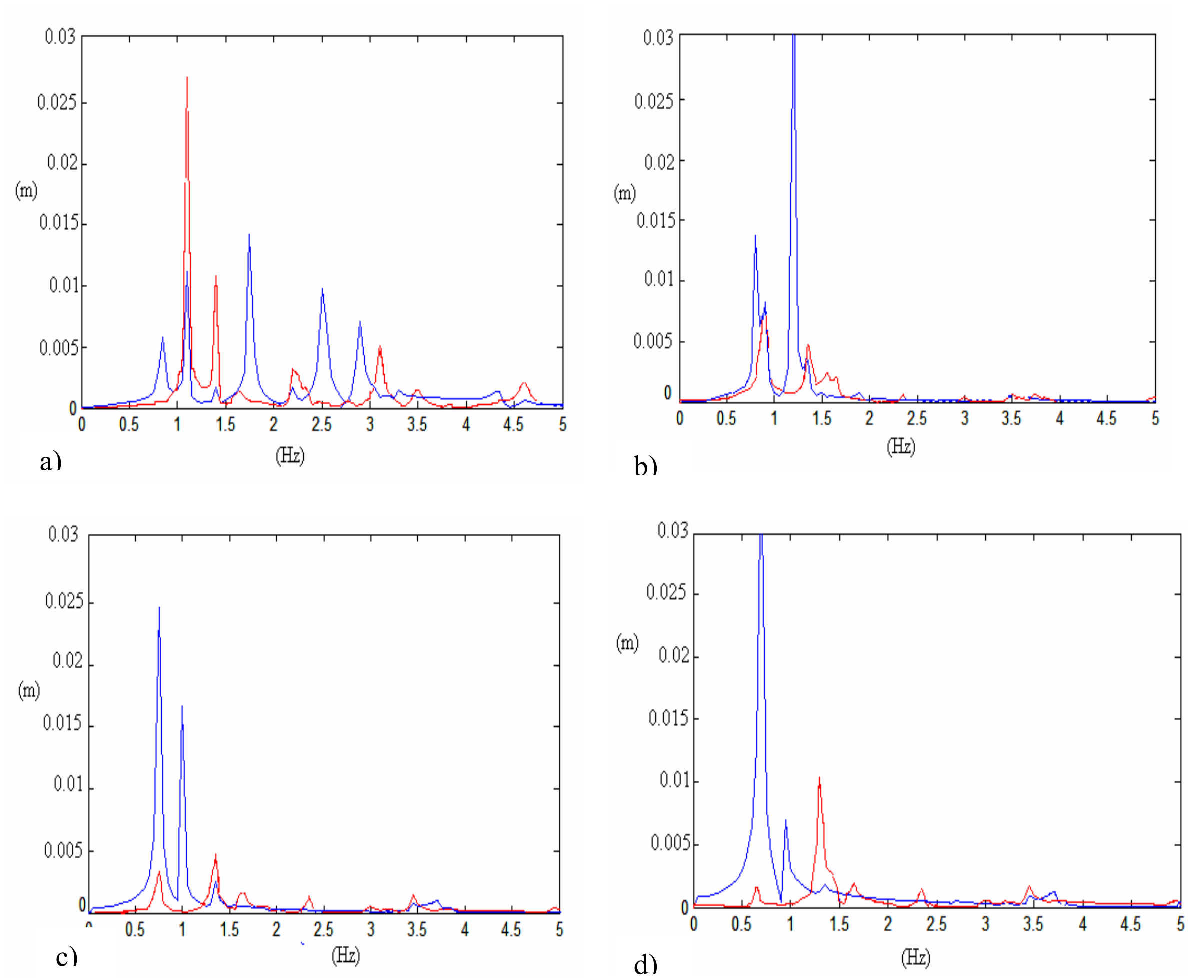

Figure 2.4.1.3: FFT plot of sloshing liquid (red-line) and structural vibration (blue-line) with various added masses, for the 25 mm mesh size and 10 ms time steps runs. Point mass amounts: (a) 0 kg, (b) 5 kg, (c) 9 kg, (d) 13 kg.

The FFT plots of liquid sloshing and structural vibration data for 0.025 m mesh size are given in Figure 2.4.1.3. The FFT plots of liquid sloshing and structural vibration data for 0.05 m mesh size are given in Figure 2.4.1.6. Red line indicates sloshing, and blue line indicates structural spectral distributions. The horizontal axis represents frequency in [Hz] and the vertical axis represents spectral magnitude [m]. All spectral plots presented in this section and for the rest of this thesis are single-sided.

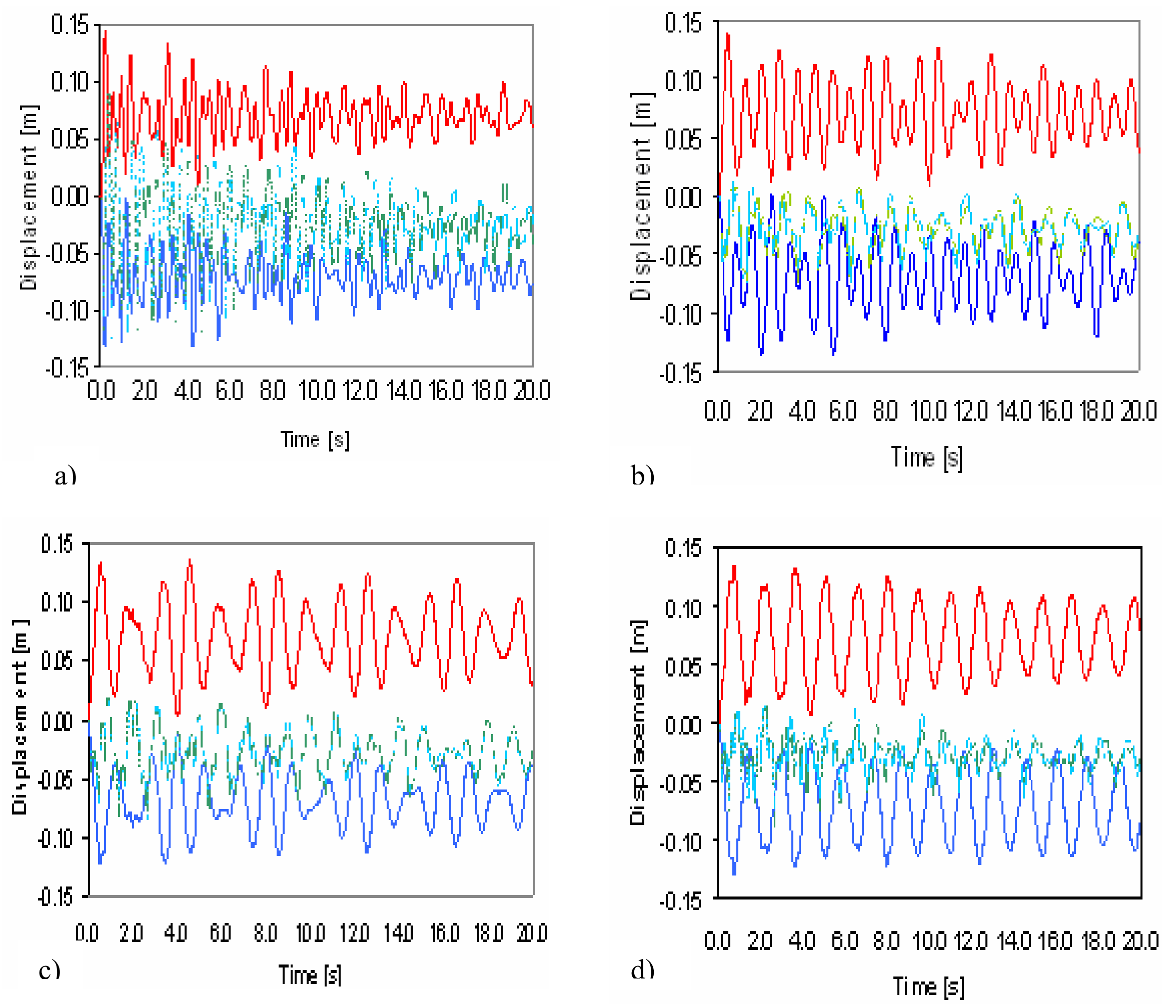

Figure 2.4.1.4 Same as in Figure 2.4.1.1 but for the 50 mm mesh size runs and 10 ms time steps.

The sloshing frequencies are dominant in Figure 2.4.1.3 (a), around 1.2 Hz and 1.4 Hz. The main structural frequencies that are around 0.8 Hz, 1.2 Hz and 1.75 Hz are lesser in magnitude. By looking at the highest peak around 1.2 Hz attributed to sloshing, it is possible to say that the structure is driven by the fluid. The addition of 5 kg and then 9 kg point masses in Figures 2.4.1.3 (b) and (c) seems to transform the system to one that is structurally driven, as opposed to one driven by the sloshing. The structural peak around 1.3 Hz in Figure 2.4.1.3 (b) which then shifts to 1.1 Hz in Figure 2.4.1.3 (c) is clearly suppressing the sloshing peaks in this range.

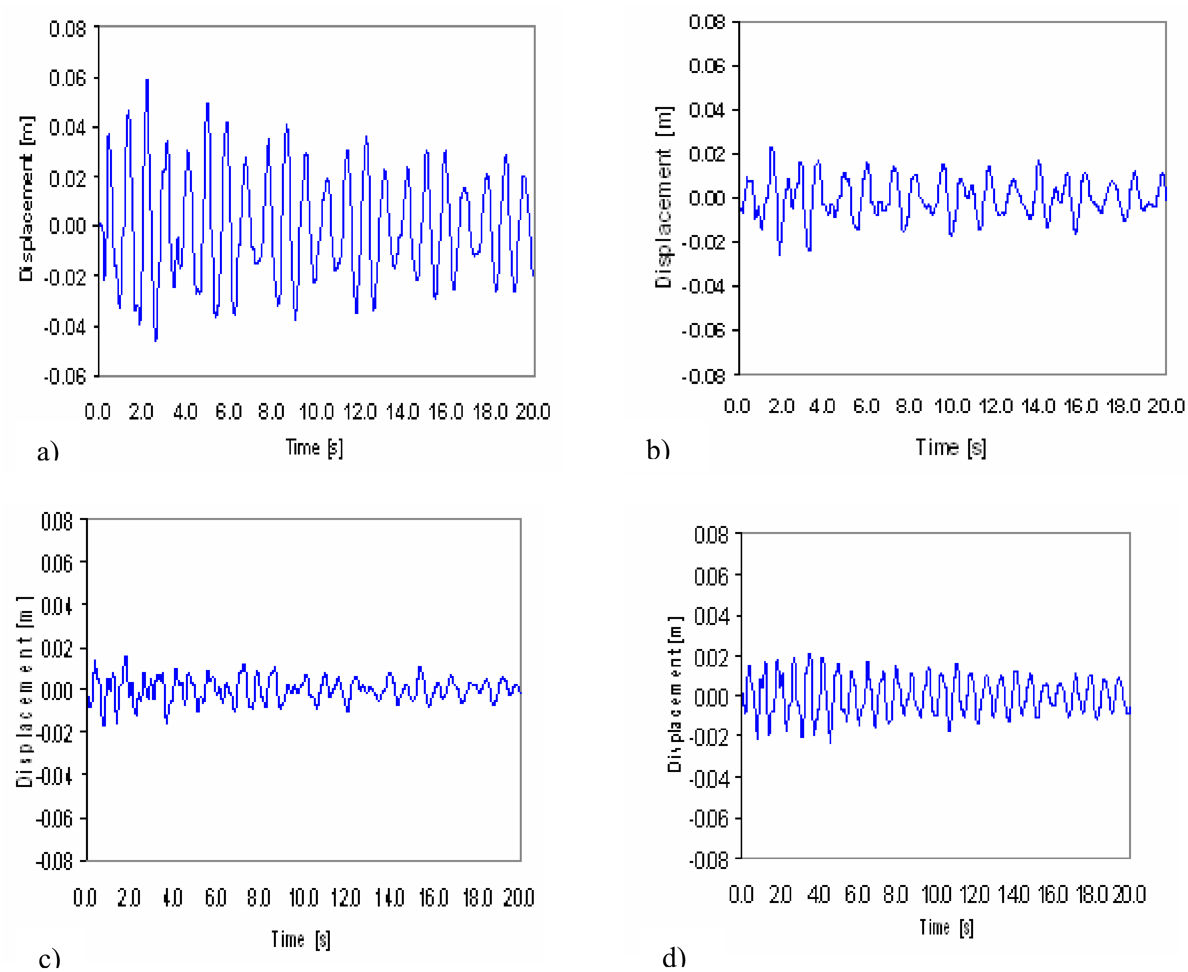

Figure 2.4.1.5 Same as in Figure 2.4.1.2 but for the 50 mm mesh size runs and 10 ms time steps.

The same observation can be made for the other major structural peak around 0.8Hz and 0.75 Hz for 5 kg and 9 kg point mass cases respectively. Again by looking at Figure 2.4.1.3 (d) it is possible to see that the fluid and the structure are not effectively controlling each other any more. Rather they are both acting in their separate ranges, - structure around 0.7 Hz and sloshing around 1.4 Hz.

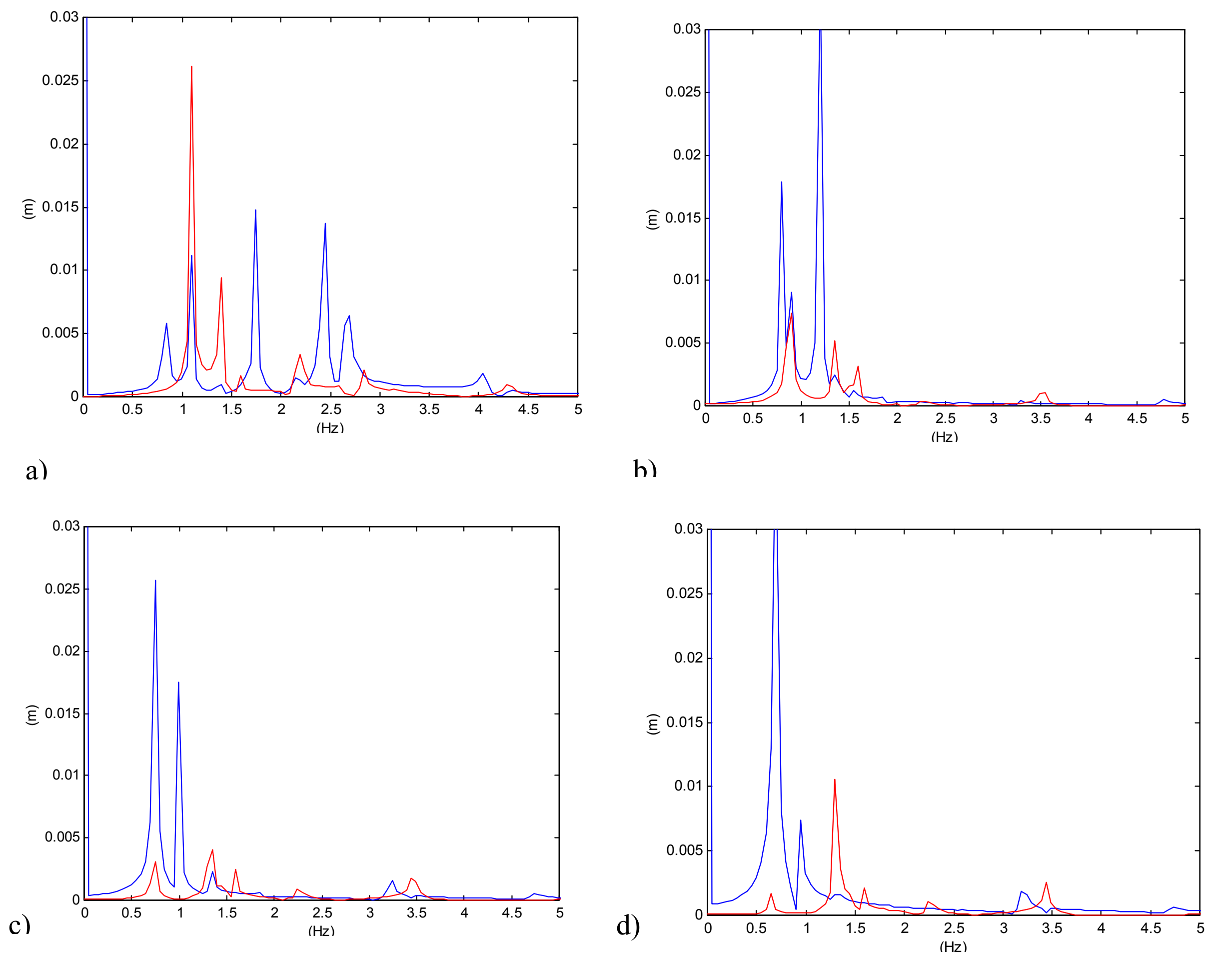

Figure 2.4.1.6 Same as in Figure 2.4.1.3 but for the 50 mm mesh size runs and 10 ms time steps.

The FFT plots of 0.0550 m mesh size are given in Figure 2.4.1.6. It can be observed that it is possible to predict the same behavior with 50 mm mesh size as that for the 25 mm mesh. This leads to the conclusion that obtained results with a finer mesh are very similar to the results of the chosen mesh size.

2.4.2 Time Step Size

A transient analysis has been conducted with 10 milliseconds (ms) time step. These 10 ms time steps were selected as there was minimal difference between 10 ms and 5 ms time steps, to be more cost effective. For verification, 25 mm mesh size run and 10 ms time step for the same selected cases have been presented here in Figures 2.4.1.7, 2.4.1.8 and 2.4.1.9

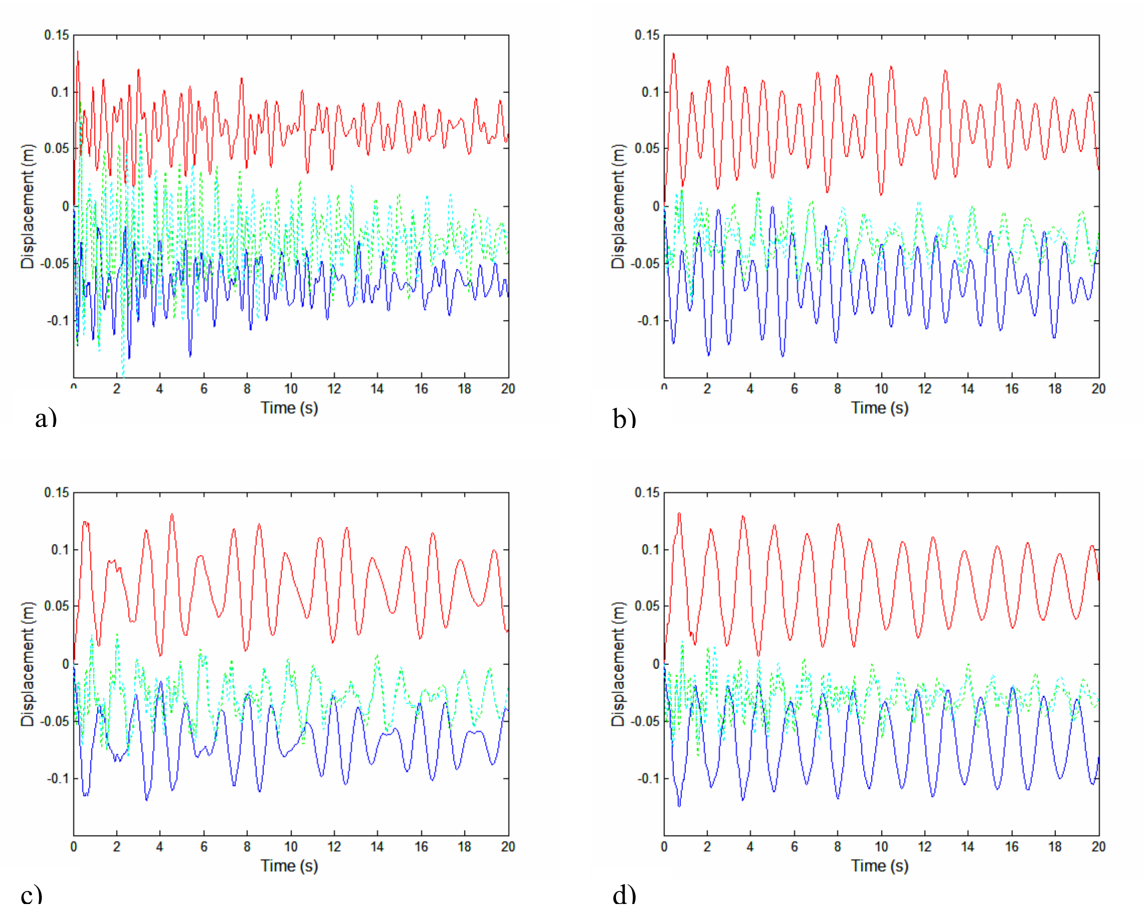

Figure 2.4.1.7: Predicted displacement histories of chosen fluid and structure nodes in a flexible container with various added masses, for the 25 mm mesh size and 10ms time steps runs. Point mass amounts: (a) 0 kg, (b) 5 kg, (c) 9 kg, (d) 13 kg.

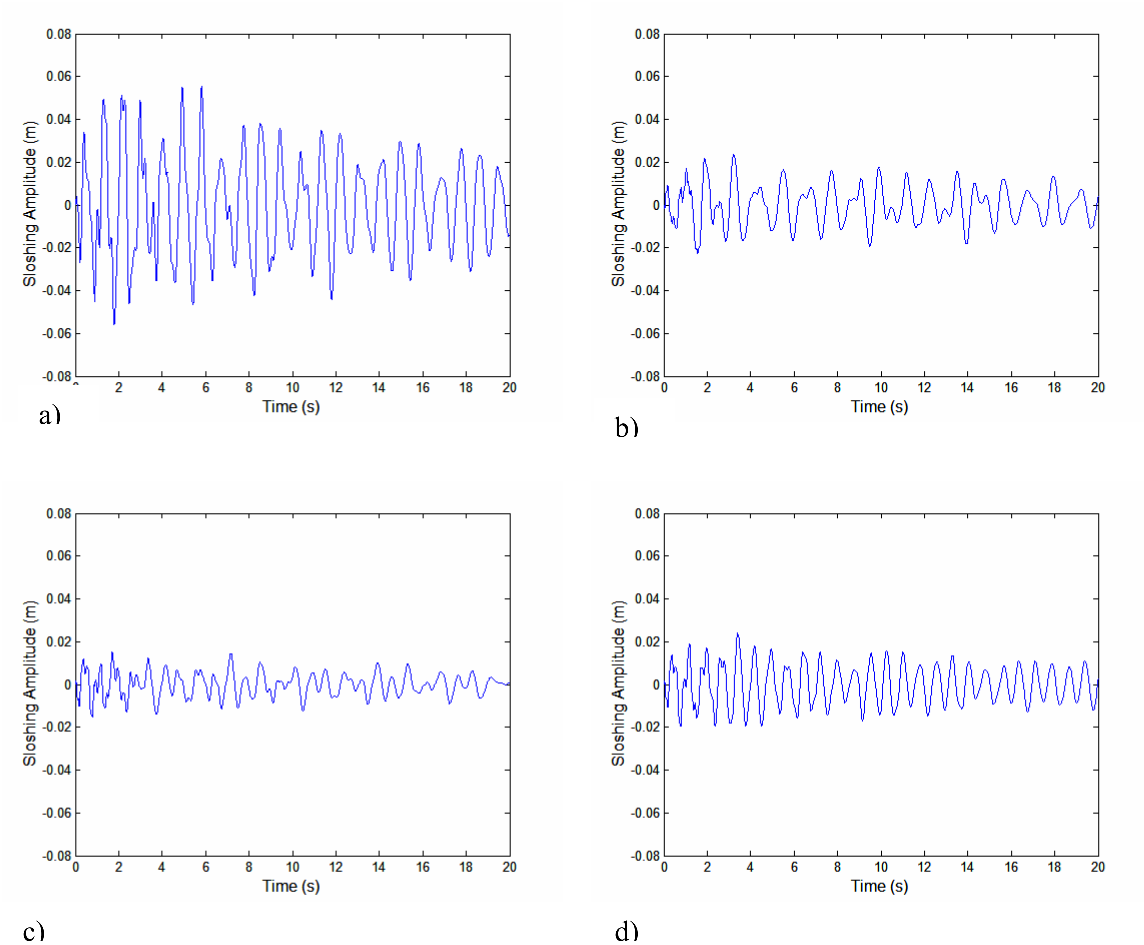

Figure 2.4.1.8: Predicted sloshing amplitude of chosen fluid nodes in a flexible container with various added masses, for the 25 mm mesh size and 10 ms time step runs. Point mass amounts: (a) 0 kg, (b) 5 kg, (c) 9 kg, (d) 13 kg.

Again, Figures 2.4.1.7 give the displacement histories; Figures 2.4.1.8 give the sloshing amplitude and Figures 2.4.1.9 give the FFT plots for structural displacement and sloshing data for the selected cases of 0 kg, 5 kg, 9 kg and 13 kg point mass respectively.

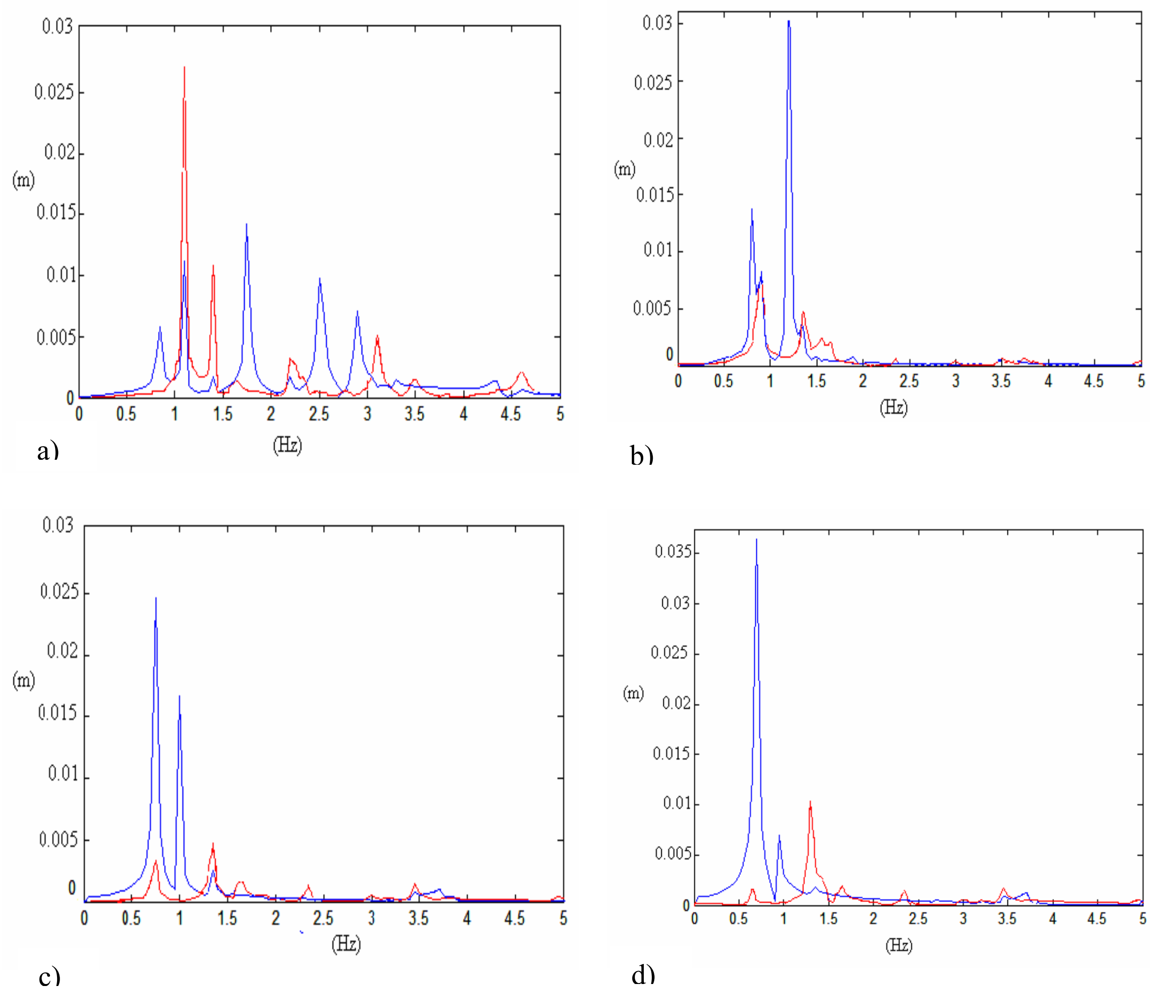

Figure 2.4.1.9: FFT plot of sloshing liquid (red-line) and structural vibration (blue-line) with various added masses, for the 25 mm mesh size and 10 ms time step runs. Point mass amounts: (a) 0 kg, (b) 5 kg, (c) 9 kg, (d) 13 kg.

A comparison with Figures 2.4.1.7, 2, 4.1.8 and 2.4.1.9 leads to the conclusion that there are no substantial differences between 5 ms and 10 ms time step runs and time step independence assumption is verified.

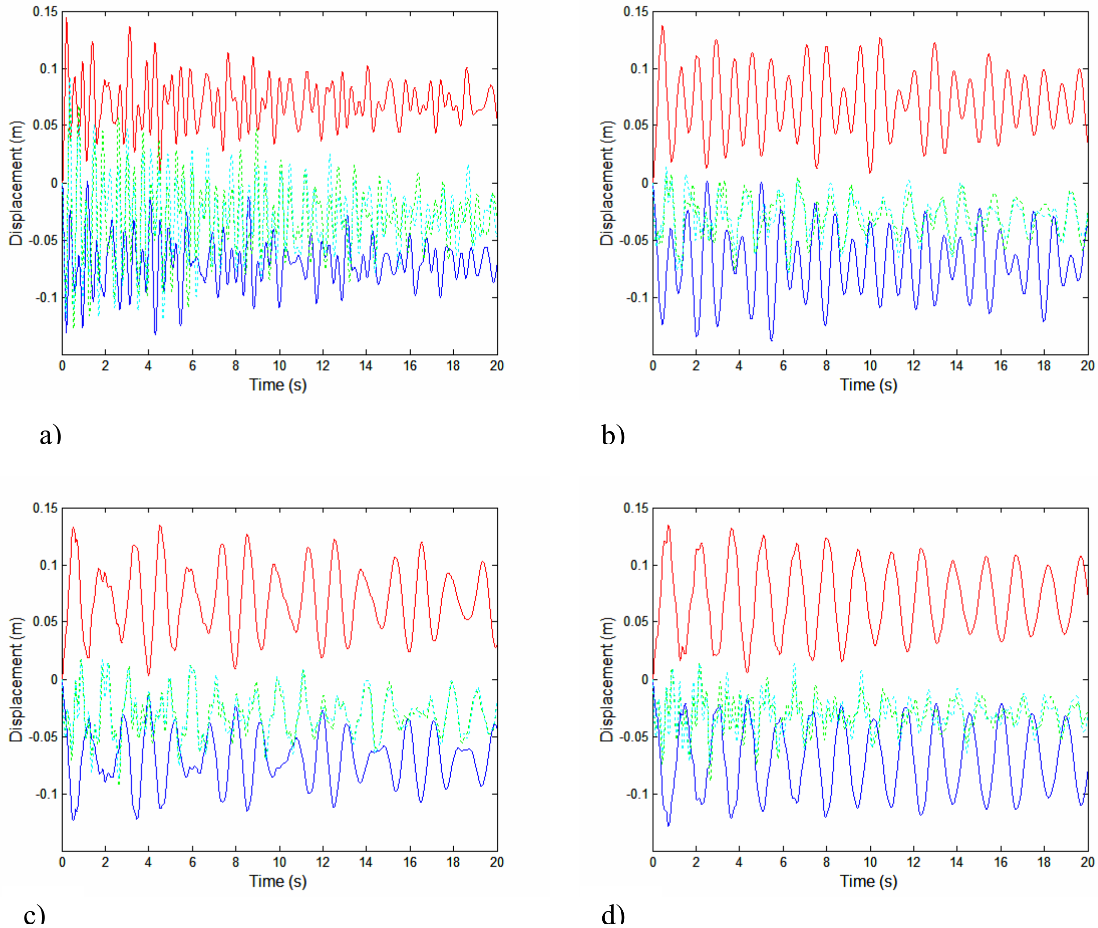

Figure 2.4.1.10: Same as in Figure 2.4.1.7 but for the 25 mm mesh size and 5 ms time step run.

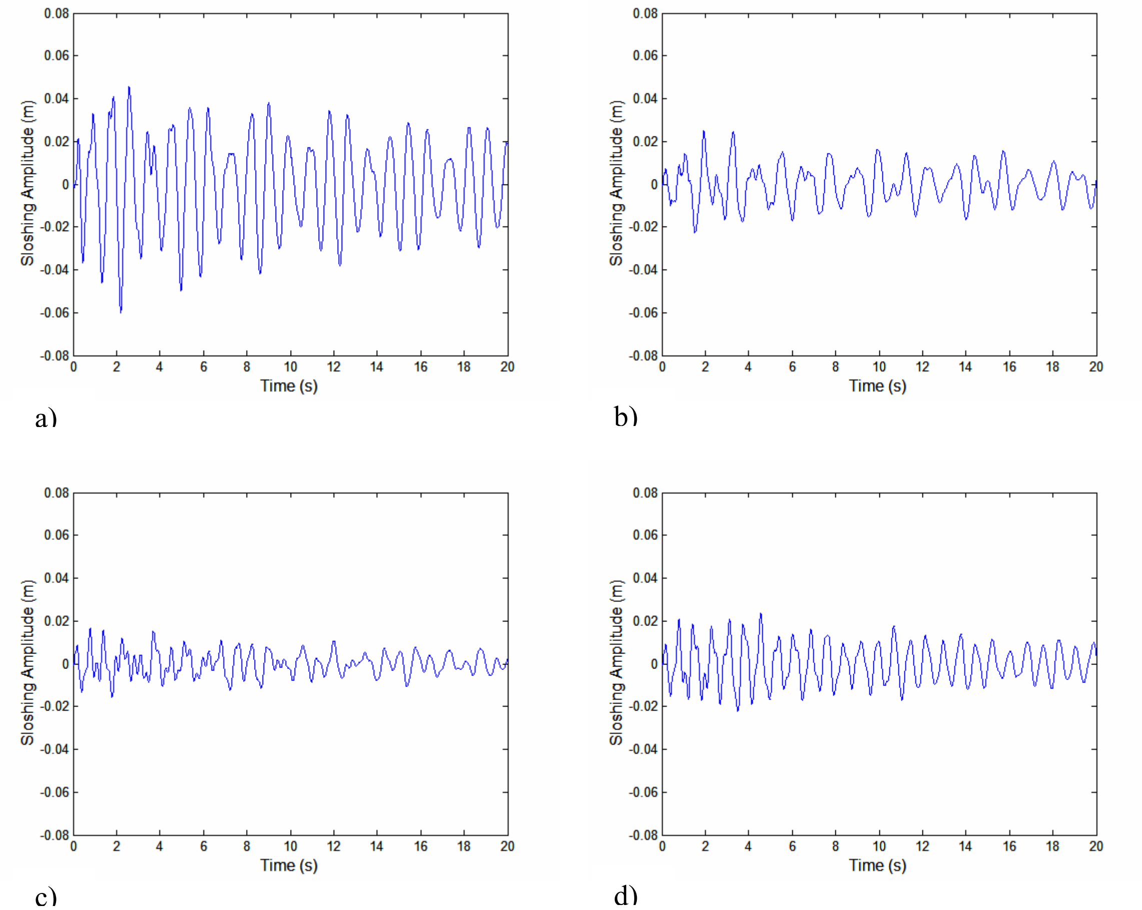

Figure 2.4.1.11: Same as in Figure 2.4.1.8 but for the 25 mm mesh size and 5 ms time step run.

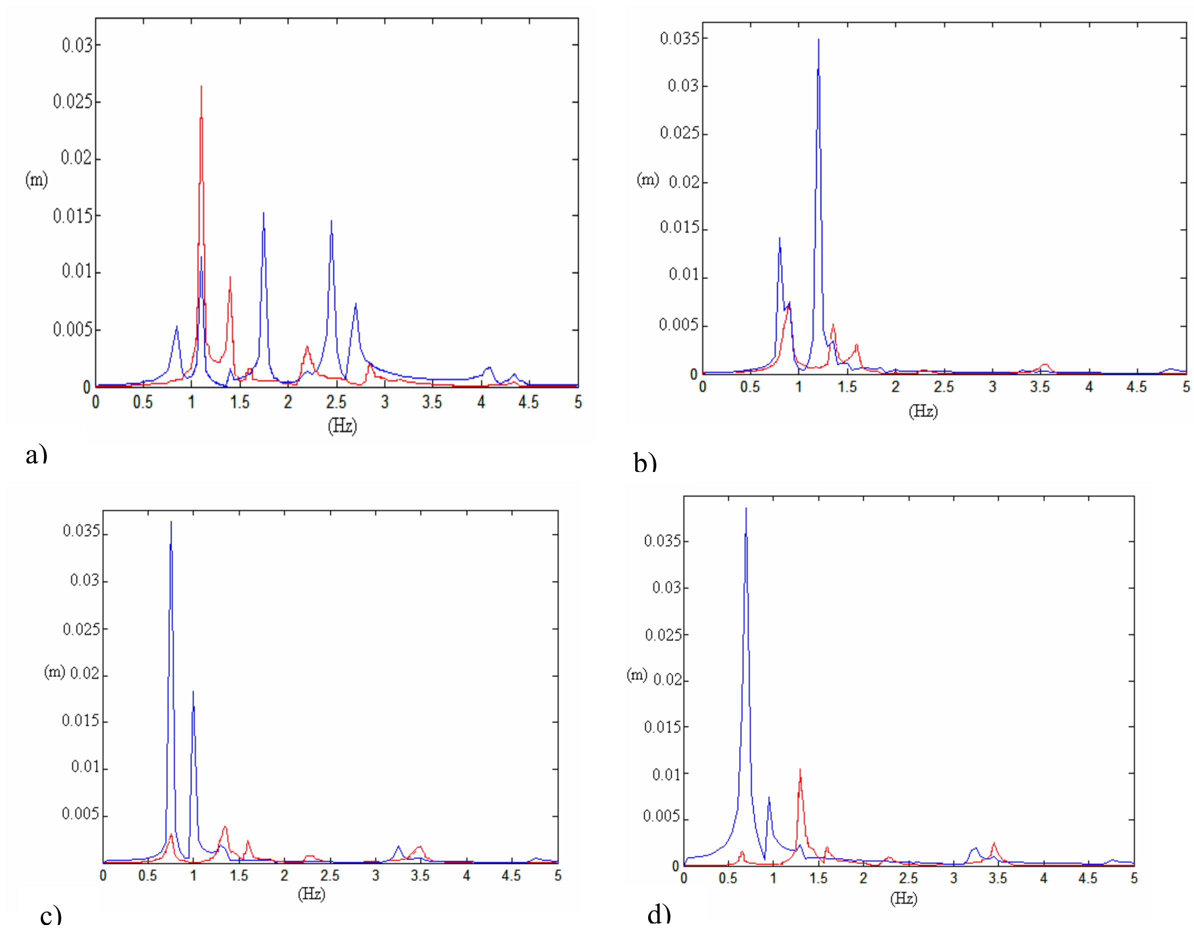

Figure 2.4.1.12: Same as in Figure 2.4.1.8 but for the 25 mm mesh size and 5 ms time step run.

2.4.3 Selection of the Length of Simulation Time

The introduction of water to the numerical model at time zero, has been of concern in determining the total duration of simulations. The flexible container gets elastically deformed by the addition of water at time zero. This deformation leads to structural oscillations of some considerable magnitude and long duration. It should be pointed out that this initial period for the container to seek the "static equilibrium" is peculiar only to the numerical process. The dynamic events of interest start only after the container reached its deformed state to accommodate the weight of its static liquid load. Until such a state is reached, container walls oscillate in the horizontal direction, and the “flat” liquid free surface oscillates in the vertical direction. No sloshing takes place.

To understand the effect of the initial settling period in which the flexible container seeks its static equilibrium, long runs of forty seconds have been obtained for the selected cases of 0 kg, 3 kg, 5 kg, 7 kg, 9 kg and 13 kg point masses. For these cases, the excitation has been introduced after twenty seconds, to allow the static equilibrium to be established. For brevity, only 0 kg, 9 kg and 13 kg point mass cases are presented here, while the remainder of the cases are in Appendix B, for completeness.

In Figures 2.4.2, 2.4.3 and 2.4.4, simulation results with a total duration of forty seconds are presented (where there is an initial twenty second waiting period before the base excitation is applied). By keeping the test conditions the same but altering the simulation time to twenty second duration (and skipping the initial twenty second period) the simulations are repeated and the corresponding results are presented in Figures 2.5.2 to 2.5.7 (within the context of the next section).

a)

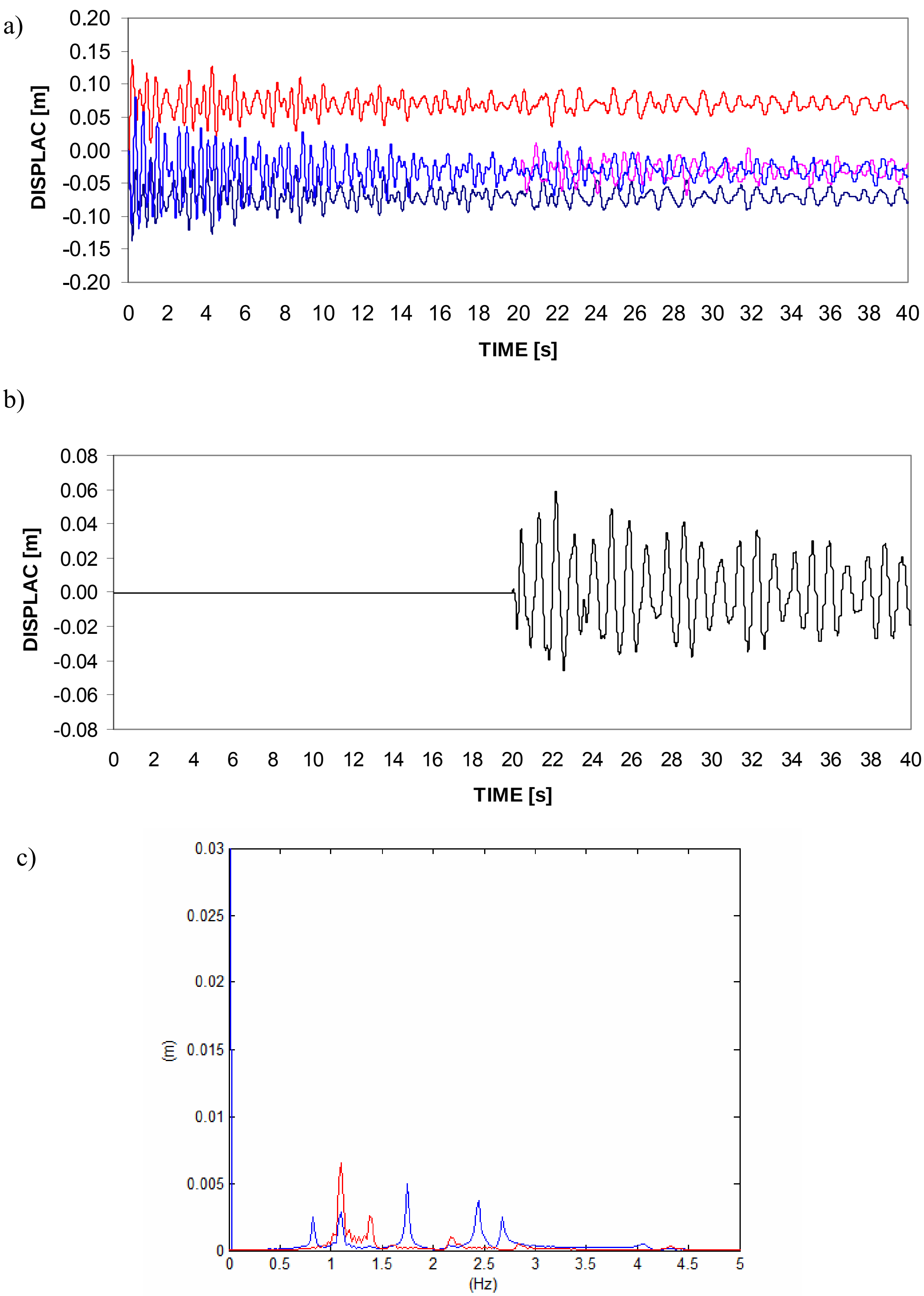

Figure 2.4.2: Displacement histories of the liquid in a flexible container with 1 mm wall thickness and 0 kg point mass (a).The liquid is undamped and structure has 1% damping. Predicted sloshing amplitude for the same case (b). Corresponding frequency spectrum of sloshing liquid (red) and structure (blue) (c).

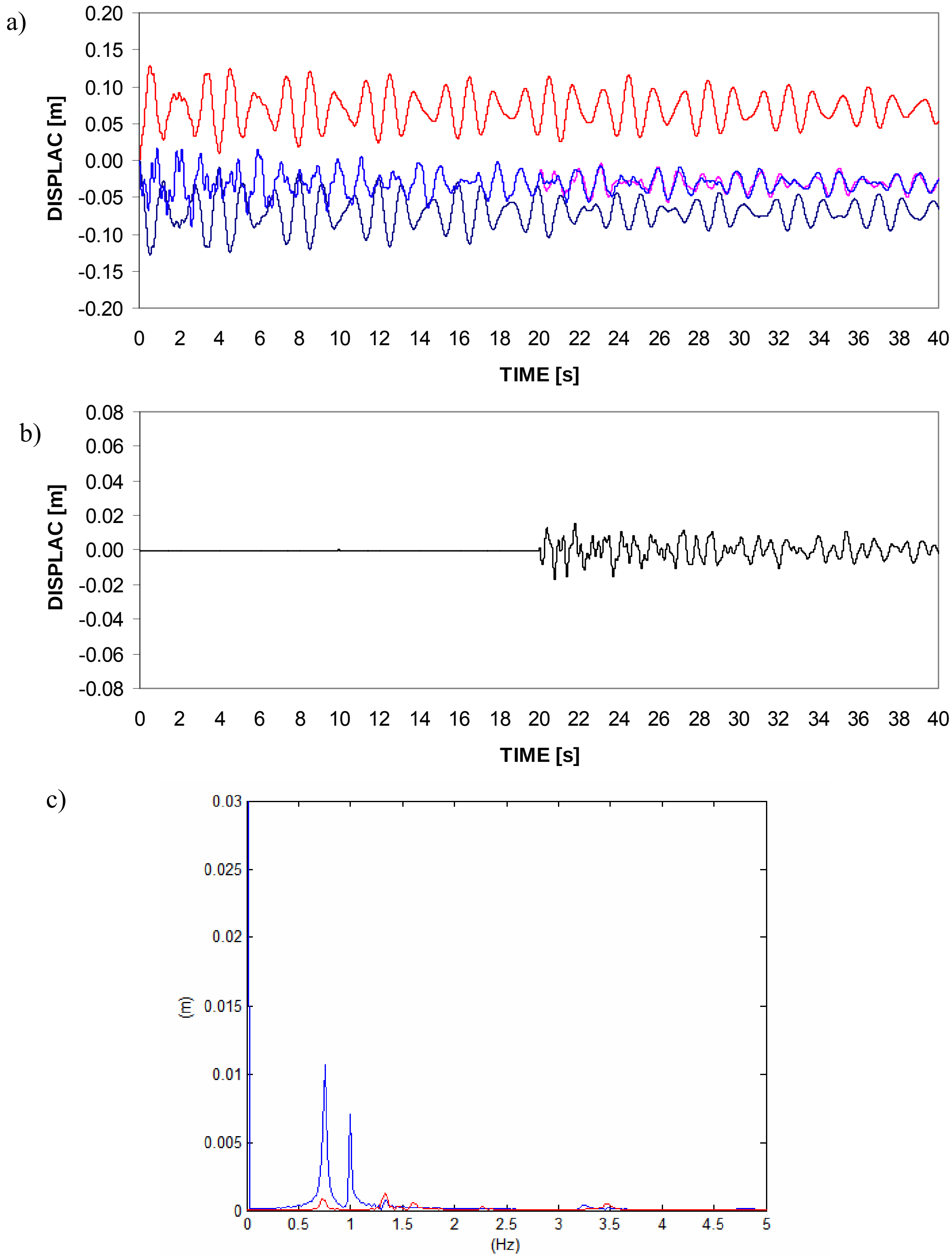

Figure 2.4.3: Displacement histories of the liquid in a flexible container with 1 mm wall thickness and 9 kg point mass (a).The liquid is undamped and structure has 1% damping. Predicted sloshing amplitude for the same case (b). Corresponding frequency spectrum of sloshing liquid (red) and structure (blue) (c).

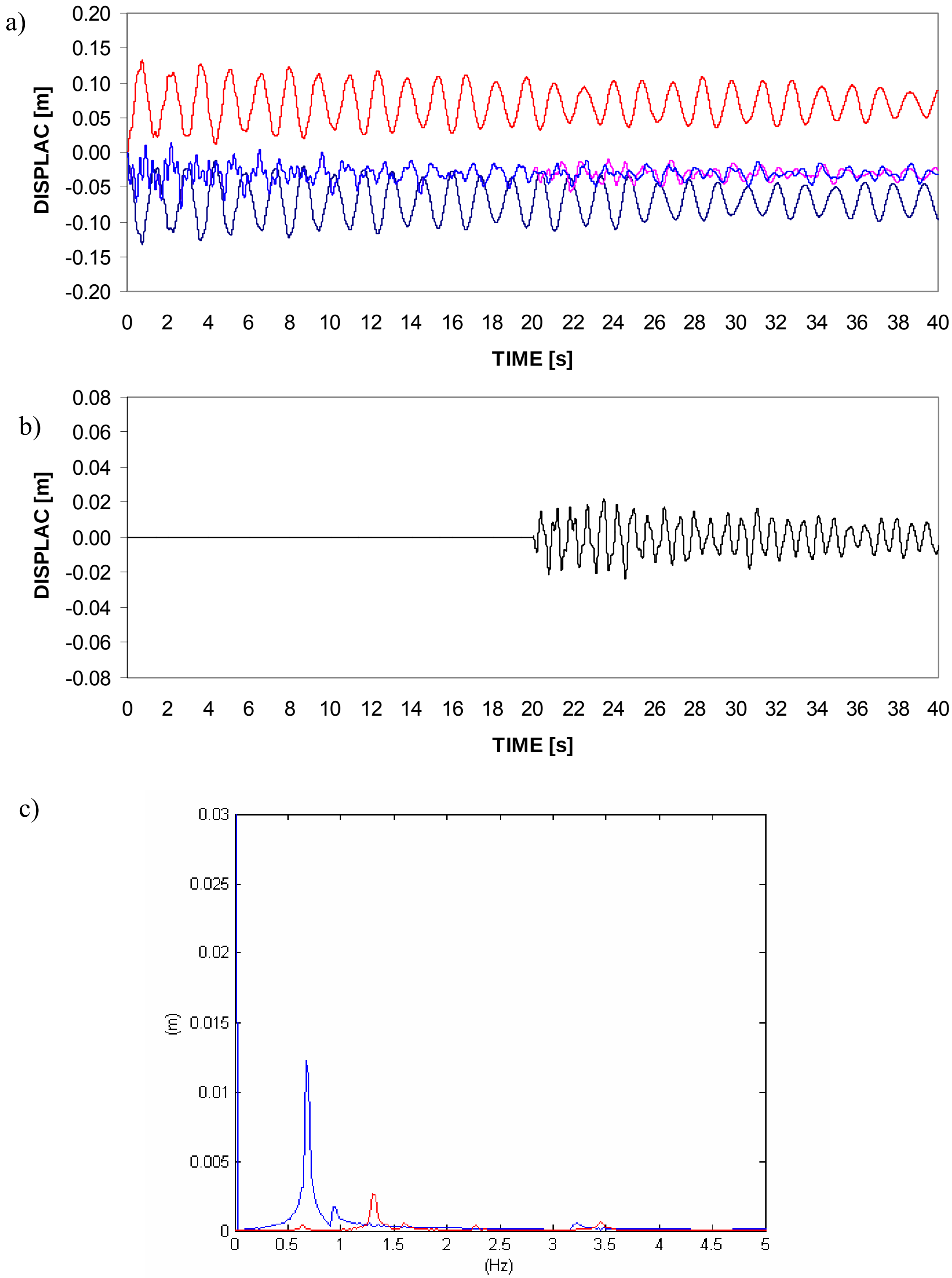

Figure 2.4.4: Displacement histories of the liquid in a flexible container with 1 mm wall thickness and 13 kg point mass (a).The liquid is undamped and structure has 1% damping. Predicted sloshing amplitude for the same case (b). Corresponding frequency spectrum of sloshing liquid (red) and structure (blue) (c).

In these figures, frame (a) contains the histories of the horizontal motion of the container nodes located in the middle of the wall near the top, as marked in Figure 2.3.1, and the vertical motion of the liquid free surface nodes. In all the following figures in frame (a), colors (■, magenta) and (■, light blue) present vertical displacement of the liquid and colors (■, red) and (■, dark blue) present horizontal displacement of the container. In the frame (b), the resulting sloshing amplitude is shown. In the frame (c), the frequency spectra of the container displacement (blue) and sloshing (red) are presented. The 40-second displacement histories in Figures 2.4.2, 2.4.3 and 2.4.4, and the 20-second ones in Figures 2.5.2, 2.5.6 and 2.5.7 are quite different in appearance, as expected.

Sloshing amplitudes for the selected cases are shown in frame (b) of Figures 2.4.2, 2.4.3 and 2.4.4. These figures represent the difference between the vertical displacements of the two liquid nodes on either side of the container. Without excitation, the two free surface nodes of the liquid are completely in phase, as mentioned earlier, thus making the sloshing amplitude zero for the first twenty seconds.

After excitation, the value of the sloshing amplitude changes. The sloshing amplitude is around 0.06 m for the 0 kg added point mass case, and this value drops to below 0.02 m for 9 kg point mass case. Following the addition of the 13 kg point mass, the sloshing amplitude again starts climbing over the 0.02 m level. Exactly the same trend is seen for the sloshing amplitude in Figures 2.5.2, 2.5.6 and 2.5.7 (b) and the sloshing patterns look quite similar (except for the first twenty seconds of the longer runs, of course). In both sets of runs, sloshing is best suppressed near the 9 kg point mass but this effect is lost by the addition of further point masses.

The FFT plots are given in frame (c) of the same figures. The red line in these plots indicates the sloshing amplitude frequency, whereas the blue line indicates the container frequency.

Sloshing frequencies which are dominant in Figure 2.4.2 (c) are around 1.2 Hz and 1.4 Hz. Major structural peaks for the 0 kg point mass are around 0.8 Hz, 1.2 Hz and 1.75 Hz. Looking at these frequency amplitudes, sloshing liquid should be driving the structure for this case scenario especially around the highest peak of 1.2 Hz.

For the 9 kg point mass case scenario, in Figure 2.4.3 (c), structural frequencies are even more dominant over the fluid ones. The structural frequency that was around 0.8 Hz significantly increases in amplitude and shifts in the spectrum to 0.75 Hz level, further suppressing the sloshing at the same frequency. The highest structural peak is switched from 1.2 Hz to 0.7 Hz. for this case.

With the introduction of 13 kg point masses, the interaction between the fluid and the container is seen to diminish as in Figure 2.4.4 (d). Sloshing peak is around 1.4 Hz once again and the structural frequency is decreased to 0.65 Hz. The fluid and the structure seem to be acting independently beyond this point. As in displacement history and sloshing amplitude plots, FFT plot results of longer runs are quite similar to results of twenty seconds runs that are displayed in Figure 2.5.7 (c). The only major difference is the higher frequency amplitudes of the forty second run plots. However, relative magnitudes in the frequency spectrum still remain the same as for the twenty second runs.

From a detailed comparison of the twenty second and forty second simulations, it is seen that a twenty second settling period is insufficient for the liquid to stabilize. However, it appears that applying the excitation at the start of a simulation, even without a settling period, the difference in the dynamic response is quite minimal. Therefore, as suggested earlier, the computational time can be halved by using a twenty-second total time, and by introducing the excitation at the beginning of the simulation.

2.5 Numerical Predictions

In Figure 2.5.1 (a), the predicted vertical displacement histories of the free surface of the liquid are given at the nodes which are located at the middle of the container near the top of two long sides of the rigid container (also indicated in Figure 2.3.1). These two histories are 180-degrees out of phase, indicating that when the liquid climbs at one wall, it drops at the other one. At the completion of one period of excitation, the liquid climbs approximately 20 mm on one wall, and it comes down by about 20 mm on the opposite wall. As there is no viscous dissipation, liquid sloshing continues with almost constant amplitude. No displacement history for the container walls is given as the walls have no detectable deflection.

The resulting sloshing amplitude for the rigid container is around 40 mm and is shown in Figure 2.5.1 (b). Sloshing history in figure (b), is given as the difference between the vertical displacements of the two liquid nodes, on the opposite sides of the container as shown in Figure 2.3.1. Figure 2.5.1 (b) may be used as a comparison base to judge the effectiveness of liquid sloshing control.

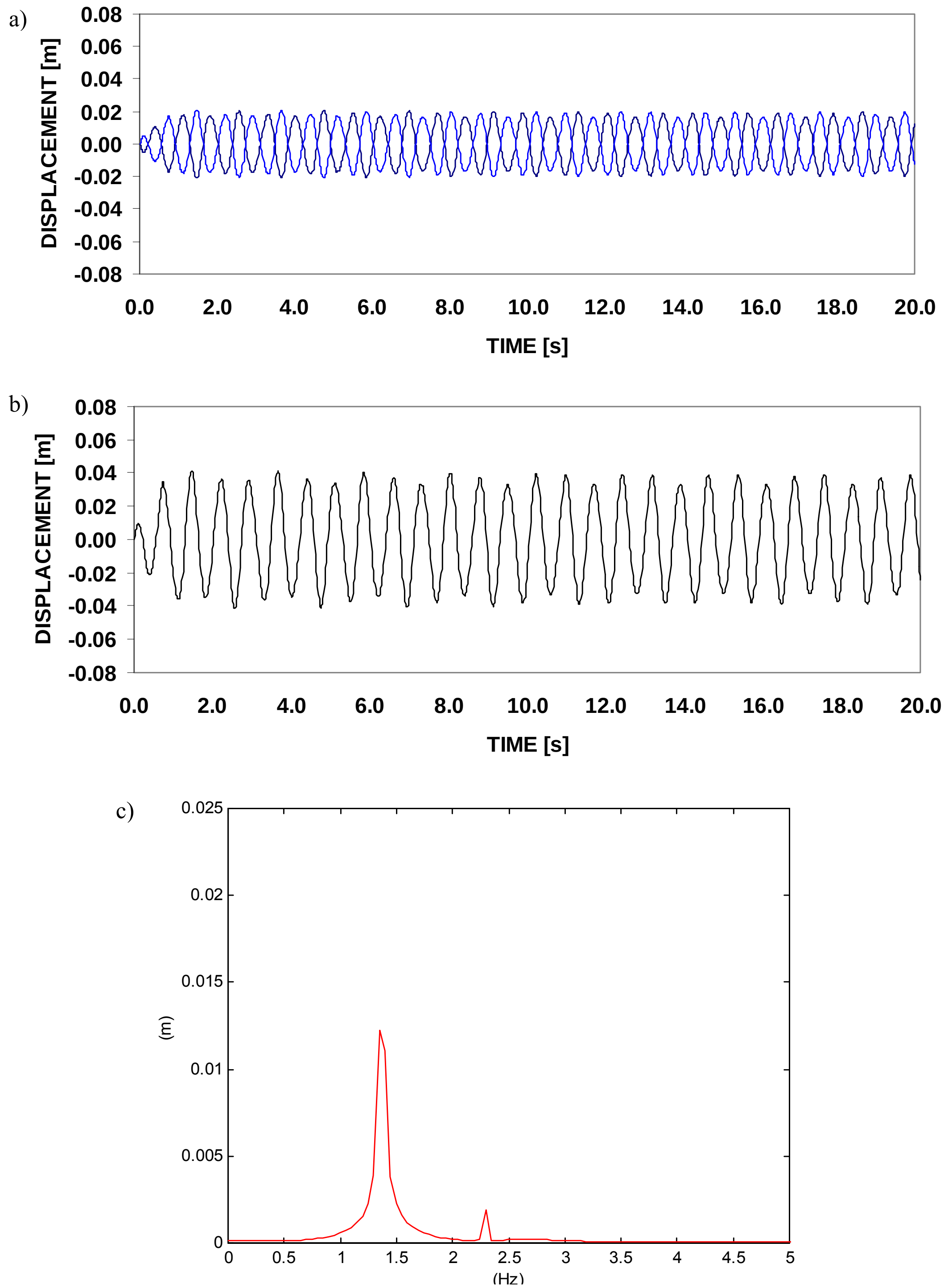

Figure 2.5.1: (a)Predicted absolute displacement histories of the liquid in a rigid container, (b) sloshing amplitude for the same case, (c) corresponding displacement frequency spectrum of sloshing liquid.

In Figure 2.5.1 (c) where the corresponding frequency spectrum of the sloshing history is given, the fundamental sloshing frequency is suggested to be around 1.4 Hz, quite close to the theoretical fundamental frequency of 1.34 Hz. Another small spectral peak is apparent, around 2.3 Hz, indicating the second sloshing frequency.

A series of numerical trials was conducted to determine the most promising container flexibility. The objective of the trials was to tune the container's natural frequency to the sloshing frequency. As mentioned before, two point masses of various magnitudes were attached to obtain tuning at the middle point of the longer container walls. The presence of significant energy transfer between the liquid and container is considered to be the sign of appropriate tuning. Tuning generally produces a beat envelope in the displacement history and two dominant spectral peaks in the corresponding frequency spectrum. This beat should be apparent both in the displacement histories of the container and at the liquid surface level.

The displacement history for the flexible container with 0 kg point mass is presented in Figure 2.5.2 (a). The horizontal displacement histories of the container nodes are the top and the bottom ones. The vertical displacement histories of the liquid surface nodes are indicated with two middle lines, with smaller displacement magnitudes than those of the container. Also, the container walls deflect substantially (an average of 0.075 m) after filling the flexible container with water. As a result, the free surface oscillations take place about a level lower that zero.

The sloshing history for the flexible container with 0 kg point mass is given in Figure 2.5.2 (b). The sloshing amplitude for the container with 0 kg point mass is around 0.06 m, larger than the 0.04 m amplitude of the rigid container. The gradual decay of the envelope of oscillations is due to 1% critical damping of the structure. Despite a weak beat in the envelope of the sloshing amplitude, the control effect is poor.

A frequency spectrum of the same case is given in Figure 2.5.2 (c). The spectral distribution of the container is rather crowded with structural peaks at 0.7 Hz, 1.1 Hz, 1.7 Hz, 2.3 Hz and 2.7 Hz. Sloshing also has a spectral peak at 1.1 Hz, possibly driving the lighter container at this frequency. Incidentally, if the deflection of the container is taken into account, the width of the flexible container at the free surface increases when compared to the case for the rigid container. In Figure 2.5.2 (a), container walls oscillate at a mean distance of approximately 0.075 m, increasing the average width of the free surface from 0.4 m to 0.55 m. It is interesting to note that a quick approximation (using the standard potential flow formulation) gives the fundamental sloshing frequency to be 1.15 Hz, for 0.55 m free surface, keeping all other parameters of the container unchanged.

Cross correlation between the histories of sloshing and structural displacement and its spectral distribution are given in Figures 2.5.2 (d) and 2.5.2 (e). Strong interaction at one dominant frequency is evident in the cross-correlation. This frequency is identified clearly at Figure 2.5.2 (e) to be 1.1 Hz, the same frequency as the one speculated to be the sloshing frequency of the deflected container in Figure 2.5.2 (c). None of the other spectral peaks are present in Figure 2.5.2 (e), reinforcing the earlier determination that this case is far removed from the tuning condition. Many spectral peaks in the sloshing and container wall displacements in Figure 2.5.2 (c), simply indicate that these two entities display their own preferred frequencies by ignoring the presence of each other.

a)

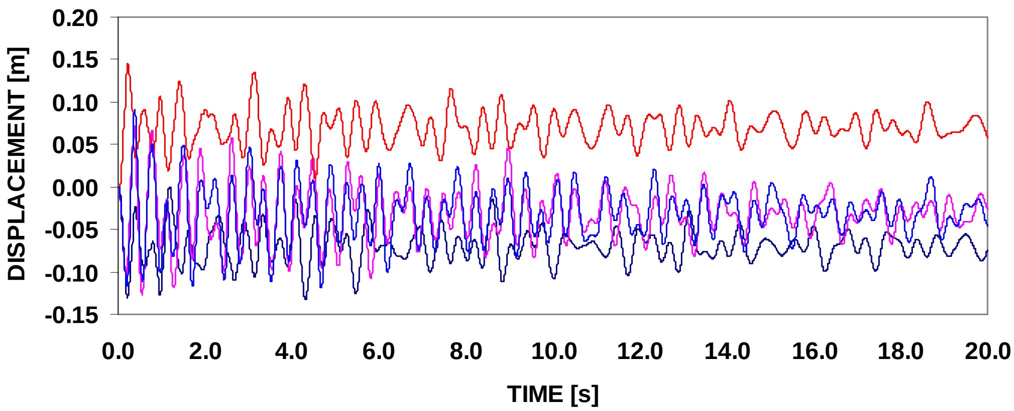
0.20
0.15
0.10
0.05
0.00
-0.05
-0.10
-0.15
DISPLACEMENT [m]
0.0
2.0
4.0
6.0
8.0
10.0
12.0
14.0
16.0
18.0
20.0
TIME [s]

b)

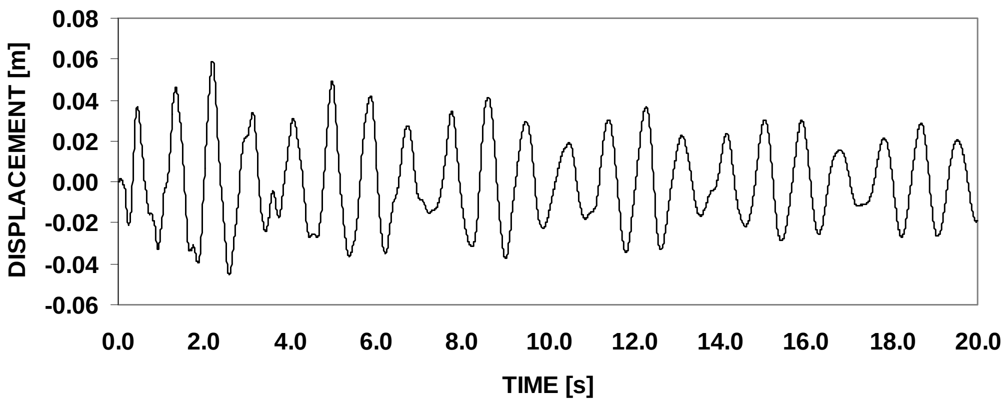
0.08
0.06
0.04
0.02
0.00
-0.02
-0.04
-0.06
DISPLACEMENT [m]
0.0
2.0
4.0
6.0
8.0
10.0
12.0
14.0
16.0
18.0
20.0
TIME [s]

c)

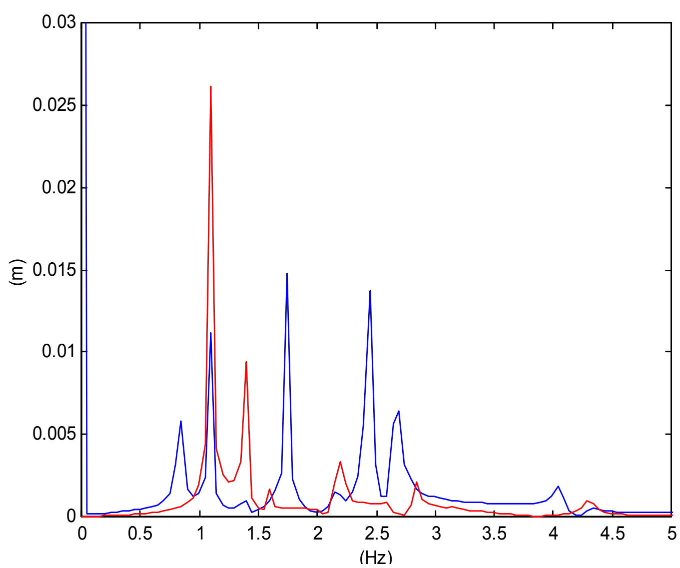
0.03
0.025
0.02
0.015
0.01
0.005
0
(m)
0
0.5
1
1.5
2
2.5
3
3.5
4
4.5
5
(Hz)

d)

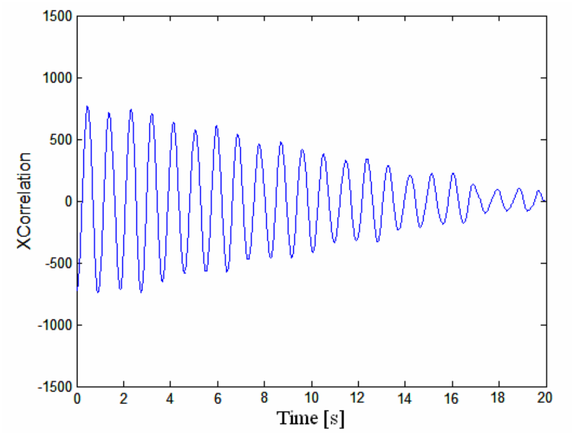

e)

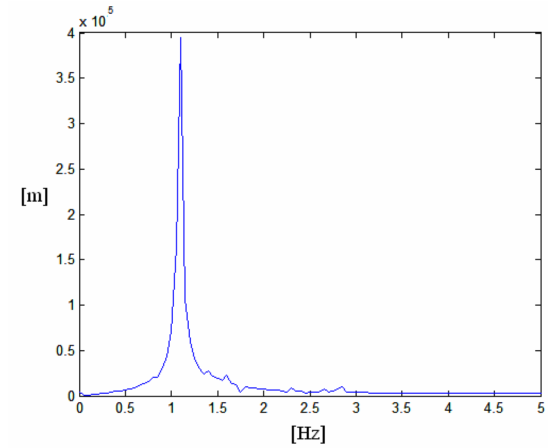

Figure 2.5.2: (a) Predicted displacement histories of the liquid in a flexible container with 1mm wall thickness and 0 kg point mass, (b) sloshing history, (c) frequency spectrum of sloshing liquid (——) and structure (——), (d) cross-correlation between container wall displacement and liquid sloshing and (d) its frequency spectrum. The liquid is undamped and structure has 1% damping.

The displacement history of the liquid and the container walls for the case with 3-kg point mass is presented in Figure 2.5.3 (a).

a)

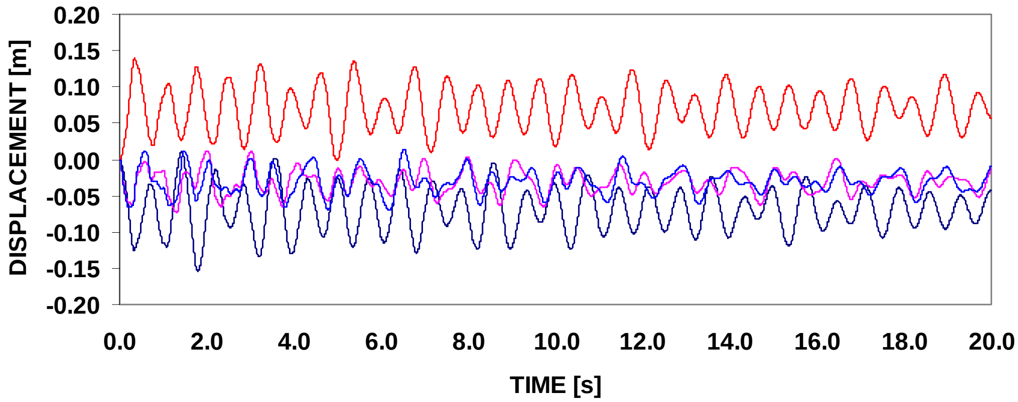

b)

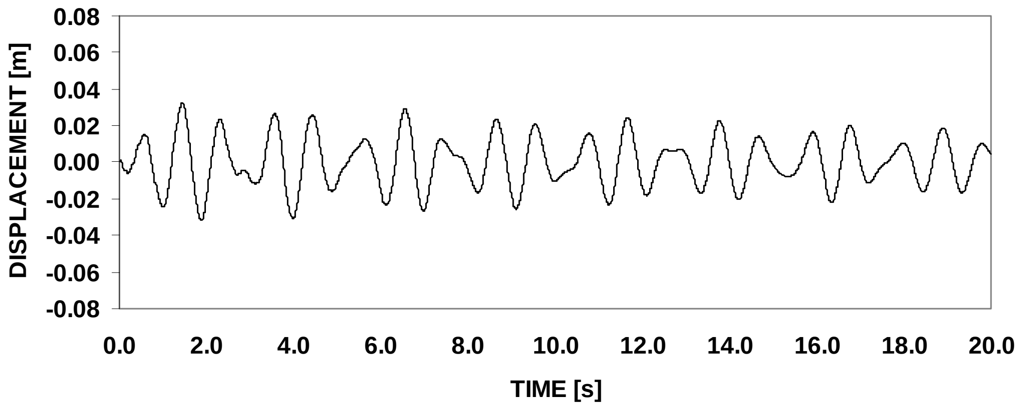

c)

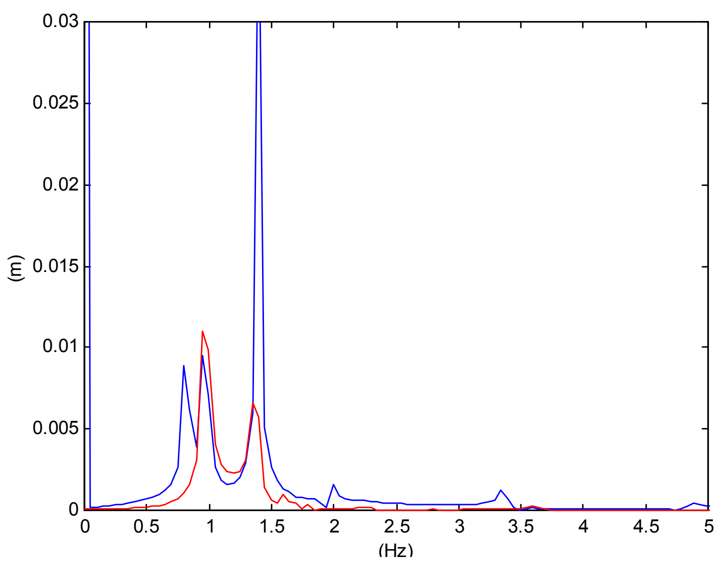

d) e)

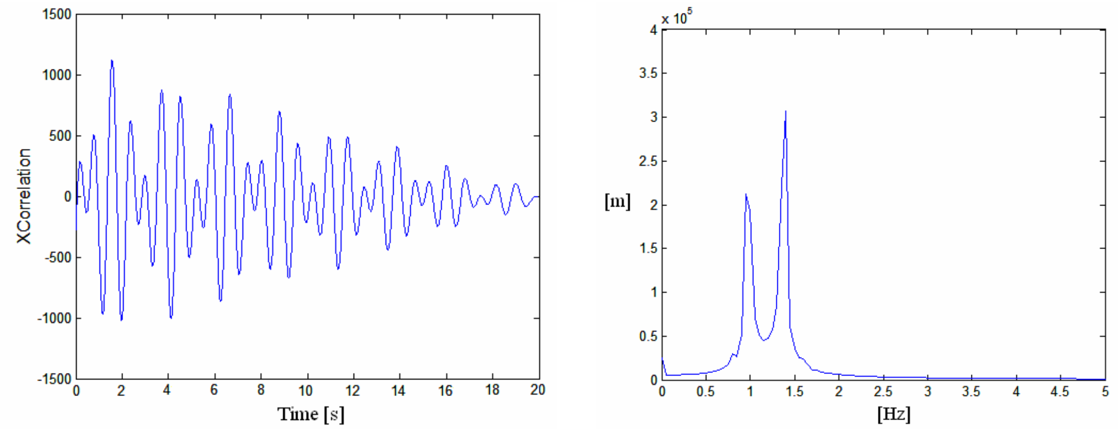

Figure 2.5.3: (a) Predicted displacement histories of the liquid in a flexible container with 1mm wall thickness and 3 kg point mass, (b) sloshing history, (c) frequency spectrum of sloshing liquid (——) and structure (——), (d) cross-correlation between container wall displacement and liquid sloshing and (d) its frequency spectrum. The liquid is undamped and structure has 1% damping.

In general, addition of mass causes the frequency of oscillations of the container to decrease as compared to those in Figure 2.5.2 (a.) which presents the figures for the 0 kg point mass case. An improvement of the sloshing magnitude is apparent in Figure 2.5.3 (b) for this same 3 kg point mass case. The sloshing amplitude decreases below 40 mm in the beginning, to around 25 mm at the end of the simulations. The beat in the container's displacement history in Figure 2.5.3 (a), and in the sloshing history in Figure 2.5.3 (b), may indicate that this case is getting close to tuning.

With 3-kg point mass, the spectral distribution of both the container and the sloshing liquid are significantly simplified and reduced, being practically limited to below 2 Hz. This is especially significant when compared to the case with 0 kg point mass. The container has spectral peaks at approximately 0.75 Hz, 1 Hz and 1.4 Hz. Sloshing has spectral peaks at 1 Hz and 1.4 Hz. The second sloshing peak coincides with that of the rigid container at this frequency. The liquid driven oscillations at 1.1 Hz from the 0 kg case now appear to be around 1 Hz.

From the cross-correlation in Figure 2.5.3 (d), a strong interaction between the liquid and structure is noticeable. Two "communication" frequencies exist between liquid and container at 1 Hz and 1.4 Hz, as shown in Figure 2.5.3 (e). Clearly, the spectral peak of the container at 0.75 Hz in Figure 2.5.3 (c), indicates an off-tuned response of the flexible walls.

The displacement history for the flexible container with 5-kg point mass is presented in Figure 2.5.4 (a).

a)

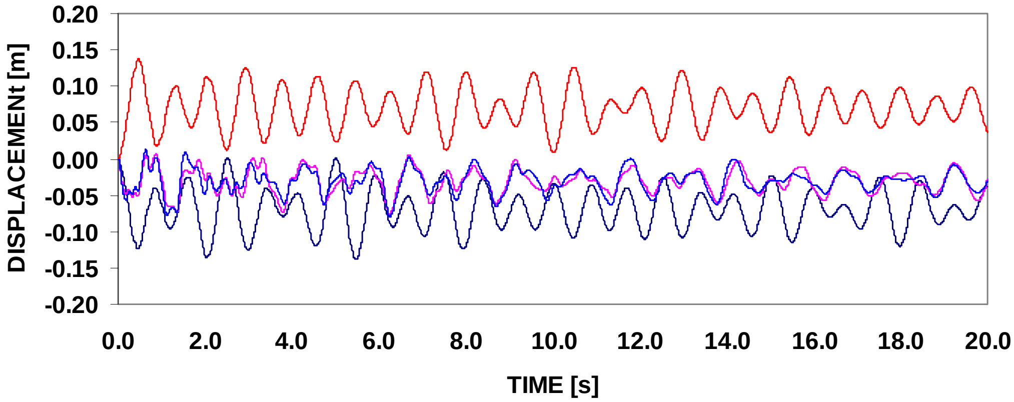
0.20
0.15
0.10
0.05
0.00
-0.05
-0.10
-0.15
-0.20
DISPLACEMENt [m]
0.0
2.0
4.0
6.0
8.0
10.0
12.0
14.0
16.0
18.0
20.0
TIME [s]

b)

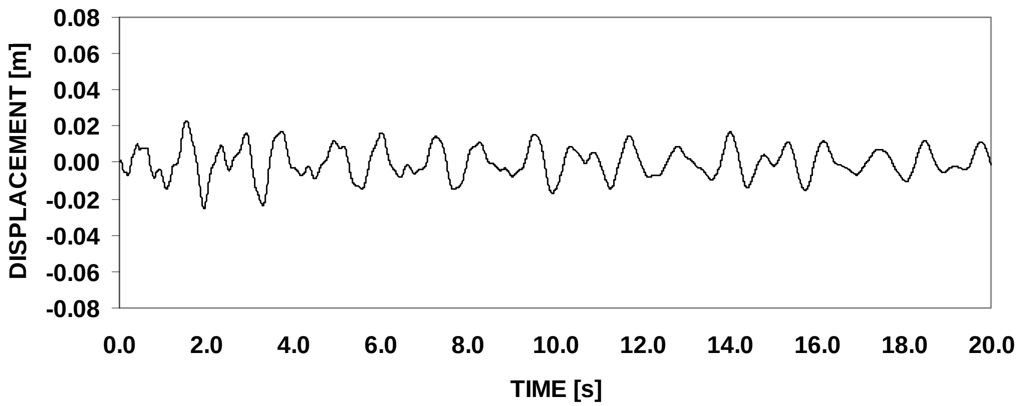
0.08
0.06
0.04
0.02
0.00
-0.02
-0.04
-0.06
-0.08
DISPLACEMENT [m]
0.0
2.0
4.0
6.0
8.0
10.0
12.0
14.0
16.0
18.0
20.0
TIME [s]

c)

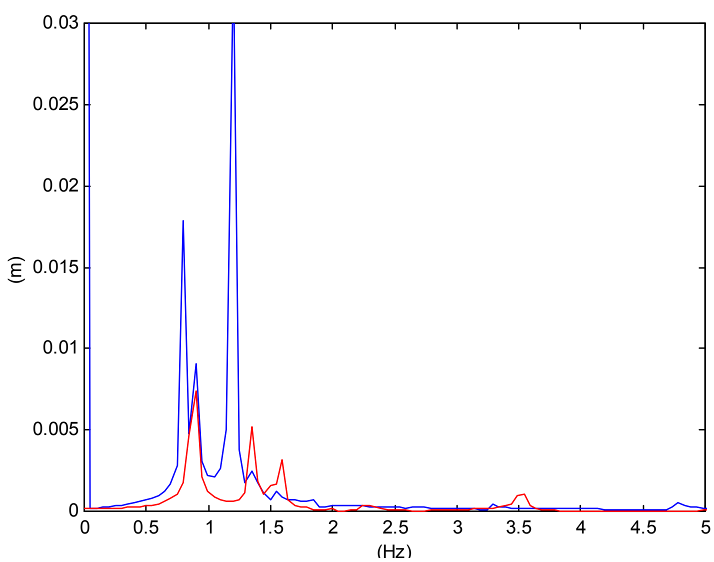
0.03
0.025
0.02
0.015
0.01
0.005
0
(m)
0
0.5
1
1.5
2
2.5
3
3.5
4
4.5
5
(Hz)

d)

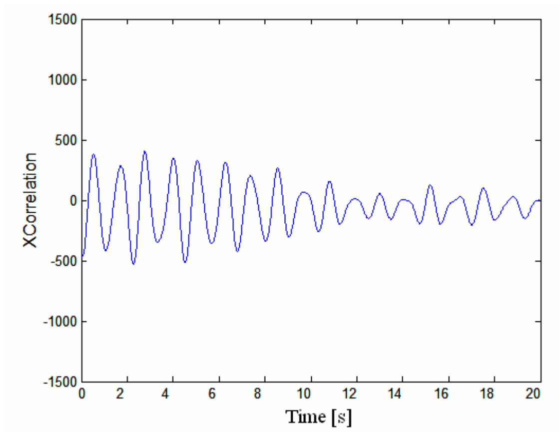

e)

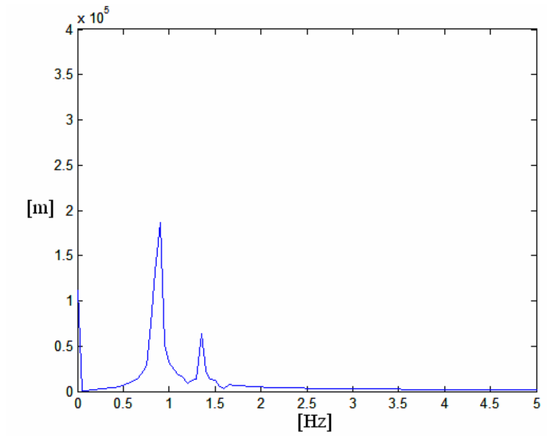

Figure2.5.4.: (a) Predicted displacement histories of the liquid in a flexible container with 1mm wall thickness and 5 kg point mass, (b) sloshing history, (c) frequency spectrum of sloshing liquid (——) and structure (——), (d) cross-correlation between container wall displacement and liquid sloshing and (d) its frequency spectrum. The liquid is undamped and structure has 1% damping.

There is a further noticeable decrease in the frequency of the displacement histories from the case of the 5-kg point mass case presented in Figure 2.5.4 (a). As shown in Figure 2.5.4 (b), sloshing amplitude decreases further to below 20 mm. In Figure 2.5.4 (c), the structure has two dominant spectral peaks around 0.75 Hz and 1.2 Hz. In addition, both the structure and the liquid have a common frequency at approximately 0.9 Hz suggesting it is approaching tuning. The spectral peak magnitude of the structure are significantly larger than those of the liquid, possibly indicating that the structure may now affect the response of the liquid more than being affected by it. The control effect of the structure is suggested quite clearly at its second spectral peak at 1.2 Hz where the sloshing magnitudes are suppressed significantly.

From the cross-correlation in Figure 2.5.4 (d), a strong interaction between the liquid magnitude and the structure magnitude is still noticeable. In the cross-spectrum, two spectral peaks are clear, one at 0.9 Hz, and the other at 1.4 Hz. The first peak is possibly the reduced sloshing frequency due to deflection of the container and the added mass. The smaller second peak is possibly due to the sloshing frequency of the rigid container, still present, although now in the background. The two spectral peaks which do not exist in the cross-spectrum are the container frequencies at 0.75 Hz and at 1.2 Hz.

As predicted earlier, the lower frequency is an inherent off-tuned frequency of the flexible walls. The higher frequency is the effect of the "tuning" sought through the design process.

The displacement history for the two best tuned cases, with 7-kg and 9-kg point masses, are presented in Figures 2.5.5 (a) and 2.5.6 (a), respectively.

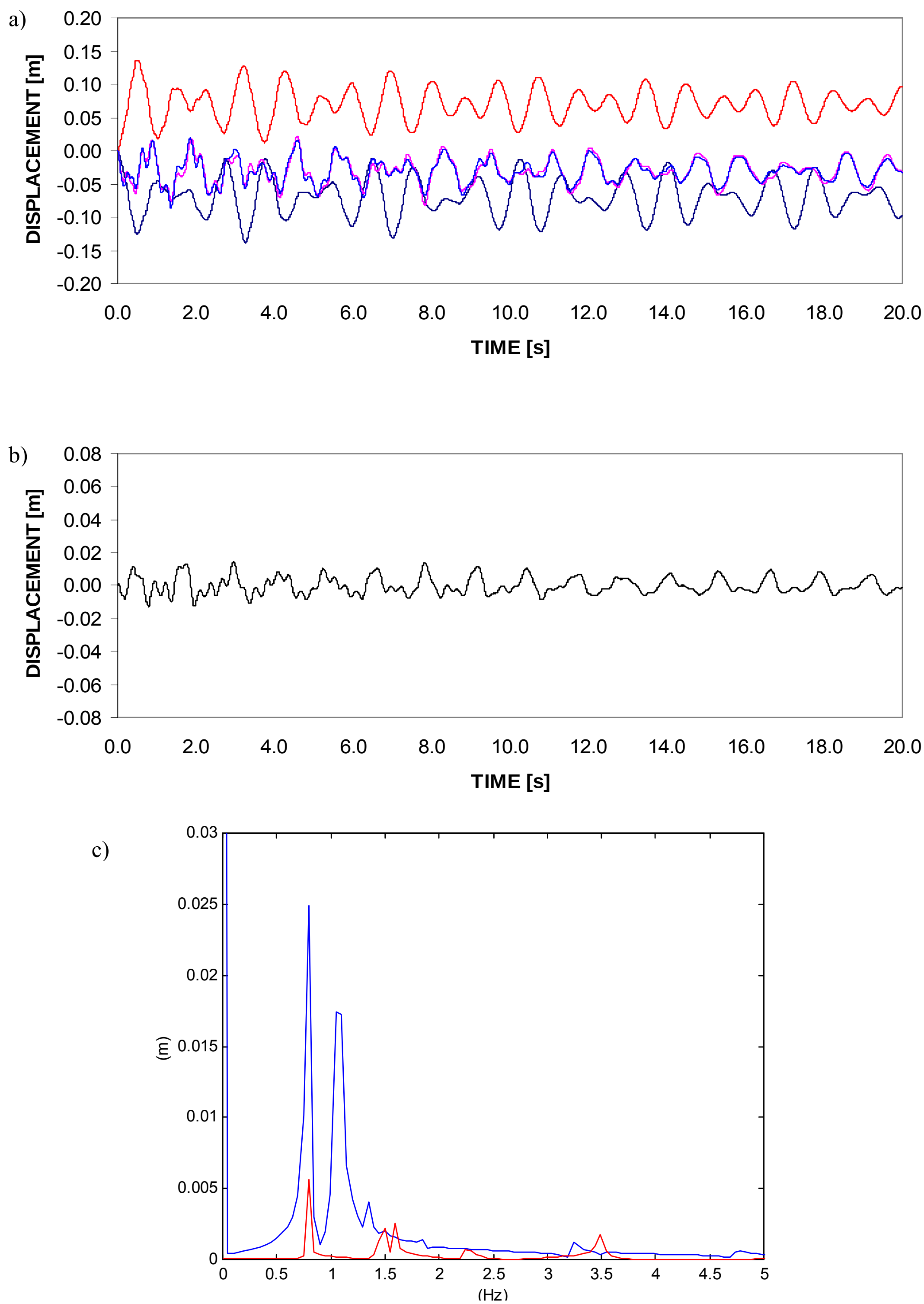

d) e)

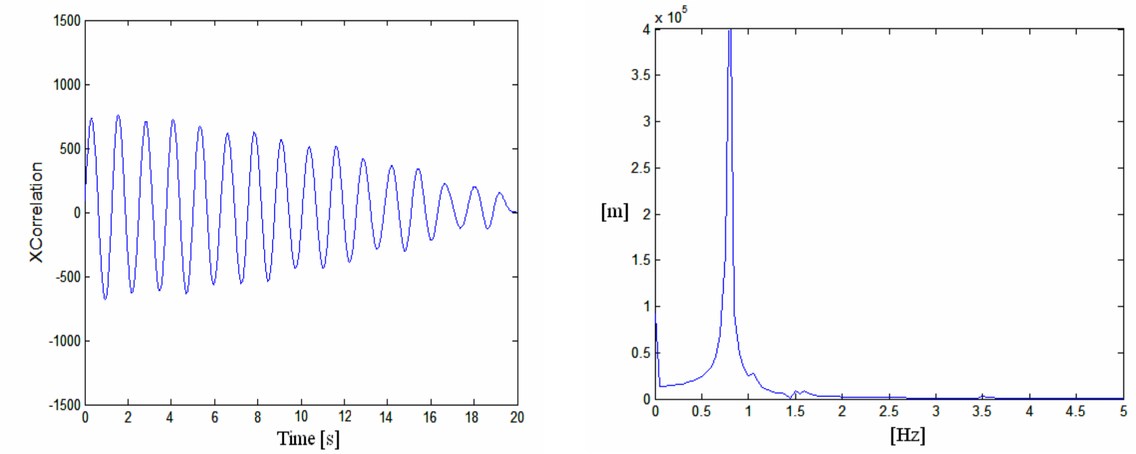

Figure 2.5.5: (a) Predicted displacement histories of the liquid in a flexible container with 1mm wall thickness and 7 kg point mass, (b) sloshing history, (c) frequency spectrum of sloshing liquid (——) and structure (——), (d) cross-correlation between container wall displacement and liquid sloshing and (d) its frequency spectrum. The liquid is undamped and structure has 1% damping.

a)

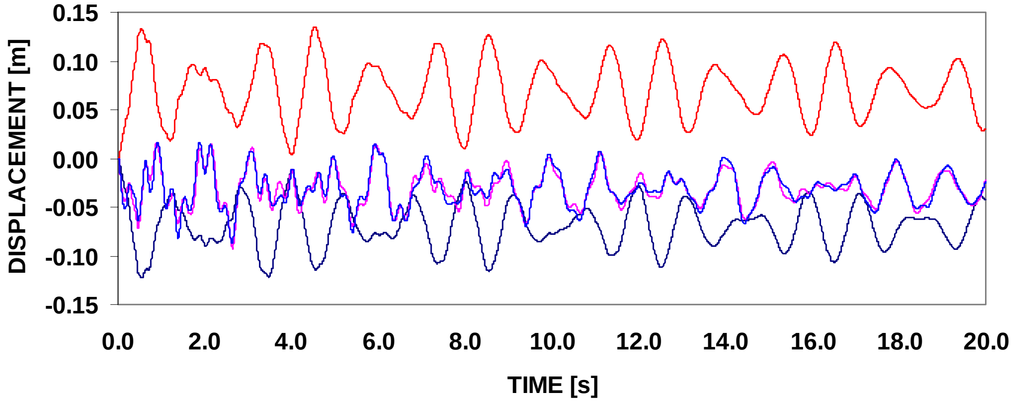
0.15
0.10
0.05
0.00
-0.05
-0.10
-0.15
DISPLACEMENT [m]
0.0
2.0
4.0
6.0
8.0
10.0
12.0
14.0
16.0
18.0
20.0
TIME [s]

b)

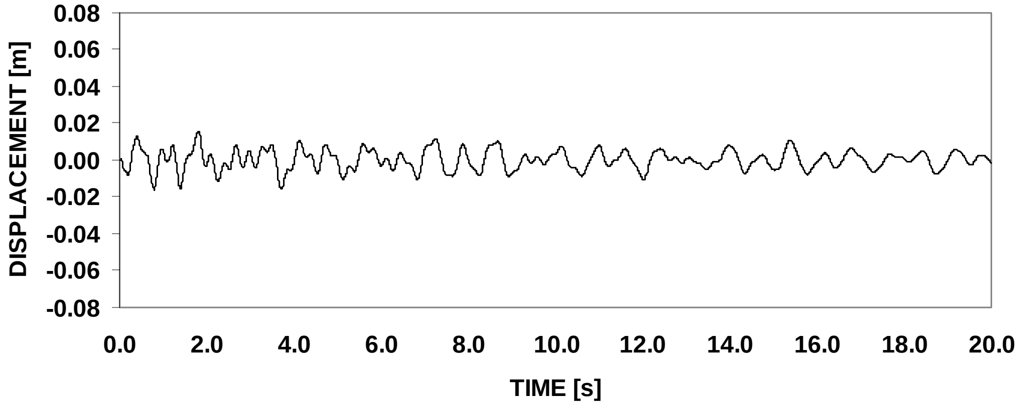
0.08
0.06
0.04
0.02
0.00
-0.02
-0.04
-0.06
-0.08
DISPLACEMENT [m]
0.0
2.0
4.0
6.0
8.0
10.0
12.0
14.0
16.0
18.0
20.0
TIME [s]

c)

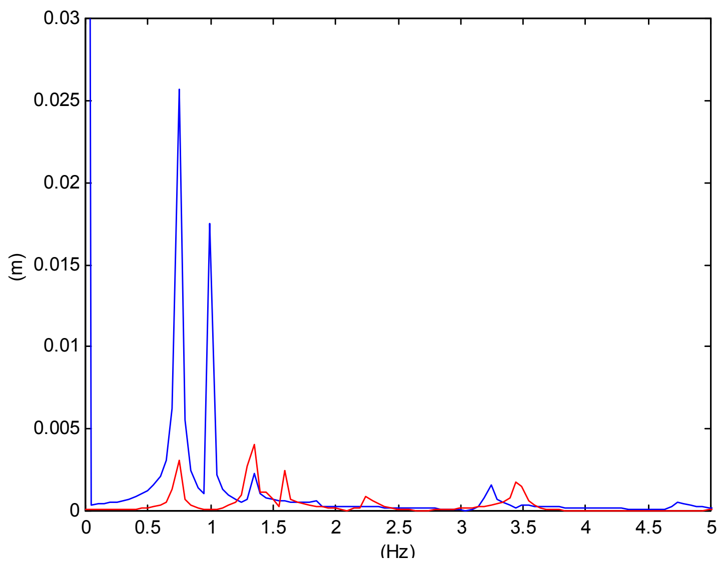
0.03
0.025
0.02
0.015
0.01
0.005
0
(m)
0
0.5
1
1.5
2
2.5
3
3.5
4
4.5
5
(Hz)

d) e)

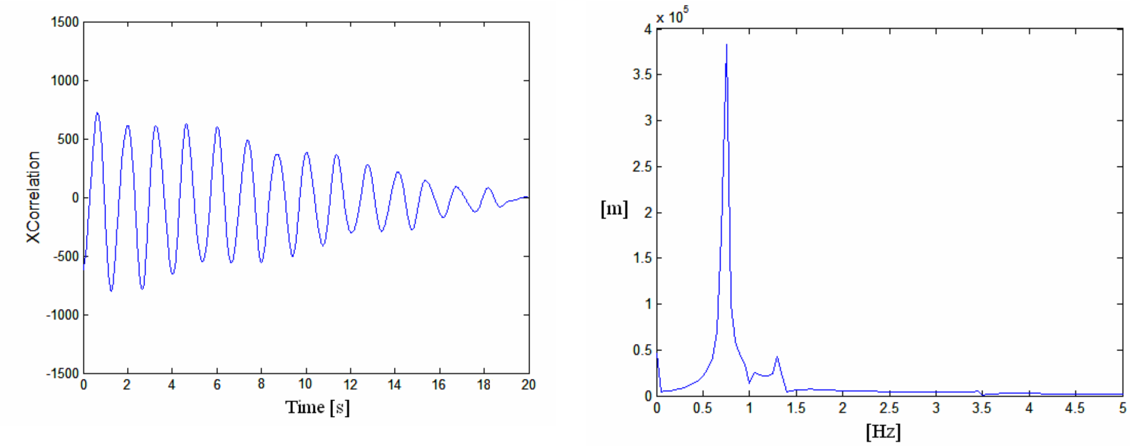

Figure 2.5.6: (a) Predicted displacement histories of the liquid in a flexible container with 1mm wall thickness and 9 kg point mass, (b) sloshing history, (c) frequency spectrum of sloshing liquid (——) and structure (——), (d) cross-correlation between container wall displacement and liquid sloshing and (d) its frequency spectrum. The liquid is undamped and structure has 1% damping.

A beat in the envelope of the container displacement is clear for both 7-kg and 9-kg cases. Sloshing amplitude decreases to below 15 mm for the 7-kg point mass, and below 10 mm for the 9-kg point mass, as shown in Figures 2.5.5 (b) and 2.5.6 (b).The structure's response in Figure 2.5.5 (c) is significantly larger than that of the sloshing liquid in general, and particularly at both of its preferred frequencies of 0.75 Hz and 1.15 Hz. The first spectral peak is again the off-tuned container frequency and it imposes a forced response on the liquid. The second is the effective frequency tuned to suppress sloshing. In this figure, the only noticeable sloshing response is that corresponding to the forced response at the off-tuned structural frequency.

It may be argued that if this frequency can be avoided, further suppression of sloshing could be achieved. In agreement with the preceding comment, cross correlation and its frequency content is limited to the off-tuned container frequency at 0.75 Hz.

Similar observations can be made for the 9 kg cases in Figure 2.5.6 (c). The difference is the slight emergence of the rigid-container frequency at approximately 1.4 Hz in the sloshing response and the forced response of the container at this frequency. The second event is quite insignificant in magnitude, and the sloshing is suppressed just as effectively for the 9kg case as it is for the 7kg case.

The displacement history for the 13-kg point mass case is presented in Figure 2.5.7 (a). The observed beat in the envelope of the container displacement from the previous case has disappeared. The sloshing amplitude starts to increase again, as shown in Figure 2.5.7 (b) and tuning is lost. In Figure 2.5.7 (c), the off-tuned container frequency appears at 0.7 Hz due to increased mass. The tuning effect of the container on the sloshing, is still quite clear around 1 Hz, although its effectiveness starts to diminish clearly. The rigid container's frequency at 1.4 Hz starts to gather importance, as the tuning condition is gradually lost. As the tuning is lost, the correlation between magnitudes become smaller in Figure 2.5.7 (d).

a)

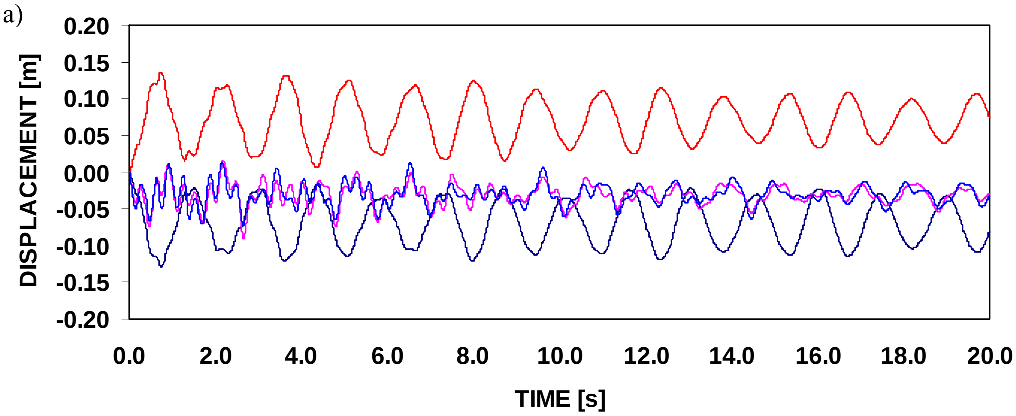
0.20
0.15
0.10
0.05
0.00
-0.05
-0.10
-0.15
-0.20
DISPLACEMENT [m]
0.0
2.0
4.0
6.0
8.0
10.0
12.0
14.0
16.0
18.0
20.0
TIME [s]

b)

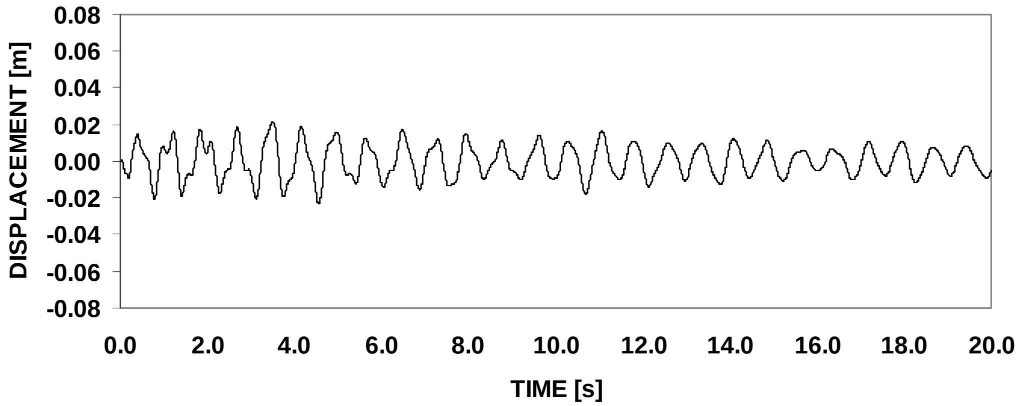
0.08
0.06
0.04
0.02
0.00
-0.02
-0.04
-0.06
-0.08
DISPLACEMENT [m]
0.0
2.0
4.0
6.0
8.0
10.0
12.0
14.0
16.0
18.0
20.0
TIME [s]

c)

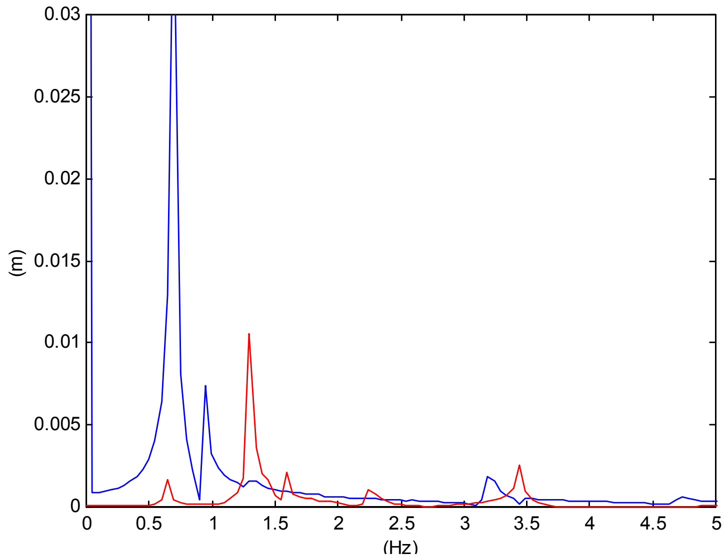
0.03
0.025
0.02
0.015
0.01
0.005
0
(m)
0
0.5
1
1.5
2
2.5
3
3.5
4
4.5
5
(Hz)

d)

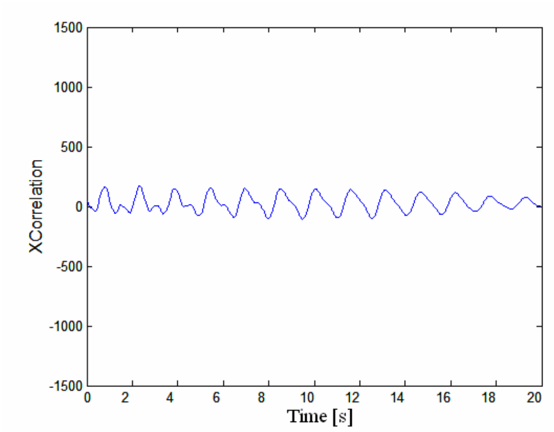

e)

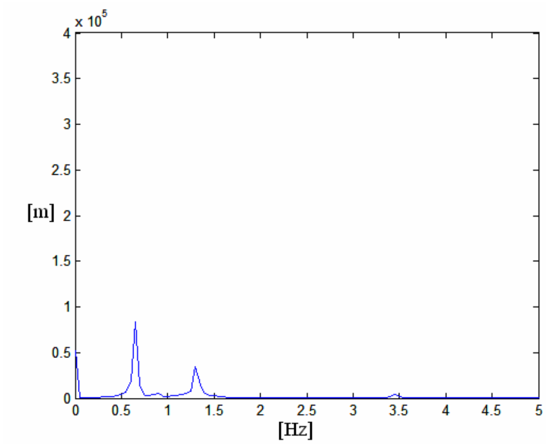

Figure 2.5.7: (a) Predicted displacement histories of the liquid in a flexible container with 1mm wall thickness and 13 kg added mass, (b) sloshing history, (c) frequency spectrum of sloshing liquid (——) and structure (——), (d) cross-correlation between container wall displacement and liquid sloshing and (d) its frequency spectrum. The liquid is undamped and structure has 1% damping.

2.5.1 Numerical prediction summary

A summary of the numerically predicted tuning process is presented in Figure 2.5.8 with the root mean square averages (from now on referred to as 'rms') of sloshing amplitude.

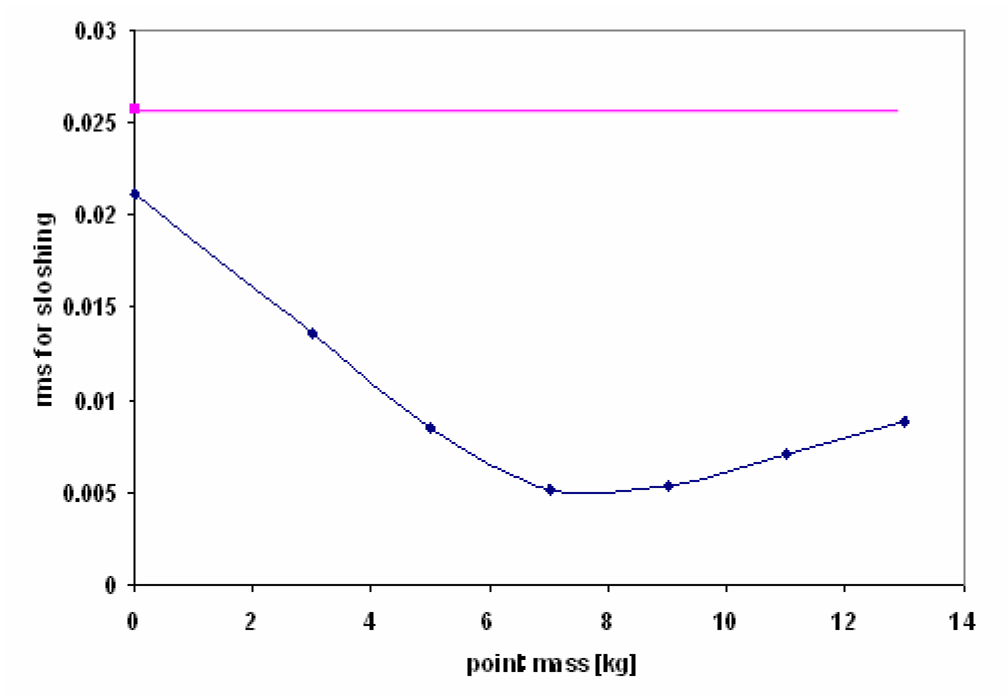

Figure 2.5.8. Variation of the rms of sloshing magnitude in m with mass for rigid (▬) and flexible (▪) containers.

The minimum sloshing amplitude for 7-kg to 9-kg point mass on the flexible container, corresponds to better than 80% attenuation as compared to that in the rigid container. Considering the respective slopes of the trend line on either sides of the best cases (7 kg to 9 kg point mass), the control effect is more sensitive as the tuning is approached from the left. Therefore, the added mass can be somewhat larger than the optimal without significant loss of effectiveness.

Figure 2.5.9 shows the frequency of occurrence of the sloshing amplitudes, of the rigid container ( ) and the flexible container with 9 kg added mass ( ). In this figure, the horizontal axis indicates the magnitude of the free surface displacement of the liquid.

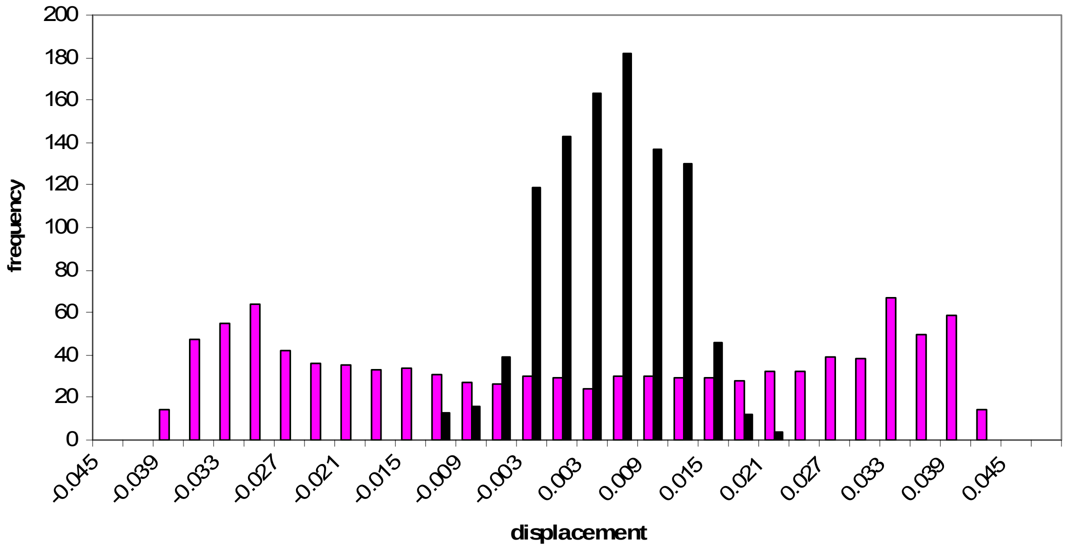

Figure 2.5.9. Probability distribution for sloshing in rigid container ( ) and flexible container with 9 kg added mass ( ).

The amplitude distribution of the rigid container case, is that of an almost harmonic function with the highest probability being around the peak displacements and the lowest probability of being around zero displacement. For the case with the tuned absorber, on the other hand, the well-organised harmonic trend of the rigid container is lost, indicating a distribution approximating that of a Gaussian function. The peak sloshing magnitudes of the tuned case are limited to less than half of the rigid container's. In addition, the probability of being around zero magnitude is approximately six times higher with the tuned case as compared to the case of the rigid container. These are, of course, the result of the strong interference of the container's flexibility with the natural sloshing oscillations.

2.6 Experiments

As the main objective of this research was numerical simulations, the following relevant experiments were performed in an attempt to validate the presence of "tuning", claimed in the preceding section. These experiments were seen as a means of verifying the numerical predictions.

The experimental setup is shown schematically in Figure 2.6.1. It consists of a (1)-personal computer; (2)-Techron 7560 power amplifier; (3)- VTS500, model VG 600-3, electromagnetic exciter; (4)-the container mounted on a trolley with a rigid platform. The container was identical to the one used for the numerical model. The moving table of the shaker was programmed to provide the required displacement history. This feature was particularly useful to provide a controlled disturbance.

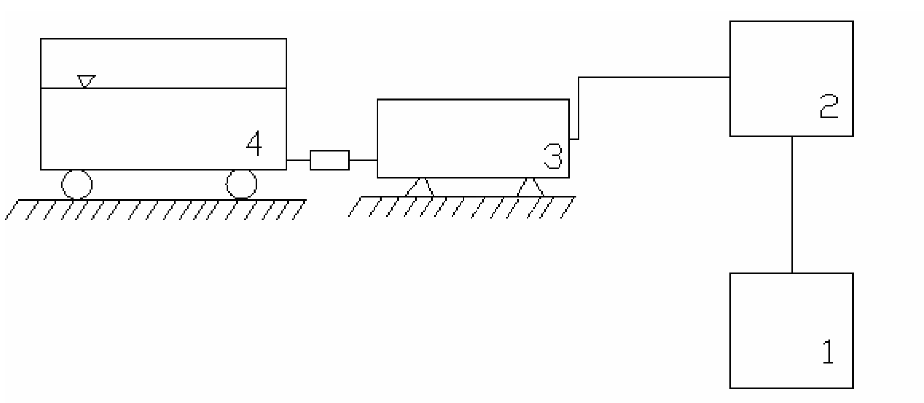

Figure 2.6.1. Schematic view of the experimental setup for the base excitation. 1: personal computer, 2: power amplifier, 3: electromagnetic shaker, 4: container.

Point masses were added to the flexible container walls, at the same location as in the numerical model, in order to vary the modal frequencies of the container. The purpose of these preliminary tests was to check the magnitude and the distribution of the liquid displacements at the free surface. To this end, the container was excited in an identical manner to that of the numerical displacements described earlier.

A transient sinusoidal displacement, same as numerical simulations at the sloshing frequency of the rigid container (1.34 Hz) was administered to the container's base. Then, the liquid motion was observed visually by placing rulers at various locations, on the inside vertical walls of the container, at the free surface of the liquid.

The magnitude of the disturbance was adjusted to provide a large enough surface displacement for reliable reading. The reported results were determined within ± 0.5 mm accuracy which was assumed to be acceptable. In addition, at least three repetitions were used to ensure the repeatability and are presented in Table 2.6.1.

Table 2.6.1 Observed liquid surface vertical peak displacement.

CASE	LIQUID DISPLACEMENT [mm]		
0 kg	56	58	60
3 kg	40	38	35
7 kg	23	20	18
9 kg	20	18	19
11 kg	25	23	24

The experimental observations are presented collectively in Figure 2.6.2, in the same format as the numerical predictions of Figure 2.5.8.

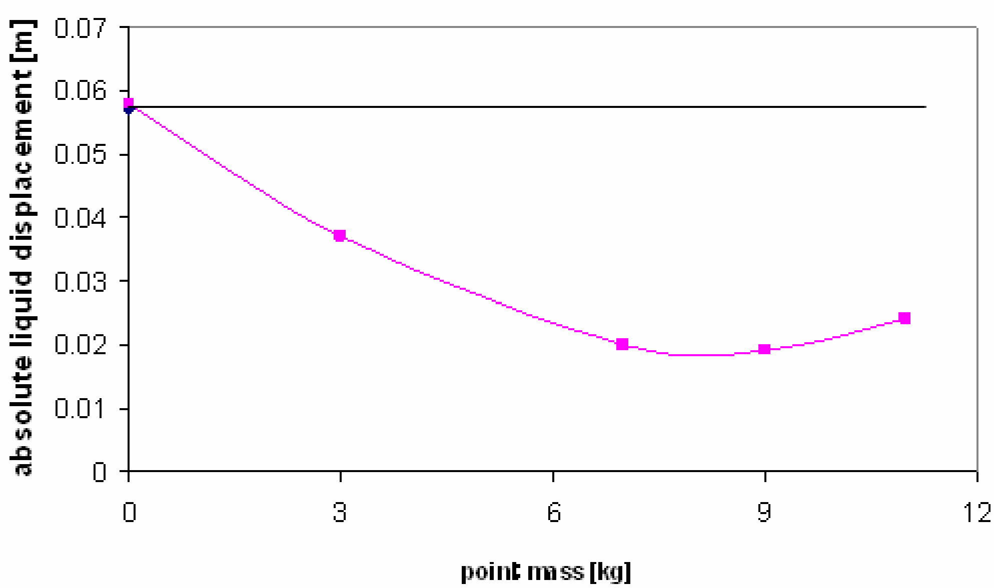

Figure 2.6.2. Absolute sloshing amplitude in m with mass for the rigid (—) and flexible (■) containers.

In Figure 2.6.2, the value of the added point mass is given along the horizontal axis, whereas the vertical axis represents the absolute displacement of the free surface of the liquid. The point at which the masses are added is the same as the nodes reported in the numerical predictions, located at the top of the container wall, in the middle of the long side.

The peak displacement of the free surface with 0 kg added mass is approximately 58 mm, virtually identical to the case of the rigid container. The rigid container case is marked with a solid horizontal line to provide the reference. As expected, as the mass increases, the displacement of the free surface becomes smaller. The displacement is 30mm with 3 kg, and 18mm with 7 kg. The change from 7 kg to 9 kg is quite marginal with approximately 70% reduction as compared to the rigid container case. After 9 kg, the change is more noticeable, but it is more gradual than the change to the left of 7 kg case. With these observations, it is assumed that the numerical predictions used in this thesis have practical merit, indicating the presence of "tuning" for effective suppression of the free surface.

Finally, it is worth noting that both the distribution of the free surface displacements around the container walls, and symmetry on both sides were checked, and confirmed to agree with the numerical predictions. Therefore, these experiments are believed to confirm the reliability of the numerical predictions.

2.7 Summary

Although sloshing has always attracted attention in the literature, attempts to control it have been relatively limited. The approach in this research is that it addresses the complexity of the problem without approximations and simplifications of its treatment. The objective is to design a container with intentional flexibility that will suppress excessive levels of liquid sloshing. Using intentional flexibility for this purpose is novel.

This chapter proves the design case studies where there is a strong interaction between the flexible container and the sloshing liquid. This strong interaction is achieved when the fundamental structural frequency, in the direction of sloshing, is tuned to the fundamental sloshing frequency of the liquid. Such a tuned flexible container should act in a similar fashion to a classical tuned absorber to control liquid oscillations. Numerical predictions suggest that the sloshing can be significantly reduced by tuning the interaction of the flexible container with liquid sloshing. Simple experiments confirm this assertion.

A summary of the extensive case studies indicate the possibility of employing container flexibility in reducing liquid sloshing. These attenuations are predicted to be in the order of 80 %, in the rms sense, as compared to a container with rigid walls. This level of attenuation is certainly quite promising. For the particular container, an optimal value of added point masses exists in a range between 7 kg and 9 kg, to achieve necessary tuning.

However, even with promising reductions of the sloshing amplitude, the practical difficulties may be caused by quite substantial wall deflections of the flexible container.

These static deflections are in the order of 0.075 m, after the flexible container is filled with water. If masses are added at the top of the container to achieve tuning, the container walls deflect even further. During the experiments, the largest added mass was found to be below 10 kg, to avoid excessive deflections. This problem is further addressed in the next chapter.

In closure, it should be stated that what is proposed in this chapter is merely the concept of “designing” flexibility to achieve sloshing control. No claim can be made for immediate practical application. Further issues related to excessive wall deflections and resulting dynamic stresses must be considered.

Use of added mass to achieve the coincidence of structural and sloshing frequencies, has been made for convenience. The same coincidence can be observed by manipulating structural stiffness as well.

Chapter 3

A FLEXIBLE CONTAINER MODIFIED USING STRAPS FOR SLOSHING CONTROL

3.1 Introduction

In Chapter 2 the possibility of using a container with flexible walls to control liquid sloshing was explored. The findings from Chapter 2 indicate that the flexibility of a container can suppress excessive sloshing only when there is strong interaction between the container and the liquid. The strong interaction between the container and the liquid was achieved when the fundamental container frequency, in the direction of sloshing, was tuned to the fundamental sloshing frequency of the liquid. This tuning between the liquid and the container walls, in this research was achieved by adding the point masses at the top of the container. However, this ideal condition may not be possible due to the structural constraints. This tuning may be further complicated by the multiple vibration modes which may be involved in the process.

When the container is filled, the container walls deflect substantially. This large deflection may cause difficulties in practical applications. Hence, it is desirable to limit those excessive wall deflections, to be able to maintain the effective control of the liquid sloshing. Large deflections are observed at the top of the container, away from the centre. Hence, rigid links (or straps) which are attached at the opposite sides of the open top, may limit the container deflections to more acceptable, practical levels. Findings obtained with this modified design suggestion are reported in this chapter.

This chapter is organized as follows:

- Section 3.2 gives details of the redesigned finite element model, developed to accommodate the structural change.
- Section 3.3 deals with predicted model parameters of the flexible container.
- Section 3.4 discusses the numerical predictions. As in chapter 2, predicted displacement histories of the liquid and the container walls are presented. Also presented are predicted sloshing amplitude and the corresponding frequency spectrum of the same cases to help the argument of "tuning". In the end, the rms liquid sloshing amplitudes are shown to summarize the presented cases.
- Section 3.5 outlines relevant experimental observations.
- Section 3.6 presents the conclusion.

3.2 Numerical Model and Procedure

3.2.1 Computational Setup

The container geometry used for this part of the study, is identical to that described in Chapter 2. It has a rectangular shape, 1.6 m in length, 0.4 m in width and 0.4 m in height. The container is modeled with two-dimensional rectangular shell elements. Each element has constant thickness, and it is defined by four nodes, ANSYS (2002). Critical damping of 1 % at the fundamental mode, is applied to the structure of the container walls without liquid. In addition, three link elements (straps) are attached at the top of the container, as shown in Figure 3.2.1. A strap's finite element is defined by two nodes, the cross-sectional area of the rectangle and material properties. The material properties of the straps, in this case, are aluminium. The cross -sectional area is taken to be 0.5e-4 [m^2].

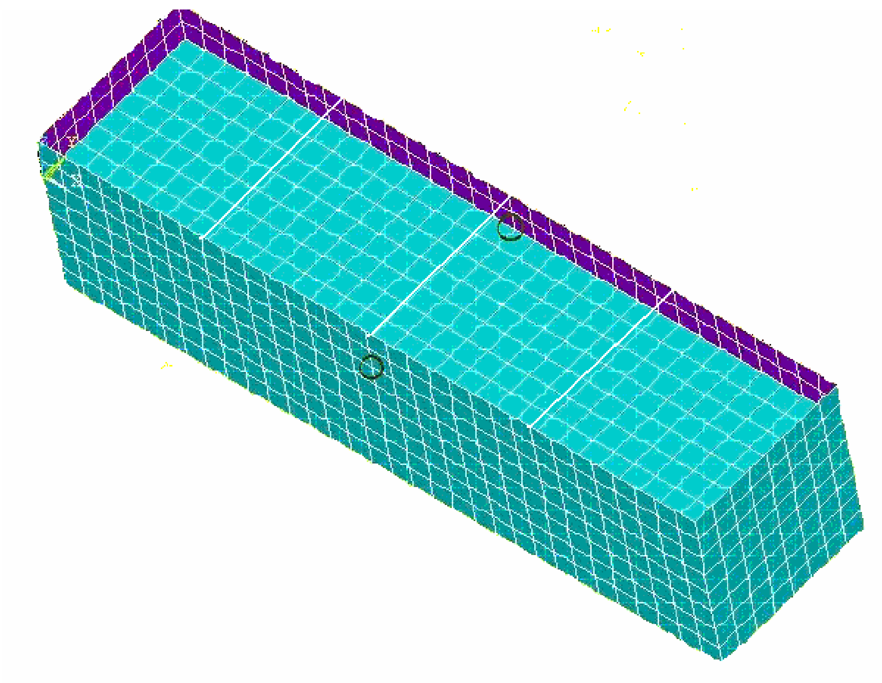

Figure 3.2.1: The numerical model, the location of straps and observation nodes (circled).

Three dimensional brick elements are used to model the liquid. The parameters are chosen for a homogenous, inviscid, irrotational and incompressible liquid. The liquid depth is 0.3 m the same as in Chapter 2. Also, the liquid is kept undamped throughout simulations. As in Chapter 2, fluid-structure interaction is achieved by coupling the liquid displacement with that of the container walls in the direction normal to the wall. The numerical model is illustrated in Figure 3.2.1 with top straps.

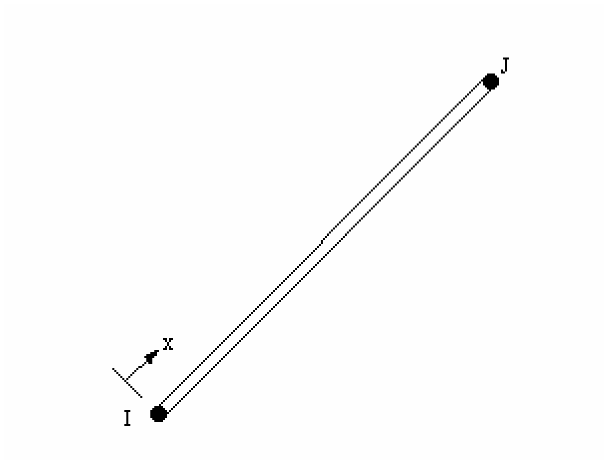

Figure 3.2.2: Finite Element-Straps

Figure 3.2.2 has a simple drawing of a link element, LINK8 (ANSYS 2002) - straps. As described earlier, this link element is defined by two nodes (I, J), cross sectional area and material properties with the element x axis oriented along the length of the element.

Similar to Chapter 2, two structural point mass elements are added to each long side of the container, on either side of the middle strap, in order to tune the dynamic response of the container to that of the sloshing liquid. A structural mass finite element is defined as a single node that has a concentrated mass.

3.3 Computational Simulations

The first three mode shapes of oscillation for the container with no straps, no added masses and no liquid are shown in Chapter 2 in a Figure 2.4.1. The first mode shape of oscillation, Figure 2.4.1 (a), showed that oscillations along the longest walls of the container were out of phase. The second mode shape of oscillation, Figure 2.4.1 (b), has showed that oscillations along the longest walls were in phase and the third mode shape of oscillation, Figure 2.4.1 (c), has showed much clearer separation of the frequency.

The first three mode shapes with straps are given in Figure 3.3.1. In contrast to Figure 2.4.1, all structural modes of oscillation along the walls are now in phase. This is, of course, expected due to the designed inflexibility of the straps. The first mode is a simple one, similar to the second mode of the case without straps. The other two modes, in Figures 3.3.1 (b) and (c) show more complex shapes as compared to those without straps.

The first three natural frequencies for the container without straps are given in Table 2.4.1 in Chapter 2. The first three natural frequencies for the container with straps are shown in Table 3.3.1 below. It is worth noting that the first natural frequency for the container without straps is slightly higher than for the case with straps.

a)

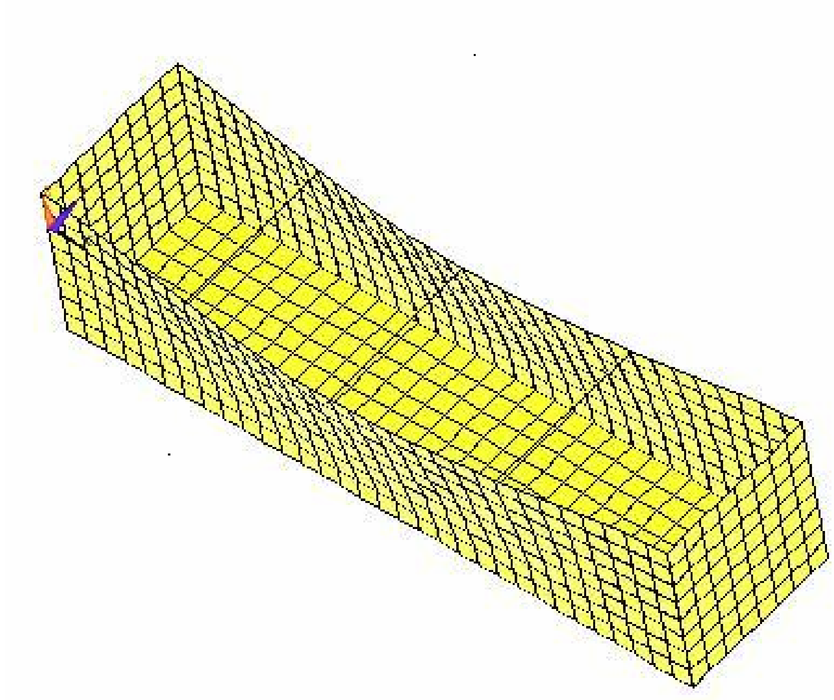

b)

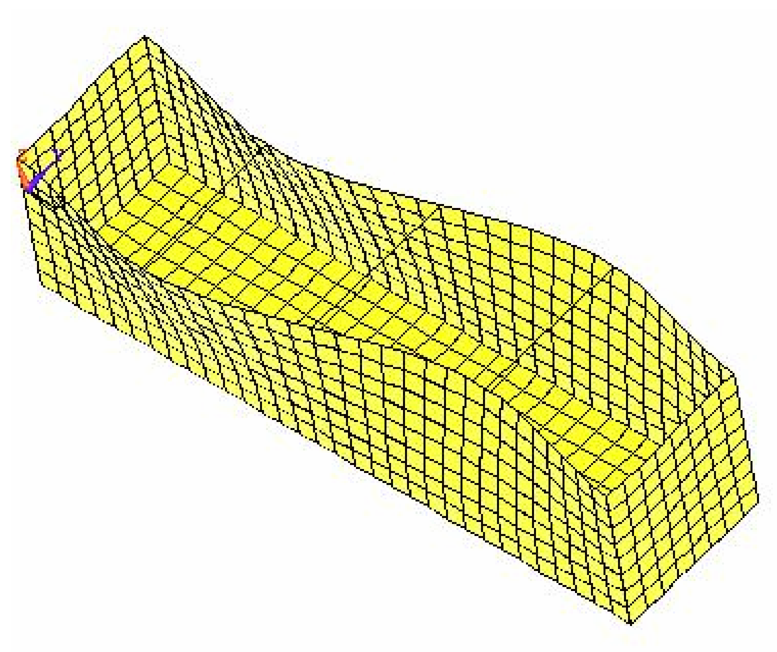

c)

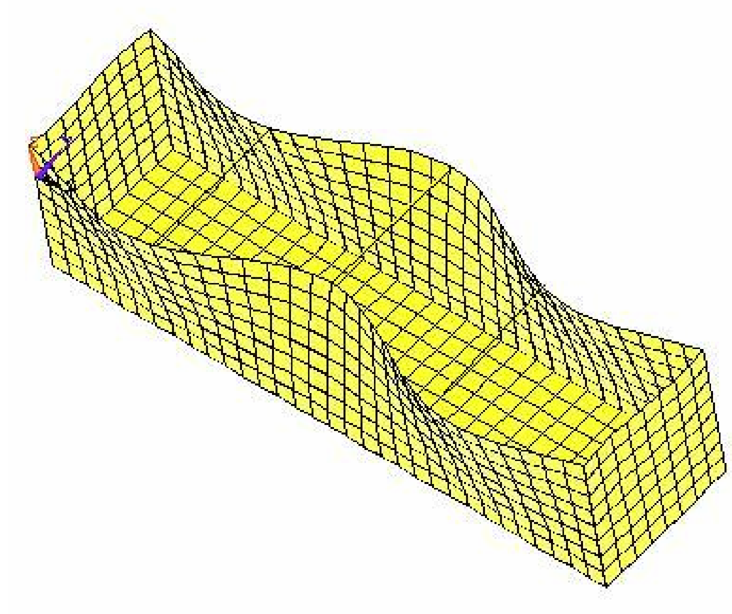

Figure 3.3.1: Mode shapes of the container with straps and no liquid

Table 3.3.1 First, second and third natural frequencies of the container without liquid for different mass.

Mass [kg]	1st natural frequency [Hz]	2nd natural frequency [Hz]	3rd natural frequency [Hz]
0	5.78	8.54	12.8
3	1.04	4.37	5.04
5	0.806	3.46	3.93
7	0.68	2.95	3.33
9	0.6	2.62	2.94
11	0.55	2.37	2.66
13	0.5	2.19	2.45

The structural frequencies without mass are significantly higher than the theoretical sloshing frequency of liquid, 1.34 Hz. By adding mass, the structural frequencies become closer to the sloshing frequency. However, starting from the lightest added mass, the fundamental structural frequency becomes significantly smaller than 1.34 Hz. (It should be kept in mind that the information in Table 3.3.1 is only for identification purposes of the container's structure.)

3.4 Numerical Predictions

In Chapter 2, the rigid container is used as the comparison base for the flexible wall cases with additional elements to demonstrate the effectiveness of sloshing control. The resulting sloshing amplitude for the rigid container is around 40 mm and is shown in Figure 2.5.1 (b).

The numerical predictions for 0, 3, 5, 7, 9, 11 and 13 kg added point mass cases, on either side of the middle strap are presented below. In all the following figures in frame (a), (▪, red) and (▪, dark blue) colors present horizontal displacement histories of the container and colors (▪, magenta) and (▪, light blue) present vertical displacement of the liquid. In the frame (b), the resulting sloshing amplitude is shown. In the frame (c), the frequency spectra of the container displacement (blue) and sloshing (red) are presented.

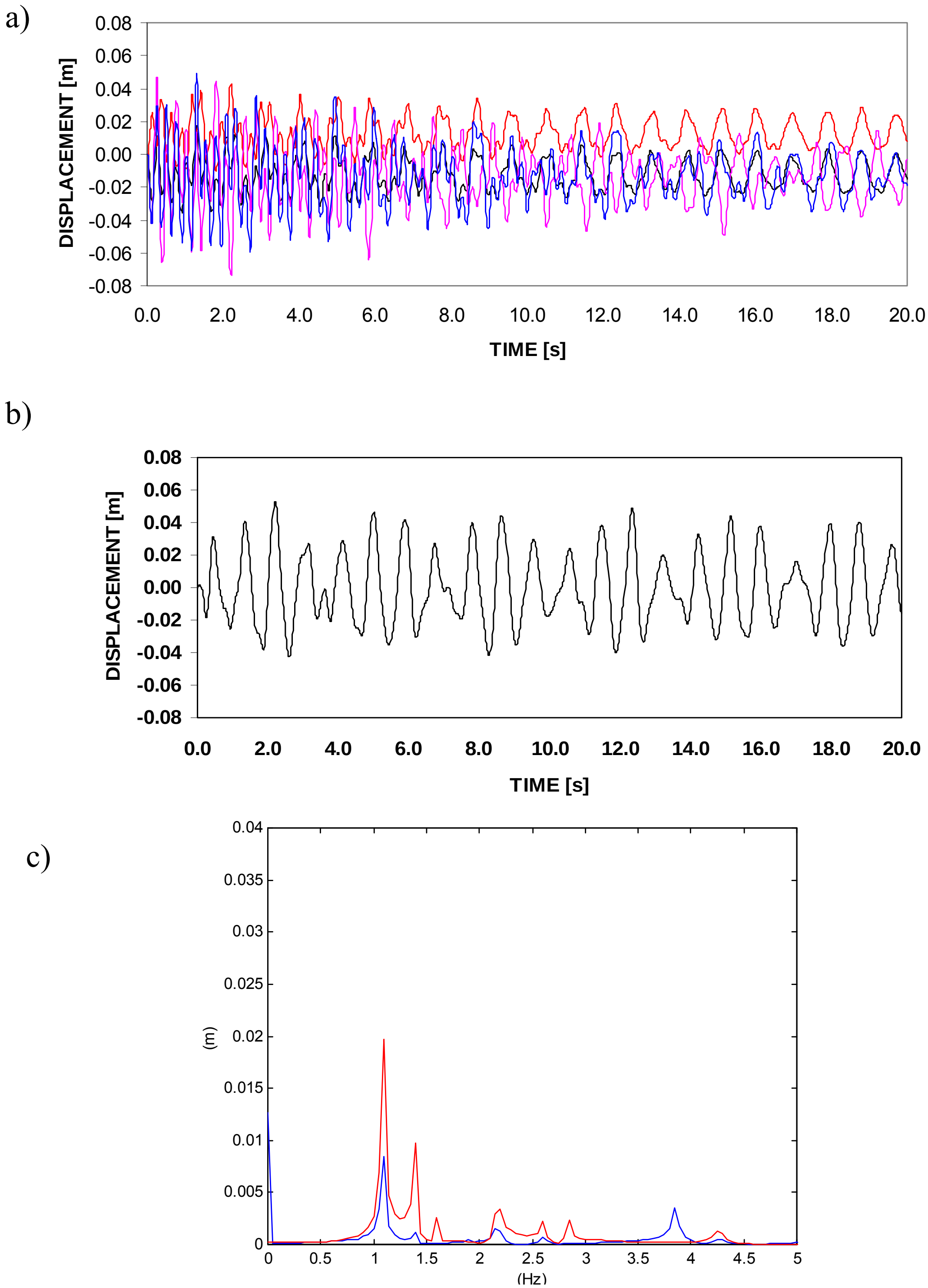

Figure 3.4.1: Displacement histories of the liquid in a flexible container with three straps on top, 1mm wall thickness and no added mass (a). The liquid is undamped and structure has 1% damping. Predicted sloshing amplitude for the same case (b). The frequency spectra of the container displacement (blue) and sloshing (red) are presented (c).

Referring to definition of the tuning process given in Chapter 2, the presence of significant energy transfer between the liquid and container is considered to be the sign of appropriate tuning. Tuning generally produces a beat envelope in the displacement history and two dominant spectral peaks in the corresponding frequency spectrum. This beat should be apparent both in the displacement histories of the container and at the liquid surface level.

The displacement history for the flexible container with 0 kg point mass is presented in Figure 3.4.1. As there is no beat clear in both histories of the container nor that of the liquid, this case is far from tuning. The sloshing history for the same case is given in Figure 3.4.1 (b). The sloshing amplitude for the case with 0 kg point mass is around 60 mm and is larger than that of the rigid container (40 mm). A slight beat envelope for the sloshing amplitude can be observed. However, despite this slight beat, there is little decay of the sloshing amplitude and the control effect is poor.

The frequency spectrum for the structural displacement of the container and the sloshing liquid are given in Figure 3.4.1 (c). Sloshing has spectral peaks at 1.1 Hz and around 1.4 Hz. This second spectral peak coincides with the theoretical fundamental sloshing frequency for the rigid container. The container has a spectral peak at 1.1 Hz, the same as the sloshing's first spectral peak. However, the spectral peak magnitude of the liquid is significantly larger than that of the structure's spectral peak, indicating forced vibration effect from the liquid on the container.

This frequency spectrum of the structure with the straps is significantly simplified when compared to the frequency spectrum of the structure without straps in the 0 kg point mass case. This can be observed comparing results from Figure 3.4.1 (c) with results shown in Figure 2.5.2 from Chapter 2. The structural peaks at 0.7 Hz, 1.7 Hz, 2.3 Hz and 2.7 Hz frequencies in Figure 2.5.2 (c), are suppressed with the addition of straps, as shown in Figure 3.4.1 (c). Only the structural peak at 1.1 Hz can be observed both with and without straps.

The displacement histories of the liquid and container walls for the case with 3 kg point mass added is presented in Figure 3.4.2 (a). With this added mass, the frequency spectrum of the structure is generally limited. In frame (b) the sloshing amplitude decreases below 40 mm. Also, the apparent beat envelope in the sloshing history, may indicate that this case is getting closer to tuning.

In frame (c) the spectral peaks for the liquid and structure move towards the left. The sloshing and the container have peaks at 0.5 Hz, 0.6 Hz and 0.7 Hz. The spectral peak magnitudes of the liquid are still significantly larger that that of the structure indicating that the forced vibration from the liquid on the container is still strong. This trend was not observed in Chapter 2 (Figure 2.5.3(c)) where the spectral magnitudes of the structure were significantly larger than those of the liquid.

a) b) c)

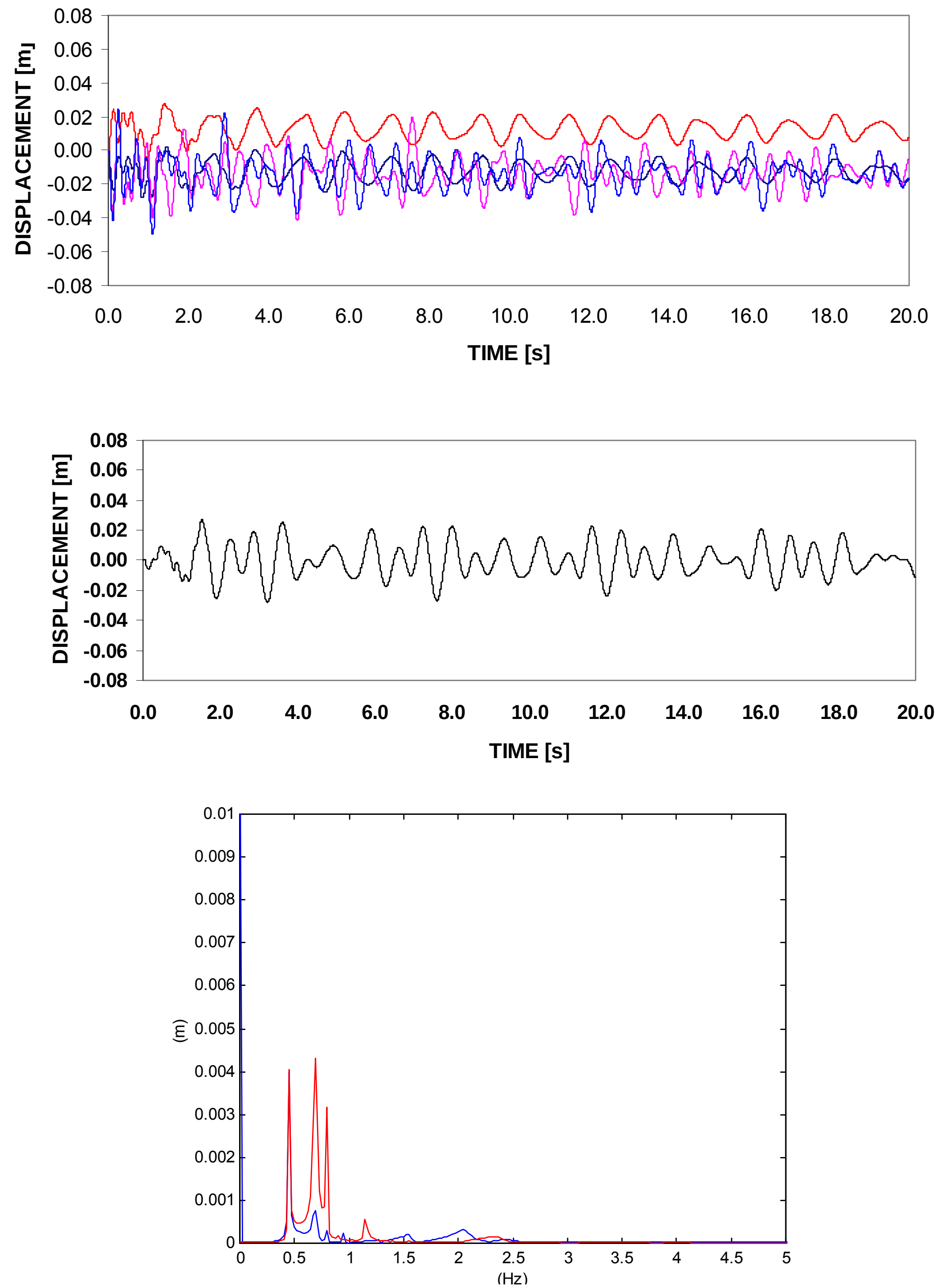

Figure 3.4.2: Same as in Figure 3.4.1, but for 3 kg mass.

The displacement history for the case with 5 kg added mass is presented in Figure 3.4.3. In frame (a), a further decrease in the frequency of the displacement histories can be observed. In frame (b), sloshing amplitude decreases further to approximately around 20 mm. There is no noticeable difference in the sloshing amplitudes at the end of the twenty second simulation time.

In frame (c), the structure has two dominant spectral peaks around 0.4 Hz and around 0.6 Hz. The liquid also has two spectral peaks that coincide with the structure's spectral peaks at 0.4 Hz and 0.6 Hz. The third sloshing peak with the largest magnitude is around 0.7 Hz. The first spectral peaks of both the liquid and the structure, at 0.4 Hz, are very close in height. The second spectral peak of the liquid, at 0.7 Hz, is still larger than that of the structure, indicating a forced vibration effect from the liquid on the container. This trend was not observed for the flexible container in the previous chapter, Figure 2.5.4.

The displacement history for the case with 7 kg point mass is presented in Figure 3.4.4. The trend in frame (a) does not change much from the previous case. In frame (b), sloshing amplitude decreases further to approximately around 15 mm.

In frame (c), the structure still has the same two dominant spectral peaks around 0.4 Hz and 0.6 Hz. The liquid still has a spectral peak around 0.4 Hz but the spectral peak around 0.6 Hz from the previous case is lost. The spectral peak around 0.7 Hz is still the largest magnitude of the liquid. At 0.4 Hz and 0.6 Hz, forced vibrations from the structure on the liquid can be observed.

a)

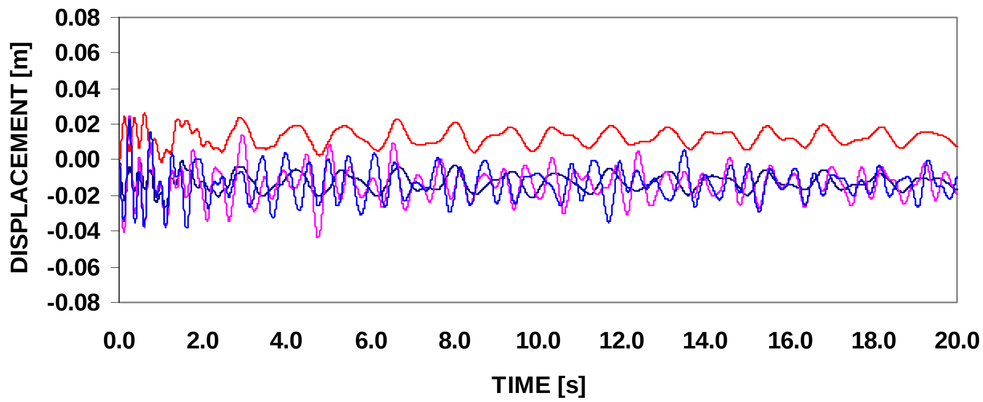

b)

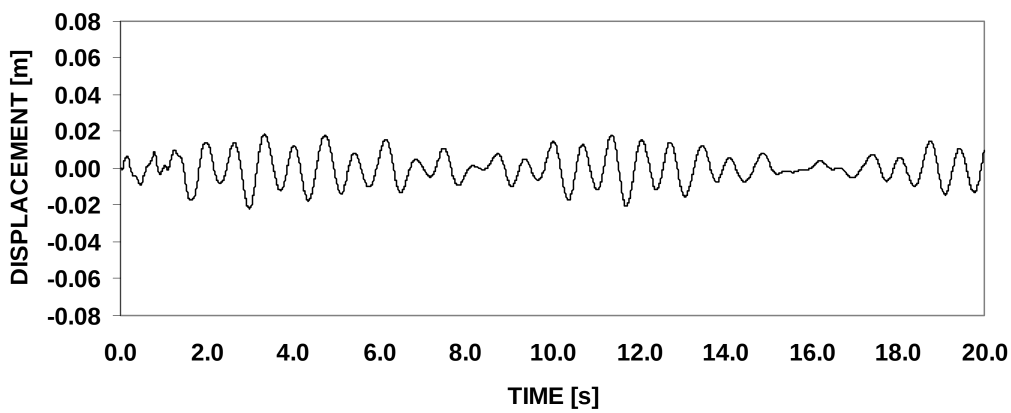

c)

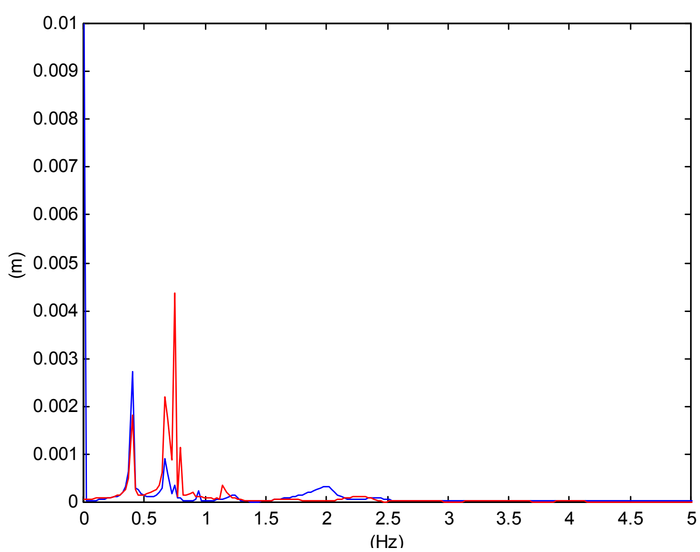

Figure 3.4.3: Same as in Figure 3.4.1, but for 5 kg mass.

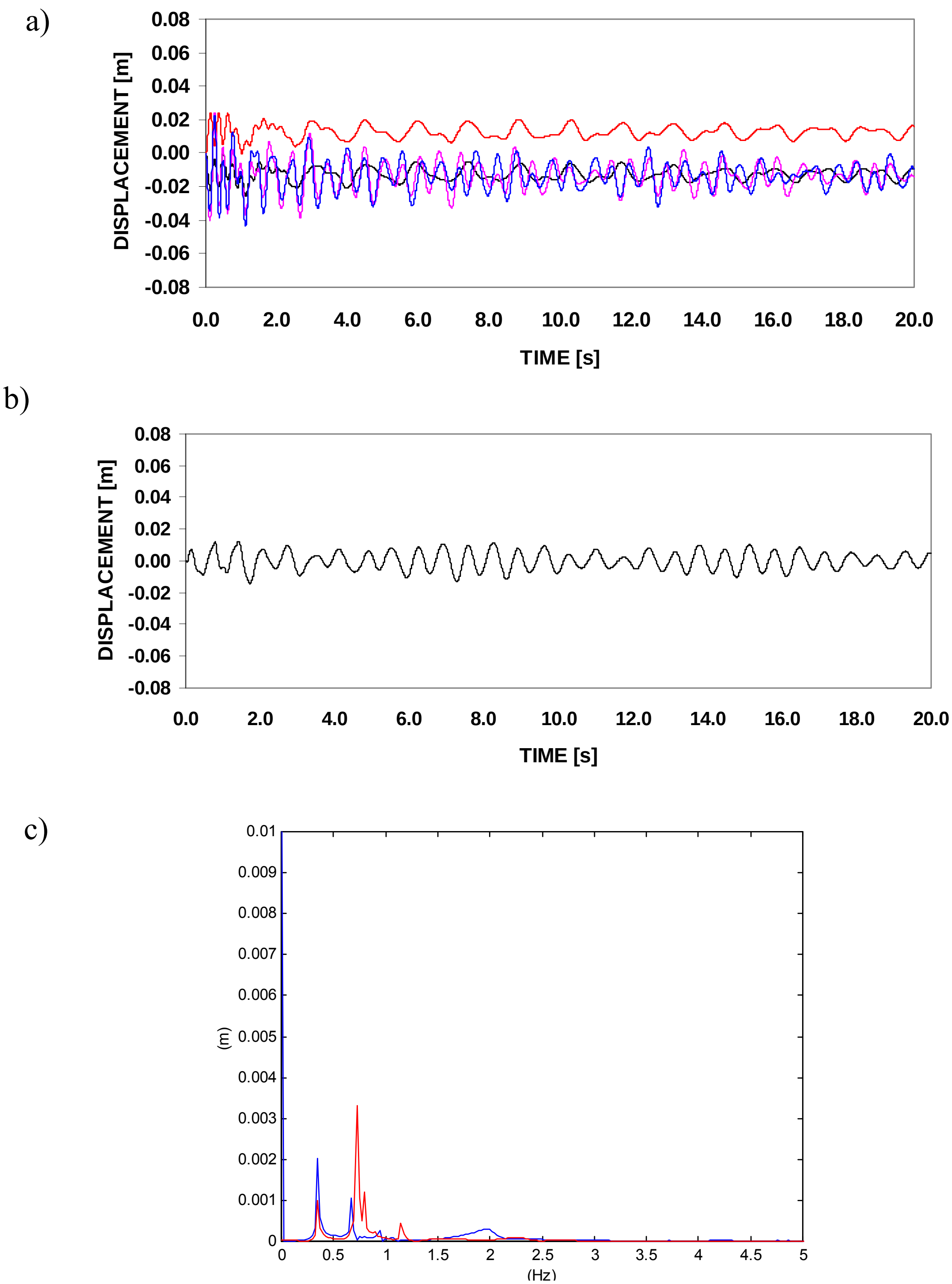

Figure 3.4.4: Same as in Figure 3.4.1, but for 7 kg mass.

a)

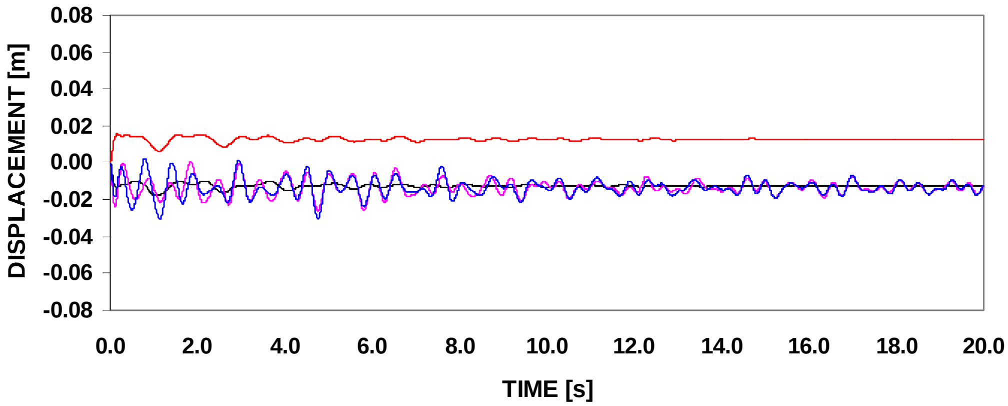

b)

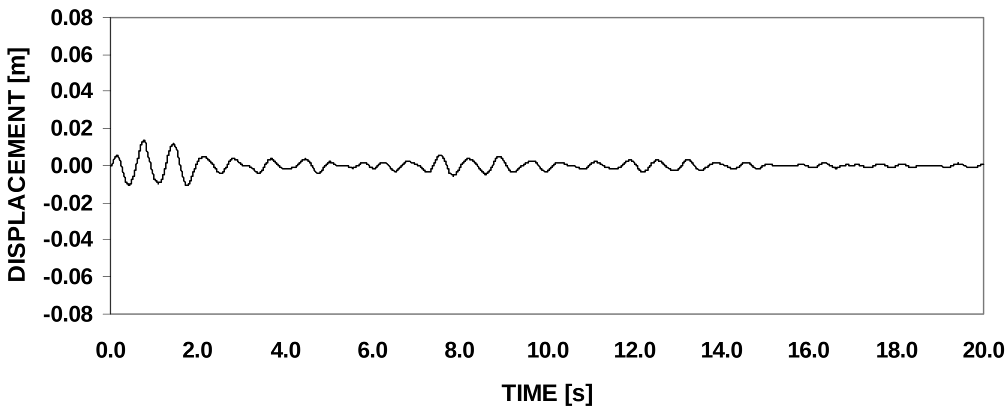

c)

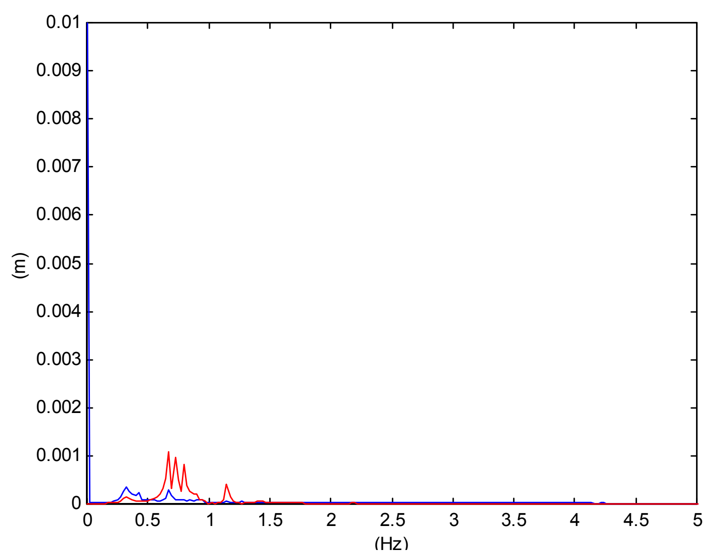

Figure 3.4.5: Same as in Figure 3.4.1, but for 9 kg mass.

The displacement history for the case with 9 kg point mass is presented in Figure 3.4.5 and this presents the most significant and surprising findings yet. The oscillation of the structure reduced drastically as can be seen from frame (a). The 9kg case corresponds to the most effective tuning for suppression of the liquid motion-sloshing. In the frame (b), the sloshing amplitude is reduced well below 5 mm by the end of the twenty second period with a very clear beat envelope in its history.

In frame (c), spectral distribution has changed drastically from the previous cases also. The structure's two spectral peaks at 0.4 Hz and 0.6 Hz have almost disappeared. There are three spectral peaks in the liquid between 0.8 Hz and 0.9 Hz. These amazing results indicate, quite unexpectedly, that the liquid has now suppressed the motion of the container very effectively. This trend is also very clear in frame (a).

With further increases of the added masses to 11 kg and 13 kg, in Figures 3.5.6 and 3.4.7, sloshing amplitudes begin to increase again, and are around 20 mm.

In figures (c), for both cases, spectral peaks that disappeared in the previous case, (9 kg point mass), start to appear again, now around 0.5 Hz. These frequencies are similar to the first natural frequencies of the container without liquid, shown in Table 3.3.1.

a)

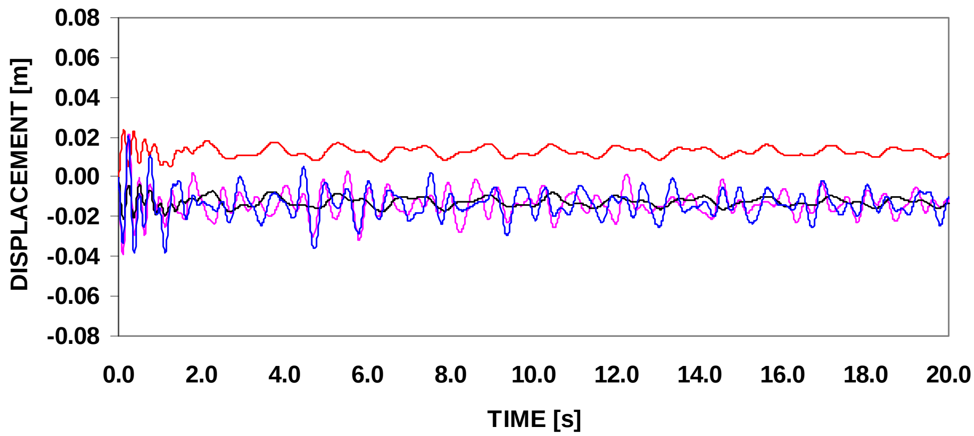

b)

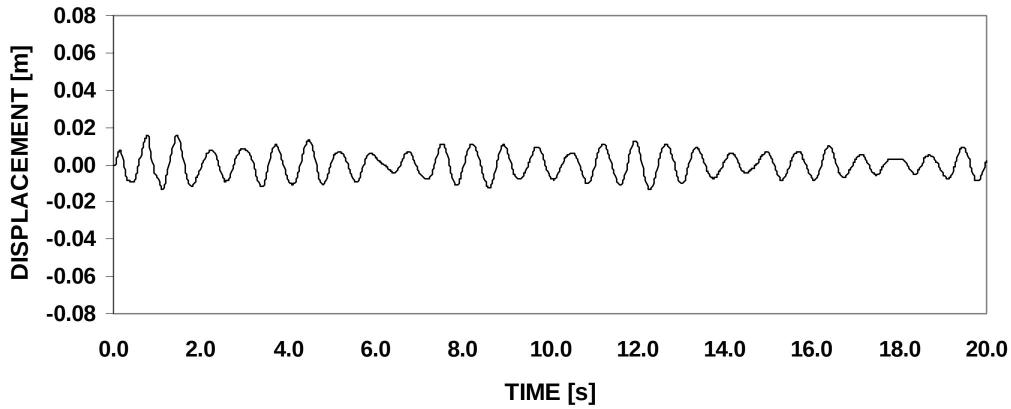

c)

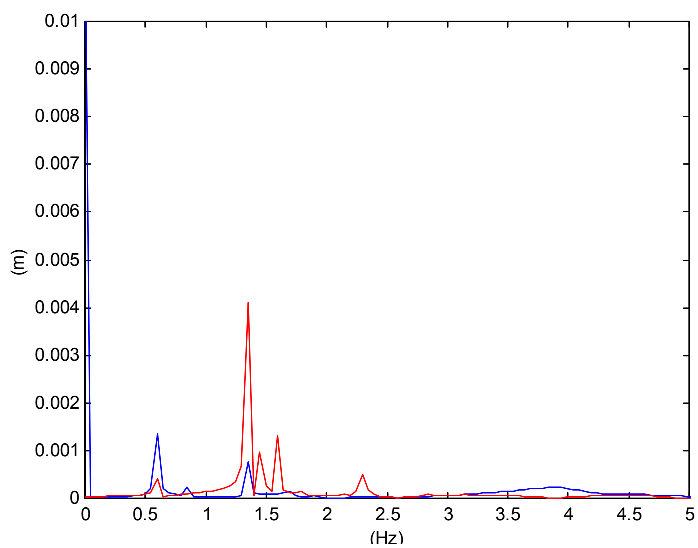

Figure 3.4.6: Same as in Figure 3.4.1, but for 11 kg mass.

a)

b)

c)

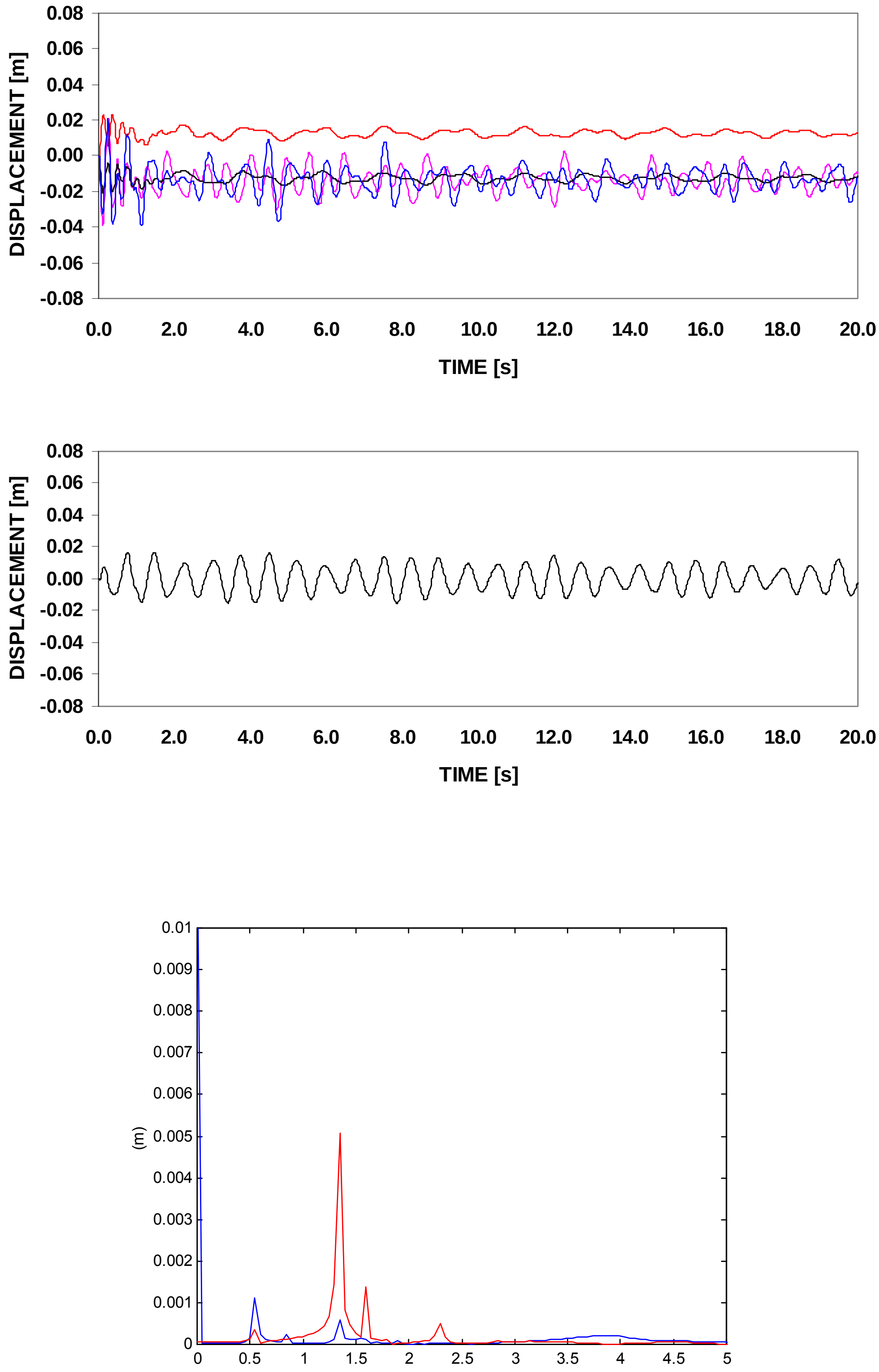

Figure 3.4.7: Same as in Figure 3.4.1, but for 13 kg mass.

In Figure 3.4.8, rms liquid sloshing amplitudes of different cases, are shown as a function of added mass for all cases, presented in Chapters 2 and 3.

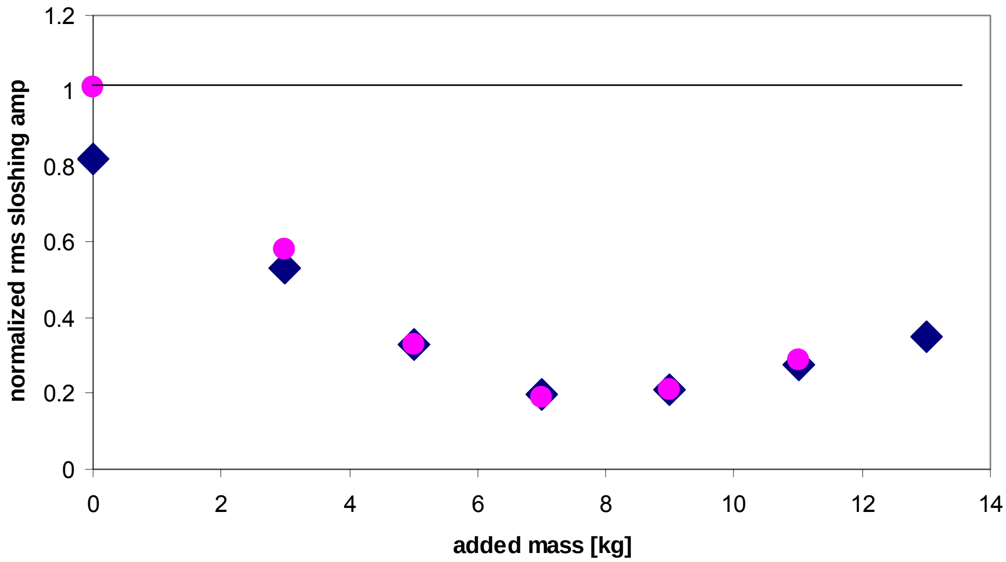

Figure 3.4.8: Variation of rms sloshing amplitude with added mass for cases: rigid container (——), flexible container without (◆) and flexible container with (●) straps.

The rms amplitudes of the flexible container are normalized by the rms sloshing amplitude in the rigid container. As seen in this figure, the optimal control achieved with straps corresponds to a decrease in the sloshing amplitude of about 80% between 6 to 10 kg added mass, another amazing result. This is similar to the results achieved for sloshing control without straps but with added masses in Chapter 2.

The control is marginally more sensitive for smaller added mass cases than for larger ones, as indicated by the steeper slope to the left of the best control case. Even considering there is no difference between results obtained in the reduction of the sloshing amplitude in Chapters 2 and 3, this new improved design has proved to be a far better practical design, given the addition of the straps at the top of the container has drastically reduced the excessive container vibrations.

3.5 Experiments

The experimental setup is identical to that in Chapter 2. As in Chapter 2, the liquid motion was observed visually by placing rulers at various locations, on the vertical walls inside the container, at the liquid's free surface. Light timber pieces (of approximately 15mm by 40mm cross-section) were added to the container to implement the rigid straps. Each case is repeated three times and data was observed for the cases with 0, 3 kg, 5 kg, 7 kg, 9 kg and 11 kg point mass added.

The experimental observations are presented collectively in Figure 3.5, in the same format as in Figure 2.6.2, given in Chapter 2.

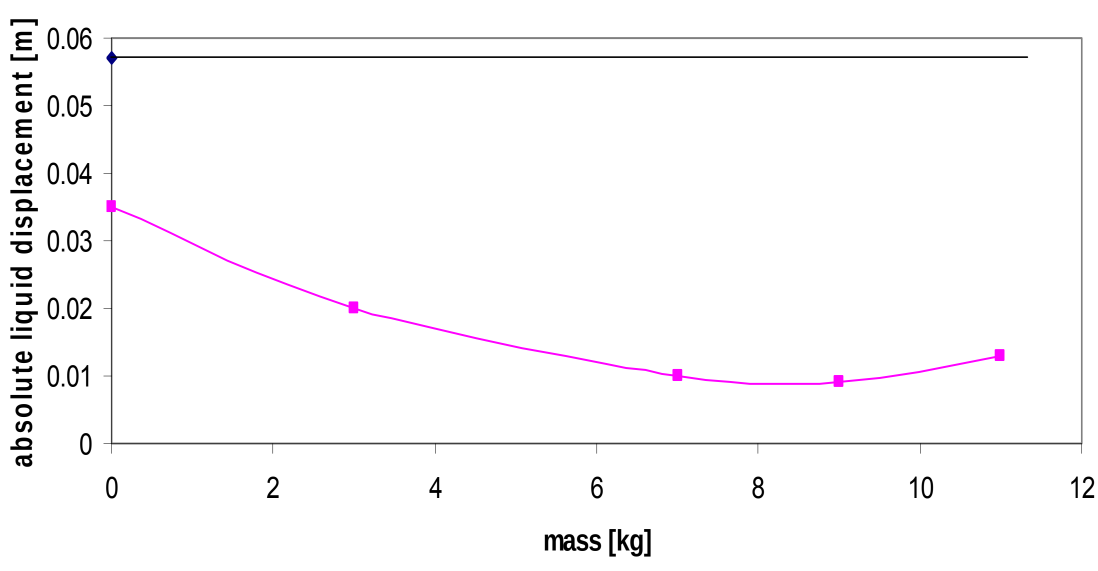

Figure 3.5: Absolute sloshing amplitude with added mass for cases: rigid container (——), flexible container with (▪) straps.

In Figure 3.5, the value of the added point mass is given along the horizontal axis, whereas the vertical axis represents the peak displacement of the liquid's free surface. The recorded point is the same as the one reported in the previous chapter.

The peak displacement of the free surface with 0 kg point mass is approximately 35 mm, lower than the displacement of the free surface for the rigid case. With increasing mass, the displacement of the free surface becomes smaller, (Figure 3.5) with a displacement around 25 mm at 3 kg, and 12 mm at 7 kg.

The change from 7 kg to 9 kg is quite marginal and shows the same trend as for the container without straps. Amazingly, the optimal control achieved with the straps corresponds to a decrease in the sloshing amplitude of about 80%, having fallen between 6 and 10 kg added point masses. After 9 kg, the sloshing amplitude begins to increases once more. Numerical predictions claimed the best suppression cases would fall between the 6 and 9 kg added point masses, these predictions are now supported by experimental data and Figure 3.6 confirms this.

3.6 Summary

A flexible container with rigid straps at the free top of the flexible container, has been investigated in this chapter for its effectiveness in suppressing the sloshing magnitudes. The motivation for the inclusion of the straps is the excessive wall deflections of the flexible container reported in Chapter 2.

Two masses are added to each long side of the container, on either side of the middle straps, in order to tune the dynamics of the container to that of the sloshing liquid.

Simulations have been run for 0 kg, 3 kg, 5 kg, 7 kg, 9 kg, 11 kg and 13 kg masses. The best suppression of sloshing is obtained around 7 6 kg to 9 kg added mass, with reductions in the sloshing amplitude of about 80%. By adding more masses the tuning effect is lost and the liquid sloshing amplitude starts to increase again. The numerical predictions of the tuning process have been verified with relevant experiments and reported here.

The modified design of the container with straps, shows a much improved performance. It enables just as effective sloshing control and significant limits the wall deflections of the flexible container, making the suggested design model more useful in practical applications.

Chapter 4

USING A FLEXIBLE CONTAINER

FOR VIBRATION CONTROL

4.1 Introduction

This chapter reports on the results of an investigation on the possibility of using intentionally induced liquid sloshing for structural vibration control. The container of the sloshing liquid is firmly attached on the structure to be controlled, and the dynamic forces which result from the sloshing in the container are used for control purposes on the structure. Although the concept has been explored earlier, the novelty here is to use the flexible container employed in the earlier chapters of this thesis. In contrast to the earlier chapters, the objective is not to suppress the magnitude of sloshing, but to employ its dynamic forces on the container walls to vibration control purposes. Such a control strategy may be useful in suppressing and unwanted excessive oscillations in structures, such as high rise buildings exposed to wind and earthquake loads.

The chapter is organized as follows:

- Section 4.2 is a literature review of previous work concerning the application of tuned liquid dampers for structural control.

- Section 4.3 gives details of the numerical procedure developed to simulate the liquid and flexible structure interaction when attached to the structure needing control. A three-dimensional numerical model of the sloshing absorber is discussed using finite element method.
- Section 4.4 discusses the numerical predictions to show the trends of the control effect.
- Section 4.5 presents the conclusions.

4.2 Background

4.2.1 Literature review

The concept of using sloshing forces for structural control has been the subject of intensive research for many years and its effectiveness in controlling those forces has been verified in theory and practice. The most commonly used liquid dampers are Tuned Liquid Dampers (TLD) and Tuned Liquid Column Dampers (TLCD). Both deep and shallow water configurations of tuned liquid dampers, which exploit the amplitude of fluid motion and wave–breaking patterns to provide additional damping, are widely explored in the literature.

Modi and Welt (1984) pioneered research on Nutation dampers and their applications in tall structures. Their approach to employing sloshing has been to use it as a means to control structural oscillations. This work is directed towards encouraging the sloshing action rather than suppressing it. Fujii et al. (1990) reported using liquid motion in a circular container to reduce wind-induced oscillations at Nagasaki Airport Tower and

Yokohama Marine Tower, to about half the uncontrolled values. Their work is also directed toward encouraging the sloshing action rather than suppressing it.

Abe et al. (1996) report effective control of structural vibration using a U-tube with a variable orifice passage. Seto and Modi (1997) present work to use fluid-structure interaction to control wind induced instabilities. Their numerical model was based on the shallow water wave theory. They assumed that relatively simple shallow water wave theory, viscosity and wave breaking are major factors that contributed to dissipation. Whilst Anderson et al. (1998, 2000a, 2000b) proposed a sloshing absorber of standing wave type. It was acknowledged that standing wave theory has poor energy dissipation characteristics, but by employing cantilevered baffle plates, the performance of a standing wave sloshing absorber could be enhanced.

Reed et al. (1998) investigate tuned liquid dampers under large amplitude excitation. Experimental and numerical modeling of the tuned liquid dampers were investigated. They concluded that in the case when a certain excitation frequency was higher than the fundamental natural frequency of the sloshing water, the response of the tuned liquid damper suddenly ceased. They also found that the tuned liquid damper‘s frequency increased as the excitation amplitude increased.

Fujino et al. (1988) studied TLD. The study expressed the advantages of TLD as they enable easy adjustment of natural frequencies and maintenance is low cost. But concern was expressed about the adverse effect that can occur if the wave motions do not diminish immediately after the excitation, as some of the energy absorbed by the TLD is transferred back to the structure. Gardarsson et al. (2001) investigate the possibilities of avoiding those adverse affects mentioned above and recommended a tuned liquid damper with a sloped bottom. Sloshing motion in a tank with 30 degrees sloped sides was studied. The outcome was softening (or lessening) of the spring characteristic of the free surface elevation due to the nonlinear effects of the wave run up onto the sloped surfaces. Energy dissipation was used in Fujino et al. (1992) when simulating a tuned liquid damper for suppressing structural oscillations. The conclusion was that the TLD, where water is used as a sloshing fluid, is effective only in a narrow frequency range.

In sloshing controllers plain water, which has poor energy dissipation characteristics, is normally used as the working fluid. In order to improve energy dissipation, Kaneko and Yoshida (1994) suggest employing a net to obstruct the flow of liquid during sloshing, and reported optimum levels of obstruction for the best structural control. Warnitchai and Pinkaew (1998) investigates the effect of flow damping devices such as vertical poles, blocks and nets on sloshing in rectangular tanks for the purpose of controlling structural oscillations. In this case, the liquid was assumed to be inviscid, incompressible and irrotational. Surface tension effects appear to be neglected. The model of liquid sloshing which included, flow-dampening devices, is restricted to two dimensional liquid sloshing in a rigid container.

Sakamoto et al. (2001) using both analytical and experimental methods proposed tuned sloshing dampers using electro-rheological fluid. Soong and Spencer (2002) propose magnetorheological and electrorheological fluid dampers, acknowledging the complexity of fluid-structure interaction when attempting to estimate energy dissipation performance. Research into shallow liquid levels in a container are likely to induce traveling sloshing waves with desirable energy dissipation. For this reason, earlier work invariably dealt with shallow liquid levels in the tuned sloshing absorbers. Even in the work of Kaneko and Yoshida (1994) which employs a relatively larger depth than those of the others, the water depth is approximately equal to 35% of the length of the container. Such small depth may be quite limiting for some geometries such as liquid storage tanks in tall structures. This particular point is addressed in this study with water depth of the absorber comparable to the length of the container. Sun et al. (1994) proposed an analytical model for a tuned liquid damper using a rectangular tank filled with shallow liquid. In this model it was assumed that the free surface was continuous and the model was valid as long as no breaking waves occurred.

Deep liquid levels cause a standing sloshing wave at the fundamental mode. Without additional measures, the suppression effect of a standing sloshing wave is quite limited. For such cases, the oscillatory energy of the structure could be easily transferred to the sloshing liquid, if there is a strong interaction. A strong interaction is assured when the sloshing frequency is close to the natural frequency of the structure. However, if there is no dissipative mechanism in the sloshing absorber, this transferred energy in the liquid may travel back to the structure to excite it quite easily. Due to phase difference, the exchange of energy between the structure and the liquid produces a beat envelope of oscillations of the structure. Such a beat drastically reduces the control effect.

There are a number of research papers involved in developing numerical models of the tuned liquid dampers. Nomura (1994) and Yamamoto and Kawahara (1999) use finite elements with moving grids based on the Arbitrary Lagrangian Eulerian formulation. Numerical instability problems, at the free surface, were reported by Yamamoto and

Kawahara (1999) and their results include smoothing functions. Pure sloshing motion studies show that it is essential to describe the free surface's nonlinear behaviour accurately in order to know if the tuned liquid damper is working.

4.2.2 Summary of literature review

All preceding work cited here has been directed to understanding the physics of the phenomenon, dealing with sloshing absorbers in rigid containers exclusively. The results reported in Chapter 2 indicate that investigation of a flexible container in this new application could again produce a practical alternative. There are no reported attempts in the literature to explore the possibilities of employing a flexible container.

This chapter outlines the research on the use of a flexible container as a sloshing absorber attached to a resonant structure. As it will be briefly discussed next, container flexibility introduces an additional tier of tuning to that of an already existing tuning issue between the sloshing liquid and the structure to be controlled. The objective of this study is to present the effect of this additional tuning effect.

4.3 Numerical Procedure

A commercial finite element package, ANSYS (2002), was used to model the dynamics of the container, sloshing liquid and the structure to be controlled. A schematic view of the model with a grid size of 50mm x 50mm, is given in Figure 4.3.1 (a).

a)

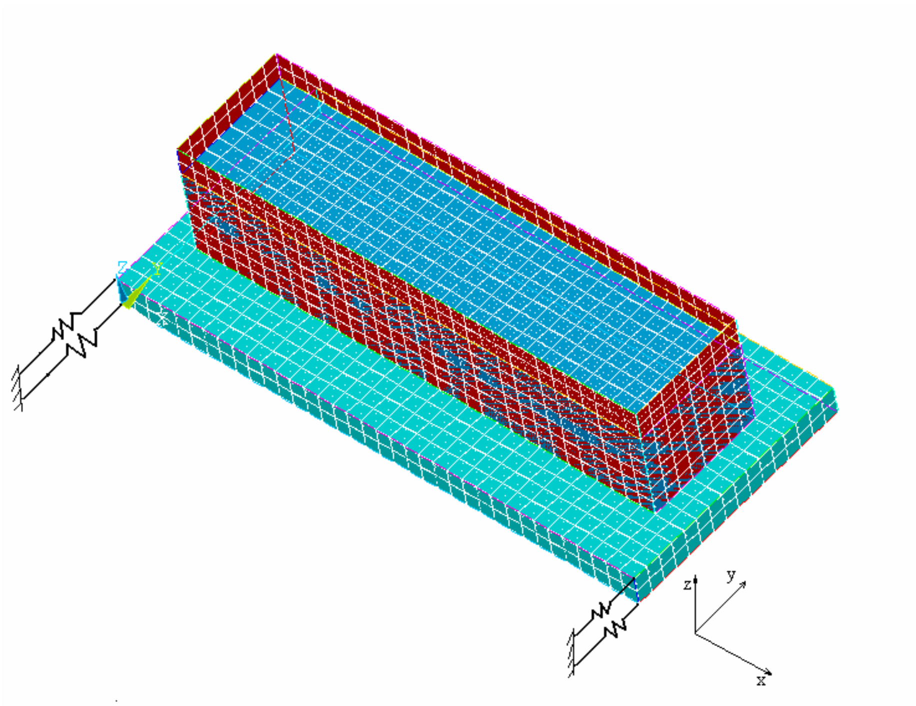

b)

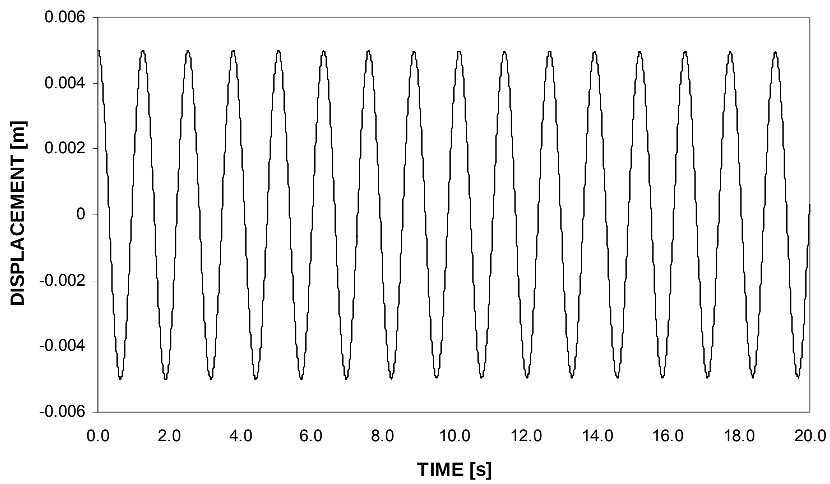

Figure 4.3.1: Showing (a) the computational model and (b) the displacement history of the structure after an initial displacement of 5 mm.

The sloshing absorber consisted of a rectangular aluminium container of 1.6m x 0.4m x 0.4m in length, width and height. The wall thickness was 1mm. Two-dimensional rectangular shell elements were used for the container walls with 1.5% critical damping in the fundamental mode. The container was filled with water to a depth of 0.3 m, corresponding to a mass of approximately 192 kg. The liquid was modelled using three-dimensional brick elements. The liquid has no damping.

Fluid and container interaction was achieved by coupling the displacement of the liquid and the container walls in the direction normal to the container walls. A solid steel element was used to model the mass of the structure. The structure was attached to a rigid wall by four springs. The base of the container was attached to the top of the structure. The mass of the structure was 2000 kg which resulted in a mass ratio between the sloshing absorber and the structure to be controlled of approximately 0.10.

The sloshing absorber was orientated such that a sloshing wave was induced in z-direction in response to a 5 mm initial displacement administered to the base of the structure in y-direction. A transient solution was obtained with a time step of 0.01s, for a total duration of twenty seconds.

The concept of using liquid sloshing in a flexible container to control structural vibration is similar to that of using a tuned absorber to control excessive vibrations of a mechanical oscillator. The fundamental sloshing frequency of the liquid in a rigid container is approximately 1.34 Hz. Hence, the natural frequency of the structure was also set to this value to achieve strong interaction, the same as that of a classical tuned absorber.

In the case of a flexible container, there is a second level of tuning between the liquid, the container and the structure to be controlled. As mentioned earlier, the primary objective of the presented work is to demonstrate the effect of this particular secondary tuning on the structure's response. Hence, the case runs include different values of tuning frequencies of the flexible container. Different frequencies of the flexible container were obtained by symmetrically adding two point masses in the middle of the 1.6m length, at the top edge of the container (as was done previously).

A solid element was used for the three-dimensional modeling of the solid structure. The element is defined by eight nodes having three degrees of freedom at each node; translations in the nodal x,y and z directions. The geometry, node locations and the coordinate system for this element are shown in Figure 4.3.2.

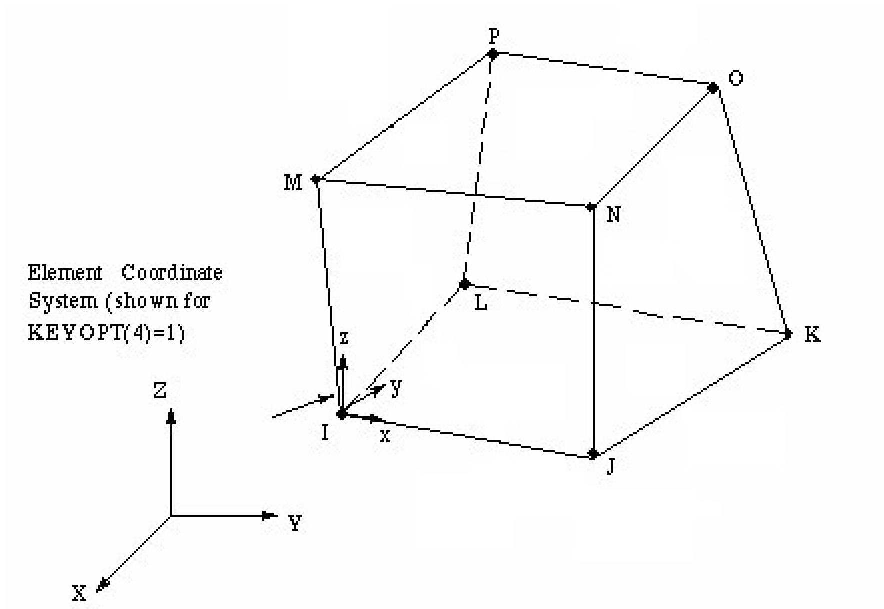

Figure 4.3.2: Three dimensional solid structure element [ANSYS 2002]

The longitudinal spring-damper option is a uniaxial tension-compression element with up to three degrees of freedom at each node: translation in x,y and z direction. The geometry, node locations, and the coordinate system for this element are shown in Figure 4.3.3.

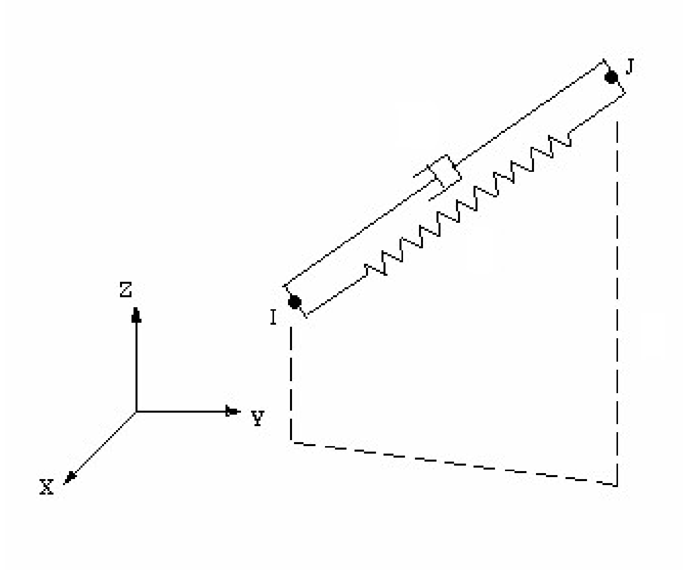

Figure 4.3.3: Spring element [ANSYS 2002]

4.4 Numerical Predictions

In Figure 4.3.1 (b), displacement history of the structure is given without the sloshing absorber in the y-direction. Since no damping is included in the structure's model, the induced initial displacement of 5 mm remains unchanged indefinitely. Figure 4.3.1 (b) is included here, as the comparison base for all cases with the sloshing absorber.

In Figure 4.4.1, the case of the rigid container is presented. The displacement of only two liquid nodes is given. These undergo an almost perfectly out-of-phase motion, in response to the initial displacement given to the structure, as shown in Figure 4.4.1 (a). The sloshing magnitude is 60 mm, as shown in Figure 4.4.1 (b). The clear beat envelope is the result of imposed "tuning" between the sloshing frequency and the natural frequency of the structure. The beat indicates strong interaction when there is the back-and-forth flow of energy between the liquid and the structure. The beat envelope is at a peak when most of the kinetic energy is with the sloshing liquid. The beat envelope diminishes to approximately zero, and the free surface becomes flat temporarily, when the energy is transferred to the structure.

The same clear beat envelope is also apparent in the displacement history of the structure in Figure 4.4.1 (c), but out-of-phase with that of Figure 4.4.1 (b). The peak displacement of the structure is 5mm, the same as in Figure 4.3.1(b), since neither the structure nor the liquid have any means of dissipating energy.

In Figure 4.4.1 (d), the tuning is clearly marked with the sharp trough at 1.34 Hz, along with the two spectral peaks at approximately 1.2 Hz and 1.45 Hz (which are responsible for the beat envelope with a 4-second period). The small spectral peak at approximately 2.3 Hz marks the second sloshing mode.

The numerical predictions presented in Figures 4.4.2 to 4.4.8 (a), include displacement histories of four nodes - two of the flexible container and two of the liquid. The histories of the container nodes are the two top and bottom ones (dark blue and red), whereas the liquid nodes (light blue and magenta) are in the middle. All nodes are selected to be at the level of the free surface, in the middle of the long side of the container. The container displacement is in the same direction with the initial disturbance, in y-direction, whereas the induced liquid motion is in z-direction.

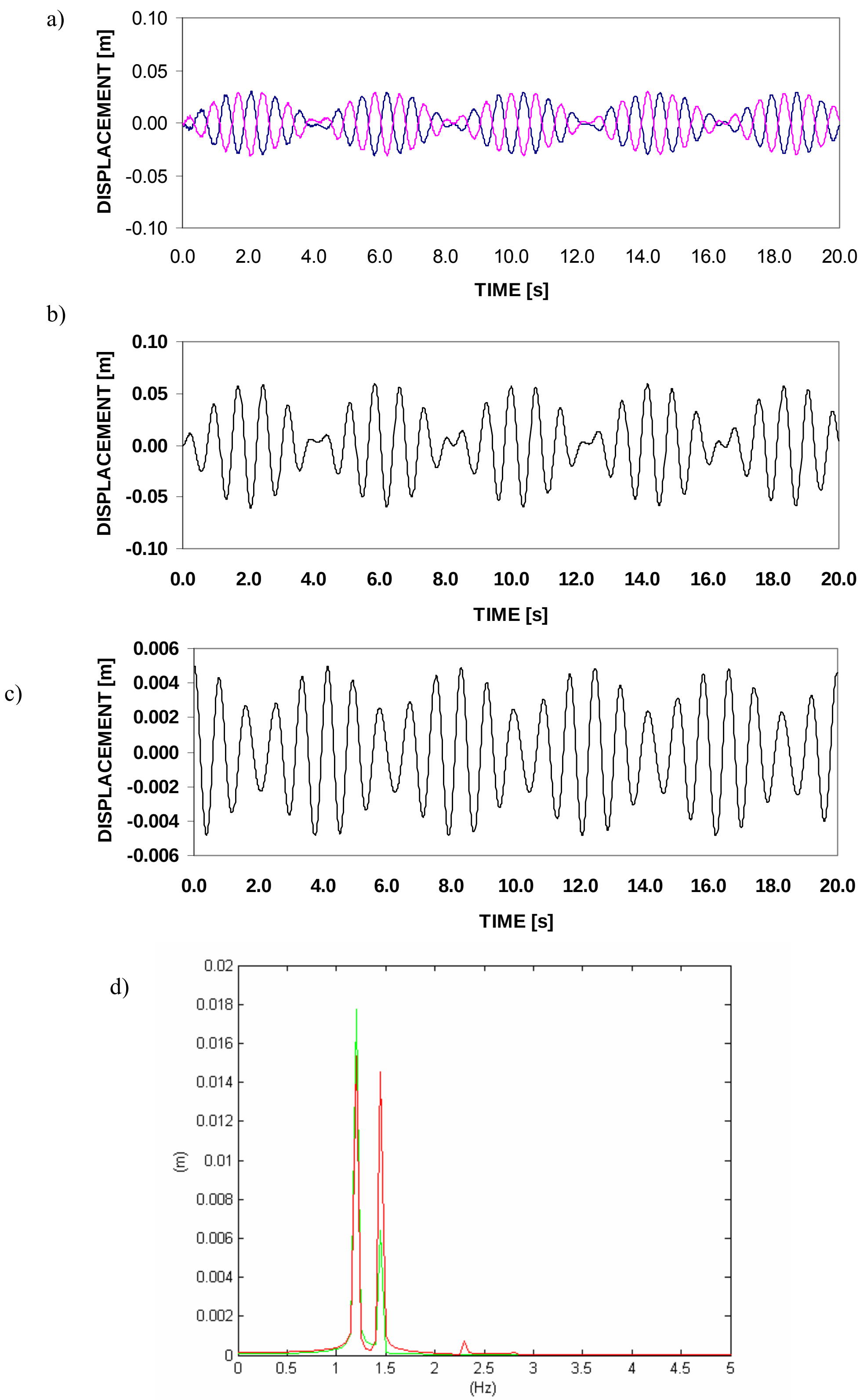

Figure 4.4.1: a) numerically predicted displacement histories of the sloshing absorber: liquid displacement histories in container with rigid walls. b) predicted sloshing amplitude, c) structure displacement and d) FFT of sloshing liquid (red) and plate displacement (green).

Figures 4.4.2 to 4.4.8 (b), include the history of sloshing which is the difference of the displacement of the two free surface liquid nodes as previously stated. As sloshing refers to the out-of-phase motion of the liquid free surface, the second column value is zero when there is no surface deflection and when the two liquid nodes move in-phase. The resulting sloshing amplitudes are for a flexible container at different tuning frequencies. As mentioned earlier, tuning of the flexible container is attempted by adding point masses to it, in the middle of the long side of the container at the top. The cases are with 0 kg, 3kg, 5kg, 7kg, 9kg, 11kg and 13kg added point masses.

In Figures (c) from 4.4.2 to 4.4.8, the displacement histories of the structure are presented. It may be worthwhile to repeat that Figure 4.3.1 (b) is the comparison base for all cases in figures (c). Again, following the same order, the corresponding frequency spectra are given in Figures (d) for the same graphs. In those figures, liquid sloshing is marked with red, the flexible container is marked with blue and the structure is marked with green.

In Figure 4.4.2, the flexible container case is shown with 0 kg point mass. With the dimensions listed earlier, and with a 1mm wall thickness, the container is clearly off-tuned. In the figure (a), the top and bottom histories, corresponding to the displacement of the container walls, show large deflections. This is clearly different than that of the liquid nodes, in the middle. In the figure 4.4.2 (b), the beat of the envelope is much less apparent than the case discussed for the rigid container. Sloshing magnitude is approximately 80mm, as compared to the 60mm magnitude of the rigid container.

In Figure 4.4.2 (c), the displacement history of the structure still suggests a beat, although it is somewhat less uniform than that in Figure 4.4.1 (c). As a result of the container oscillations, the peak displacement of the structure is attenuated to 4mm, from the starting 5mm by the end of the twenty second simulation. Hence, amplification of the sloshing from 60 mm to 80 mm, is not necessarily detrimental to the control action on the structure which is the primary objective of the investigation. In addition, despite the off-tuned container, it is interesting to note that the frequency of oscillations of the structure within the envelope is quite comparable to that of sloshing, shown in the Figure 4.4.2 (c).

The spectral distributions in Figure 4.4.2 (d) are rather complicated, partly due to the presence of multiple modes of the container in this off-tuned case. Multiple spectral peaks make it difficult to comment on their relative importance, with the exception of the original sloshing frequency of approximately 1.34 Hz.

As a result of the lack of any coherent interaction with the flexible container, sloshing largely reverts to its original frequency, also forcing a response from both the structure and the container at the same frequency.

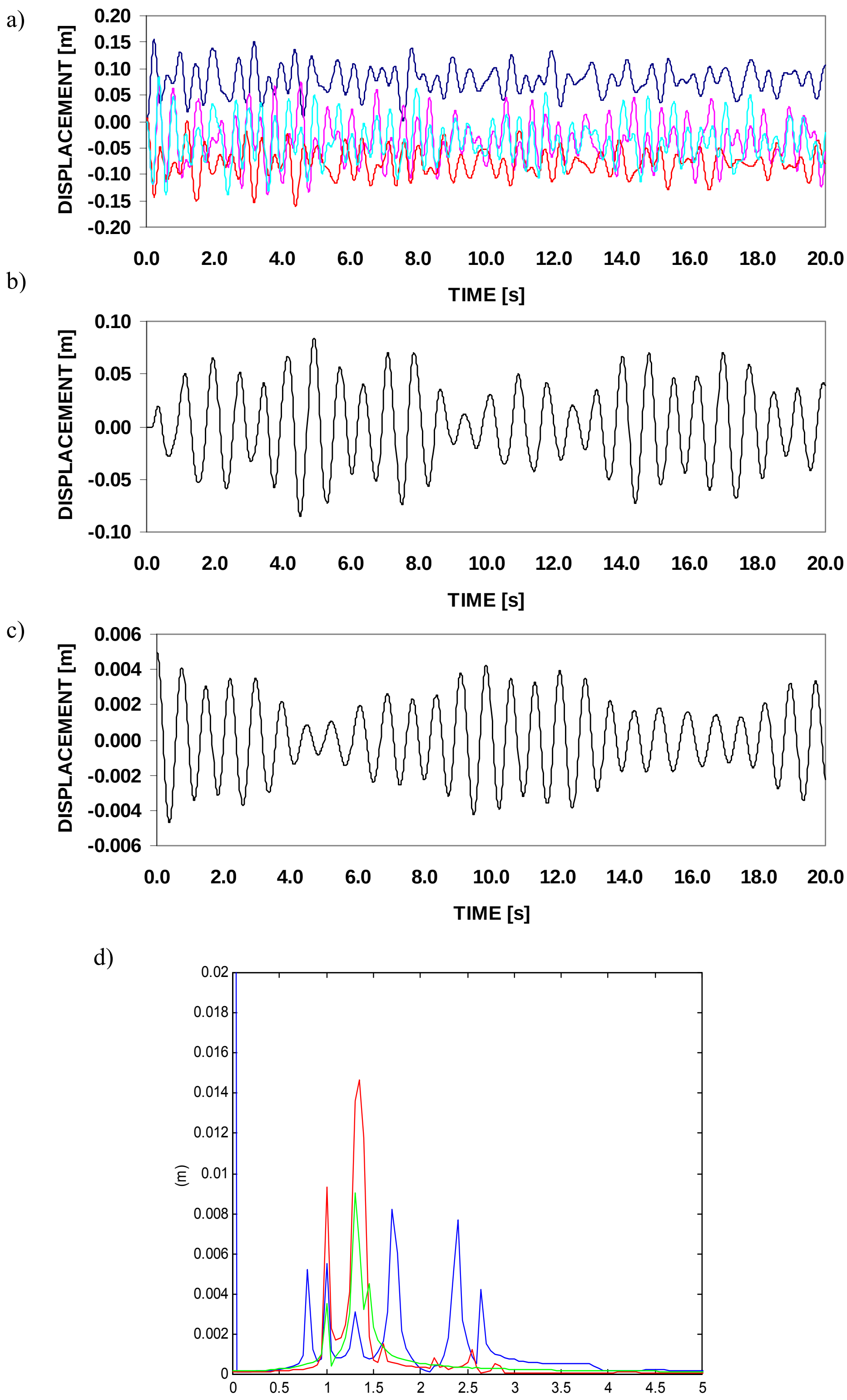

Figure 4.4.2: a) numerically predicted displacement histories of the container walls and liquid. b) predicted sloshing amplitude in flexible container with 0 kg point mass, c) structure displacement and d) FFT of wall displacement (blue), sloshing liquid (red) and plate displacement (green).

Figure 4.4.3 (a) shows the predicted displacement histories when pairs of a 3 kg point mass are added to the container. One immediate observation in the displacement graph of the container, is the lowered frequency of the oscillations. The oscillations of the two liquid nodes are mostly in-phase, especially during the last 5 seconds of simulation, indicating suppressed sloshing. There is a clear beat in the sloshing amplitude graph, figure 4.4.3 (b), with the magnitude reduced to approximately 20 mm towards the end of the simulation. The beat is also clear in the structural oscillations in Figure 4.4.3 (c), with a period of 8 seconds. In addition, the third peak of the beat envelope, around 17 seconds, displays a reduction from the initial 5mm deflection to approximately 2mm.

In Figure 4.4.3 (d), the dominant structure's (green) and sloshing (red) response is at 1.4 Hz, and it is split by the spectral peak of the flexible container (blue). This split and the resulting double spectral peaks are responsible for the beat envelope with a long duration. The flexible container also has a spectral peak of significant magnitude around 0.7 Hz.

Observations with 5 kg and 7 kg point mass cases, in Figures 4.4.4 and 4.4.5, are quite close to those with 3kg. One exception is the further suppression of the sloshing magnitudes to about 15 mm, as shown in Figure 4.4.4 (b), and to 10 mm in Figure 4.4.5 (b). These cases are included to show the transition of the split double peaks in the response of the structure and the sloshing in Figure 4.4.3 (d).

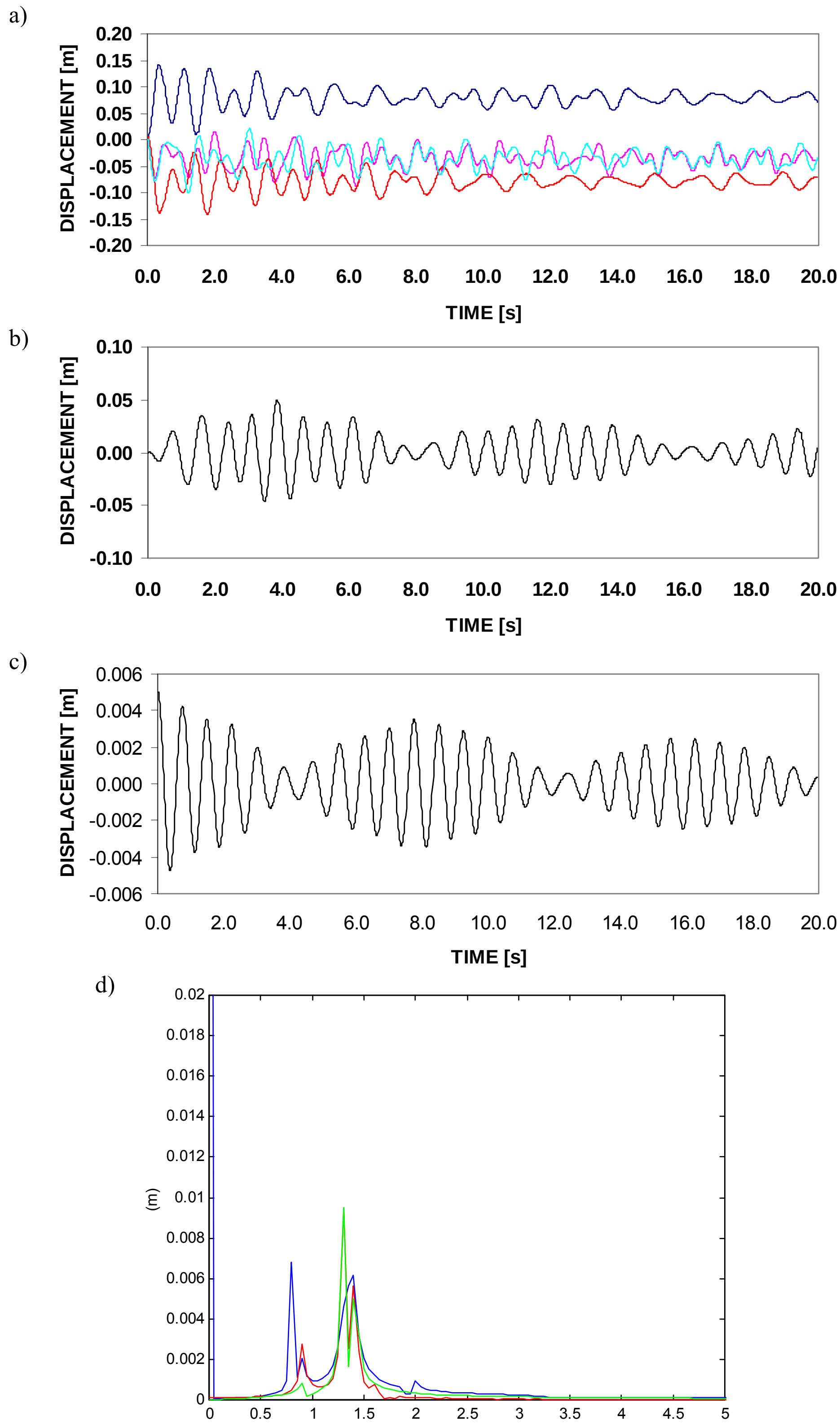

Figure 4.4.3: Same as in Figure 4.4.2 but with 3 kg point mass.

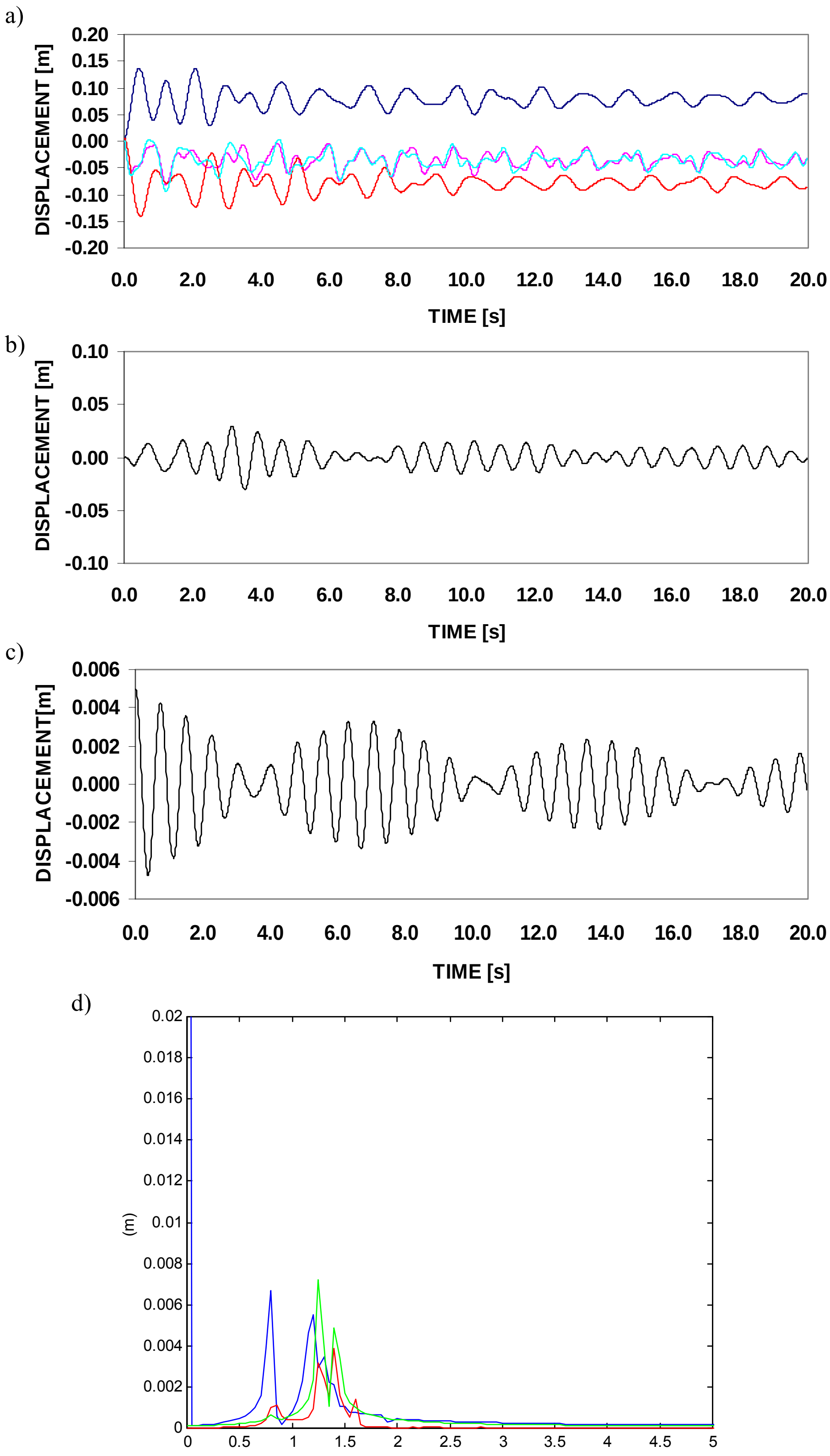

Figure 4.4.4: Same as in Figure 4.4.2 but with 5 kg point mass.

Observations with 9kg point masses, in Figure 4.4.6, correspond to the most effective tuning reported earlier by Gradinscak et al. (2006) for suppression of the liquid motion. In Figure 4.4.6 (a), the liquid surface moves in almost perfect phase, resulting in a virtual elimination of sloshing as shown in Figure 4.4.6 (b).

In Figure 4.4.6 (c), the beat duration is about 5.5 seconds, and the peak of the last beat around 18 seconds, is reduced to less than 1.5 mm. The two dominant peaks are now clearly separated for both the structure and the liquid in Figure 4.4.6 (d). In some ways, these two peaks around 1.3 Hz and 1.45 Hz behave quite similarly to the two peaks of the case with the rigid container in Figure 4.4.1 (d), but the difference, of course, is the drastically reduced magnitudes as a result of the container flexibility. It is also interesting to note that the spectral distribution of the flexible container started to favor lower frequencies.

With further increases of the added point masses to 11kg and 13 kg, in Figures 4.4.7 and 4.4.8 of the respective figures, sloshing magnitudes start to grow, as the container flexibility now starts to de-tune from the dynamics of sloshing. However, the beat in the structure's response is still very clear in Figures 4.4.7 (c) and 4.4.8 (c), with a further reduction of the peak response to about 1mm, around 17 seconds. Hence, the liquid in the container and the structure seem to interact quite strongly, almost ignoring the loss of tuning of the container. This observation is supported by the spectral distribution given in Figure 4.4.7 (d) and 4.4.8 (d). Extrapolating on these results, it is reasonable to expect similar outcomes for even larger added point masses.

a)

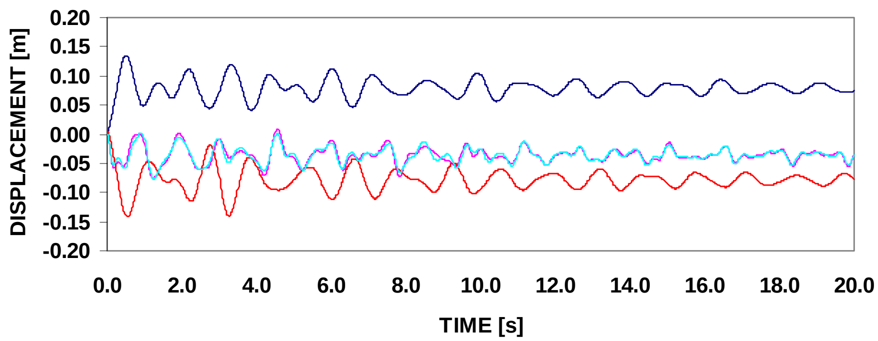

b)

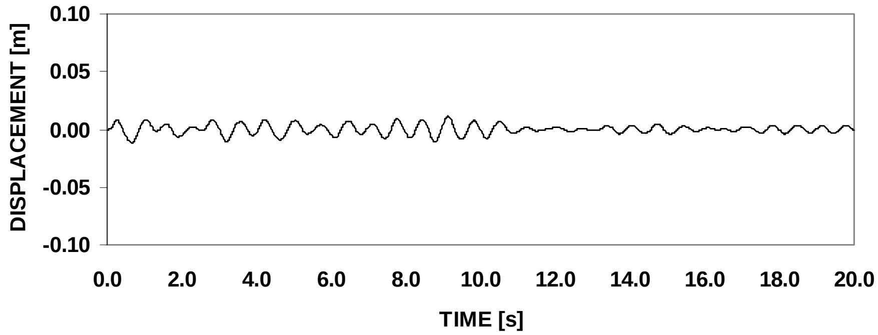

c)

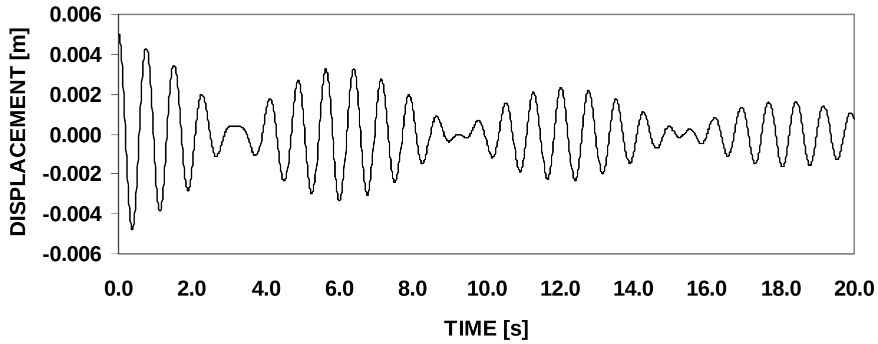

d)

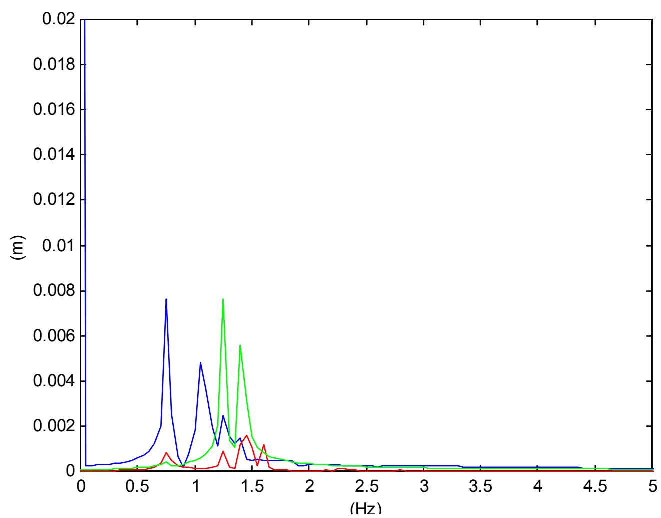

Figure 4.4.5: Same as in Figure 4.4.2 but with 7 kg added mass.

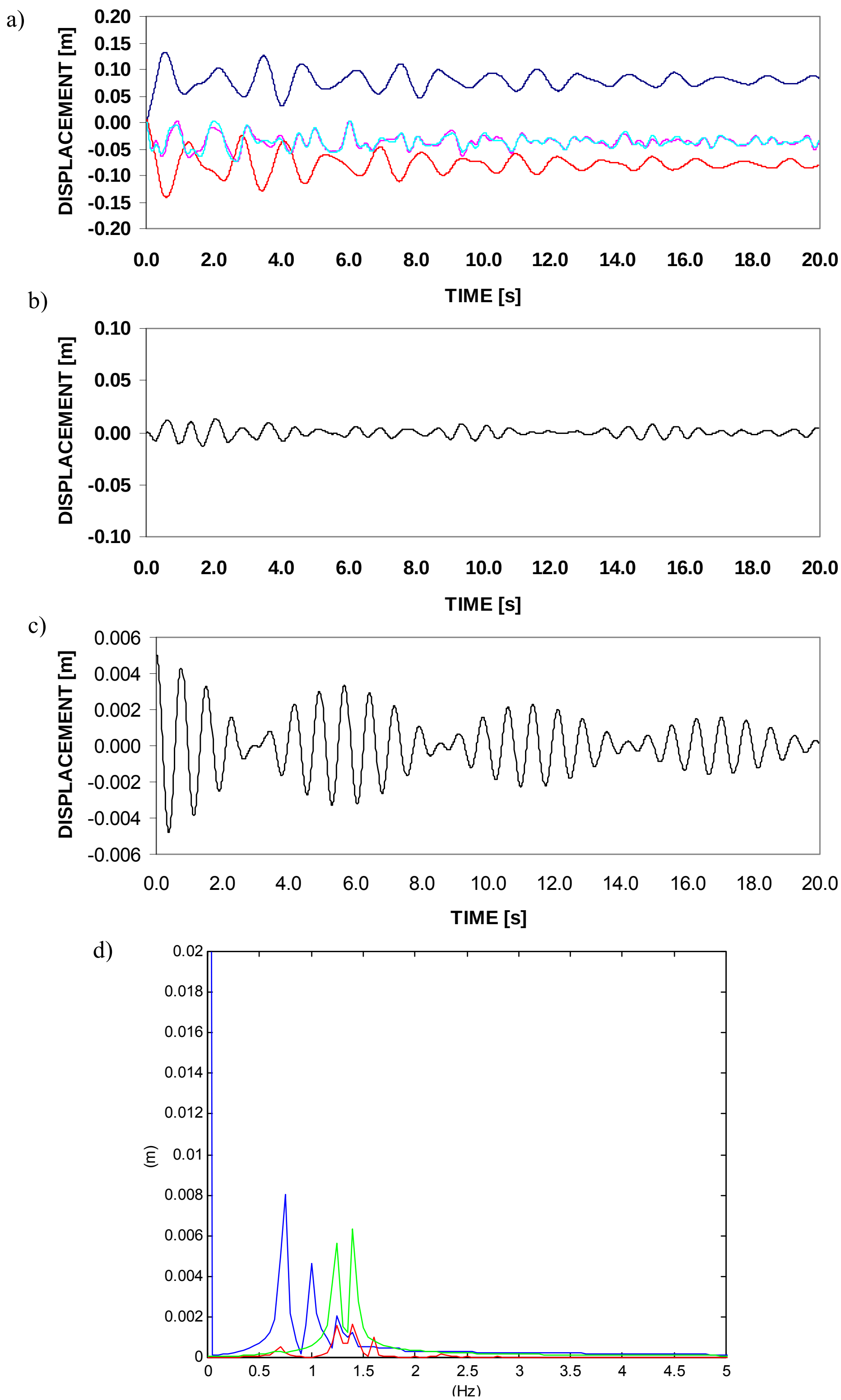

Figure 4.4.6: Same as in Figure 4.4.2 but with 9 kg added mass.

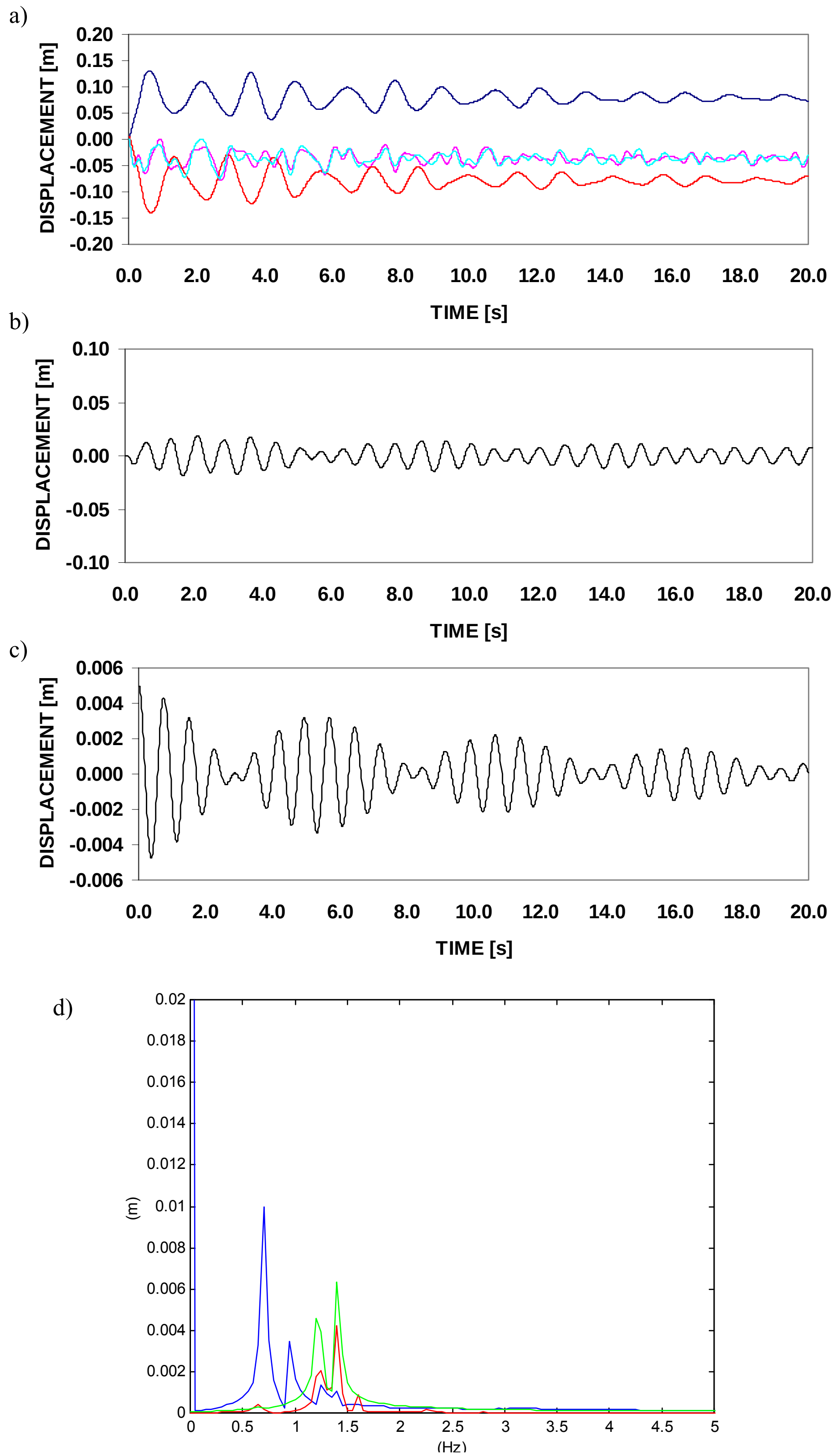

Figure 4.4.7: Same as in Figure 4.4.2 but with 11 kg added mass.

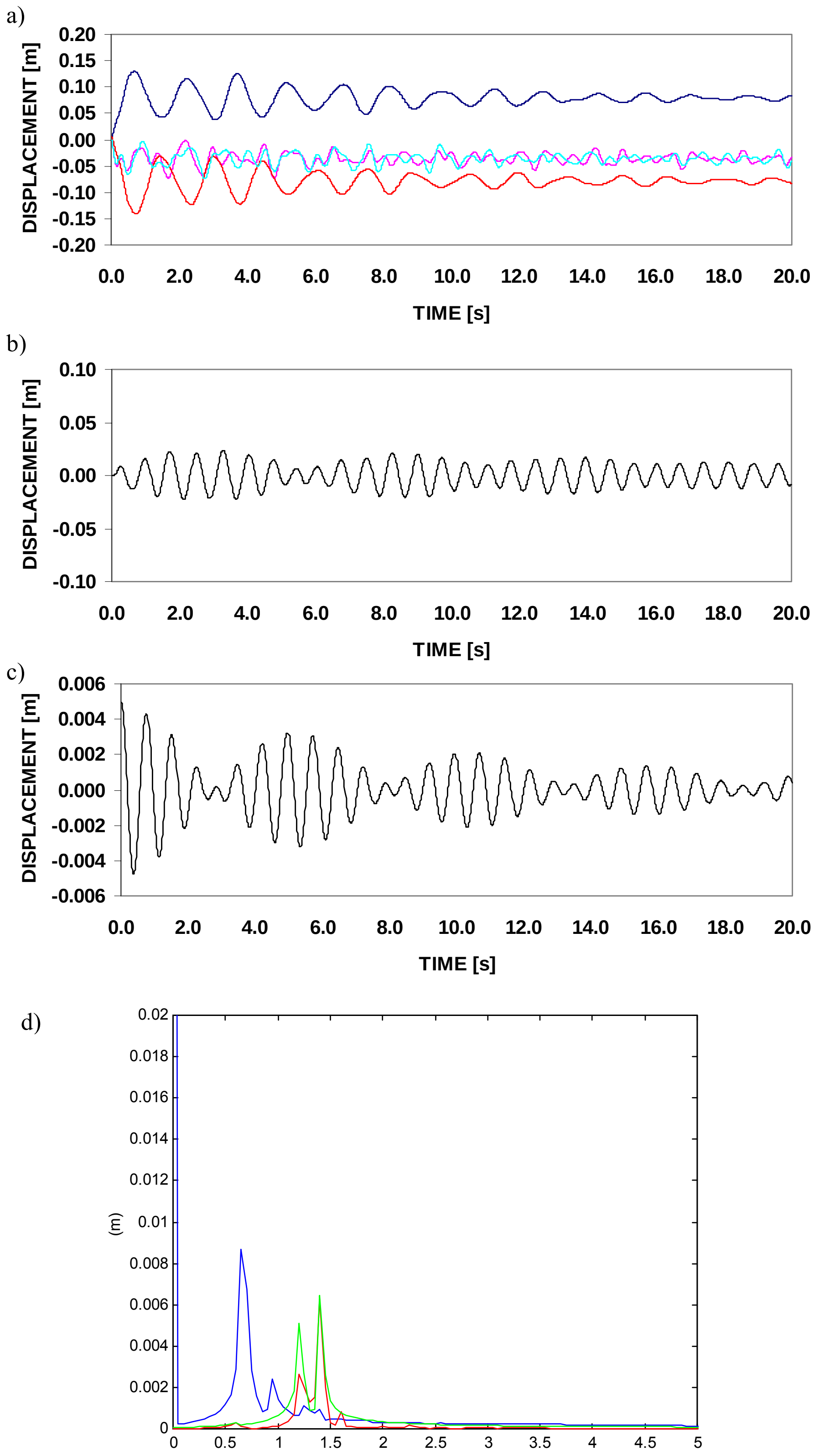

Figure 4.4.8: Same as in Figure 4.4.2 but with 13 kg added mass.

4.4.1 Selective cases with different critical structural damping applied to the container.

In the previous section structural damping applied to the container model was taken to be 1.5%. In this subsection structural damping is increased to 5% and 10%. The study shows that if the flexible container is made with larger rates of dissipation, the displacement of the controlled structure is reduced further. Only selective cases with 0 kg, 9 kg and 13 kg point masses are presented here, to show the effect of critical structural damping of the container, on structural displacement. The rest of the results are presented in Appendix C.

In Figures 4.4.1.1 to 4.4.1.3, the critical damping ratio is increased to 5%. In Figure 4.4.1.1, the flexible container case is shown with 0 kg point mass. Displacement history of the container walls and liquid in the Figure 4.4.1.1 (a) and sloshing amplitude in Figure 4.4.1.1 (b) remained similar compared to Figure 4.4.2 (a) from the previous section. Some differences exist in the displacement histories of the controlled structure in Figure 4.4.1.1 (c) as compared to those in Figure 4.4.2 (c). Most noticeably, at the end of the simulation period, the displacement of the structure is smaller.

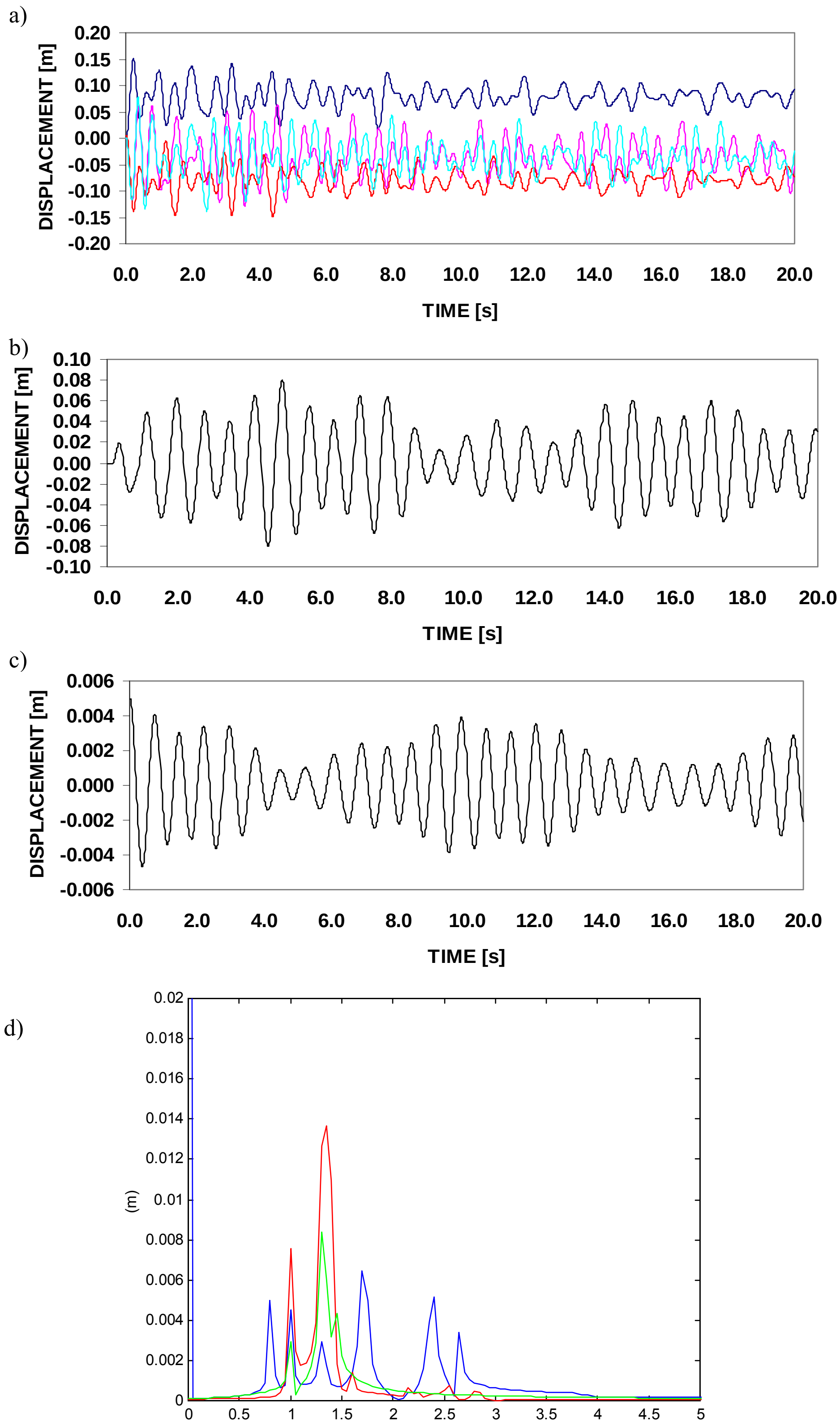

Figure 4.4.1.1: a) numerically predicted displacement histories of the container walls and liquid. b) predicted sloshing amplitude in flexible container with 0 kg point mass, c) structure displacement and d) FFT of wall displacement (blue), sloshing liquid (red) and plate displacement (green). Liquid is undamped and container has 5% damping.

In Figure 4.4.1.2, the flexible container case is shown when a pair of 9 kg point masses is added to the container. In the Figure 4.4.1.2 (b), the sloshing amplitude is almost eliminated as compared to that Figure 4.4.6 (b). In Figure 4.4.1.2(c), the displacement history of the controlled structure is significantly smaller as compared to Figure 4.4.6 (c). In Figure 4.4.1.2 (d), the magnitudes of the structural peaks of the container are smaller than for the flexible container shown in 4.4.6 (d).

In the Figure 4.4.1.3, the flexible container case is shown, when a pair of 13 kg point masses is added to the container. In the Figure 4.4.1.3 (b), the sloshing amplitude is starting to increase again. In the Figure 4.4.1.3(c), the displacement history of the controlled structure is even further reduced compared to Figure 4.4.1.2 (c). In Figure 4.4.1.2 (d), the magnitudes of the structural peaks of the container are smaller than for the flexible container shown in 4.4.6 (d).

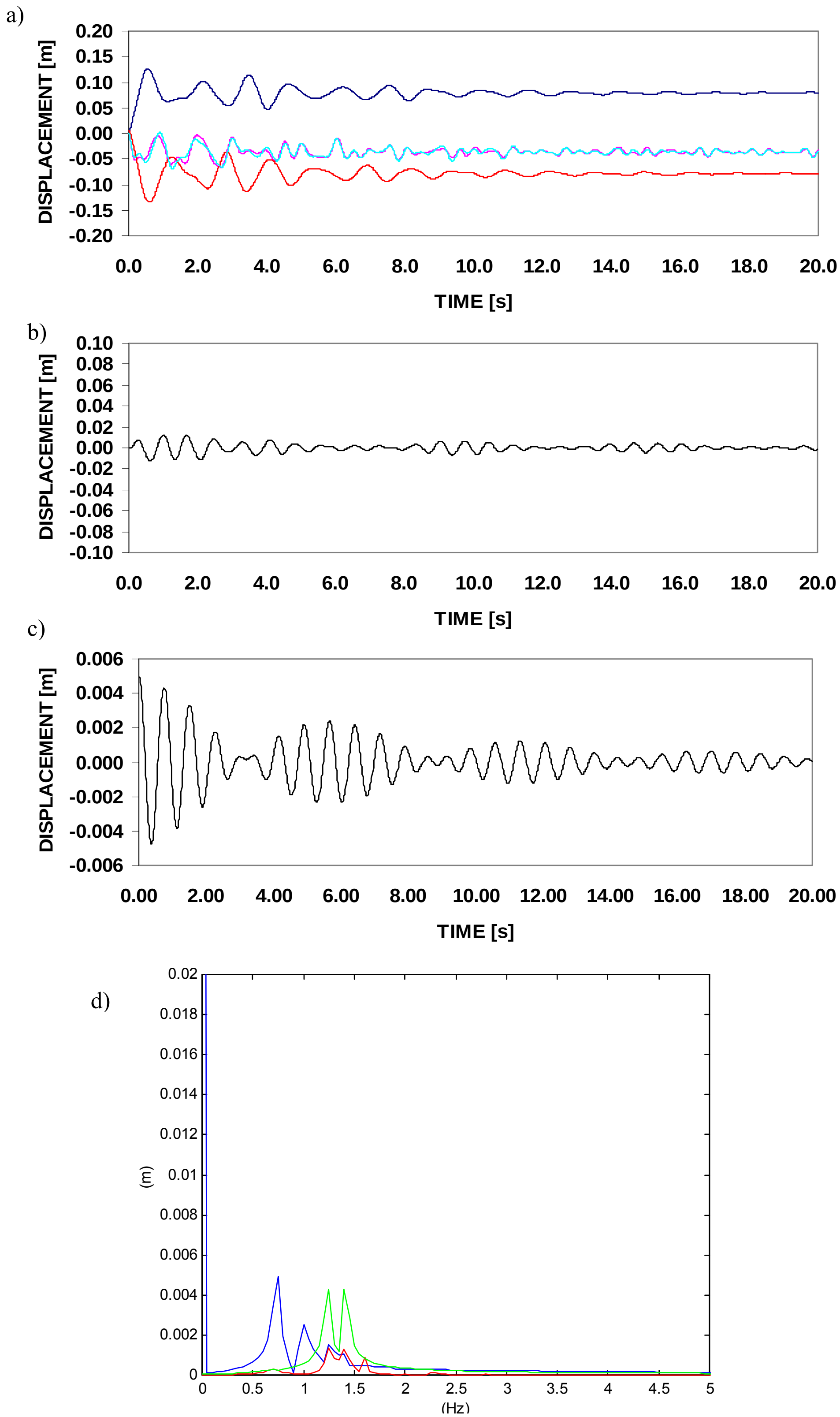

Figure 4.4.1.2: Same as in Figure 4.4.1.1 but for 9 kg point mass.

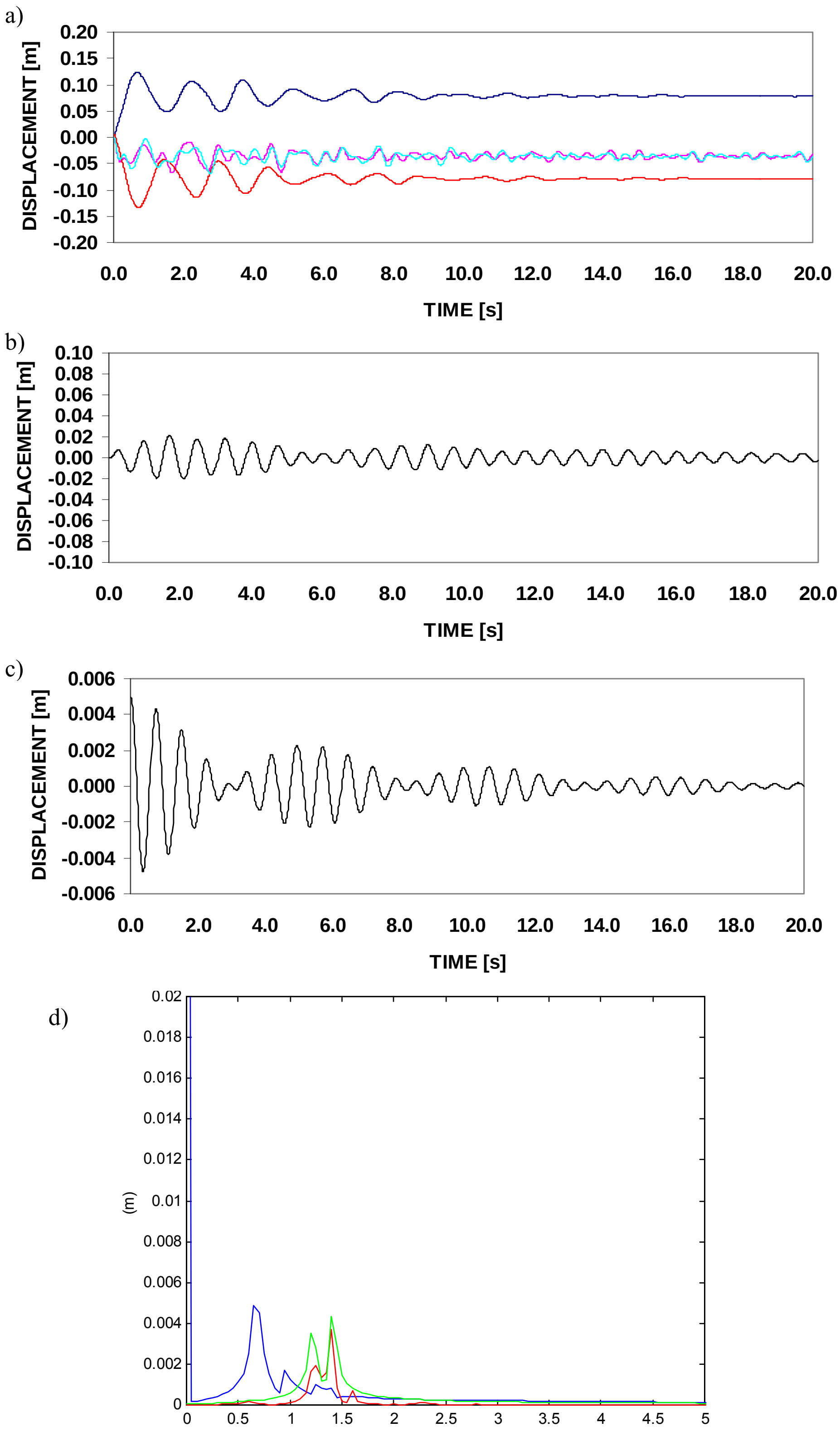

Figure 4.4.1.3: Same as in Figure 4.4.1.1 but for 13 kg point mass.

In Figure 4.4.1.4 to 4.4.1.6, the critical structural damping of the container is increased further to 10%. In Figure 4.4.1.4, the flexible container case is shown with 0 kg point mass. In the Figure 4.4.1.5 and Figure 4.4.1.6, the flexible container cases with 9 kg and with 13 kg added point masses are presented. The displacement histories of the sloshing amplitude are shown to be quite close to those when the critical structural damping of the container was 5%. The difference in the displacement history of the controlled structure has been noticed. The controlled structure's displacement decreased even further.

In conclusion when critical structural damping of the container is increased, the controlled structure's displacement can be reduced further. From the results achieved in this section, clearly the best reduction in the controlled structure's displacement is in the scenario with a 10% critical damping of the container. There is undoubtedly a level of damping where too much damping is going to inhibit structural deflections, and the case will start approaching to that with a rigid container.

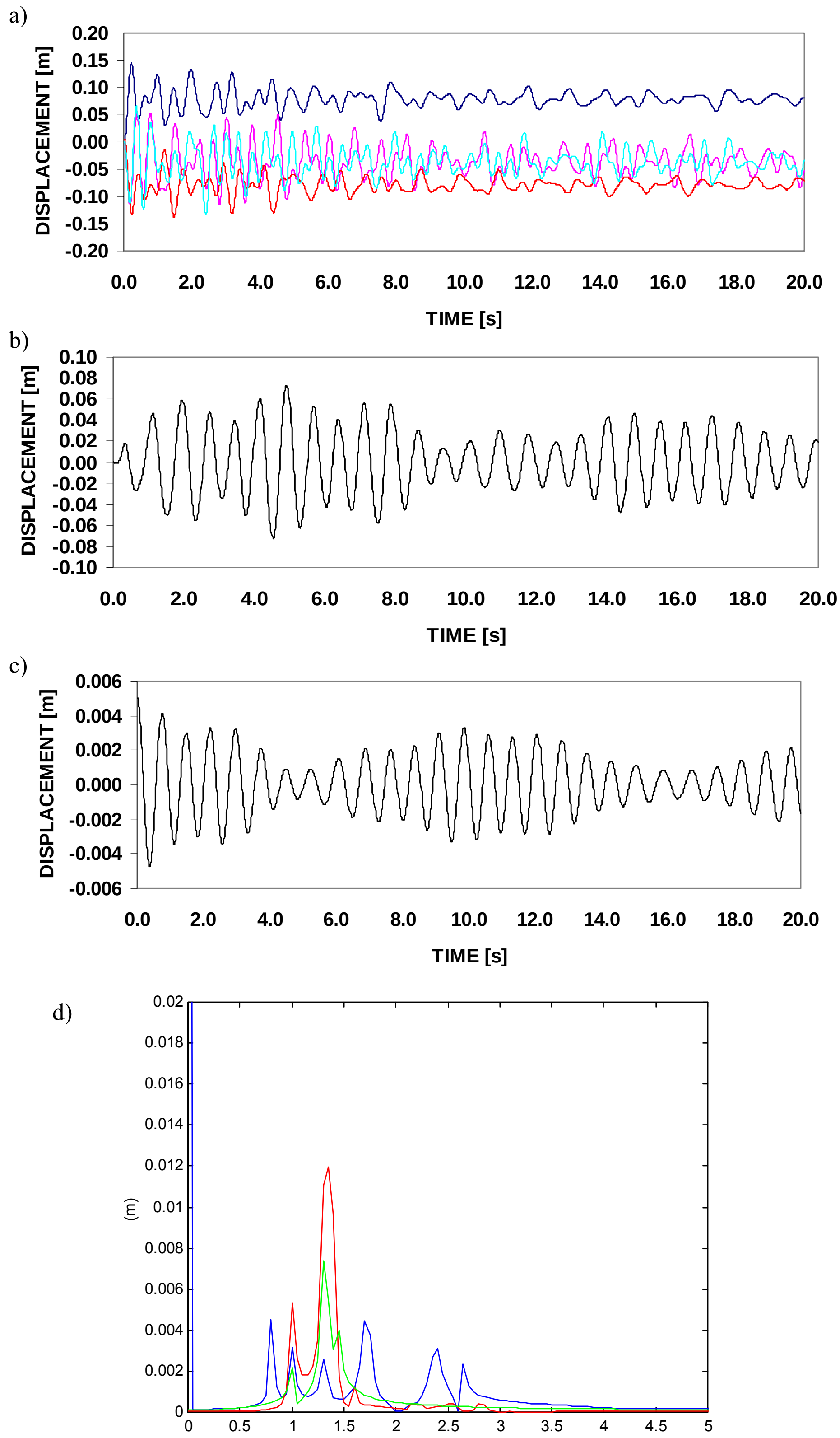

Figure 4.4.1.4: a) numerically predicted displacement histories of the container walls and liquid. b) predicted sloshing amplitude in flexible container with 0 kg point mass, c) structure displacement and d) FFT of wall displacement (blue), sloshing liquid (red) and plate displacement (green). Liquid is undamped and container has 10% damping.

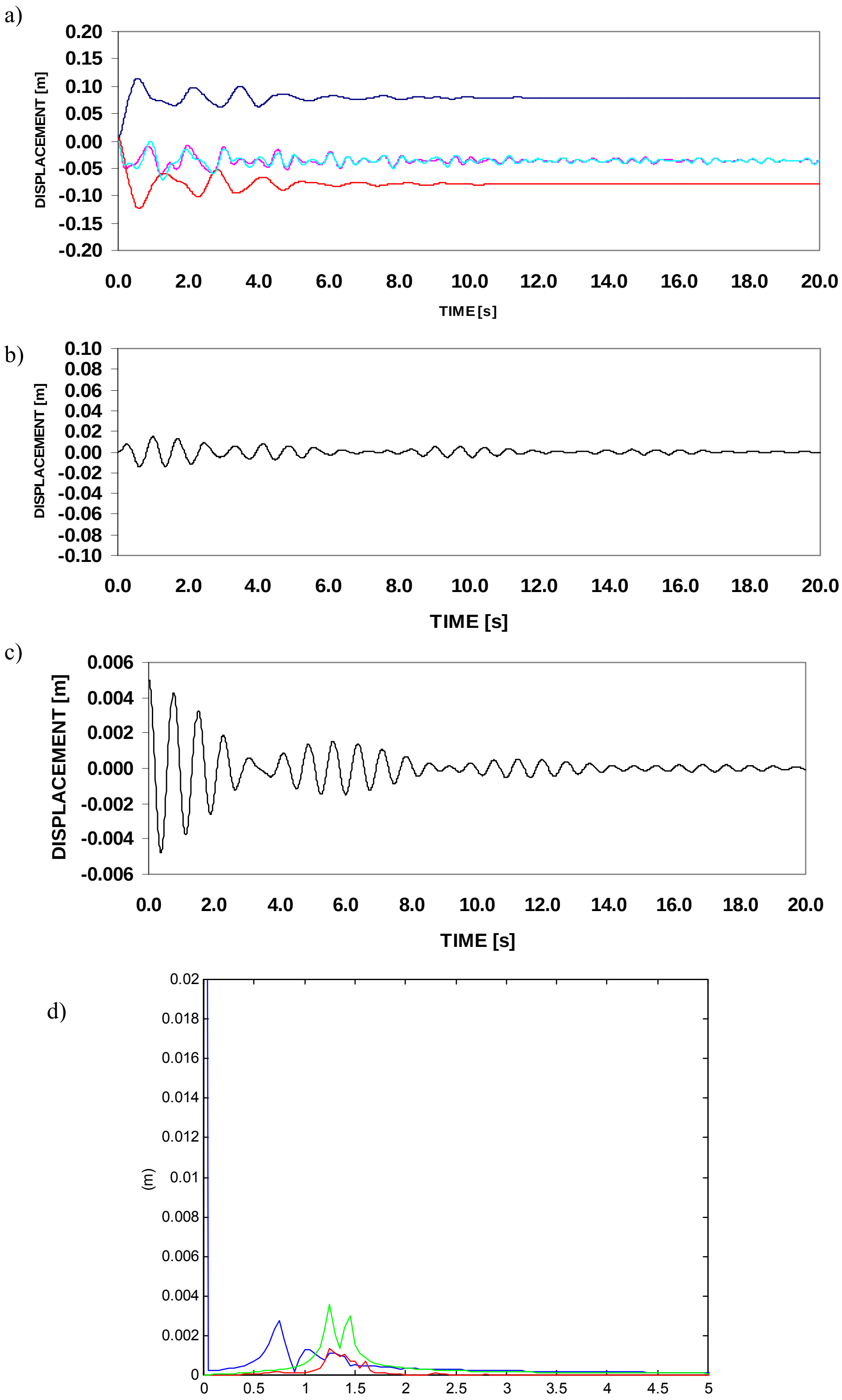

Figure 4.4.1.5: Same as in Figure 4.4.1.4 but for 9 kg point mass.

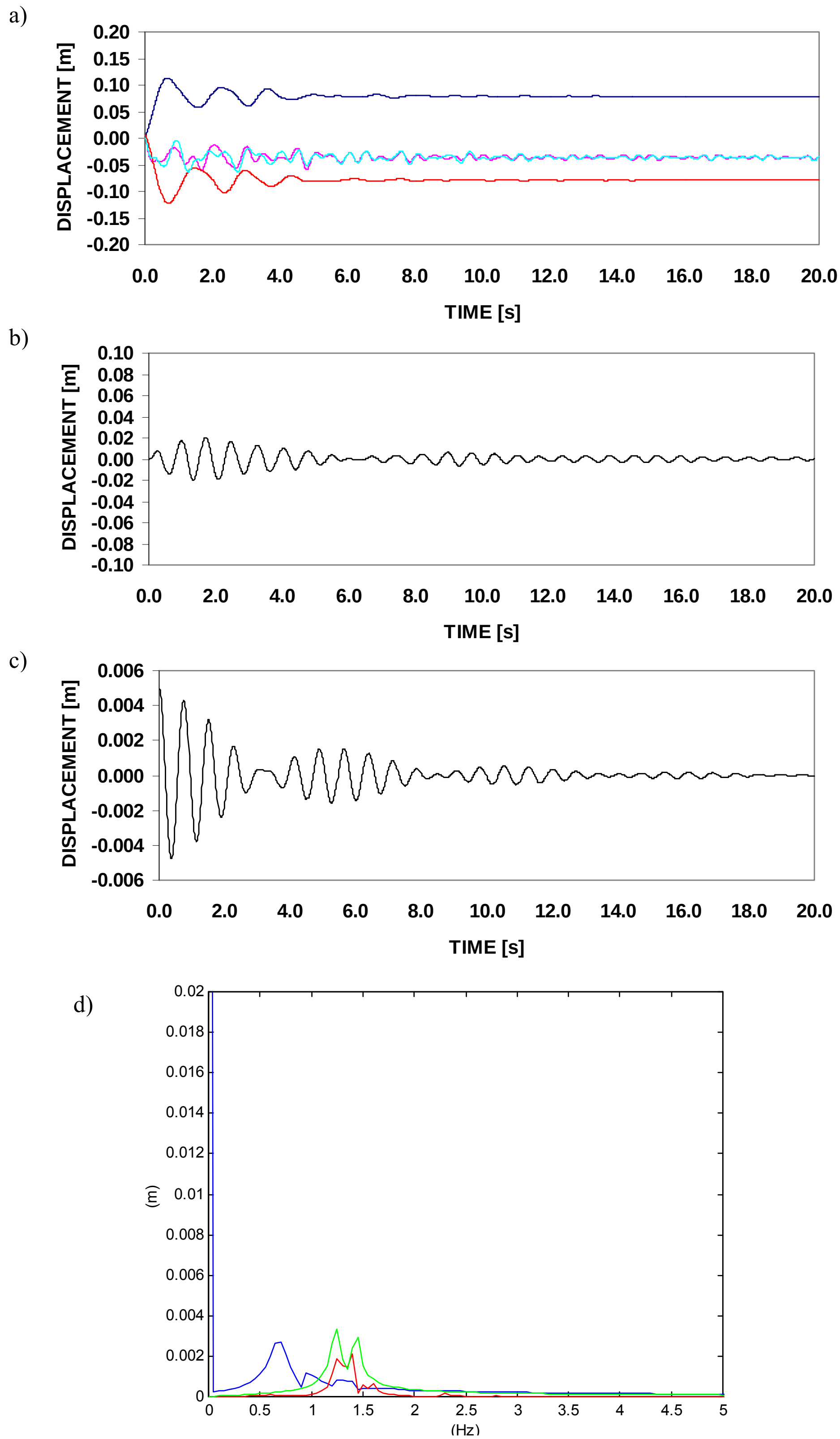

Figure 4.4.1.6: Same as in Figure 4.4.1.4 but for 13 kg point mass.

The rms average of sloshing amplitudes, Figure 4.4.9 (a), and rms average of the controlled structure's displacements, Figure 4.4.9 (b), are shown as functions of added point mass. In the frame figure (a), the rms is given for the rigid container, and for the flexible container with different structural damping of 1.5%, 5%, 10%.

a)

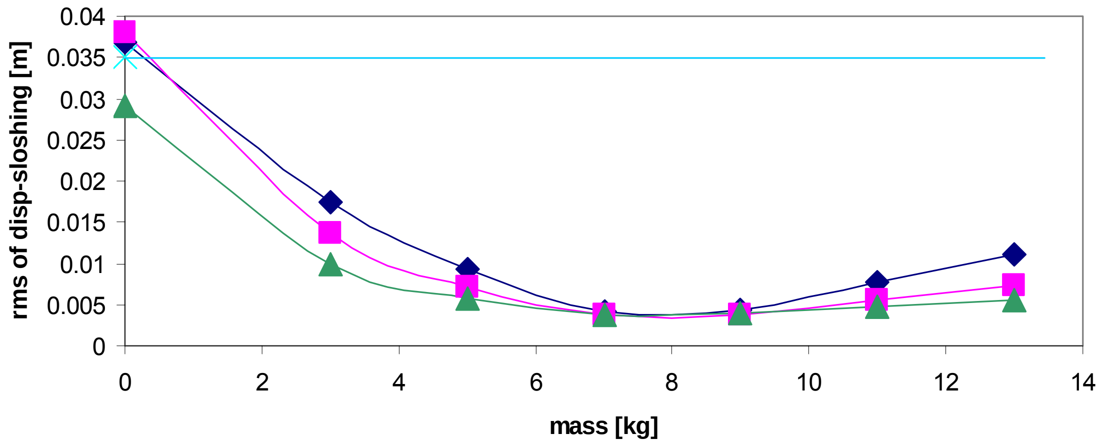

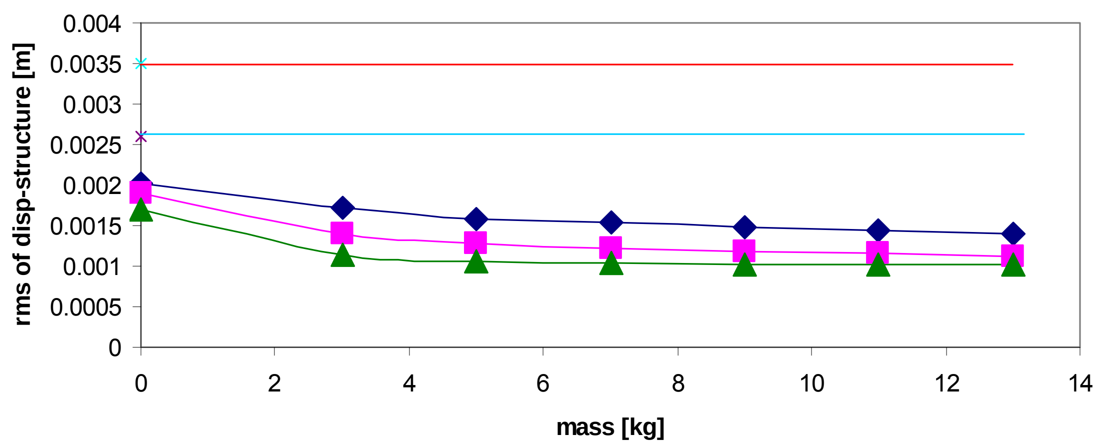

b)

Figure 4.4.9: Variations of the rms of (a) sloshing amplitude and (b) structure's displacement. (structure alone, rigid container; and flexible container with structural damping of ◆ 1.5% , ■ 5% and ▲ 10%) .

When the flexibility of the container is introduced with 0 kg mass, some deterioration from the case with rigid container is noted. When the 3 kg mass is added, the sloshing amplitude starts to decrease. Not surprisingly, the lowest sloshing amplitude is between 7 kg and 9 kg point mass, again verifying the best tuned case from Chapter 2. The sloshing amplitude starts to increase when 11 kg is added and once again the tuning is lost.

In Figure 4.4.9 (b), the rms of the controlled structure's displacement is shown. The top horizontal line indicates the case with the largest displacement of 3.5 mm, the case that shows the structure alone. The next horizontal line, case with a slightly lower displacement of 2.6 mm, indicates the case with the rigid walled container. With added mass and increasing damping of the flexible container, the structure's displacement is reduced significantly. The best control of displacement is with the 10 % critical structural damping of the container. More importantly, the structures's response seems to reamin quite unaffected by the tuning which takes place between the liquid and its container. This point may be quite advantageous from a design point of view, and certainly deserves further attention.

4.4.2 Selective cases with different mass ratios

This section explores the effect of different mass ratios between the structure's mass and that of the added container used to control it. To this end, cases have been tried by reducing the mass of the structure from 2000 kg (10% mass ratio) to 1500 kg (15% mass ratio) and finally to 1000 kg (20% mass ratio). The tuning condition is maintained between the structure and the sloshing liquid (with rigid walls) by varying the stiffness of the structure accordingly. The study shows no significant differences when the mass ratio is changed. As in the previous subsection, only selective cases are presented here while the rest are given in Appendix D.

In the Figures 4.4.2.1 to 4.4.2.3, the cases for the 1500 kg structural mass are presented, with 0 kg, 9 kg and 13 kg mass. For the 0 kg case, in Figure 4.4.2.1 (a), there is no decay in sloshing magnitudes. The sloshing history is quite similar to that with 2000 kg structural mass in Figure 4.4.2. In frame (c), a clearer beat in the envelope of the structure's displacement can be observed as compared that in frame (c) with 2000 kg structural mass. However, no considerable difference in spectral distributions is observed with increase of the mass ratio of the controller from 10% to 15%. Same argument is true for the 9 kg and 13 kg cases, in Figures 4.4.2.2 and 4.4.2.3.

There is a change in the beat envelope of the structure's displacement history observed in Figures 4.4.6 (c) and 4.4.8 (c) when compared to Figures 4.4.2.2 (c) and 4.4.2.3 (c). The number of beats increased to around five compared to the case with 2000kg mass, where there were only four beats. Once again looking at the 9 kg case (Figure 4.4.2.2 (c)) with the 13 kg case (Figure 4.4.2.3 (c)), there is a complete beat at the end of the run in the 13 kg case, compared to an incomplete beat in the 9 kg case.

In the Figures 4.4.2.4 to 4.4.2.6, the cases for the 1000 kg structural mass are given given for the 0 kg, 9 kg and 13 kg added mass cases. Observations with 1000 kg are quite close to those of the 1500 kg.

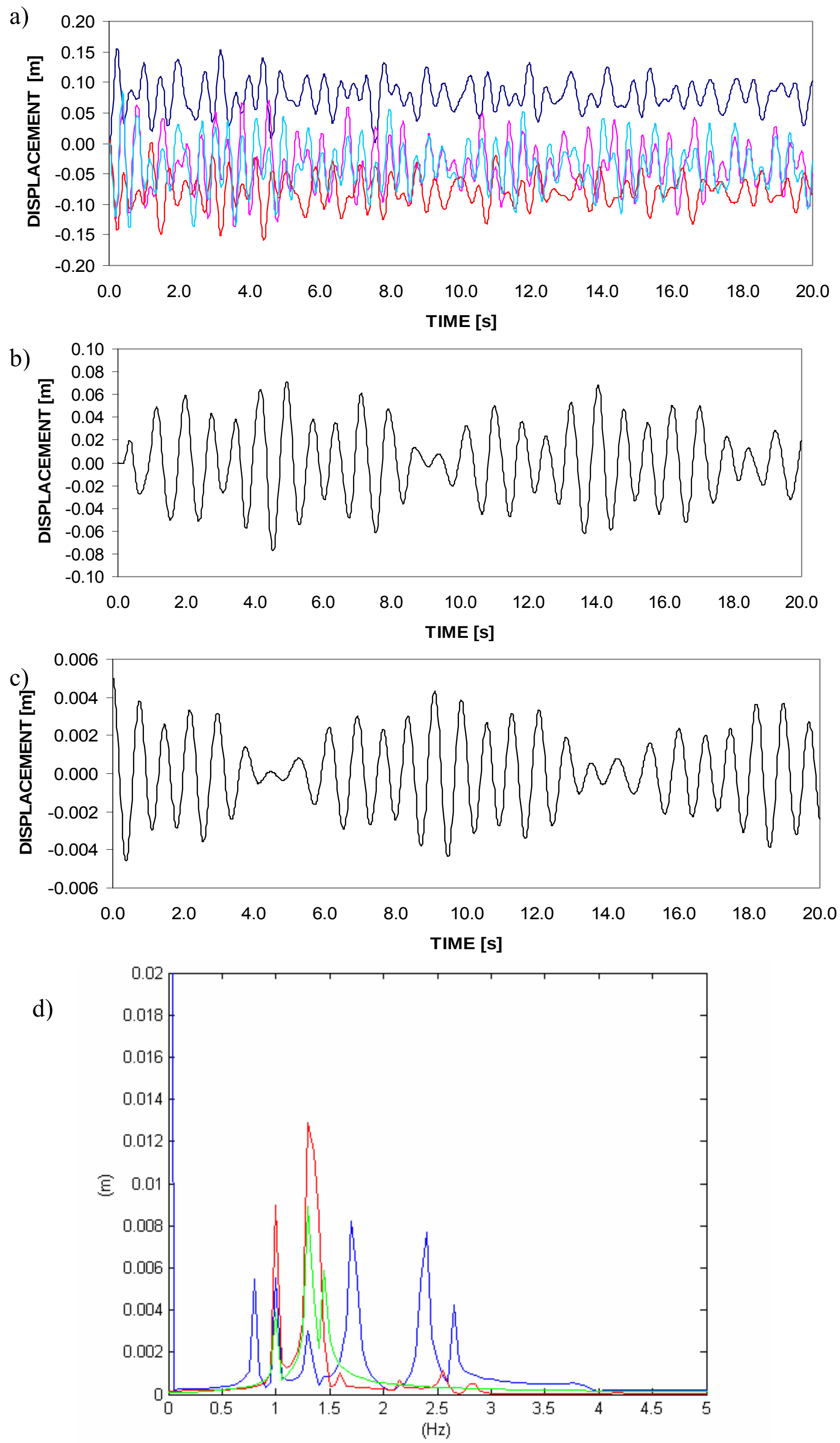

Figure 4.4.2.1: a) numerically predicted displacement histories of the container walls and liquid. b) predicted sloshing amplitude in flexible container with no added mass, c) structure displacement and d) FFT of wall displacement (blue), sloshing liquid (red) and plate displacement (green). The mass of the structure is 1500 kg.

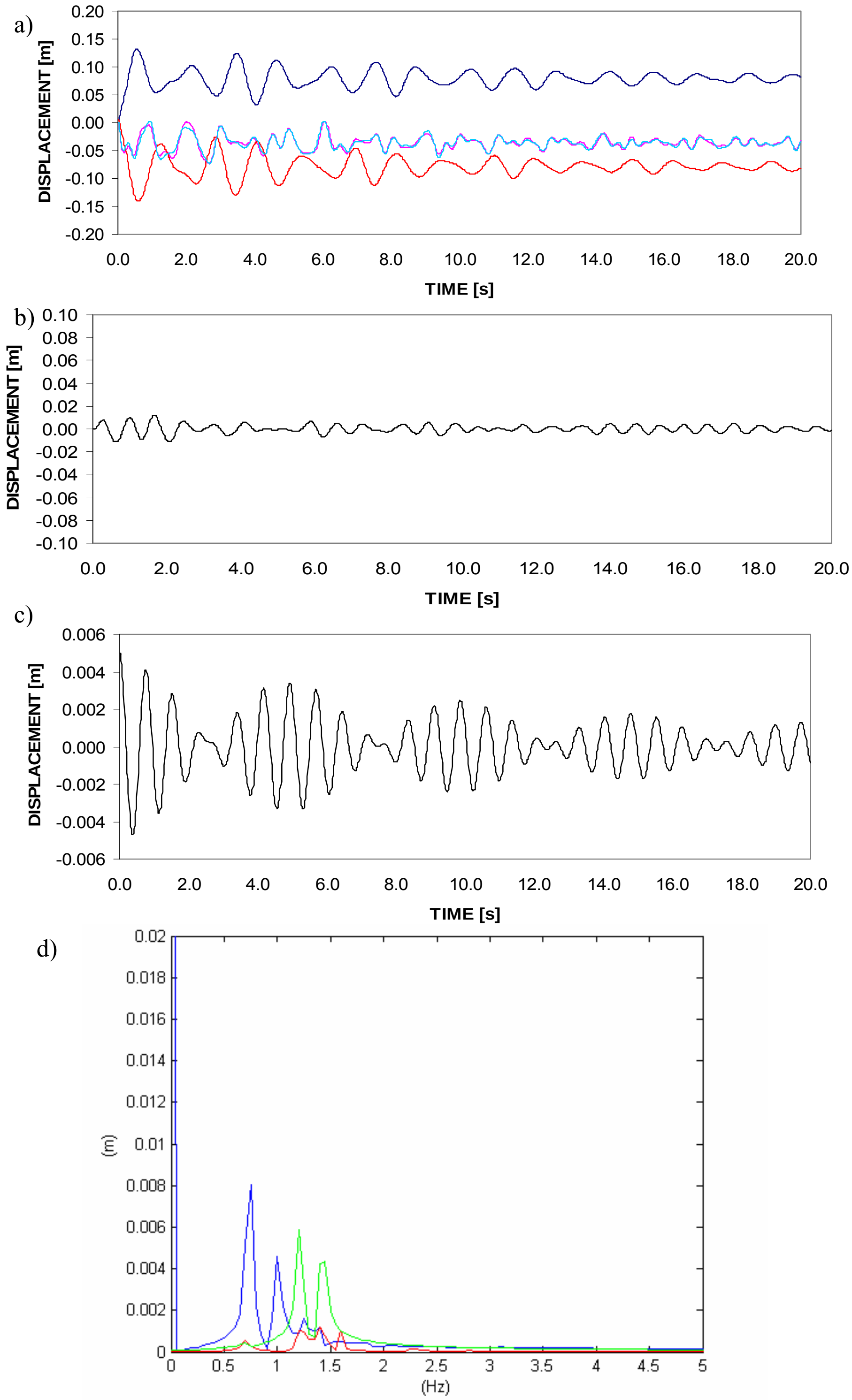

Figure 4.4.2.2: Same as in Figure 4.4.2.2 but for 9 kg added mass.

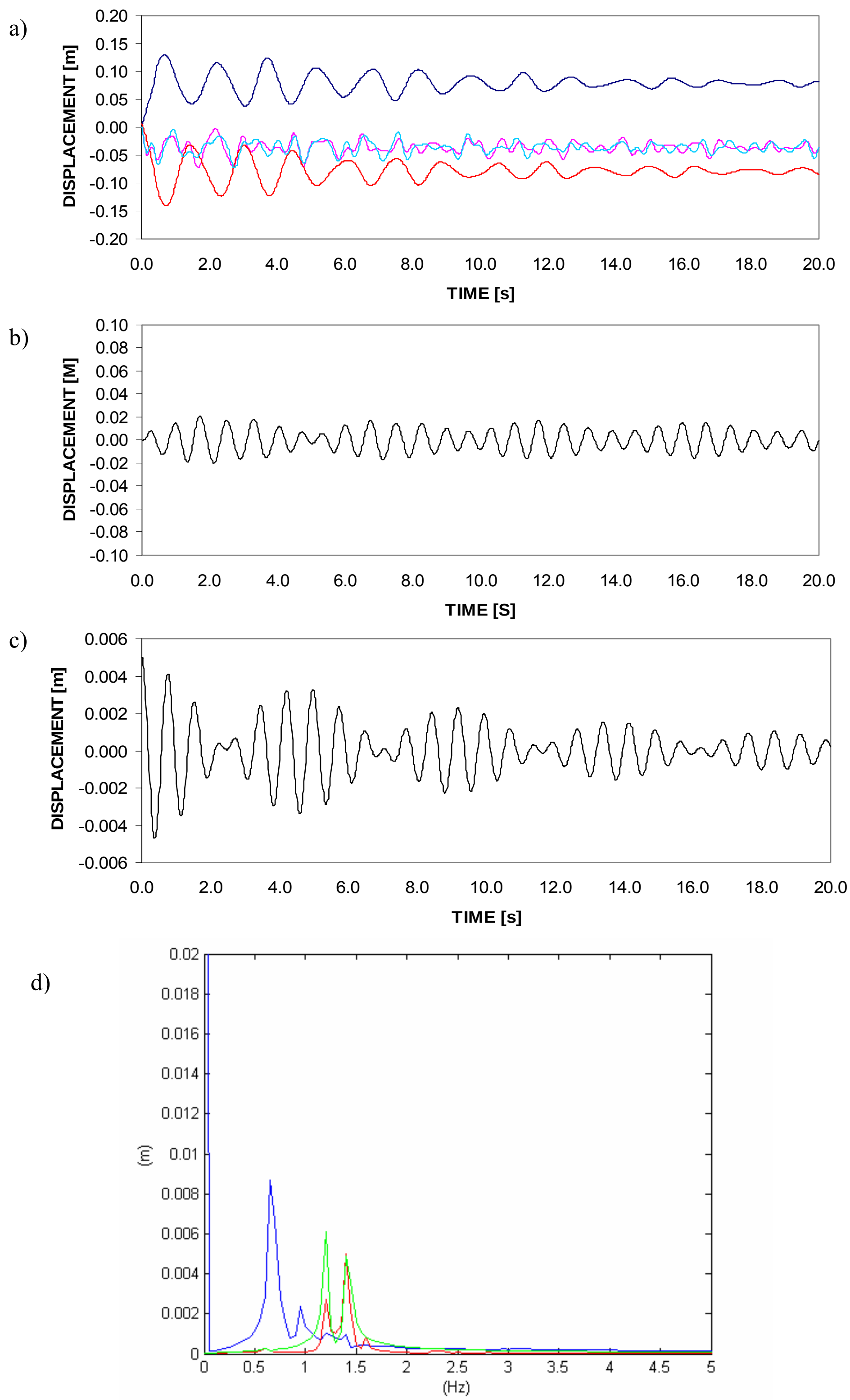

Figure 4.4.2.3: Same as in Figure 4.4.2.3 but for 13 kg added mass.

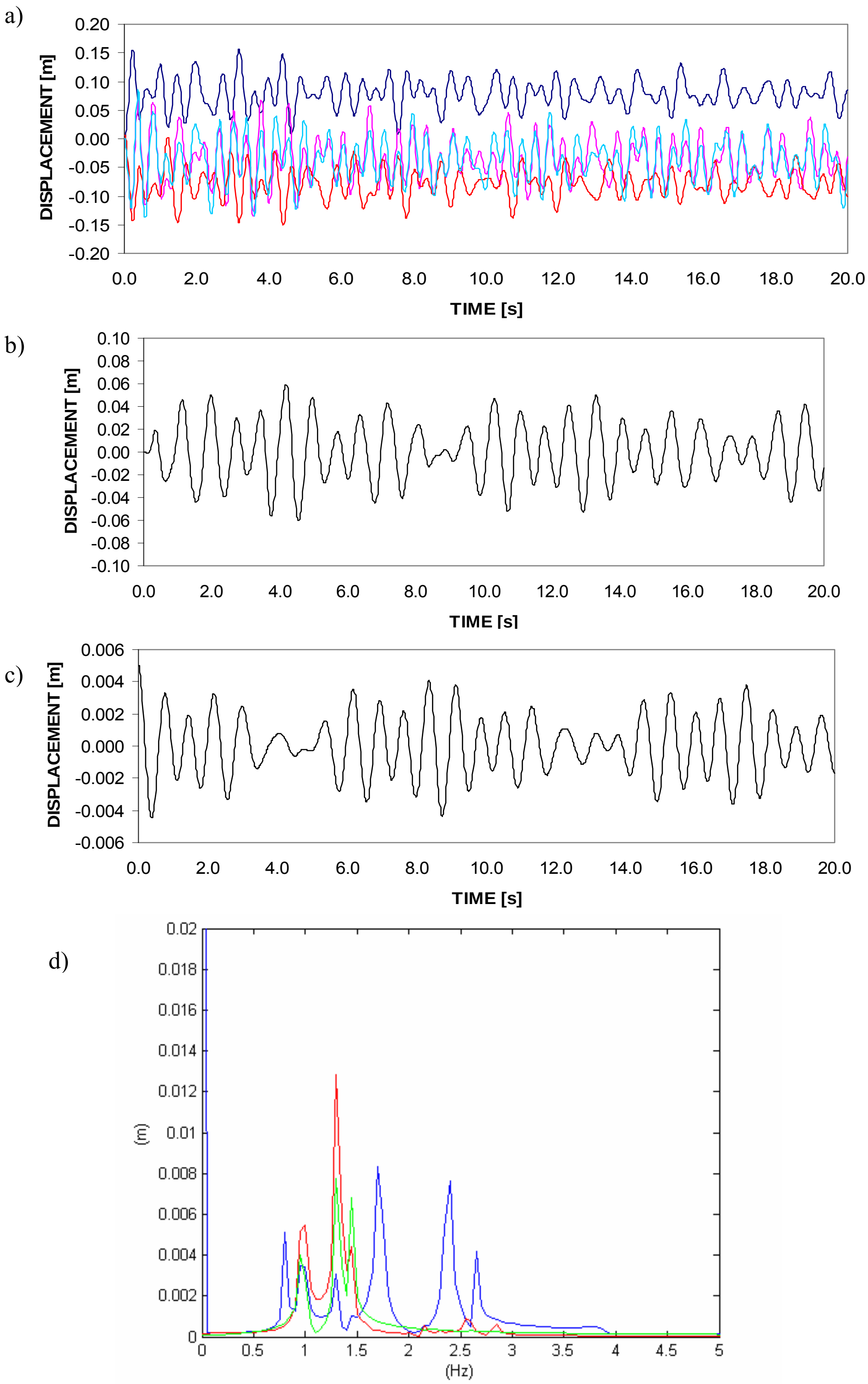

Figure 4.4.2.4: a) numerically predicted displacement histories of the container walls and liquid. b) predicted sloshing amplitude in flexible container with 0 kg point mass, c) structure's displacement and d) FFT of wall displacement (blue), sloshing liquid (red) and plate displacement (green). The mass of the structure is 1000 kg.

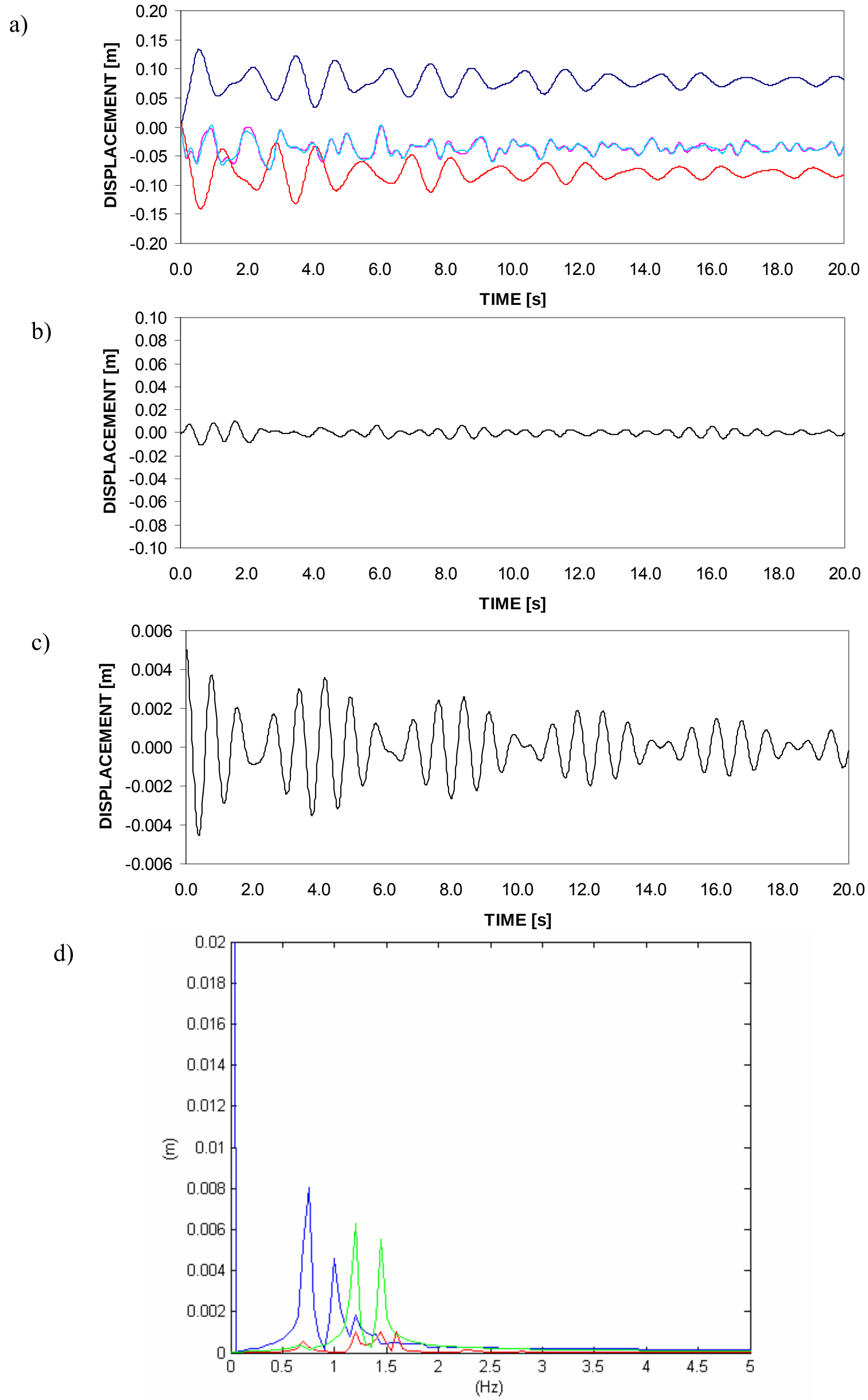

Figure 4.4.2.5: Same as in Figure 4.4.1.4 but for 9 kg added point mass.

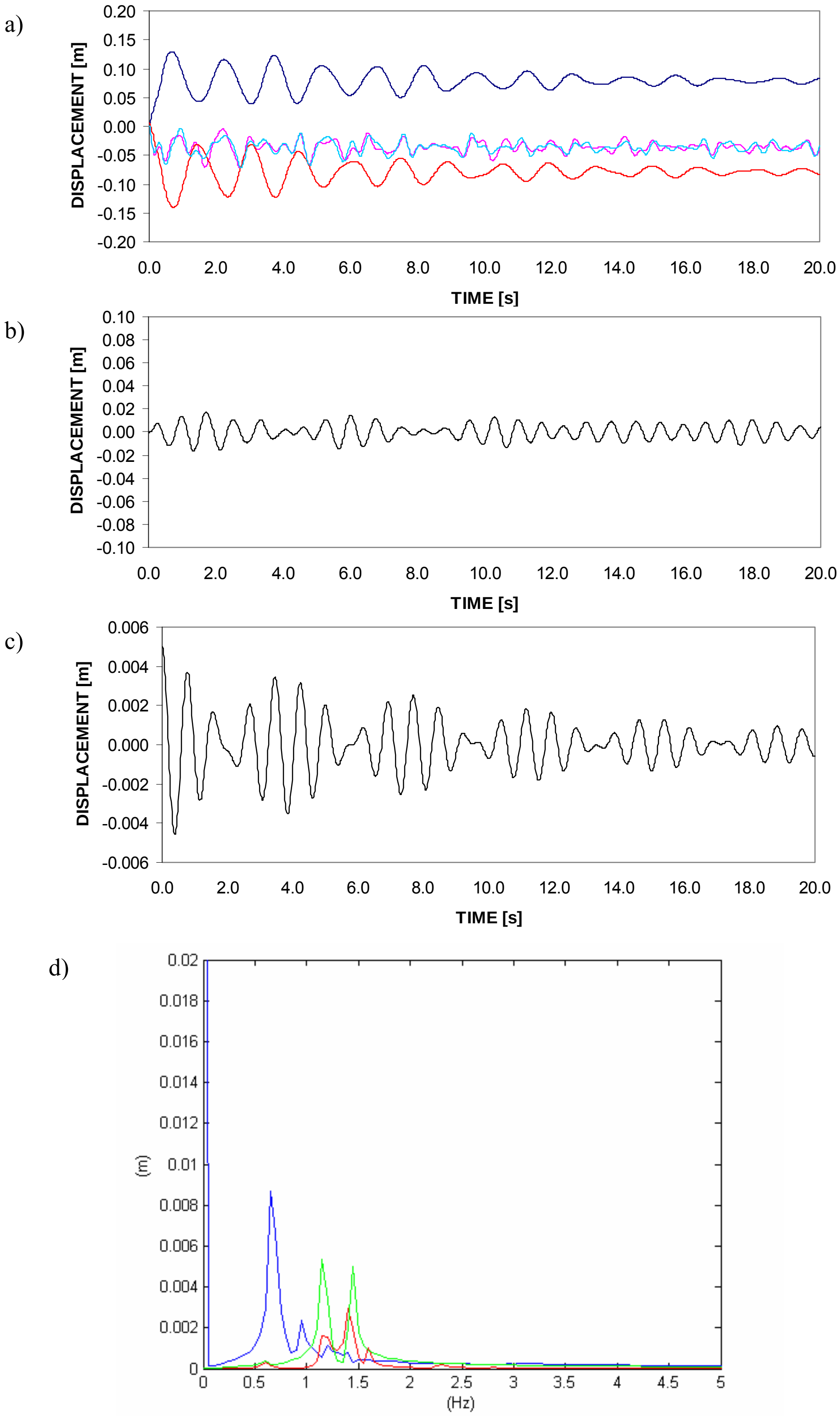

Figure 4.4.2.6: Same as in Figure 4.4.1.4 but for 13 kg added point mass.

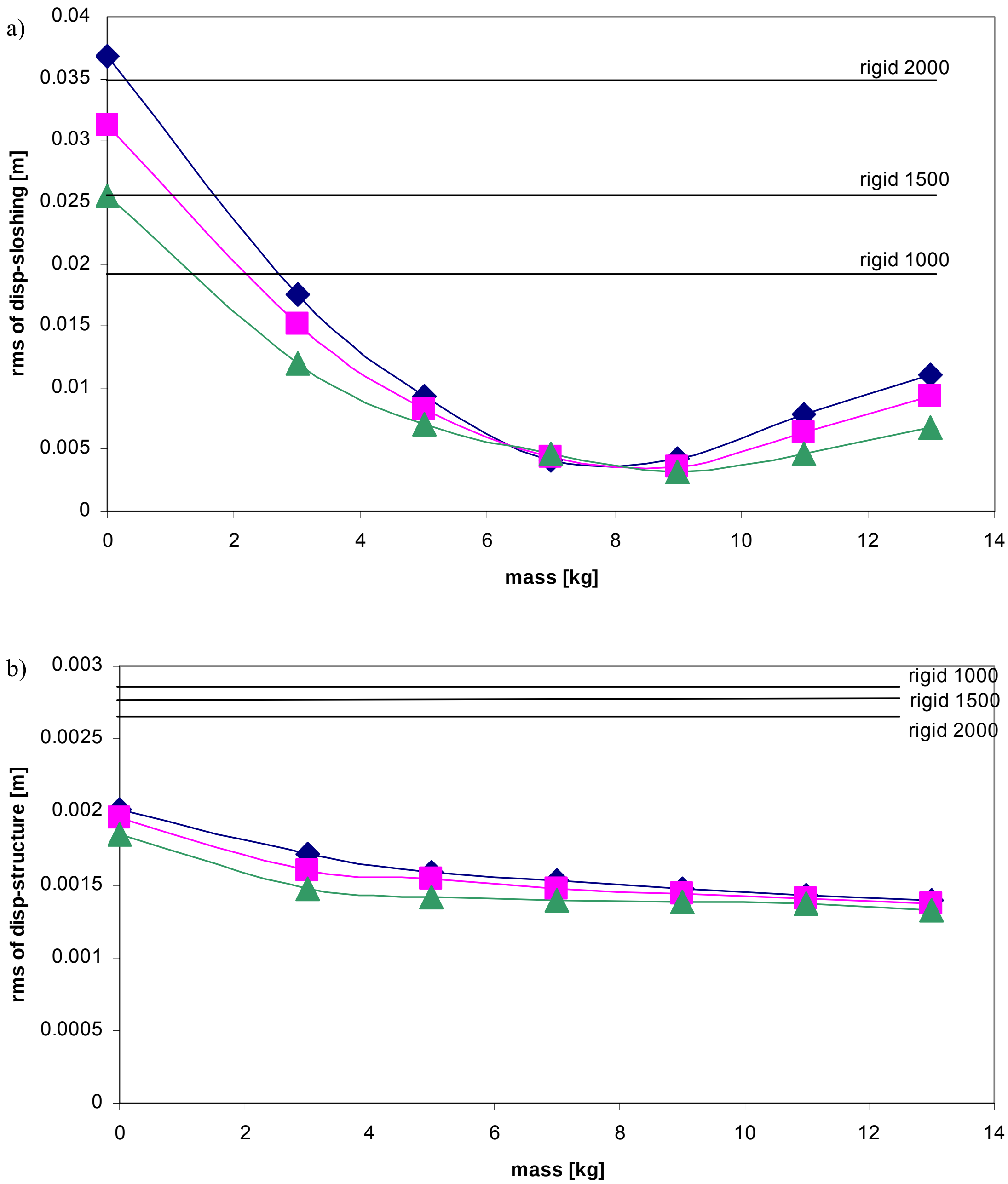

Figure 4.4.10: Variations of the rms of (a) sloshing amplitude and (b) structural displacement. (▬ rigid container; and flexible container with mass ratio of ◆ 2000 kg , ■ 1500 kg and ▲ 1000 kg) .

Summaries of all the simulations are given in Figure 4.4.10 for the structural mass of 2000 kg (◆),1500 kg (■) and 1000 kg (▲). The rms averages of the sloshing amplitudes are given in figure (a), whereas the same information is shown in figure (b) for the structure's displacement.

In the Figure 4.4.10 (a), a flexible container with 0 kg point mass results in a larger sloshing magnitude than the rigid container. The smallest sloshing magnitude is again around 7 kg to 9 kg of added masses which is in close agreement with the earlier predicted tuning. With 1000 kg structural mass, the lowest sloshing magnitudes are observed. The largest sloshing magnitudes are for the 2000 kg structural mass case. In Figure 4.4.10 (b), the structural displacement for all three cases reduces when the point masses are added. The structural response is quite insensitive to the tuning condition between the flexible container and the sloshing liquid.

4.5 Summary

This chapter outlines results on possibility of using intentionally induced liquid sloshing for the purposes of controlling structural vibrations. The objective is to employ the liquid sloshing dynamic forces on the container walls to control structural vibrations. The novelty is the presence of the flexible container of the sloshing absorber. The study in this chapter involves the complex two-level of tuning between the liquid, the flexible container and the structure to be controlled.

The primary tuning is maintained by designing the fundamental sloshing frequency of the liquid in a rigid container to be the same as the structural natural frequency. The second level of tuning is due to the interaction of the flexible container with the sloshing liquid, and it is not as straightforward as the primary tuning. The difficulties arise from the many vibration modes of the flexible container which interact with the sloshing liquid all at once. The second tuning is sought by adding point masses to the flexible container.

Majority of the presented cases are to investigate the effect of second level of tuning on the overall dynamics. For these, an approximately 10% mass ratio is maintained, between the structure to be controlled and the sloshing absorber. In order the clearly observe the effects of tuning, the structure is kept undamped and a critical damping ratio varying from 1.5% to 10% is used for the flexible container.

All cases clearly demonstrate the effect of secondary level of tuning on sloshing amplitudes where the most effective tuning is achieved with the flexible container with 7 kg to 9 kg of added mass Gradinscak et al. (2006). Sensitivity to tuning gradually diminishes with added structural damping of the flexible container.

All sloshing absorbers, including the rigid container, cause a smaller structural displacement. The flexible container cases exhibit decreasing structural displacements with increasing added mass on the container. This trend seems to be consistent even after the tuning is completely lost between the container and the liquid. The fact that the structure and the liquid can interact through a de-tuning flexible container is quite unexpected and deserves further attention.

Finally, the numerical investigations are presented to demonstrate the effect of the varying mass ratio (from 10% to 20%) of the sloshing absorber on the structure to be controlled. With increasing mass ratio, the structural control is enhanced. Again marginal sensitivity is observed to the tuning condition of the flexible container when the mass ratio is changed.

The numerical predictions presented in this chapter clearly suggest that a flexible container certainly holds promise for the effective control of excessive vibrations in resonant structures. The observations so far are exciting and warrant further investigation. These may open up opportunities to gain further insight to the dynamics and design of better controllers to increase the safety of light structures.

Chapter 5

CONCLUSIONS

AND SUGGESTIONS FOR FURTHER WORK

Sloshing is the low frequency oscillations of the free surface of a partially filled container. If not controlled effectively, sloshing may cause excessive dynamic loads that strongly interact with their adjacent structures which can then lead to structural failure or loss of stability. Hence, study and control of liquid sloshing is well justified in engineering and science.

The inherent flexibility of a liquid container has been generally treated in earlier studies as a problem. Container flexibility causes moving boundaries which further complicates the treatment of this already challenging problem. Container flexibility, on the other hand, may be treated as a design parameter to gain benefit in controlling the free surface oscillations. The novelty of the presented thesis is to investigate the required flexibility parameters of a container to achieve either the suppression of its content or to utilize intentionally induced sloshing as a vibration control agent for light and flexible structures.

As demonstrated in Chapter 2, a flexible container is able to suppress excessive sloshing when a strong interaction between the container and the liquid is made possible by tuning the flexible container. This tuning has been achieved by adding point masses to the container, for no other reason than convenience at this very exploratory stage. Tuning can of course be achieved by designing the stiffness properties of the container either in addition or along with its mass. Optimal tuning corresponded to added mass values between 7 kg and 9 kg producing about 80% reduction of sloshing magnitudes as compared to a rigid container of same dimensions. Chapter 2 represents the most significant contribution of this thesis.

Following on from the clearly positive outcome of Chapter 2, Chapter 3 reports on observations with a modified design for the flexible container. The motivation for this modification is the rather excessive wall deflections of the flexible container to achieve the levels of control reported in Chapter 2. Modification in the form of "tying" the two flexible walls to each other at their free end, using rigid linkages, has overcome the problem of excessive deflections without deterioration of the level of sloshing control.

Chapter 4 deals with concept of tuned sloshing dampers to control excessive oscillations of light resonant structures, such as transmission towers, long-span suspension bridges and high-rise buildings which are adversely affected by wind and earthquake loads. A tuned sloshing absorber with a flexible container is able to reduce structural response in the order of 80 %, in rms sense. This suggestion appears to be quite important practically to increase the safety and serviceability of such structures.

Being the first of its kind, and given the exploratory nature of the presented work, extensive experimental verifications could not be undertaken following the computational work. The simple experiments reported in Chapters 2 and 3 clearly demonstrate the validity of the predictions, but they lack detailed observations. Hence, the most important follow-up study of the investigation reported in this study is detailed experiments. Only then, it is meaningful to study the practical implementation of the quiet impressive levels of control, for industrial benefit. These studies may well include different, and possibly more practical, means of achieving tuning between the container and the sloshing liquid. In addition, variations of the design proposed in Chapter 3 may prove useful to overcome practical problems in application, due to large container deflections.

References

Abe, M., Kimura, S. and Fujino, Y., 1996, Semi-active Tuned Column Damper with Variable Orifice Openings, Third International Conference on Motion and Vibration Control, Chiba, pp.7-11.

Anderson, J. G., 2000, Liquid Sloshing in Containers, Its Utilisation and Control.

Anderson, J. G., Semercigil, S. E. and Turan, **Ö. F.,** 2000a, A Standing-Wave Type Sloshing Absorber to Control Transient Oscillations, Journal of Sound and Vibration, 232(5), pp. 839-856.

Anderson, J. G., Semercigil, S. E. and Turan, **Ö. F.,** 2000b, An Improved Standing-Wave Type Sloshing Absorber, Journal of Sound and Vibration, 235(4), pp. 702-710.

Anderson, J. G., Semercigil, S. E. and Turan, **Ö . F.,** 1998, Comparison of a Sloshing Absorber and Tuned Absorber for Optimal Vibration Control, Proceedings of the Australasian Conference on Structural Optimisation, Sydney, Australia, pp. 199-206.

ANSYS , 2002, User Manual, ANSYS Inc. Houston USA.

Bauer, H. F. and Chiba, M., 2004, Axisymetric Oscillation of a Viscous Liquid Covered by an Elastic Structure, Journal of Sound and Vibration, 281 (2005), pp. 835-847.

Chen, W. and Haroun, M. A., 1994, Dynamic Coupling Between Flexible Tanks and Seismically Induced Nonlinear Liquid Sloshing, Fluid Transients ASME,FED-Vol. 198/PVP-Vol.291.

Dimarogonas, A., 1995, Vibration for Engineers, second ed., Prentice-Hall, New Jersey, pp. 286-295.

Fotia, G., Massida, L. and Siddi, G., 2000, Computational Modelling of Sloshing in Flexible Tanks, CRS4-Waves & Structures, Tech. Rep 00.

Fujii, K., Tamura, W. and Wakahara T., 1990, Wind-Induced Vibration of Tower and Practical Applications of Tuned Sloshing Damper, Journal of Wind Engineering and Industrial Aerodynamics, Vol.33, pp.263-272.

Fujino, Y., Sun, L. M, Pacheco, B. M. and Chaiseri P., 1992, Tuned Liquid Damper (TLD) for Suppressing Horizontal Motion of Structure, Journal of Engineering Mechanics, Vol.118, No. 10, pp.263-272.

Fujino, Y., Pacheco, B. M., Chaiseri, P., and Sun, L. M., 1988, Parametric Studies on Tuned Liquid Damper (TLD) Using Circular Containers by Free-Oscillation Experiments, JSCE Journal of Structural Engineering/Earthquake Engineering 5 (2), pp.381-391.

Gardarsson, S., Yeh, H., and Reed, D., 2001, Behavior of Sloped-Bottom Tuned Liquid Dampers, Journal of Engineering Mechanics 127, (3), pp.266-271.

Garrido, M. F, 2003, On the Sloshing of Liquids in Parallelepiped – Shaped Containers, European Journal of Physics, PII:SO143-0807(03)57766-2 , No. 24, pp. 277-288.

Gradinscak, M. Semercigil, S. E. and Turan, **Ö. F.,** 2001, Sloshing Control with Container Flexibility, 14th Australasian Fluid Mechanics Conference, Adelaide University, Adelaide, Australia.

Gradinscak, M., Semercigil, S. E. and Turan, **Ö. F.,** 2002, Design of Flexible Containers for Sloshing Control, Proceedings of ASME FEDSM'02, ASME 2002 Fluids Engineering Division Summer Meeting, Montreal, Quebec, Canada.

Gradinscak, M., Guzel, U. B, Semercigil, S. E. and Turan, **Ö. F.,** 2004, Control of Liquid Sloshing in Flexible Containers: Part 2. Added Mass, 15th Australasian Fluid Mechanics Conference, University of Sydney, Sydney, Australia.

Gradinscak, M. Semercigil, S. E. and Turan, **Ö. F.,** 2006, Liquid Sloshing in Flexible Containers, Part1: Tuning Container Flexibility for Sloshing Control, Fift International conference on CFD in the Process Industries, CSIRO, Melbourne, Australia, 13-15 December.

Gradinscak, M. Semercigil, S. E. and Turan, **Ö. F.,** 2006, Liquid Sloshing in Flexible Containers, Part2:Using a Sloshing Absorber With a Flexible Container for Structural Control, Fift International conference on CFD in the Process Industries, CSIRO, Melbourne, Australia, 13-15 December.

Grundelius, M. and Bernhardsson, B., 2000, Constrained Iterative Learning Control of Liquid Slosh in an Industrial Packaging Machine, Proceedings of the 39th IEEE Conference on Decision and Control, Sydney, Australia.

Guzel, U. B, Gradinscak, M., Semercigil, S. E. and Turan, **Ö. F.,** 2004, Control of Liquid Sloshing in Flexible Containers: Part 1. Added Mass, 15th Australasian Fluid Mechanics Conference, University of Sydney, Sydney, Australia.

Guzel, U. B, Gradinscak, M., Semercigil, S. E. and Turan, **Ö. F.,** 2005, Tuning Flexible Containers for Sloshing Control, Proceedings of the IMAC-XXIII: A Conference & Exposition on Structural Dynamics, January 31-February 3, Orlando, Florida.

Haroun, M.A., and Housner, G.W., 1981, Seismic design of liquid storage tanks, Journal of Technical Councils of ASCE, Vol.107, No.TC1, pp. 191-207.

Jain, S.K. and Medhekar, P.S., 1993a, Proposed Provisions for Aseismic Design of Liquid Storage Tanks: Part I – Codal Provisions, Journal of Structural Engineering, Vol.20, No.3, pp.119-128.

Jain, S.K. and Medhekar, P.S., 1993b, Proposed Provisions for Aseismic Design of Liquid Storage Tanks: Part II – Commentary and Examples, Journal of Structural Engineering, Vol.20, No.4, pp.167-175.

Jeong, K. H. and Kim, K. J., 1998, Free Vibration of a Circular Cylindrical Shell Filled with Bounded Compressible Fluid, Journal of Sound and Vibration, Vol. 217, No.2, pp. 197-221.

Kana, D. D. and Abramson, H. N., 1966, Experimental Study of Liquid Instability in a Vibrating Elastic Tank, Journal of Spacecraft, Vol. 3, No. 8, pp. 1183-1188.

Kaneko, S. and Yoshida, O., 1994, Modelling of Deep Water Type Rectangular Tuned Liquid Dampar with Submerged Nets, The American Society of Mechanical Engineers, Fluid-Structure Interaction and Structural Response Due to Shock and Impact Loads, PVP-Vol.272,

pp. 31-42.

Malhotra, P. K., Wenk, T., and Wieland, M., 2000, Simple procedure for seismic analysis of liquid storage tanks, Structural Engineering, IABSE, Vol. 10, No.3, pp. 197-201.

Milne-Thomson, L. M., 1968, Theoretical Hydrodynamics 5th ed. Macmillan Press, London, pp. 427-442.

Mitra, S., and Sinhamahapatra, K. P, 2005, Coupled Slosh Dynamics of Liquid Containers Using Pressure Based Finite Element Method, Exploring Innovation in Education and Research, Tainan, Taiwan.

Modi, V. J, and Welt, F., 1984, Nutation Dampars and Suppresion of Wind Induced Instabilities, The American Society of Mechanical Engineers Joint Multidivisional Symposium on Flow-Induced Oscillations, Vol. 1, pp.173-187.

Nomura, T., 1994, ALE Finite Element Computations of Fluid-Structure Interaction Problems, Computer Methods and Applied Mechanics and Engineering 112, pp. 291-308.

Pal, N. C., Bhattacharya, S. K and Sinha, P. K, 2003, Non-Linear Coupled Slosh Dynamics of Liquid-Filled Laminated Composite Containers: a Two Dimensional, FE Approach, Journal of Sound and Vibration 261, pp. 729-749.

Popov, G., Sankar, S., Sankar, T. S and Vatistas, G. H., 1992, Liquid Sloshing in Rectangular Road Containers, Computers in Fluids, pp. 551-569.

Rao, S. S., 1995, Mechanical Vibrations, 3rd ed. Addison-Wesley Publishing Company, USA, pp. 603-613.

Reed, D., Yeh, H., Yu, J. and Gardarsson, S., 1998, Tuned Liquid Dampers Under Large Amplitude Excitation, Journal of Wind Engineering and Industrial Aerodynamics 74-76, pp. 923-930.

Sakamoto, D., Oshima, N., and Fukuda, T., 2001, Tuned Sloshing Damper Using Electro-Rheological Fluid, Institute of Physics Publishing, Smart Materials and Structure.10, PII:S0964-1726(01)27860-4,pp.963-969.

Schulkes, R. M., 1990, Fluid Oscillations in an Open Flexible Container, Journal of Engineering Mathematics 24, pp. 237-259.

Seto, M. L., and Modi, V. J., 1997, A Numerical Approach to Liquid Sloshing Dynamics and Control of Fluid-Structure Interaction Instabilities, The American Society of Mechanical Engineers, Fluid Engineering Division Summer Meeting, Paper no. FEDSM97-3302.

Soong, T. T., and Spencer Jr. B. F., 2002, Supplemental Energy Dissipation: State of Art and State of the Practice, Engineering Structures 24, pp.243-259.

Sun, L.M. and Fujino, Y., 1994**,** A Semi – Analytical Model for Tuned Liquid Damper (TLD) with Wave Breaking, Journal of Fluids and Structur (8)e, pp.471-488.

Takahara, H. Kimura, K. and Sakata, M., 1995, Frequency Response of Sloshing in a Circular Cylindrical Tank Subjected to Pitching Excitation, Proceedings of Asia Pacific Vibration Conference, Kuala Lumpur, pp. 703-708.

Tang, Y., 1994, SSI Effects for a Tank Containing Two Liquids, Sloshing, Fluid-Structure Interaction and Structural Response Due to Shock and Impact Loads, Vol. 272, Edited by D.C. Ma, Argonne National Labaratory, The Pressure Vessels and Piping Conference , Minnesota, pp. 67-71.

Veletsos, A.S, 1984, Seismic Response and Design of Liquid Storage Tanks, Guidelines for Seismic Design of Oil& Gas Pipelines system, ASCE, NY, pp. 255-370.

Wang, C. Z. , and Khao, B. C., 2004, Finite Element Analyses of Two-Dimensional Nonlinear Problem in Random Excitations, Ocean Engineering 32 (2005), pp: 107-113.

Warnitchai, P. and Pinkaew, T., 1998, Modelling of Liquid Sloshing in Rectangular Tanks with Flow-Damping Devices, Engineering Structures, 20(7), pp. 593-600.

Welt, F. and Modi, V. J., 1992, Vibration Damping Through Liquid Sloshing, Part1: A Nonlinear Analyses, ATransactions of the ASME, Journal Vibration and Acoustics, Vol. 114, pp. 10-16.

Yamamoto, K., and Kawahara, M., 1999, Structural Oscillation Control Using Tuned Liquid Dampers, Computers and Structures 71, pp.435-446.

Yano, K., Higashikawa, S. and Terashima, K., 2002, Motion Control of Liquid Container Considering an Inclined Transfer Path, Control Engineering Practice 10, pp. 465-472.

Yao, Y., Tulin, M.P. and Kolaini, A. R., 1994, Theoretical and Experimental Studies of Three-Dimensional Wavemaking in Narrow Tanks, Including Nonlinear Phenomena Near Resonance, Journal of Fluid Mechanics, Vol. 276, pp. 211-232.

APPENDIX A

Tuned Absorber

The concept of using a flexible container to control sloshing of a liquid is similar to that of using a tuned absorber to control excessive vibrations of a mechanical oscillator. In this Appendix a brief treatment of the classical undamped and damped dynamic absorber is presented for completeness.

A tuned absorber is a mechanical oscillator whose resonance frequency is tuned at a critical frequency of the structure to be controlled. As shown in Figure 1. the primary system with mass m_1, and stiffness k_1 represents the structure to be controlled, whereas the auxiliary oscillator with m_2 and stiffness k_2 is the tuned absorber. The purpose of adding the mass is to limit the motion of the structure when it is subjected to a particular excitation. A brief treatment of the subject is presented next. Detailed explanation of the classical tuned absorbers can be found in any standard textbook such as in Rao (1995) and Dimarogonas (1995).

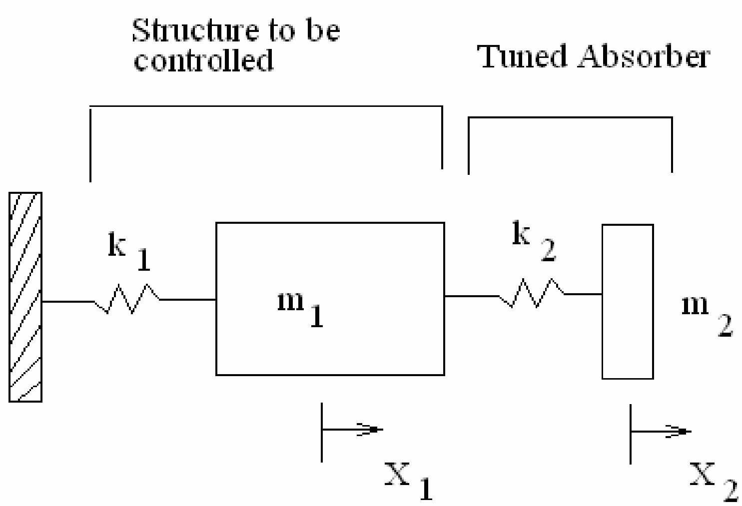

Figure1. Undamped dynamic vibration absorber.

In what follows, three different parameters of importance will be discussed. First, the effect of different tuning frequencies on the vibration control of the primary system will be demonstrated. Secondly, the effect of different mass ratios on a frequency range will be discussed. The motion of the primary mass will be significantly influenced by the absorber in a frequency range centered on the natural frequency of the primary system. For smaller values of mass ratio, the sensitivity of the absorber to tuning will increase. Outside of this frequency range absorber will have no influence on primary system movement. With increasing mass ratio the separation between those two frequencies will increase and the wider frequency range will be obtained. Thirdly, the effect of applying different damping ratios of the absorber will be discussed in order to reduce the amplitude of the vibration of the primary system at off-tuned frequencies.

The differential equations of motion, when a harmonic excitation of $F_0\, e^{i\omega t}$ is applied on the primary mass m_1, are

$$m_1\ddot{y}_1 + k_1 y_1 + k_2\,(y_1 - y_2) = F_0\, e^{i\omega t} \tag{1}$$

$$m_2\ddot{y}_2 + k_2\,(y_2 - y_1) = 0 \tag{2}$$

By assuming a harmonic solution in the steady state, in the form of the excitation

$$y_1 = X_1\, e^{i\omega t} \qquad \ddot{y}_1 = -\omega^2 X_1\, e^{i\omega t} \tag{3}$$

$$y_2 = X_2\, e^{i\omega t} \qquad \ddot{y}_2 = -\omega^2 X_2\, e^{i\omega t} \tag{4}$$

and substituting these assumed forms in the equations of motion

$$- m_1\omega^2 X_1\, e^{i\omega t} + k_1 X_1\, e^{i\omega t} + k_2\,(X_1\, e^{i\omega t} - X_2\, e^{i\omega t}) = F_0\, e^{i\omega t} \tag{5}$$

$$- m_2\omega^2 X_2\, e^{i\omega t} + k_2\,(X_2\, e^{i\omega t} - X_1\, e^{i\omega t}) = 0 \tag{6}$$

with elimination of $e^{i\omega t}$ in (5) and (6)

$$- m_1\omega^2 X_1 + k_1 X_1 + k_2 X_1 - k_2 X_2 = F_0 \quad (7)$$

$$- m_2 \omega^2 X_2 + k_2 X_2 - k_2 X_1 = 0 \quad (8)$$

From equation (8)

$$X_2 = k_2 X_1 /(k_2 - m_2 \omega^2) \quad (9)$$

By substituting expression (9) into the equation (7) the following is obtained

$$X_1 (k_1 + k_2 - m_1\omega^2) = F_0 + k_2 k_2 X_1 / (k_2 - m_2\omega^2) \quad (10)$$

$$X_1 = \mathbf{F_0 (k_2 - m_2\omega^2) / [(k_1 + k_2 - m_1\omega^2) (k_2 - m_2\omega^2) - k_2^2]}$$

(11)

Using equation (9), the steady state magnitude of the absorber becomes

$$X_2 = \mathbf{k_2F_0 / [(k_1 + k_2 - m_1\omega^2) (k_2 - m_2\omega^2) - k_2^2]} \quad (12)$$

The primary interest is to reduce amplitude X_1 of m_1 to zero.

$$F_0 (k_2 - m_2\boldsymbol{\omega}^2) / [(k_1 + k_2 - m_1\boldsymbol{\omega}^2) (k_2 - m_2\boldsymbol{\omega}^2) - k_2^2]= 0 \quad (13)$$

Equation (13) is satisfied if its numerator equals to zero. Hence,

$$k_2 - m_2\boldsymbol{\omega}^2=0$$

(14)

or

$$\omega^2 = k_2/m_2 \quad (15)$$

which means that the natural frequency of the auxiliary absorber should coincide with the square of the exciting frequency. In the case when device is used to reduce vibration at resonance of the primary component, it is desired to have the natural frequency of the absorber to be the same as that of the structure to be controlled:

$$(k_1/m_1)^{1/2} = (k_2/m_2)^{1/2.} \qquad (16)$$

If the absorber is designed using equation (16), the amplitude of vibration of the system, while operating at its original resonant frequency, will be zero. By defining

$\delta_{st} = F_o/k_1$ and

$\omega_1^2 = k_1/m_1$ as the natural frequency of the primary system alone and

$\omega_2^2 = k_2/m_2$ as the natural frequency of the absorber, as a single degree-of-freedom oscillator, equations can be put into a compact form as:

$$X_1/\boldsymbol{\delta_{st}} = \mathbf{[1-(\omega/\omega_2)^2]/\{[1+k_2/k_1-(\omega/\omega_1)^2]\ [1-(\omega/\omega_2)^2]-k_2/k_1\}} \qquad (17)$$

$$X_2/\boldsymbol{\delta_{st}} = \mathbf{1/\{[1+k_2/k_1-(\omega/\omega_1)^2]\ [1-(\omega/\omega_2)^2]-k_2/k_1\}} \qquad (18)$$

For $X_1 = 0$ and $\omega = \omega_2$ and from equation (18)

$$X_2 = -k_1/k_2\delta_{st} = -F_0/k_{2.} \qquad (19)$$

$$k_{2.}\ X_2 = -F_0 \qquad (20)$$

In other words, the force $k_{2.}\ X_2 = -Fo$ is the spring force exerted by oscillations of mass m_2 on mass m_1. This “control force” is equal in magnitude, but opposite in sign with the force applied to mass m_1 making the net force on m_1 to be zero, thus justifying the effect of “tuning”.

In Figure 2, the variation of the amplitude of vibration of the primary system when the absorber is tuned to four different frequencies, is presented. X axis represents the non-dimensional frequency (ω). The Y axis represents variation of the amplitude of vibration of the system (X_1/δ_{st}). The first case (——) is the case when the natural frequency of absorber coincides with the excitation frequency, frequency ratio of 1. The second (——), third (——) and fourth (——) cases correspond to tuning the absorber to 0.96, 0.88 and 0.76 of the natural frequency of the primary system, respectively. In Figure 2, the value of $X_1/\delta st$ is consistently brought to zero at the tuning frequency of each of the four cases.

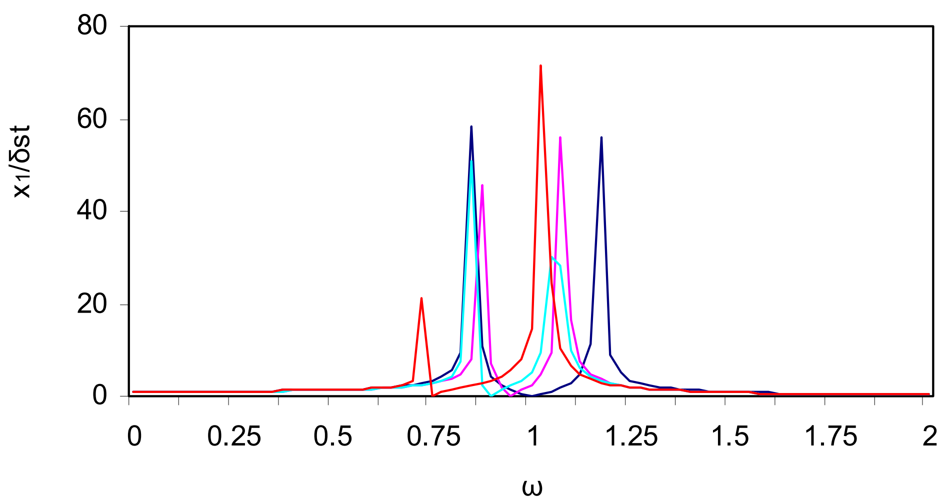

Figure 2. Effect of different tuning frequencies on the frequency response of an undamped dynamic vibration absorber. Mass ratio is 0.10.

As demonstrated graphically in Figure 2, the system now has two resonance frequencies, neither of which equals to the original resonance frequency of the main mass or of the absorber. If there is no damping in this system, the response at these new resonance frequencies will be infinitely large. If those two frequencies are also very close, there may be practical difficulties to employ this system safely. For such cases, any slight deviation from the tuning frequency may cause large amplitude oscillations. One way to avoid having these two resonance frequencies close to each other may be to increase the mass of the absorber as discussed below. Well separated resonance frequencies will enable a safe margin of frequencies around the tuning frequency.

In Figure 3, the variation of the amplitude of vibration of the system (X_1/δ_{st}) with the non-dimensional frequency ratio 'ω' is shown. For an undamped single-degree-of freedom system (----), amplitude ratio is infinite when frequency ratio is close to 1. Other two cases are for the case of 10% mass ratio (—), and 20% mass ratio (—) between the absorber and the primary system. With the larger mass ratio (20%), the separation between the two new natural frequencies is larger. For 10 %, the resonances are located at 0.975 and 1.03, whereas for 20%, they are at 0.95 and 1.06. But, even if the resonances are well separated the magnitude of those frequencies are still infinite. One solution is to add damping that will be explained below.

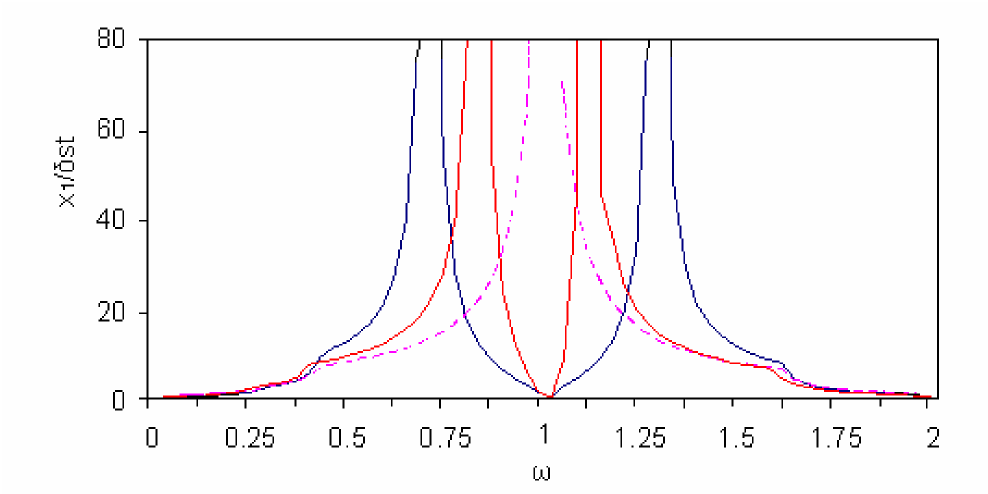

Figure 3. Variation of the displacement of the undamped vibration absorber with frequency without an absorber (----), and with an absorber of mass ratio 10% (——) and 20% (——). Tuning frequency is ω_1.

As mentioned above with applying damping to an absorber the spectral magnitudes of the two resonance frequencies are expected to decrease. Figure 4.

schematically illustrates such a system. As before, the primary system with mass m_1 and stiffness k_1 represents the structure to be controlled, whereas the auxiliary oscillator with m_2, c_2 and k_2 is the tuned absorber.

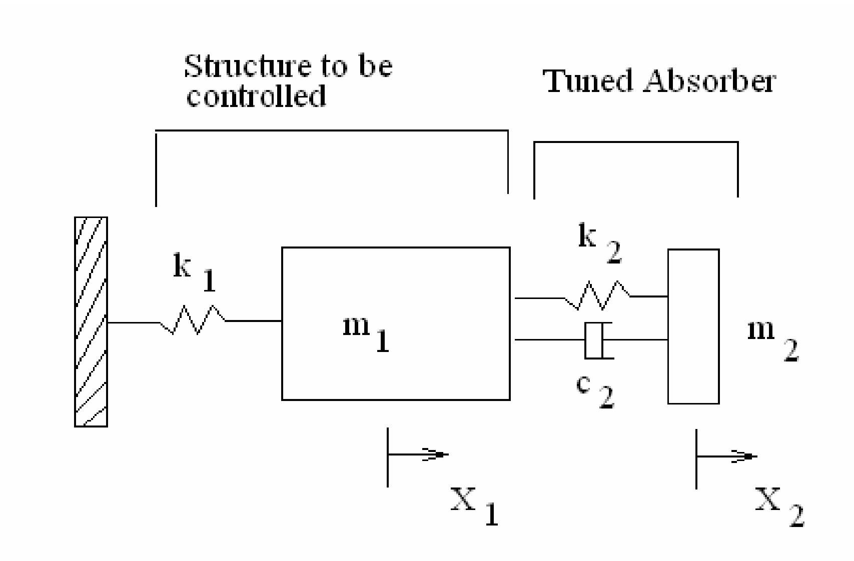

Figure 4. Damped dynamic vibration absorber

The governing equations of motion of the system for the case of damped absorber are

$$\mathbf{m_1\ddot{y}_1 + k_1y_1 + k_2(y_1\text{-}y_2) + c_2(\dot{y}_1 - \dot{y}_2) = F_0\, e^{i\omega t}} \tag{20}$$

$$\mathbf{m_2\ddot{y}_2 - k_2(y_2 + y_1) + c_2(\dot{y}_2 - \dot{y}_1) = 0} \tag{21}$$

By assuming harmonic solution

$$y_1(t) = X_1e^{i\omega t} \qquad \ddot{y}_1(t) = -\omega^2 X_1e^{i\omega t}$$

$$y_2(t) = X_2e^{i\omega t} \qquad \ddot{y}_2(t) = -\omega^2 X_2e^{i\omega t}$$

from the equation (20)

$$-m_1\omega^2 X_1e^{i\omega t} + k_1 X_1e^{i\omega t} + k_2 (X_1e^{i\omega t} - X_2e^{i\omega t}) + c_2(i\omega X_1e^{i\omega t} - i\omega X_2e^{i\omega t}) = F_0\, e^{i\omega t} \tag{22}$$

$$-m_1\omega^2 X_1e^{i\omega t} + k_1 X_1e^{i\omega t} + k_2 X_1e^{i\omega t} - k_2 X_2e^{i\omega t} + ic_2\omega X_1e^{i\omega t} - ic_2\omega X_2e^{i\omega t} = F_0\, e^{i\omega t} \tag{23}$$

dividing both sides with the exponential term and grouping

$$X_1 = \mathbf{[F_0} + X_2\, \mathbf{(k_2 + ic_2\, \omega)]/(-m_1\omega^2 + k_1 + k_2 + ic_2\omega)} \quad (24)$$

Similarly, for the second equation from (21)

$$-m_2\omega^2 X_2e^{i\omega t} + k_2 X_2e^{i\omega t} - k_2 X_1e^{i\omega t} + ic_2\omega X_2e^{i\omega t} - ic_2\omega X_1e^{i\omega t} = 0$$

$$-m_2\omega^2 X_2 + k_2 X_2 - k_2 X_1 + ic_2\omega X_2 - ic_2\omega X_1 = 0$$

$$X_2 = X_1\, \mathbf{(k_2 + ic_2\, \omega)/(-m_2\omega^2 + k_2 + ic_2\omega)} \quad (25)$$

By substituting expression (25) into the equation (24) the following is obtained

$$X_1 = [F_0 + X_1 (k_2 + ic_2\, \omega)^2/(-m_2\omega^2 + k_2 + ic_2\omega)]/(-m_1\omega^2 + k_1 + k_2 + ic_2\omega) \quad (26)$$

and grouping the real and imaginary components

$$X_1 = \mathbf{F_0(-m_2\omega^2 + k_2 + ic_2\omega)/\{[(k_1 - m_1\omega^2)(k_2 - m_2\omega^2) - m_2 k_2\omega^2] + i\omega c_2(k_1 - m_1\omega^2 - m_2\omega^2)\}}$$

$$X_2 = \mathbf{F_0(k_2 + i\omega c_2)\{[(k_1 - m_1\omega^2)(k_2 - m_2\omega^2) - m_2 k_2\omega^2] + i\omega c_2(k_1 - m_1\omega^2 - m_2\omega^2)\}} \quad (27)$$

By defining

$\mu = m_2/m_1$ - mass ratio, $f = \omega_2/\omega_1$ –ratio of natural frequencies, $g = \omega/\omega_1$ – forced frequency ratio, $\delta_{st} = F_0/k_1$ – static deflection of the system, $\omega_2^2 = k_2/m_2$ – square of natural frequency of absorber, $\omega_1^2 = k_1/m_1$ - square of natural frequency of main system, $c_c = 2m_2\omega_2$ - critical damping constant, ξ- damping ratio

and

$$X_1/\delta_{st} = [(2\xi g)^2 + (g^2 - f^2)]/\{(2\xi g)^2(g^2 - 1 + \mu g^2)^2 + [\mu f^2 g^2 - (g^2 - 1)(g^2 - f^2)]^2\}^{1/2} \quad (28)$$

$$X_2/\delta_{st} = [(2\xi g)^2 + f^2)]/\ \{(2\xi g)^2(g^2 - 1 + \mu g^2)^2 + [\mu f^2 g^2 - (g^2 - 1)(g^2 - f^2)]^2\}^{1/2} \tag{29}$$

If equation (28) is compared with equation (17) for the undamped system, it is obvious that there is a significant difference in their numerators. As result, the value of $X_1/\delta st$ cannot be tuned to be zero anymore, and therefore it is impossible to get perfect tuning. Hence, if damping is present in the absorber it is not possible to eliminate steady state vibrations of the primary mass. But it is still expected to have reduced spectral amplitudes.

In Figure 5, four different cases are shown, one for the case without absorber (----), undamped absorber (——) and two different damping cases. First, for the damping ratio of 0.1 (——) , the resonance peak amplitudes are suppressed to finite values, as compared to the undamped case, as a result of energy dissipation. For the case with 0.1 damping ratio, spectral peaks move left from those of the ideal undamped case. Secondly, when damping ratio is increased to 0.3(——), the absorber mass is practically rigidly attached to the mass of the primary component. For this excessively large damping ratio, absorber moves in phase with the primary structure. Such a system starts to behave as a one degree of freedom system.

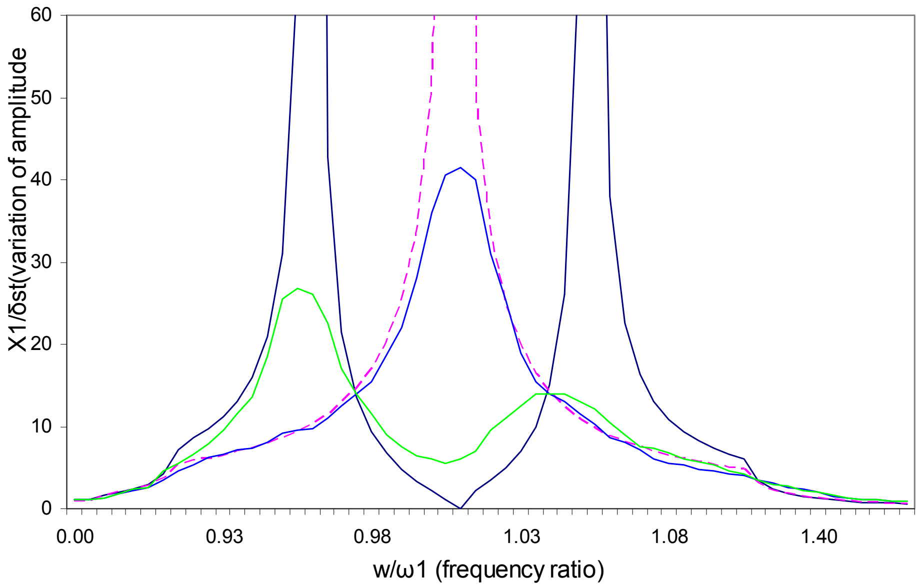

Figure 5. Variation of the displacement of the undamped vibration absorber with frequency without an absorber (----), and with an undamped absorber (——) damping ratio of 0.10 (——) and 0.3 (——). Tuning frequency and mass ratio are ω_1 and 0.10, respectively.

APPENDIX B

Selection of the length of Simulation Time

This Appendix presents results obtained in forty second time frames of the simulation for suppression of sloshing in a flexible container. The 0 kg, 9 kg and 13 kg added point masses are detailed in Chapter 2. The remainder, 3, 5, 7 and 11 kg are presented here.

Again, frame (a) contains the histories of the horizontal motion of the container nodes located in the middle of the wall near the top, (refer Figure 2.3.1), and the vertical motion of the liquid free surface nodes. In all the following figures in frame (a), colors (■) (■) present horizontal displacement histories of the container and colors (■) (■) present vertical displacement of the liquid. In the frame (b), the resulting sloshing amplitude is shown. In the frame (c), the frequency spectra of the container displacement (blue) and sloshing (red) are presented. All FFT figures in this thesis are presented as single sided spectrum, while FFT results from MatLab are double sided spectrum. Therefore all results need to be multiplying by two.

The horizontal axis represents frequency in [Hz] and the vertical axis represents spectral magnitude [m]. There is a difference between magnitude from time series figures and spectral magnitude from FFT figures.

As for the 20 seconds run cases an improvement of the sloshing magnitude is apparent when point masses are added at the top of the container. Again the best tuned case can be observed between 7 kg and 9 kg added point masses, with observable decreases in sloshing occurring as the point masses of 3 kg through to the 7 kg were added. The tuning was lost when 11 kg point masses were added to the container. As in Chapter 2, it also shows that initially a twenty second settling period for the liquid did not let the liquid reach it static equilibrium.

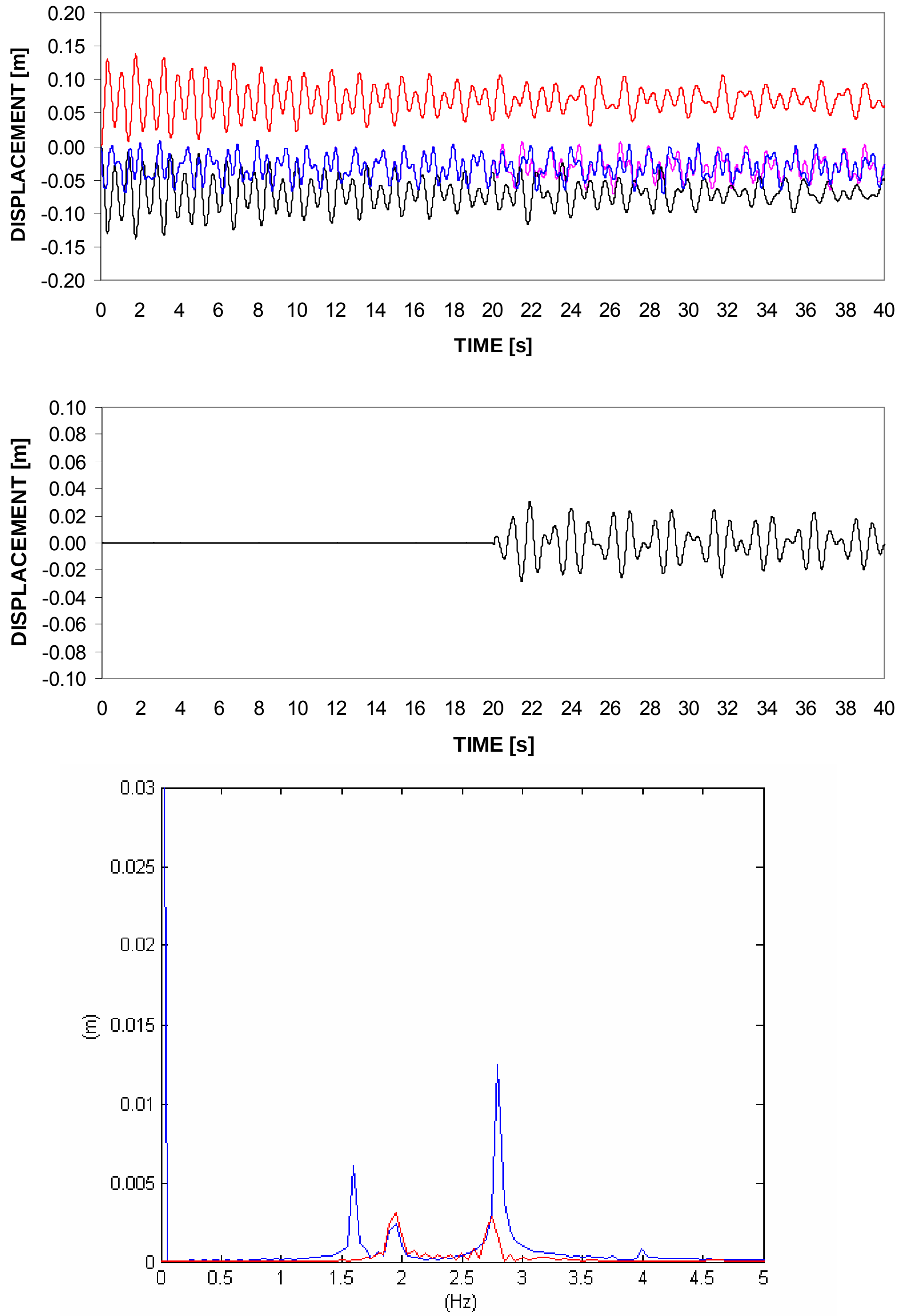

Figure B.1: Displacement histories of the liquid in a flexible container with 1 mm wall thickness and 3kg added mass (a).The liquid is undamped and structure has 1% damping. Predicted sloshing amplitude for the same case (b). Corresponding frequency spectrum of sloshing liquid (red) and structure (blue) (c).

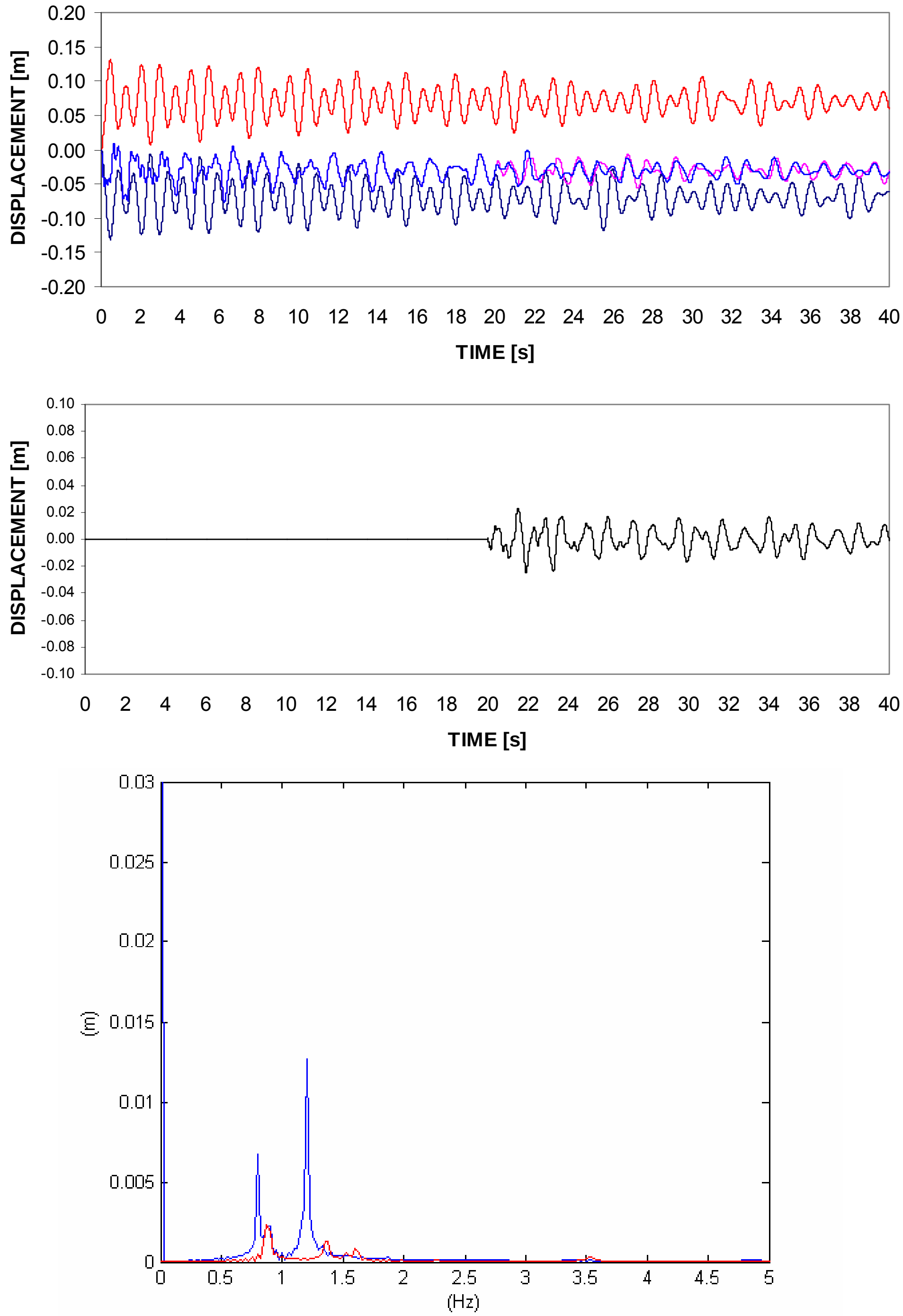

Figure B.2: Same as in Figure B.1 but for 5 kg added point mass.

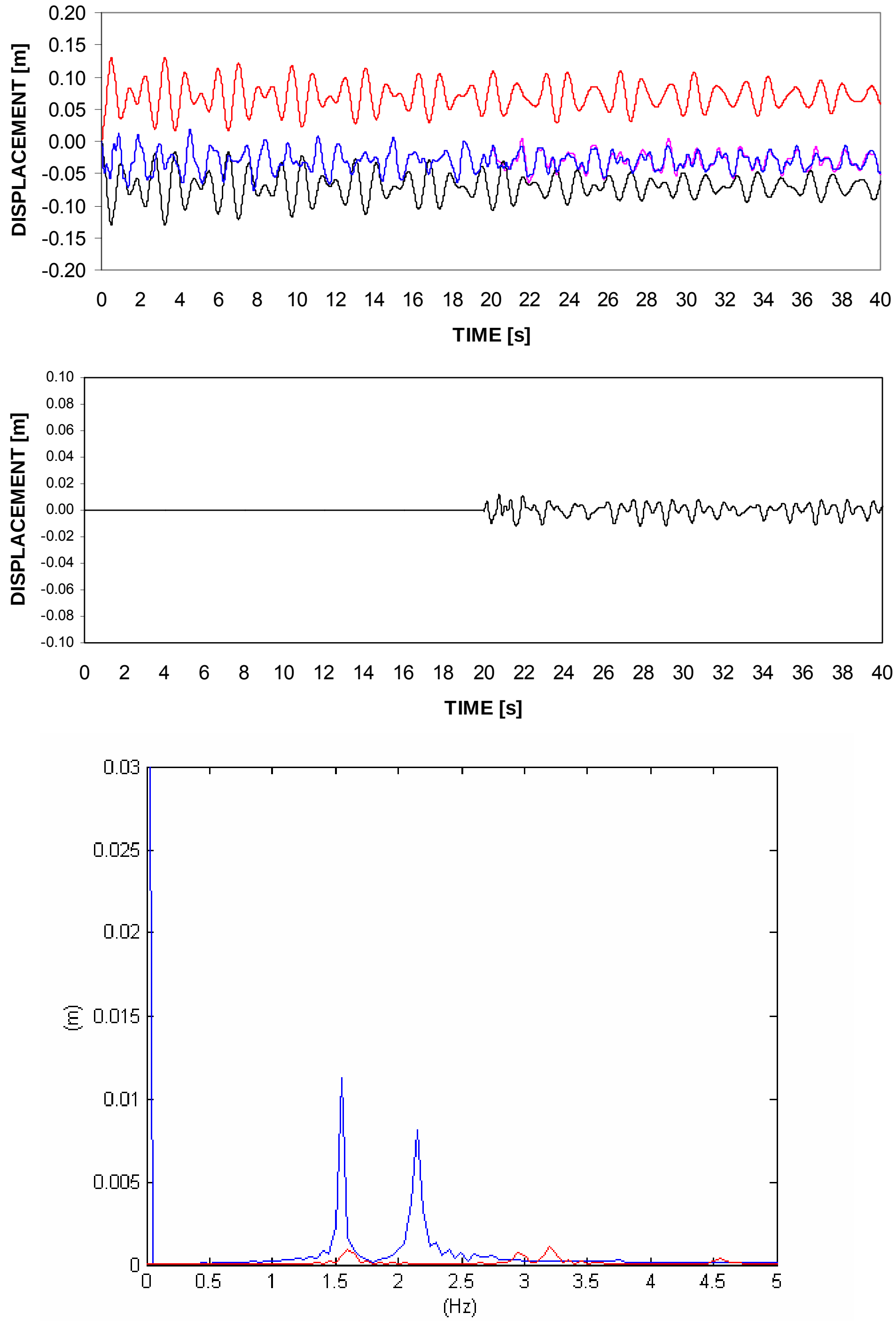

Figure B.3: Same as in Figure B.1 but for 7 kg added point mass.

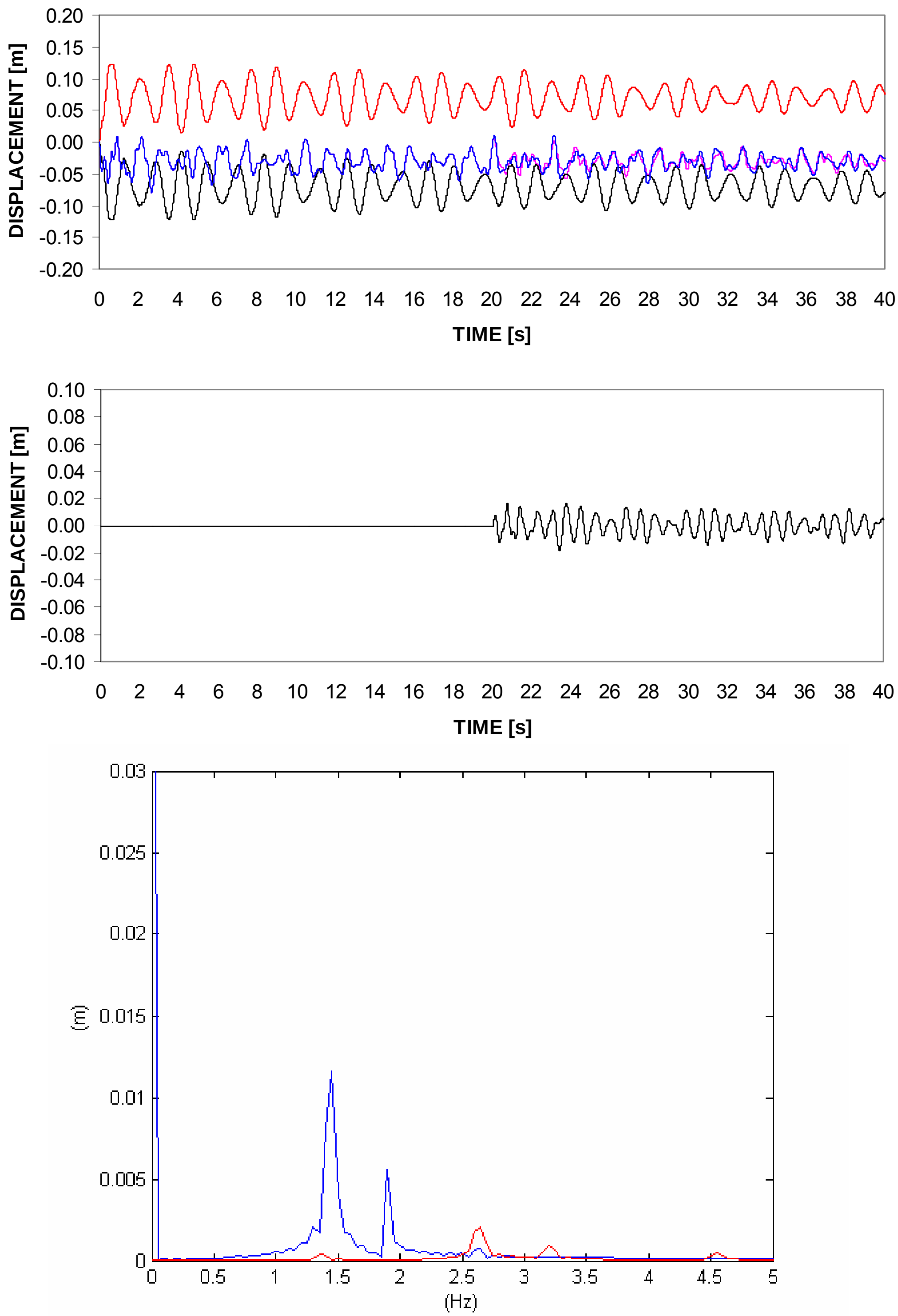

Figure B.4: Same as in Figure B.1 but for 11 kg added point mass.

APPENDIX C

Cases with different critical structural damping applied to the container

This Appendix presents additional results obtained for 5 % and 10 % structural damping of the container and its affect on displacement of the controlled structure.

Figures C.1, C.2, C.3 and C.4 are presented here for the cases of 3 kg, 5 kg, 7 kg and 11 kg added point masses. The critical structural damping applied to the container was 5%.

Figures C.5, C.6, C.7 and C.8 present cases with 3 kg, 5 kg, 7 kg and 11 kg added point masses and 10% critical structural damping applied to the container.

It confirmed that when critical damping was increased, the structure's displacement was reduced further. As outlined before, the best controlled case was that with the 10% added critical damping.

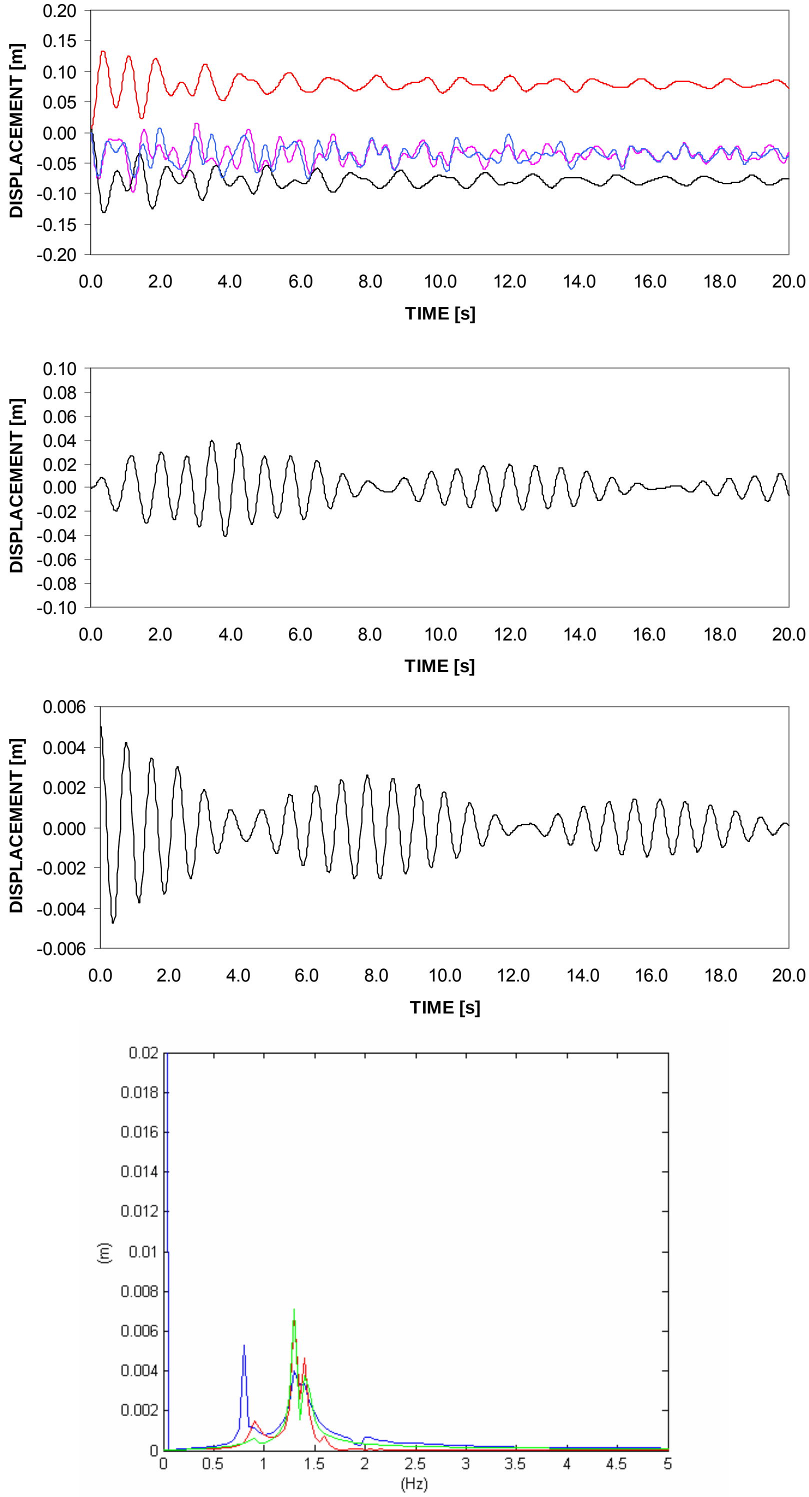

Figure C.1: a) numerically predicted displacement histories of the container walls and liquid. b) predicted sloshing amplitude in flexible container with 3 kg point mass, c) structure displacement and d) FFT of wall displacement (blue), sloshing liquid (red) and plate displacement (green). Liquid is undamped and container has 5% damping.

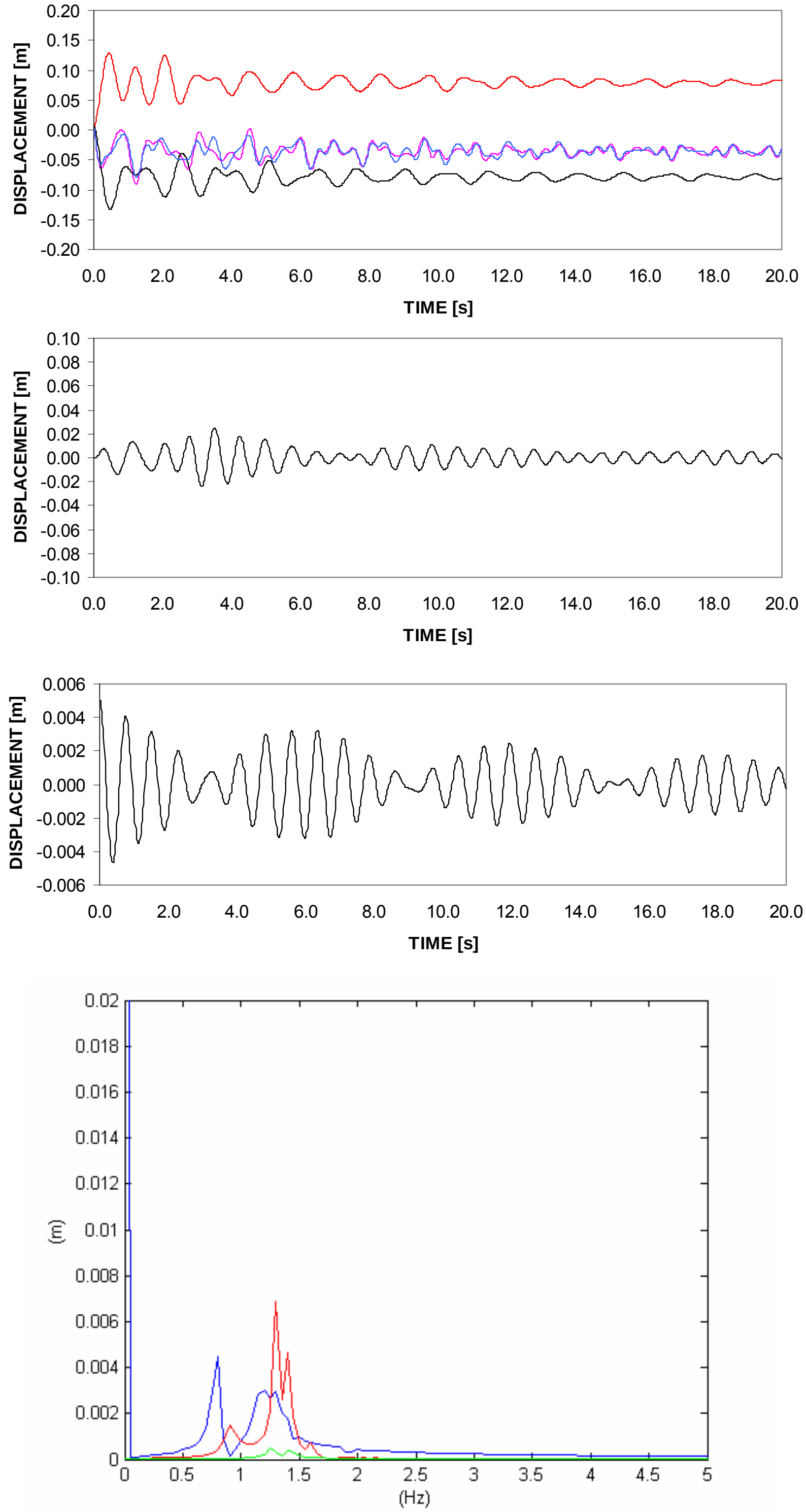

Figure C.2: Same as in Figure C.1 but for 5 kg point mass.

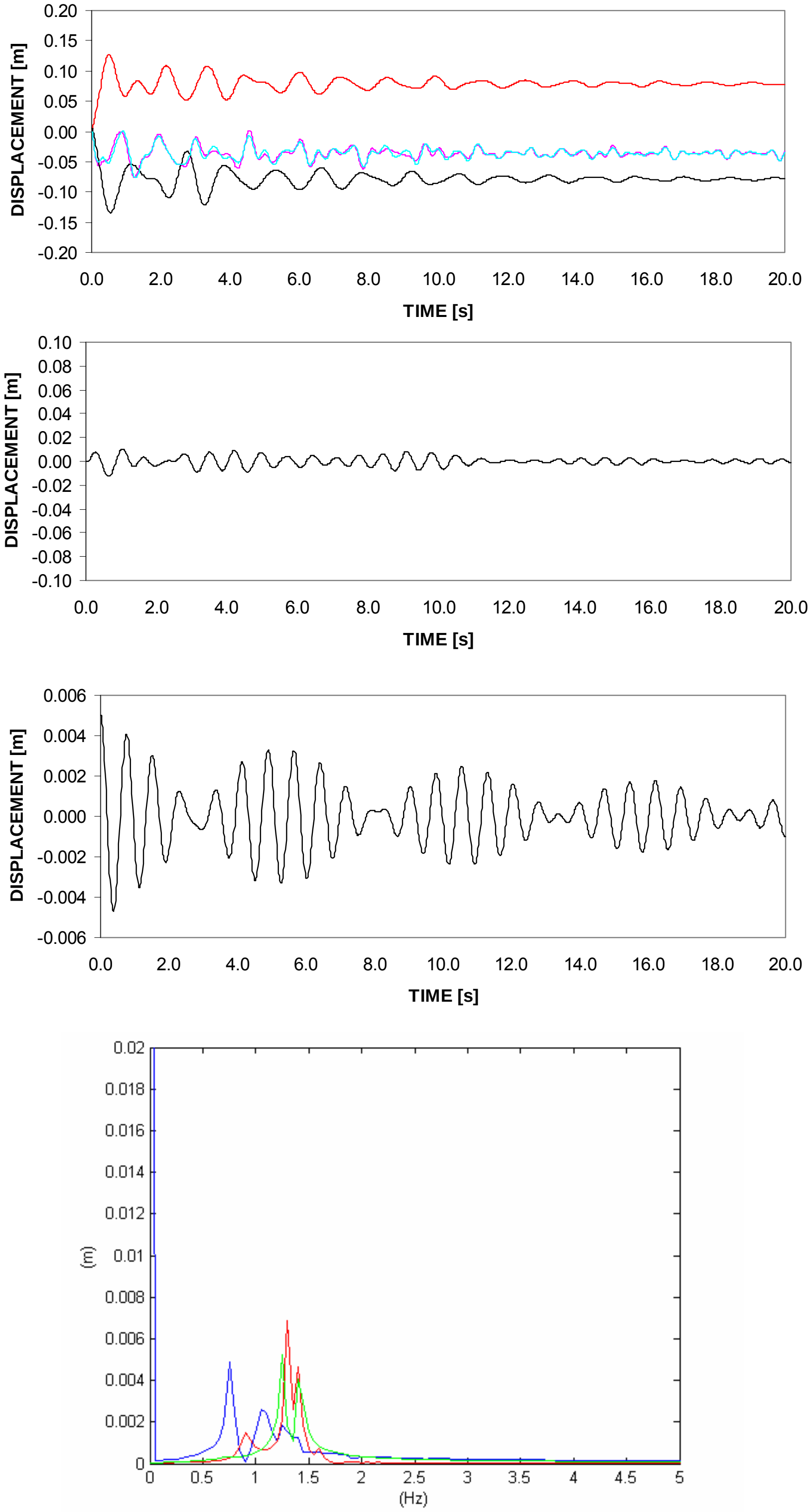

Figure C.3: Same as in Figure C.1 but for 7 kg point mass.

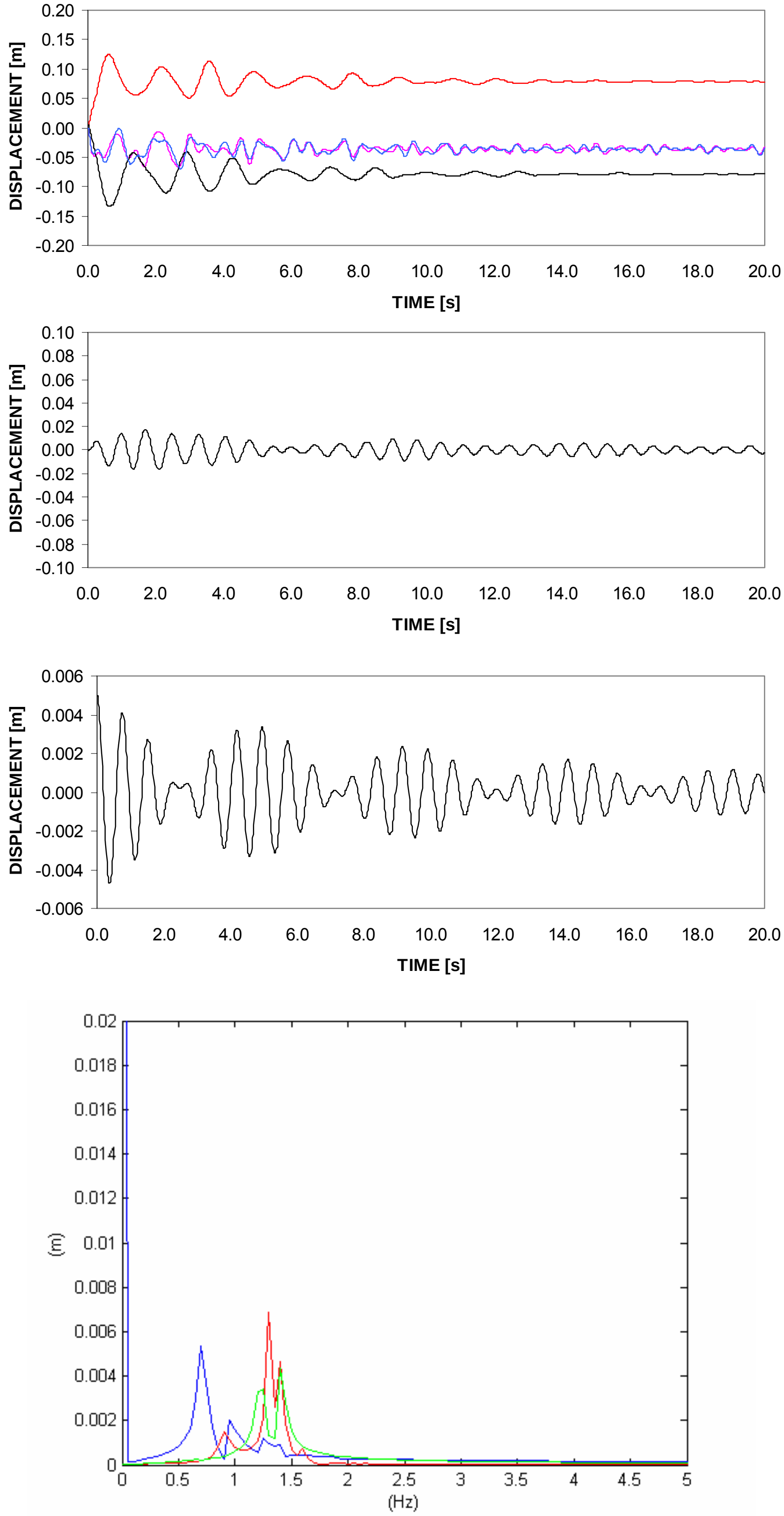

Figure C.4: Same as in Figure C.1 but for 11 kg point mass.

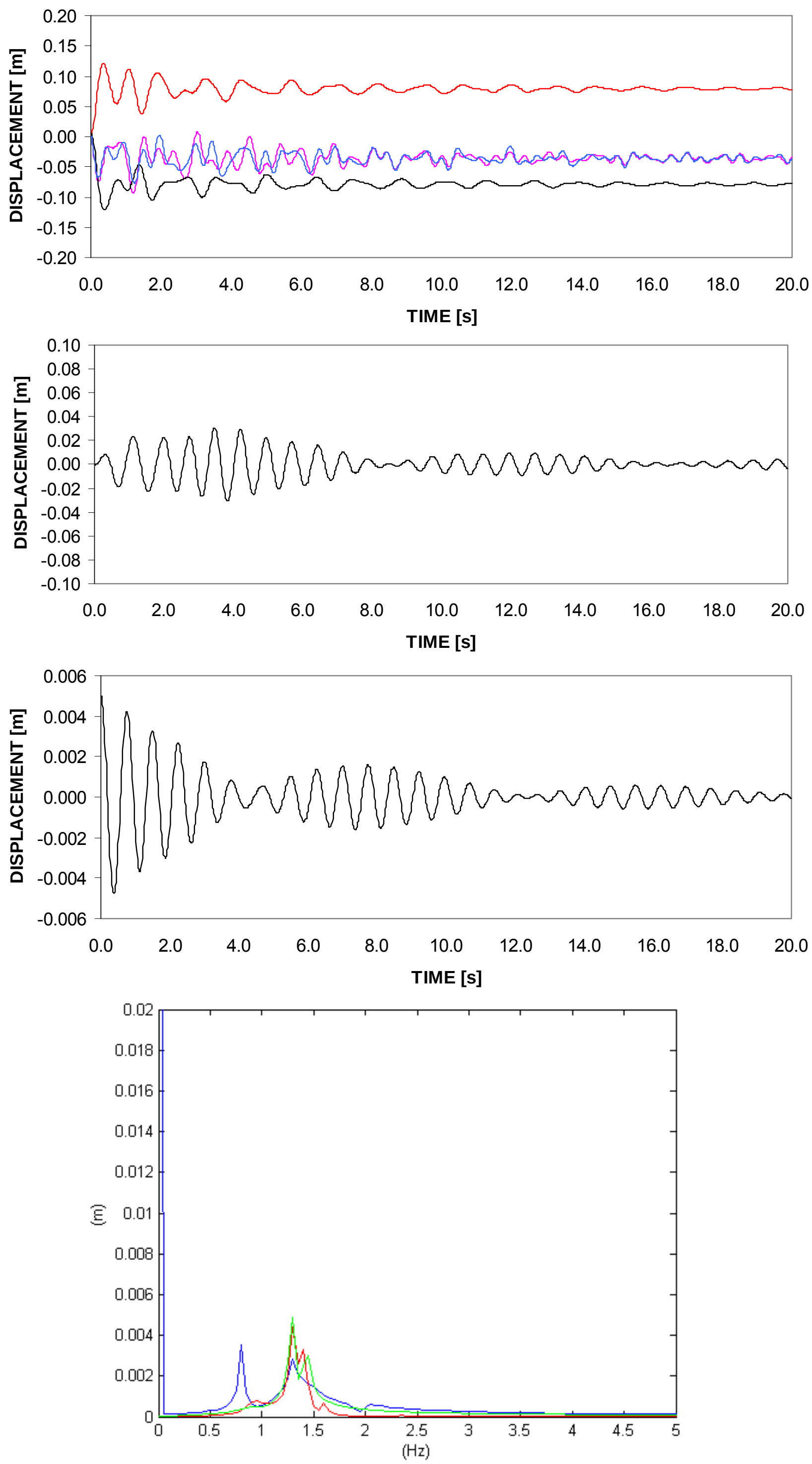

Figure C.5: a) numerically predicted displacement histories of the container walls and liquid. b) predicted sloshing amplitude in flexible container with 3 kg point mass, c) structure displacement and d) FFT of wall displacement (blue), sloshing liquid (red) and plate displacement (green). Liquid is undamped and container has 10% damping.

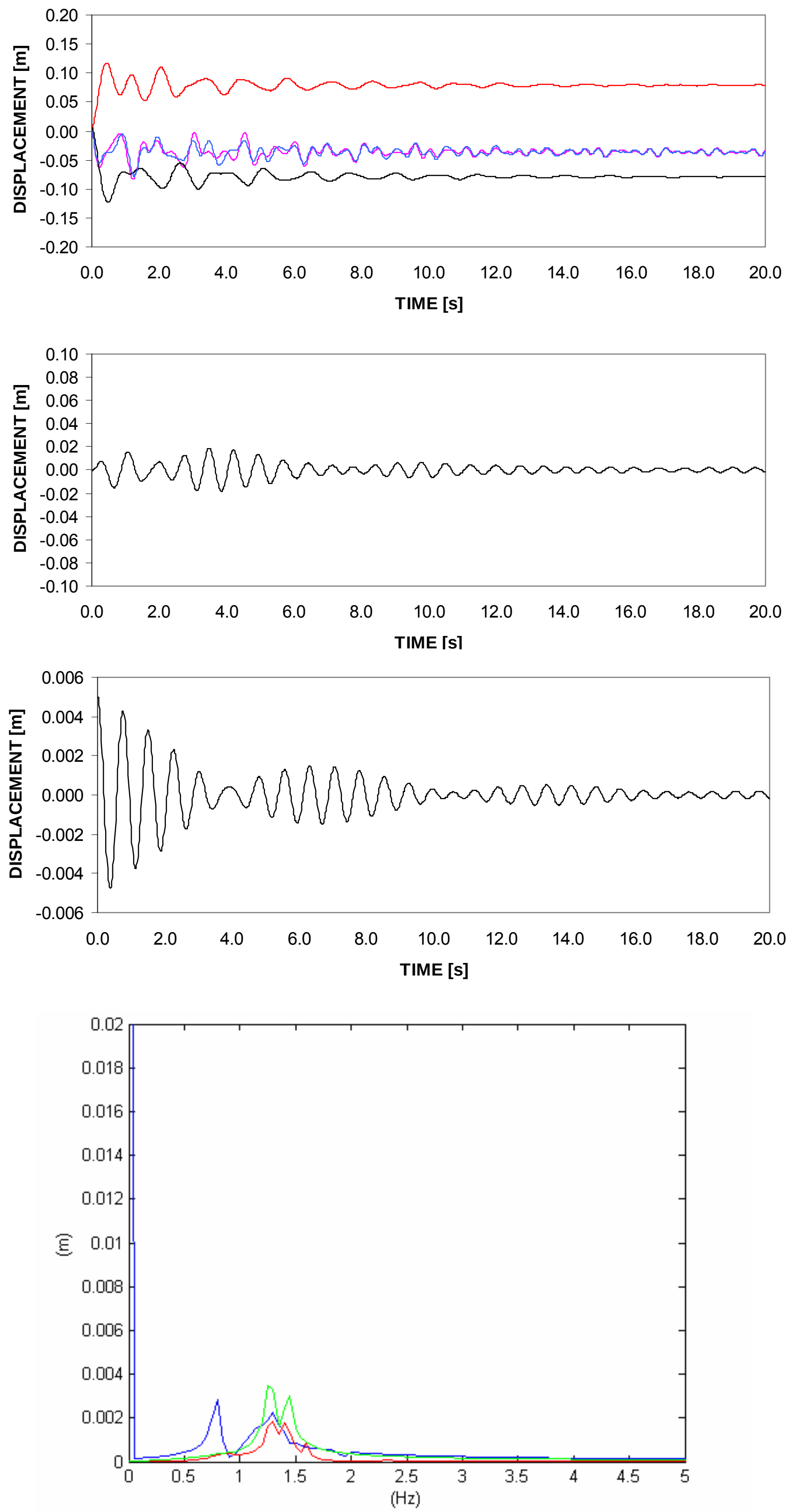

Figure C.6: Same as in Figure C.5 but for 5 kg point mass.

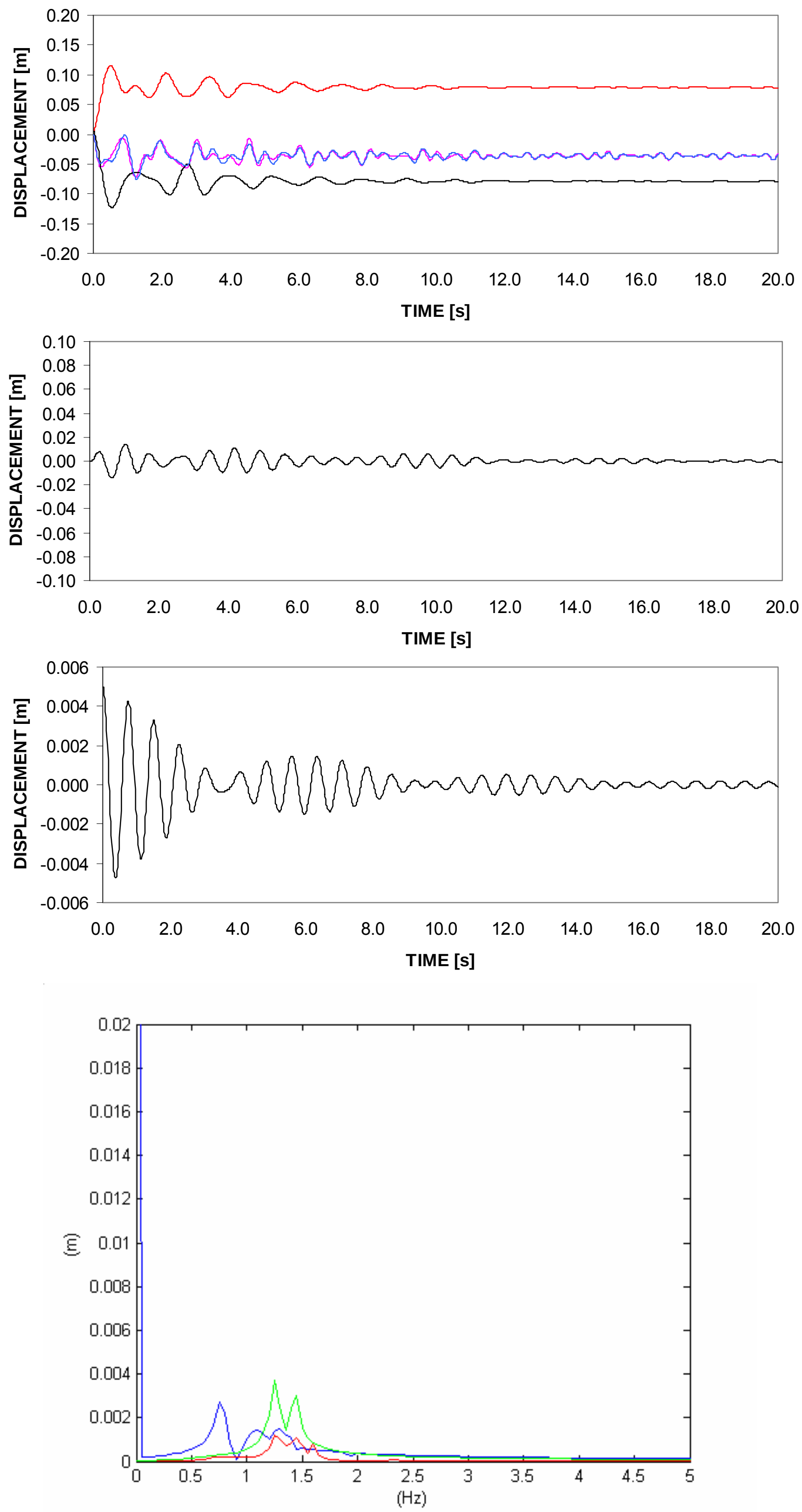

Figure C.7: Same as in Figure C.5 but for 7 kg point mass.

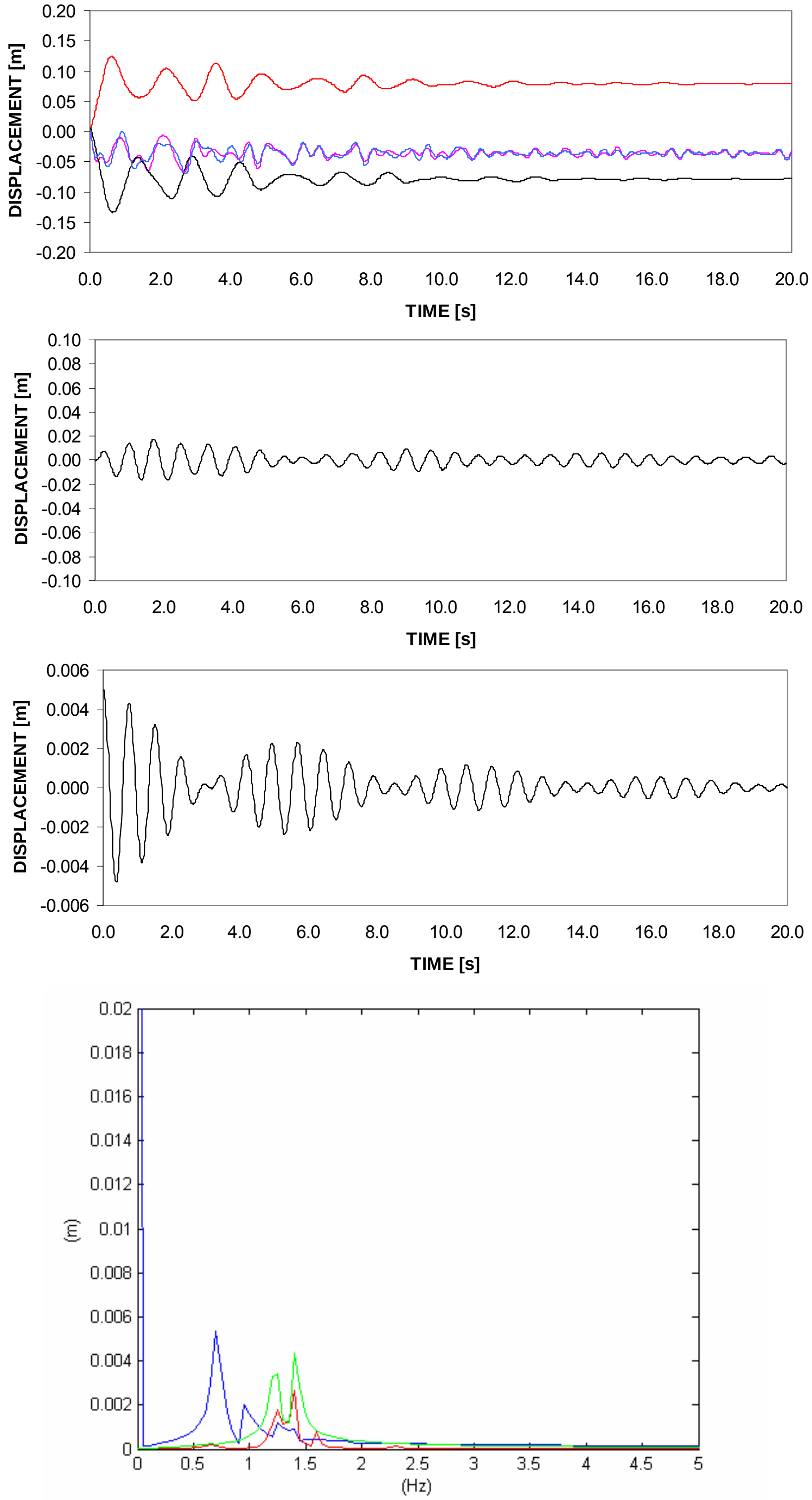

Figure C.8: Same as in Figure C.5 but for 11 kg point mass.

APPENDIX D

Cases with different mass ratio

This Appendix presents additional information in regard to the effect of different mass ratios on the structure's displacement when liquid dampers are applied. For completeness of the thesis, Figures D.1, D.2, D.3 and D.4 are presented here for the cases of 3 kg, 5 kg, 7 kg and 11 kg added point masses. For these figures, the mass of the structure is taken to be 1500 kg.

Figures C.5, C.6, C.7 and C.8 present cases with 3 kg, 5 kg, 7 kg and 11 kg added point masses to a structure with a mass of 1000 kg.

As already outlined in Chapter 4, the structural displacement was reduced when the point masses were added.

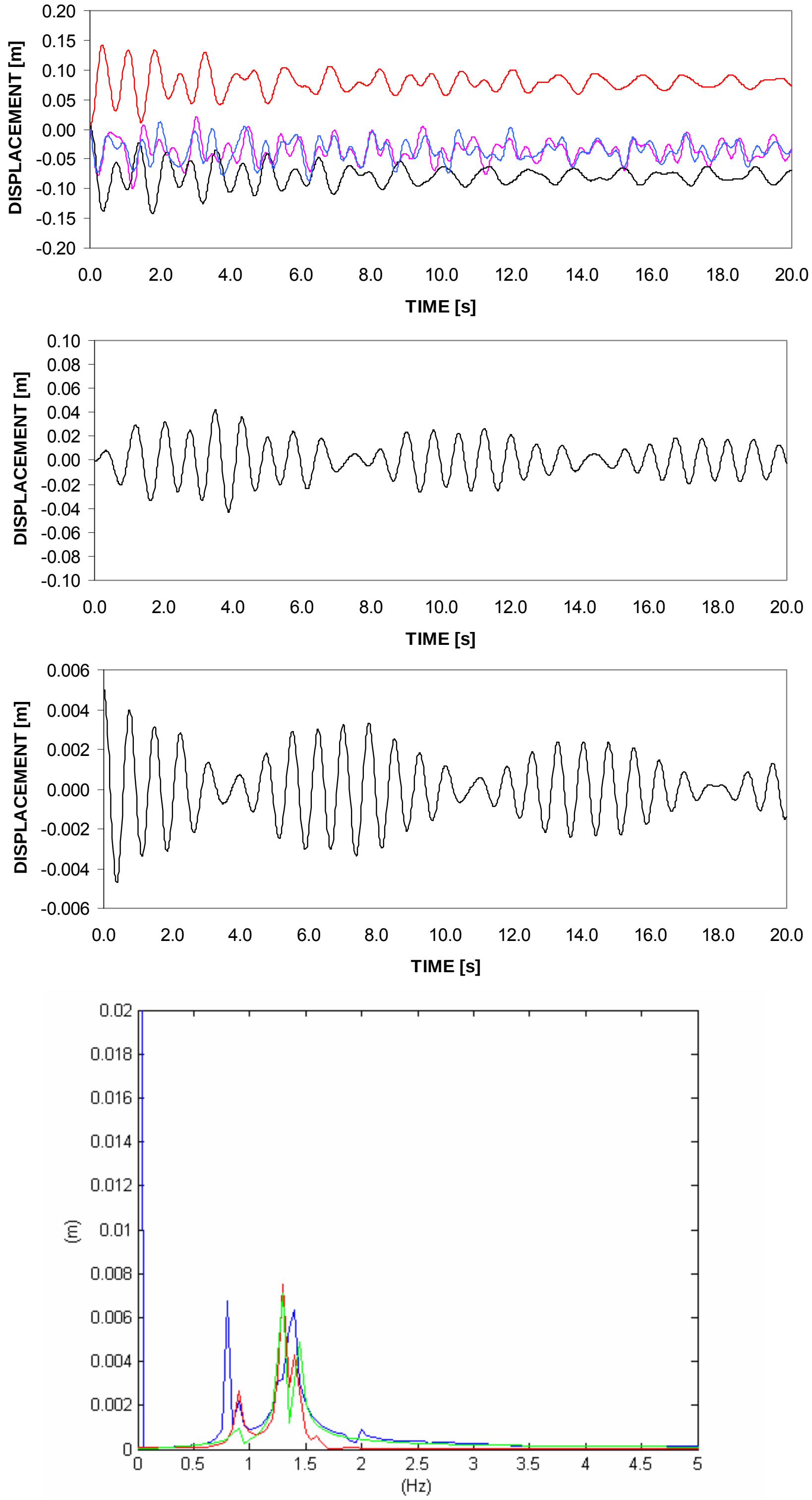

Figure D.1: a) numerically predicted displacement histories of the container walls and liquid. b) predicted sloshing amplitude in flexible container with 3 kg added mass, c) structure displacement and d) FFT of wall displacement (blue), sloshing liquid (red) and plate displacement (green). The mass of the structure is 1500 kg.

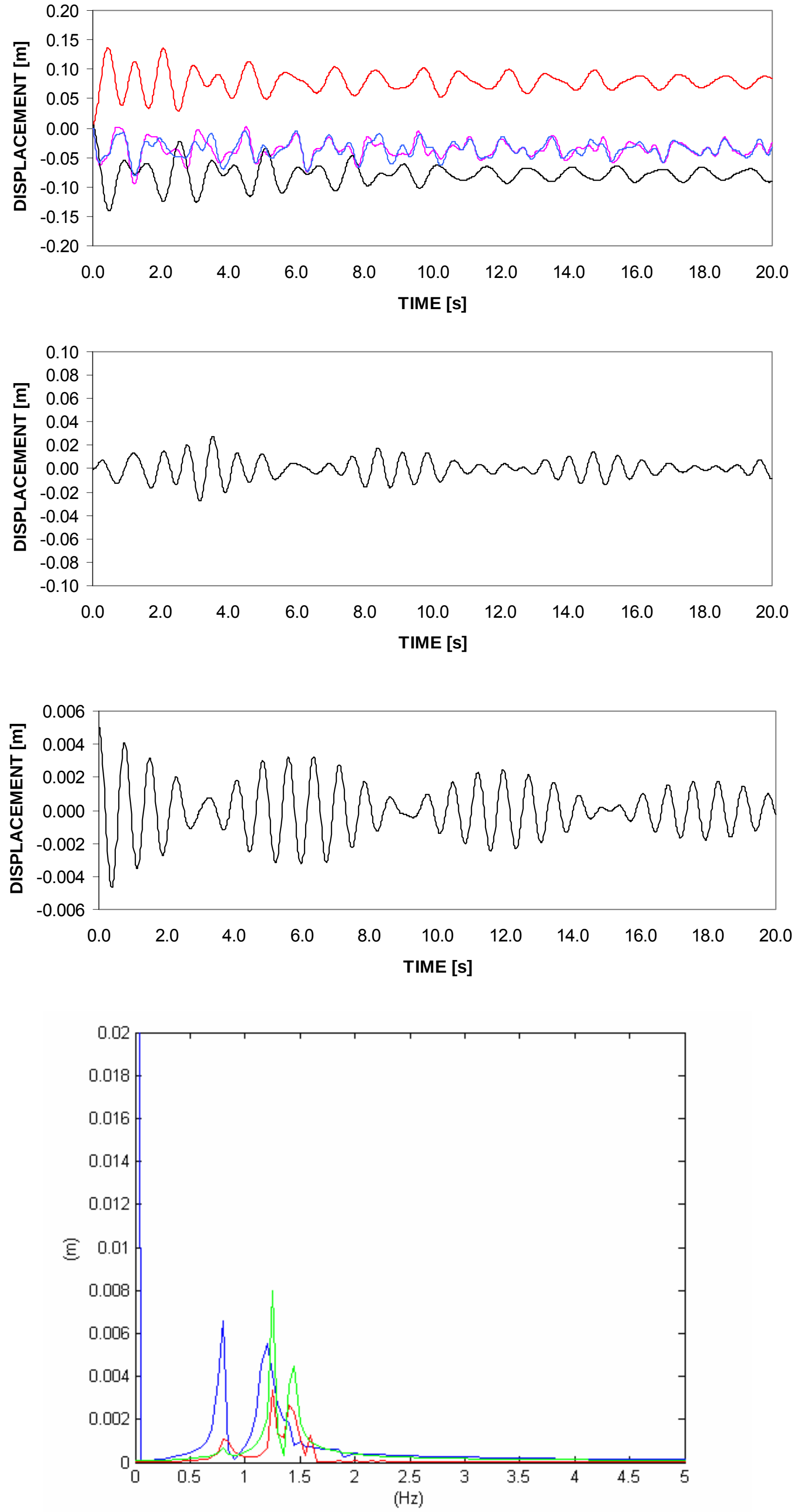

Figure D.2: Same as in Figure D.2 but for 5 kg added mass.

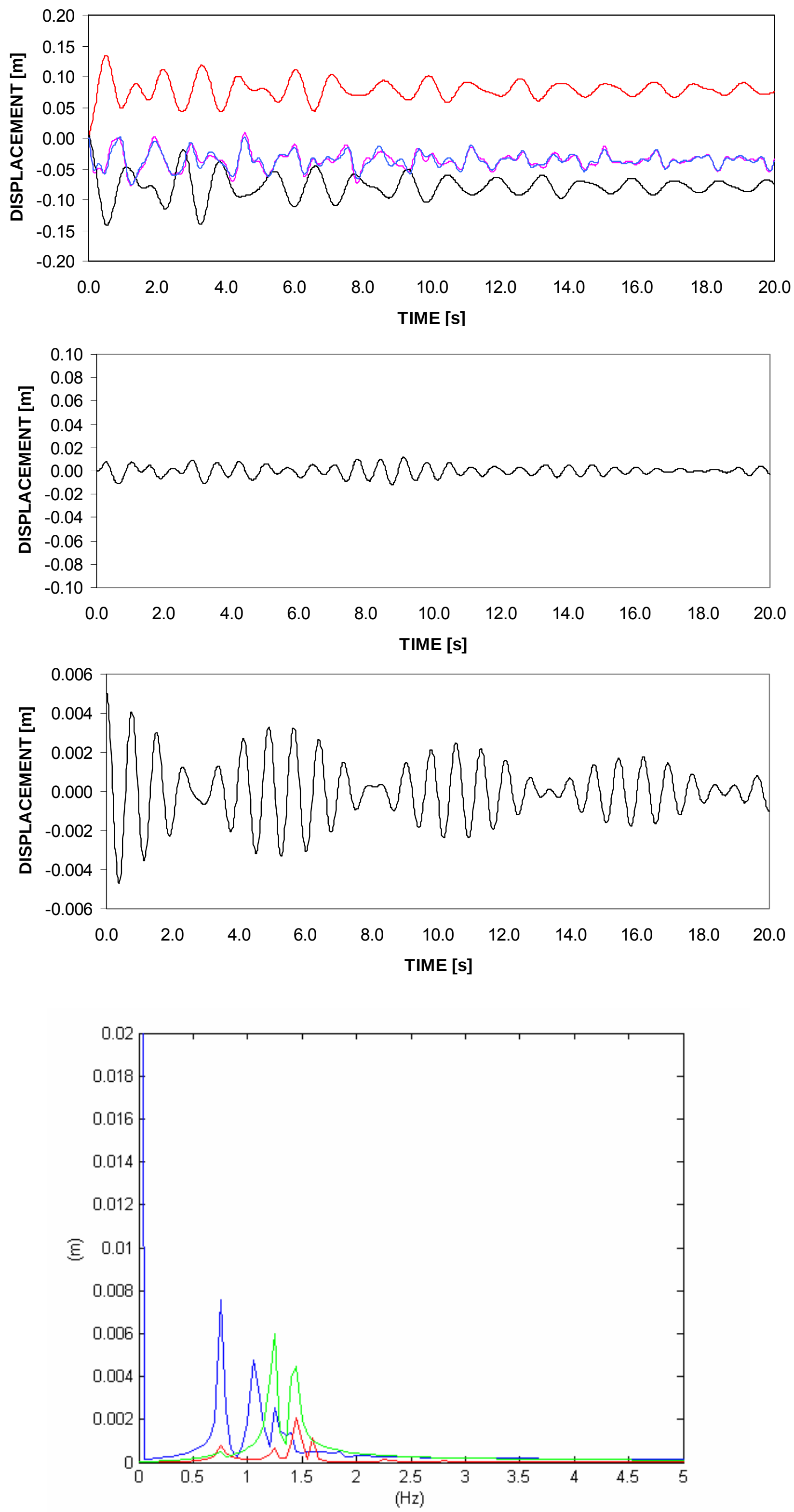

Figure D.3: Same as in Figure D.2 but for 7 kg added mass.

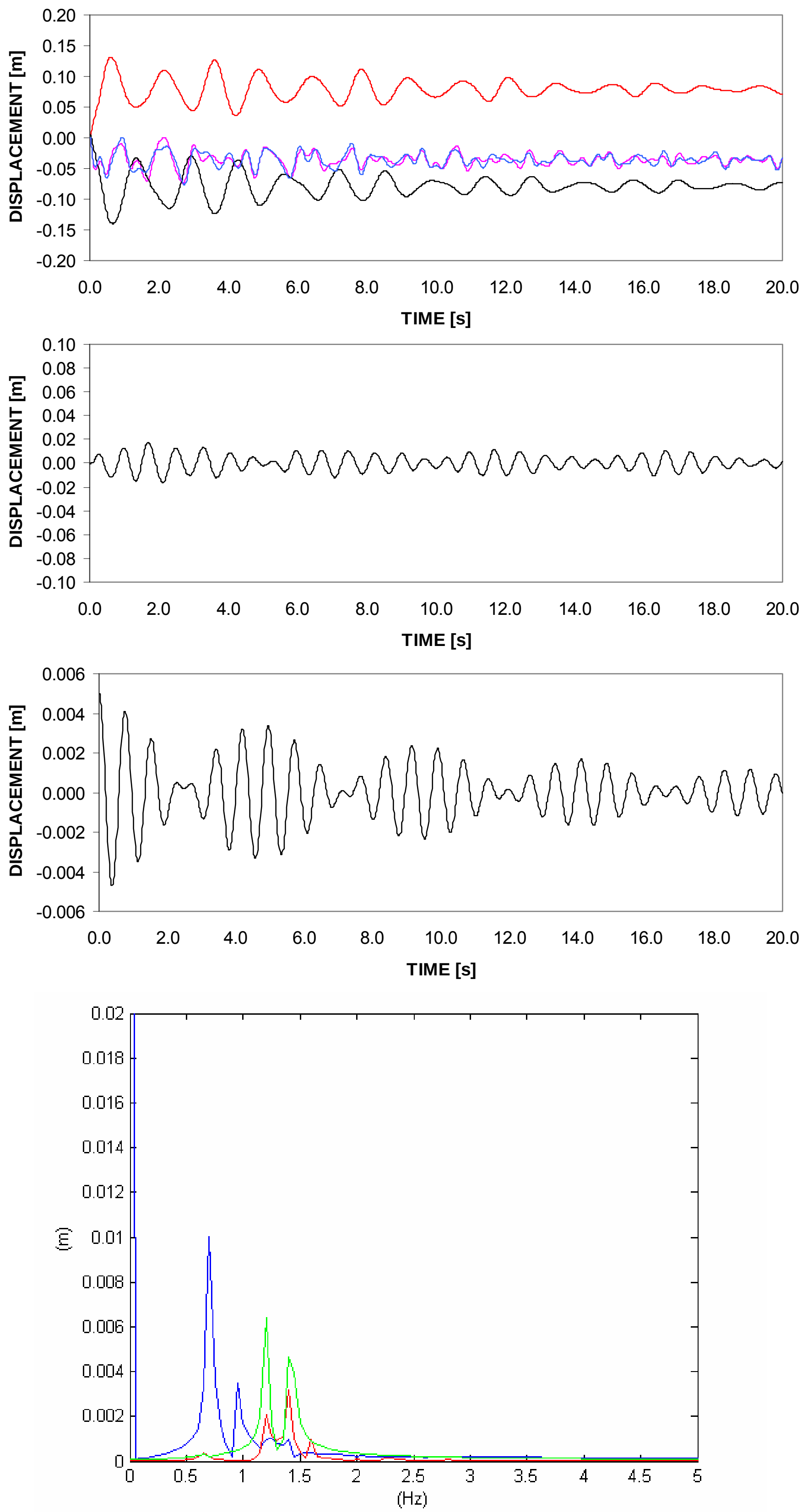

Figure D.4: Same as in Figure D.2 but for 11 kg added mass.

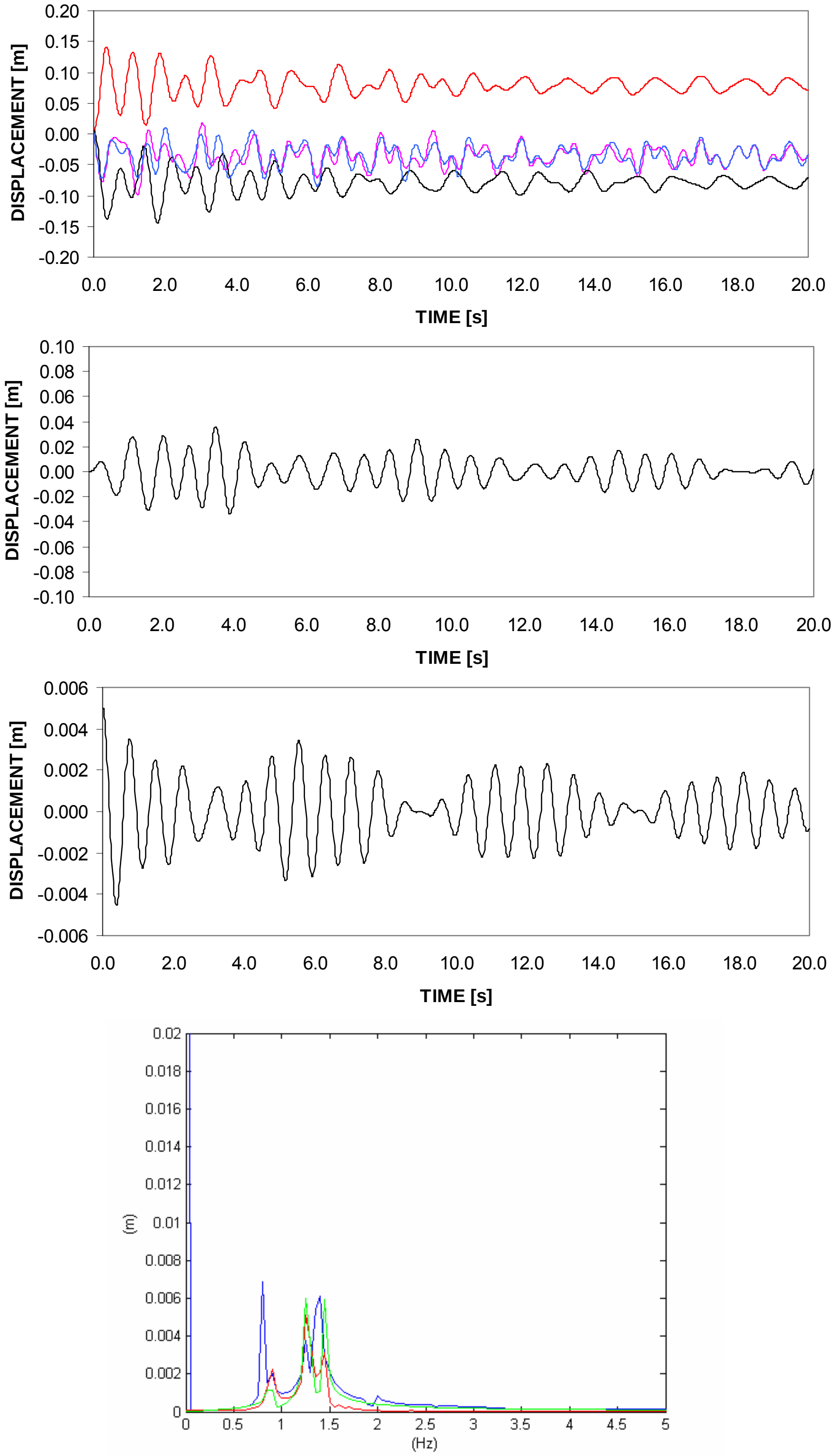

Figure D.5: a) numerically predicted displacement histories of the container walls and liquid. b) predicted sloshing amplitude in flexible container with 3 kg added mass, c) structure displacement and d) FFT of wall displacement (blue), sloshing liquid (red) and plate displacement (green). The mass of the structure is 1000 kg.

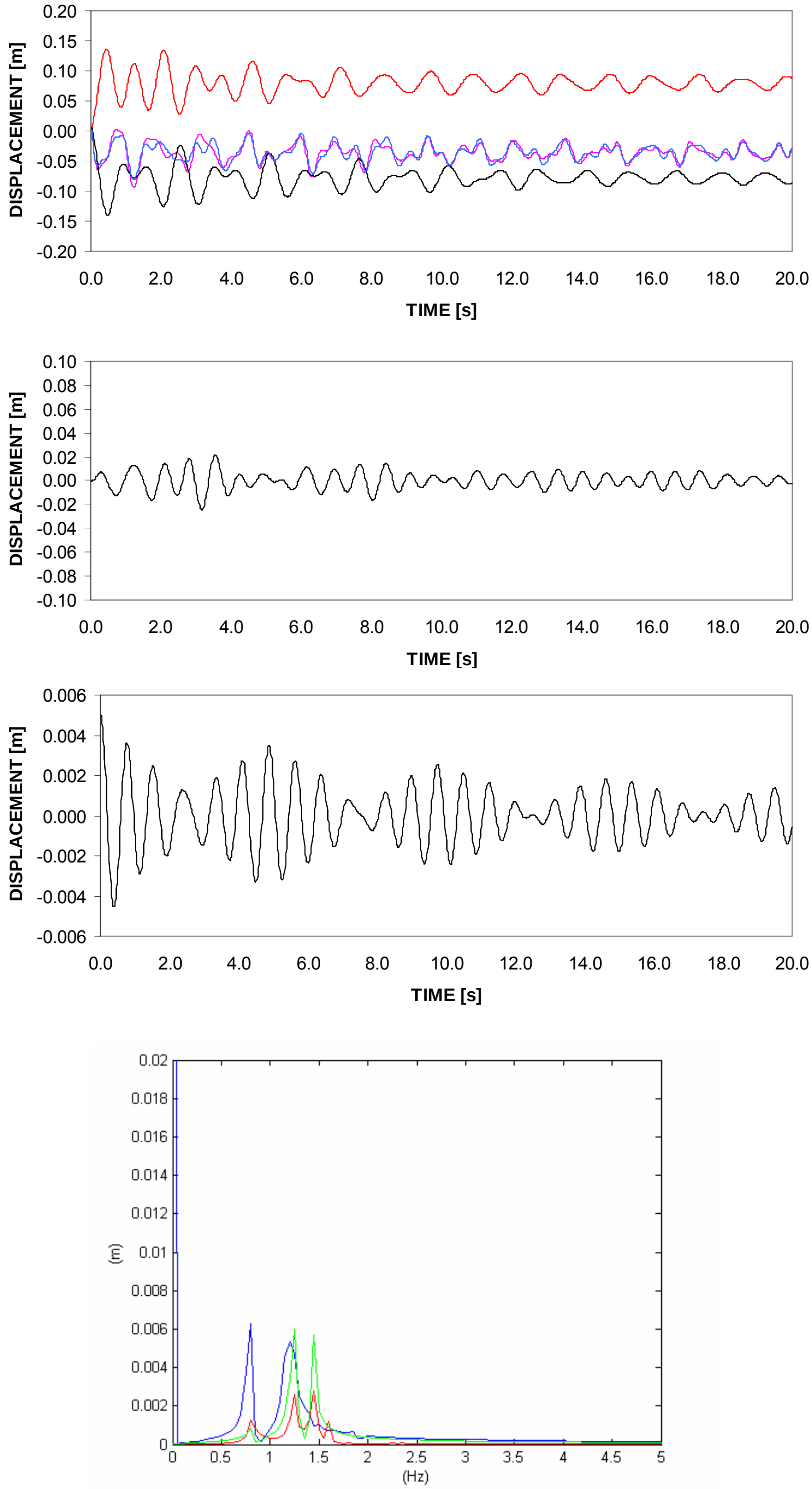

Figure D.6: Same as in Figure D.5 but for 5 kg added mass.

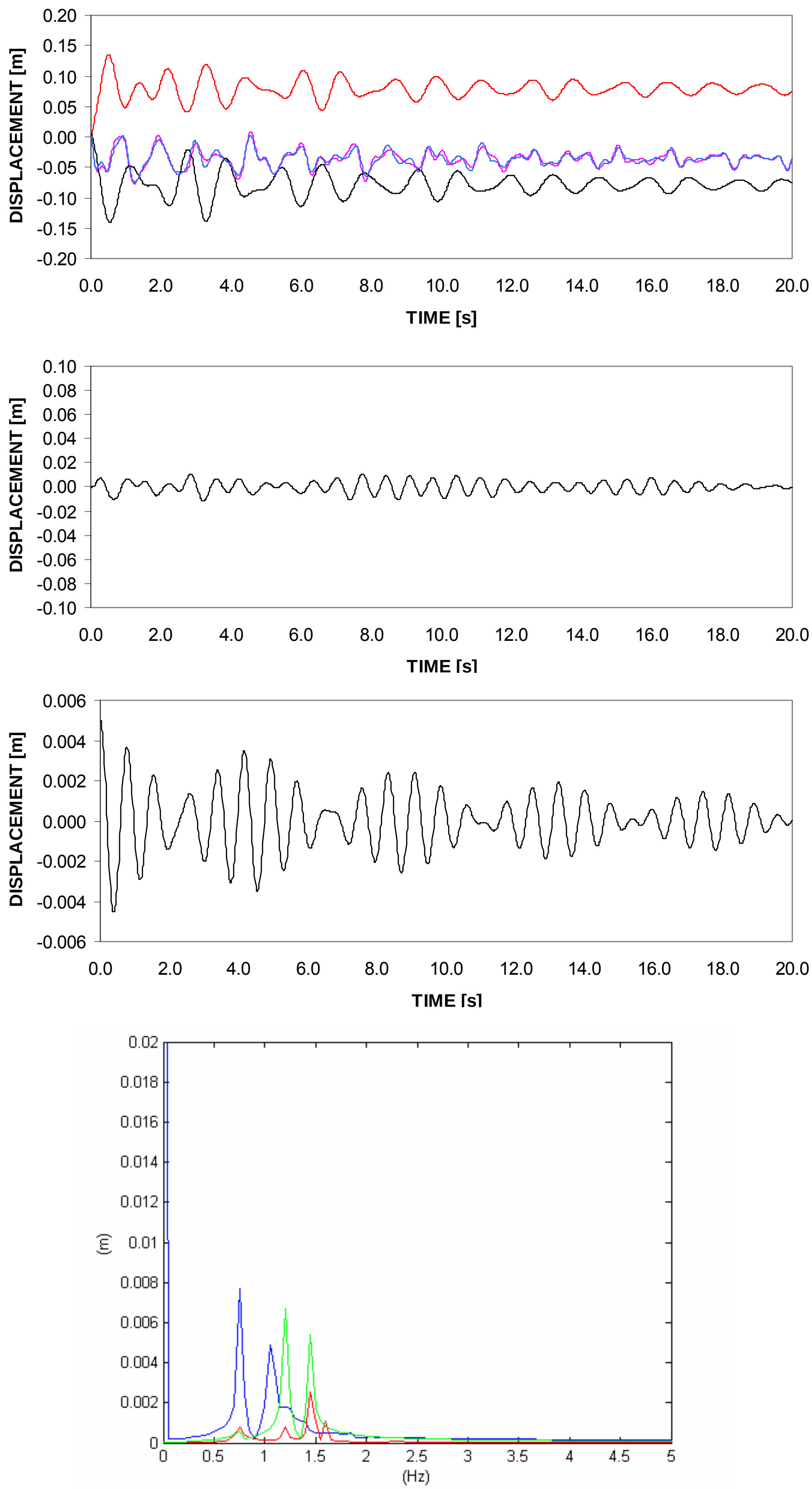

Figure D.7: Same as in Figure D.5 but for 7 kg added mass.

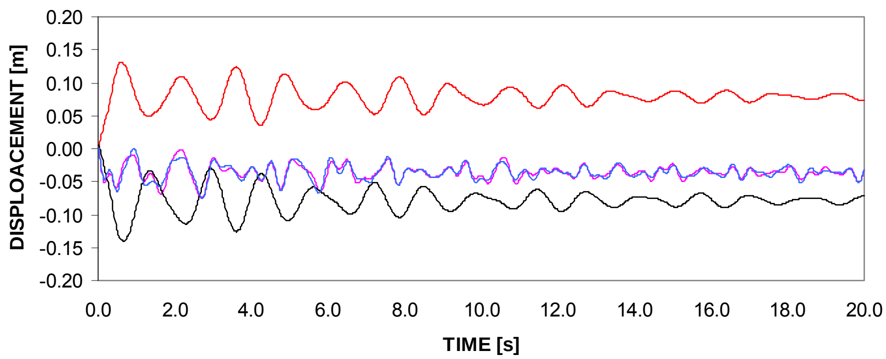

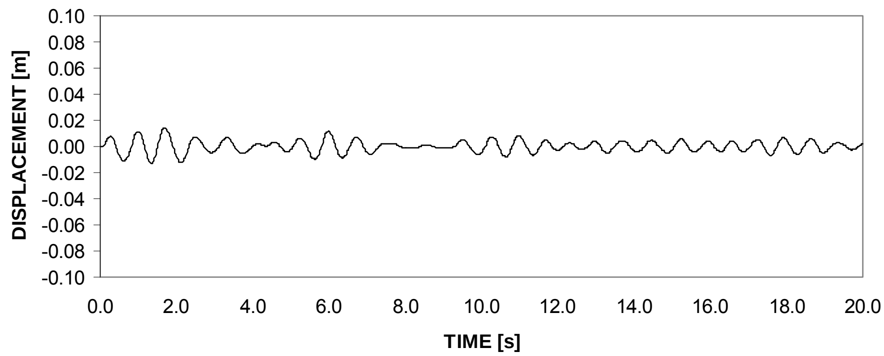

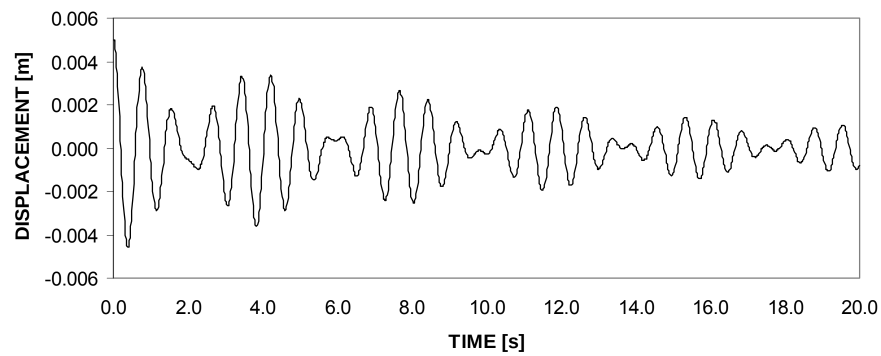

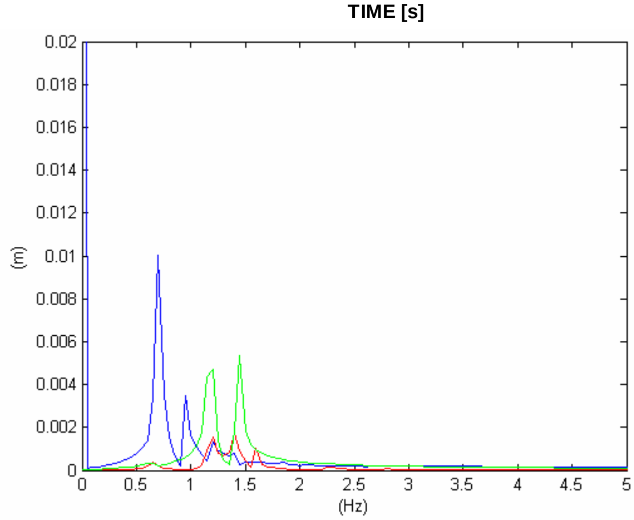

Figure D.8: Same as in Figure D.5 but for 11 kg added mass.